

**INVESTIGATIONS ON THE EFFECT OF
DEMAND SIDE MANAGEMENT AND
BATTERY STORAGE IN FREQUENCY
REGULATION OF POWER SYSTEM**

Thesis Submitted

By

SWETALINA BHUYAN

Doctor of Philosophy (Engineering)

**Department of Electrical Engineering
Faculty Council of Engineering & Technology
Jadavpur University
Kolkata, India**

2023

JADAVPUR UNIVERSITY

KOLKATA-700032, INDIA

Index No. 246/20/E

1. Title of the Thesis:

**INVESTIGATIONS ON THE EFFECT OF
DEMAND SIDE MANAGEMENT AND
BATTERY STORAGE IN FREQUENCY
REGULATION OF POWER SYSTEM**

2. Name, Designation & Institution of the Supervisors:

Prof. SUNITA HALDER NEE DEY

Professor

Electrical Engineering Department

Jadavpur University

Kolkata, India

Prof. SUBRATA PAUL

Professor

Electrical Engineering Department

Jadavpur University

Kolkata, India

3. List of Publications:

Journal Publication

- [1] **Swetalina Bhuyan**, Sunita Halder Nee Dey, and Subrata Paul. "A robust MPC design concerning on battery variables for frequency regulation and saving battery life collaborating with demand response." *Electrical Engineering*, Springer, DOI :10.1007/s00202-023-01924-1.
- [2] **Swetalina Bhuyan**, Sunita Halder Nee Dey, and Subrata Paul. "Modified delay compensation in demand response for frequency regulation of interconnected power systems integrated with renewable energy sources." *Cogent Engineering* 9(1), 2022: 2065899.
- [3] S. Chaine, **Swetalina Bhuyan** "Analysis of DFIG based wind integration in conventional thermal power system for frequency regulation" *International journal of science and technology research*, volume-8, issue11. nov2019.
- [4] **Swetalina Bhuyan**, Sunita Halder Nee Dey, and Subrata Paul. " Experimental Assessment of Parameter Driven MPC for frequency regulation in Collaboration with Delay Compensated Demand Response of an Isolated Micro grid." **(communicated)**
- [5] Mounadeep Poddar, **Swetalina Bhuyan**, Sunita Halder nee Dey "An Assessment Model of Demand Response in Indian Electricity Market." **(communicated)**

Conference Publication

- [1] **Swetalina Bhuyan**, Sunita Halder nee Dey, Subrata Paul, Sabita Chaine, 'Analysis of Frequency Regulation for a Hydro-Thermal System with ALFC-DR Model', *International Conference on Power Electronics and Energy (ICPEE-2021)*, 2-3 January 2021, KIIT Deemed to be University, Bhubaneswar, Odisha.
- [2] **Swetalina Bhuyan**, Sunita Halder nee Dey, Subrata Paul, 'Role of demand side management in automatic load frequency control', *The first International conference on Emerging Frontiers in electrical and electronic Technologies (ICEFEET-2020)*, NIT, Patna 10-11th July, 2020.

4. List of Patents: Nil

5. List of Presentation in National/International/Conference/Workshop:

Presentation in International Conference:

- [1] **Swetalina Bhuyan**, Sunita Halder nee Dey, Subrata Paul, Sabita Chaine, ‘Analysis of Frequency Regulation for a Hydro-Thermal System with ALFC-DR Model’, International Conference on Power Electronics and Energy (ICPEE-2021), 2-3 January 2021, KIIT Deemed to be University, Bhubaneswar, Odisha.
- [2] **Swetalina Bhuyan**, Sunita Halder nee Dey, Subrata Paul, ‘Role of demand side management in automatic load frequency control’, The first international conference on Emerging Frontiers in electrical and electronic Technologies (ICEFEET-2020), NIT, Patna 10-11th July, 2020.

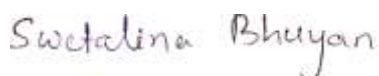
Statement of Originality

I, Swetalina Bhuyan registered on **18/02/2020** do hereby declare that this thesis entitled ***“Investigations on the Effect of Demand Side Management and Battery Storage in frequency regulation of Power System*** “contains literaturesurvey and original research work done by the undersigned candidate as part of Doctoral studies.

All information in this thesis have been obtained and presented in accordance with existing academic rules and ethical conduct. I declare that, as required by these rules and conduct, I have fully cited and referred all materials and results that are not original to this work.

I also declare that I have checked this thesis as per the “Policy on Anti Plagiarism, Jadavpur University, 2019”, and the level of similarity as checked by iThenticate software is 5 %.

Signature of Candidate:



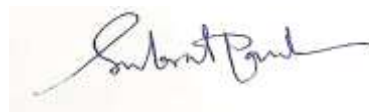
Swetalina Bhuyan

Date: 23/08/2023

Certified by Supervisors:



Prof. Sunita Halder nee Dey
Professor
Electrical Engg. Department
Jadavpur University



Prof. Subrata Paul
Professor
Electrical Engg. Department
Jadavpur University

CERTIFICATE FROM THE SUPERVISORS

This is to certify that the thesis entitled “*Investigations on the Effect of Demand Side Management and Battery Storage in frequency regulation of Power System*” submitted by **Swetalina Bhuyan**, who got her name registered on 18/02/2020, for the award of the Ph.D. (Engineering) Degree of Jadavpur University is absolutely based upon her own work under the supervision of Prof. Sunita Halder nee Dey and Prof. Subrata Paul and that neither of her thesis nor any part of the thesis has been submitted for any degree/diploma or any other academic award anywhere before.



Prof. Sunita Halder nee Dey
Professor
Electrical Engg. Department
Jadavpur University



Prof. Subrata Paul
Professor
Electrical Engg. Department
Jadavpur University

ACKNOWLEDGEMENT

I convey my sincere thanks and gratitude to my supervisors Prof. Sunita Halder nee Dey, Professor, Department of Electrical Engineering, Jadavpur University and Prof. Subrata Paul, Professor, Department of Electrical Engineering, Jadavpur University for their expert guidance, encouragement and invaluable suggestions in carrying out this research work. Due to their great effort, support and lot of enlightening ideas during the course of this research, it was possible to achieve the results in shortest time. My association with them will remain a memorable part of my life.

I am thankful to the authorities of Jadavpur University for providing the facilities for carrying out the research and allowing me to submit the Thesis for Ph.D. (Engineering) Degree.

I express my sincere thanks to the Head of the Department of Electrical Engineering, Jadavpur University for extending all help to complete the work.

It is my great pleasure to thank all the faculty members of the Department of Electrical Engineering, Jadavpur University for their encouragement.

I want to express my thanks to all the research scholars and friends in the Department of Electrical Engineering, Jadavpur University for their help.

I express my sincere thanks to all the staffs of the Department of Electrical Engineering, Jadavpur University for their help.

Finally, I express my heart-felt gratitude to my family members for their continuous support and encouragement.

Date: 23/08/2023

Swetalina Bhuyan
Swetalina Bhuyan

Dedicated to

my Husband

Shri Durga Shankar Dalai,

my Parents

Shri Bijay Kumar Bhuyan

&

Smt. Santi Lata Bhuyan

And also

my loving Daughter

Tannishtha

ABSTRACT

In this thesis, different methods are proposed for overall improvement of frequency regulation of power system mainly with the help of demand side management (DSM) and battery energy storage system (BESS). At the beginning of the thesis, the different components of the power system are modeled including conventional and renewable generation units, battery storage unit and different modern equipment's for power system control. These components have impedances, time constants, gains, power ratings, capacities, start -up time etc, all of which are to be inputted into the computer model for simulation study. In view of the above information, this research uses different components of power system for frequency regulation analysis.

These modelling are used in the thesis to examine the role of demand side management (DSM) in automatic load frequency control (ALFC) in presence of distributed generations (DGs). DSM has been introduced in ALFC in terms of demand response (DR). DR is introduced in the ALFC model of two area power system consisting of wind energy conversion system (WECS). The frequency regulation due to load variation is studied and better results are obtained after introduction of DR.

In the next part of the thesis, the research investigated the dynamic behavior of a hydrothermal power network with the aid of demand side management (DSM). DSM provides prime to consumers about the usage of electricity and prevent cross subsidies among consumers with the aim to manage the supply and demand through an elegant program. In the present work DSM is incorporated in the automatic load frequency control (ALFC) of an interconnected hydrothermal power network to get better frequency regulation. Particle swarm optimization (PSO) technique is utilized to obtain optimal control parameter of the controller employed for DSM. The presence of DSM is found to be promising in the enhancement of dynamic stability of the hydro-thermal power network.

As DR found to be a promising technique for frequency regulation, so in the nest part of the thesis puts forward a lead compensator-based PI controller for DR loop which is included in the conventional ALFC model to improve the frequency control process of power system. Though DR is a good solution for ALFC but the vital problem in DR is the

existence of communication delay between control center and appliances. The proposed lead compensator can generate phase lead at the output of the DR loop to eliminate the adverse effects of the delay on the system performance. To verify the effectiveness of the proposed controller for ALFC problem, two different two-area transfer function models of power system are tested. At first the approach is analyzed for a wind integrated two-area thermal power system, later the same is extended for a two-area hydrothermal system. The system dynamic performances in presence of proposed compensator are obtained with all the controllers tuned. The Particle Swarm Optimization (PSO) technique is used to tune all the controller parameters of the DR loop as well as the ALFC loop. The results demonstrate the usefulness of the proposed lead compensator in the event of communication delay and step load variation. Finally, the performance of lead compensator in DR exhibits robust performance even with the variation in disturbance parameters and operating conditions in the system.

Furthermore, the thesis has taken a challenge to design a model predictive controller (MPC) for ALFC of two area, wind integrated thermal power system equipped with BESS and DR for frequency regulation task. Primarily, the incremental BESS model employs a new state of charge (SOC) based strategy to regulate the power from battery for saving battery life. Then DR, along with the SOC based BESS, is employed in ALFC for frequency regulation. A modified state space model of MPC incorporating all BESS variables is developed and employed in ALFC of the studied power system. The performance of the designed MPC is examined for inertia issues arising from wind in the conventional two area power system. Furthermore, the capability of BESS for frequency regulation and effect on the life of BESS with the proposed control strategy is measured through MPC based ALFC and results compared with system performance when integral controller in ALFC and inertia controller from wind are present. In addition to DR and BESS in ALFC, doubly fed induction generator (DFIG) based proportional derivative (PD) inertia controller also contributes in the power system for frequency support from wind energy section to avoid inertia issues. So, all the controllers of the test power system such as integral controller in ALFC and PD controller in wind are tuned concurrently for smooth frequency control. However, performance of MPC is tested for smooth frequency regulation by tuning PD controller gain of wind only while keeping MPC gain parameters as available in literature. particle swarm optimization (PSO) is used to tune the integral controller gain of ALFC for the studied power system to compare the results with MPC based ALFC. A transfer function model of wind integrated two area thermal power system is taken into

consideration in the present study to verify the effectiveness of the battery variable concerning MPC design for ALFC collaborating with DR for smooth frequency control and provide safe battery life. Finally, results confirm the effectiveness of the designed MPC based ALFC, collaborating with DR and SOC based incremental BESS through various case studies.

Finally, the thesis proposes a PSO based MPC for ALFC of microgrid (MG). The generalized state space analysis is considered to model the MPC including all controllable and uncontrollable generation unit. The proposed MPC is developed as a single input multi output system. The MPC is considered as parameter driven controller whose input parameter R_w is tuned with the help of widely used robust PSO technique to get better frequency control. Moreover, the proposed MPC is collaborated with demand response (DR) which in turn, is accompanied with a proportional plus integral (PI) controller with lead compensator-based delay compensator to avoid the delay issue in DR. So, the input parameter R_w of MPC for its online optimization, and PI controller gain parameters of DR are tuned by minimizing the performance index like integral time square error (ITSE) to get smooth frequency regulation for an isolated MG. To evaluate the effectiveness of the proposed scheme of frequency regulation, an isolated MG equipped with conventional diesel unit, fuel cell, wind energy, solar energy and battery cell is taken as the test system. The effectiveness of the proposed scheme for frequency control is evaluated and compared with a robust fuzzy adaptive MPC. Finally, the results prove the efficacy of the proposed scheme through various case studies. In view of practical validation, the proposed frequency control scheme for the studied isolated MG is realized in real time through OPAL-RT OP5600 with RT lab version of 19.3.0.228.

CONTENTS

	Page No.
List of Figures	xvi
List of Tables	xix
CHAPTER 1: INTRODUCTION	1
1.1. General Introduction	1
1.2. Literature Survey	3
1.2.1. Frequency Regulation	3
1.2.2. Demand Side Management	7
1.2.3. Battery Management for Frequency Regulation	9
1.2.4. Model Predictive Controller (MPC)	10
1.3. Objectives of the Thesis	13
1.4. Contributions of the Thesis	14
1.5. Organization of Thesis	15
CHAPTER 2: TEST MODELS FOR THE STUDY	18
2.1 . Introduction	18
2.2 . Modelling of Hydro-Electric Governing System	19
2.3 . Modelling of DFIG based Wind generator	19
2.4 . DR Modelling for ALFC	22
2.5 . Modelling of BESS	23
2.6 . PSO Optimization Technique	29
CHAPTER 3: ROLE OF DEMAND SIDE MANAGEMENT FOR FREQUENCY REGULATION	31
3.1. Introduction	31
3.2. ALFC Modelling with DR for Different Power System	32

3.2.1.	Wind Integrated Two-Area Thermal Power System	33
3.2.2.	Hydro Thermal Two-Area Power System	33
3.2.3.	Power Balance Equations	34
3.3.	Proposed Methodology of Tuning Of AGC Parameters For Two-Area Power System	35
3.3.1.	PSO Algorithm for Wind Integrated Two-Area Thermal Power System	36
3.2.1.	PSO Algorithm For Hydro Thermal Two-Area Power System	36
3.4.	Simulation And Results	37
3.4.1.	Comparative Analysis with And Without DR	
3.4.1.1.	Wind Integrated Two-Area Thermal Power System	37
3.4.1.2.	Hydro Thermal Two-Area Power System	40
3.4.2.	Overall Frequency Regulation with DR	42
3.4.2.1.	Wind Integrated Two-Area Thermal Power System	43
3.4.2.2.	Hydro Thermal Two-Area Power System	47
3.5.	Conclusion	50
3.6.	Publication From This Work	50
CHAPTER 4:	MODIFIED DELAY COMPENSATION IN DEMAND RESPONSE FOR FREQUENCY REGULATION OF INTERCONNECTED POWER SYSTEMS INTEGRATED WITH RENEWABLE ENERGY SOURCES.	51
4.1.	Introduction	51
4.2.	Frequency response modelling	52
4.2.1.	ALFC Modelling of Two-Area Power System	52
4.2.2.	Inertia Control DFIG	55
4.2.3.	Mathematical Background with DR	55
4.3.	The Proposed Controller	57
4.3.1.	Stability Analysis with Proposed Controller	57
4.3.2.	Synthesis Of Lead Compensator	59
4.3.3.	The Structure of Two Stage Lead Compensator Plus PI-Based DR Delay Controller	61
4.3.4.	Problem Formulation	61

4.4.	Simulation And Results	63
4.4.1.	Study On Wind Integrated Two- Area Thermal Power System	64
4.4.1.1.	Comparative Study of Proposed Delay Control DR In LFC With Other Controllers In LFC	64
4.4.1.2.	Comparative Study Between Lead Compensator in DR and without Lead Compensator in DR Controller	68
4.4.2.	Study on Wind Integrated Two-Area Hydrothermal Power System	71
4.5.	Sensitivity Analysis with The Proposed Controller	74
4.6.	Discussion	77
4.7.	Conclusion	78
4.8.	Publication From This Work	79

CHAPTER 5: ROLE OF DR IN PRESENCE OF BATTERY MANAGEMENT SYSTEM IN A MPC BASED ALFC STUDY

5.1.	Introduction	80
5.2.	ALFC Modelling with BESS, DR and DFIG	81
5.3.	Mathematical Analysis of ALFC	83
5.4.	Proposed Approach	85
5.4.1.	SOC Strategy with BESS Model for Frequency Regulation	86
5.4.2.	Implementation of MPC for ALFC	87
5.4.2.1.	Basic of MPC for ALFC Study	87
5.4.2.2.	MPC Formulation for its Adaptive Optimization	89
5.4.2.3.	MPC Stability and Optimization Algorithm Execution Time	90
5.4.2.4.	Objective Function of MPC	90
5.4.2.5.	Problem Formulation	91
5.5.	Simulation and Results	93
5.5.1.	Simulation Procedure for Frequency Regulation	93
5.5.2.	Impact of DFIG Controller in Presence of BESS	93
5.5.3.	Impact of SOC based BESS and DR in ALFC	95
5.5.4.	Impact of MPC in ALFC	97
5.5.4.1.	MPC for Two-Area Thermal Power System	97
5.5.4.2.	MPC for Battery (BESS)Integrated Two Area Thermal Power System	99
5.5.4.3.	MPC for Wind and Battery (BESS) Integrated	101

Two Area Thermal Power System

5.5.5.	Impact of DR in MPC Based ALFC for SOC Change in BESS	104
5.6.	Discussion	105
5.7.	Conclusion	110
5.8.	Publication from This Work	110
CHAPTER 6:	REAL TIME PERFORMANCE ANALYSIS OF DR AND MODEL PREDICTIVE CONTROL FOR ALFC STUDY IN MG	
6.1.	Introduction	111
6.2.	Modelling of Isolated Micro Grid for Frequency Regulation	112
6.3.	MPC formulation for Micro-Grid	113
6.4.	Proposed Scheme for Frequency Regulation	115
6.4.1.	Model Predictive Control implementation in ALFC of MG	115
6.4.2.	Lead Compensator Based DR for Frequency Regulation	118
6.4.3.	BESS Modelling for Frequency Regulation	118
6.4.4.	PSO Optimization to Tune R_w , K_{pc} , K_{ic} for Overall Frequency Control	119
6.5.	Simulation and Results	120
6.5.1.	Performance Analysis of Proposed Frequency Control Scheme Compared to Others Existing Control Scheme for ALFC in MG	122
6.5.2.	Proposed MPC Combined with and without Lead Compensator in DR Loop	123
6.5.3.	Comparison of SOC Control Based BESS and Simple BESS Model for Frequency Regulation in MG.	124
6.5.4.	Sensitivity Analysis with the Proposed Frequency Control Scheme.	127
6.6.	Experimental Test Analysis.	129
6.7.	Discussion	131
6.8.	Conclusion	133
6.9.	Publication from This Work	133
CHAPTER 7:	CONCLUSION	
7.1.	General Conclusion	134
7.2.	Future Scope of Work	136

REFERENCES	138
APPENDIX A: Details of Components of Power System under Investigation	148

LIST OF FIGURES

	Page No.
Fig. 1.1. A conceptual Representation of Demand Response Considering Inelastic Demand.	2
Fig. 2.1. Electro-hydraulic Governors with PID Action	19
Fig. 2.2. Transfer Function Model of DFIG Controller	21
Fig. 2.3. Demand Price curve	22
Fig. 2.4. Schematic Description of a BESS Plant.	25
Fig. 2.5. Equivalent Circuit of BESS.	26
Fig. 2.6. Transfer Function Model of BESS.	26
Fig. 3.1. The ALFC Model of Two-Area Interconnected Power System In Presence of DR and DFIG.	33
Fig. 3.2. The ALFC Model of The Hydro-Thermal Test System.	34
Fig. 3.3. The flowchart to obtain gain parameters.	36
Fig. 3.4. The System Frequency and Tie Line Power Deviations for 1% Load Change in Area-1 with and without DR.	44
Fig. 3.5. The System Frequency and Tie Line Power Deviations For 2% Load Change in Area-2.	45
Fig. 3.6. The System Frequency and Tie Line Power Deviations For 2% Load Change in Area-1 And 1% Load Change in Area-2 Simultaneously and With Without DR.	47
Fig. 3.7. Deviations In Frequencies and Tie Line Power for Load Change in Area-1.	48
Fig. 3.8. Deviations In Frequencies and Tie Line Power for Load Change In Area-2.	49
Fig. 4.1. Transfer Function Model of The Test System with Proposed DR Controller.	53
Fig. 4.2. Proposed Controller for Delay Compensation in DR Loop.	54
Fig. 4.3. Modified i^{th} Area Wind Integrated Power System Model with Delay Compensated DR Model in Frequency Control Loop.	59
Fig. 4.4. Phase Lead Network.	61
Fig. 4.5. PSO flow chart to tune control parameters.	64

Fig. 4.6.	The Tie Line Power Deviation and Area Frequency Deviations for 1% Load Change in Area-1 For Different Schemes of Controllers.	66
Fig. 4.7.	Verdict Of Settling Time with Different Controllers.	67
Fig. 4.8.	Comparison of MDR with Different Controllers.	67
Fig. 4.9.	The Tie Line Power Deviation and Area Frequency Deviations For 1% Load Variation in Area-1 with Lead Compensator in DR and without lead compensator in DR.	70
Fig. 4.10.	Judgement of Maximum Overshoot with and without Lead Compensator in DR controller.	70
Fig. 4.11.	The Tie Line Power Deviation and Area Frequency Deviations For 1% Load Change in Area-1 With and Without Different DR controller for hydrothermal system.	73
Fig. 4.12.	ΔF_1 , ΔF_2 and ΔP_{Tie} of Different Power System for Continuous load change (from 0% to 50%) in Area-1 With Proposed DR in ALFC.	76
Fig. 5.1.	Transfer function model of studied two area power system.	82
Fig. 5.2.	Transfer function model of BESS with proposed SOC strategy.	86
Fig. 5.3.	Configuration of MPC for ALFC for the test system.	89
Fig. 5.4.	Flow chart for MPC in ALFC of the two -area power.	91
Fig. 5.5.	Frequency deviation in each area and tie line power deviation when BESS collaborated with ALFC.	94
Fig. 5.6.	Responses of BESS under discharging mode in area-1 for 1% load change in area-1.	95
Fig. 5.7.	Frequency and Tie line power deviation when both BESS and DR collaborated in ALFC for 1% load change in area-1.	96
Fig. 5.8.	Comparison of dynamic performances in terms of tie line power deviation and area frequency deviations for 1% load variation in area-1 with different controller in ALFC.	99
Fig. 5.9.	Comparison of dynamic performances in terms of tie line power deviation and area frequency deviations for 1% load variation in area-1 with different controller in ALFC in presence of BESS.	100
Fig. 5.10.	Simulation results of SOC variation for 1% step load variation in area-1 with different controller in ALFC.	101
Fig. 5.11.	Comparison of dynamic performances in terms of tie line power deviation and area frequency deviations for 1% load variation in area-1 with different controller in ALFC and DFIG.	102
Fig. 5.12.	Simulation results of SOC variation for 1% step load variation in area-1 with different controller in ALFC.	103
Fig. 5.13.	Comparison of responses of Cost functions of different MPC designs over simulation period.	104
Fig. 5.14.	SOC variation for 1% step load variation in area-1 for different	105

	type of controller.	
Fig. 5.15.	Damping ratio with different controllers in ALFC.	107
Fig. 5.16.	Pattern of step load change.	107
Fig. 5.17.	Frequency deviations and tie line power deviation for continuous load change.	108
Fig. 6.1.	Transfer function model of studied microgrid with MPC for secondary frequency control.	112
Fig. 6.2.	Basic structure of a Model predictive controller-based plant.	114
Fig. 6.3.	PSO algorithm to tune R_w, K_{pc}, K_{ic} .	121
Fig. 6.4.	Responses from case A in terms of a). comparison of frequency deviations of MG b). cost function of proposed MPC.	123
Fig. 6.5.	Comparison of frequency deviation of the MG with and without delay compensator in DR.	124
Fig. 6.6.	Responses from case C in terms of a). comparison of frequency deviations of MG b). cost function of proposed MPC c). control input to diesel cell d). control input to fuel cell.	126
Fig. 6.7.	Pattern of step load change.	128
Fig. 6.8.	Comparison of frequency deviation with different controller for continuous load variation.	129
Fig. 6.9.	OP5600 Set-up for real time application of the proposed control scheme.	130
Fig. 6.10.	Real time response in OPAL-RT of MG with proposed scheme for frequency regulation.	130
Fig. 6.11.	Real time response in OPAL-RT of MG for continuous load variation in the range of 0-5% in a step of 1% for first 50 second.	131

LIST OF TABLES

		Page No.
Table 2.1.	Actual values of BESS parameters.	27
Table 2.2.	Power System parameters where BESS is applied.	27
Table 3.1.	Nominal Parameters of two area wind integrated thermal Power System Model.	32
Table 3.2.	Parameters taken for the hydrothermal System Model [2].	32
Table 3.3.	Tuned controller parameters and settling time of frequency deviations and tie line power deviation for load change in the area-1 in absence of DR.	38
Table 3.4.	Controller parameters and settling time of frequency Deviations and tie line power deviation for load change in the area-1 in presence of DR.	38
Table 3.5.	Tuned controller parameters and settling time of frequency deviations and tie line power deviation for load change in the area- 2 in absence of DR	39
Table 3.6	Controller parameters and settling time of frequency Deviations and tie line power deviation for load change in the area-2 in presence of DR	39
Table 3.7.	Tuned controller parameters and settling time of frequency deviations and tie line power deviation for load changes in the area-1 and area-2 simultaneously in absence of DR.	39
Table 3.8.	Controller parameters and settling time of frequency Deviations and tie line power deviation for load change in both the areas in presence of DR.	40
Table 3.9.	Optimal controller gains and corresponding settling times for 1% SLP in the area-1 without DR.	41
Table 3.10.	Optimal controller gains and corresponding settling times for 1% SLP in the area-1 with the aid of DR.	41
Table 3.11.	Optimal controller gains and corresponding settling times for 1% SLP in the area-2 without DR.	41
Table 3.12.	Optimal controller gains and corresponding settling times for 1% SLP in the area-2 with the aid of DR.	42
Table 3.13.	Comparison of various performance indices with and without DR in ALFC.	42

Table 4.1.	Comparison of performance indices and MDR with different controllers in LFC by considering 20% frequency support from DFIG.	67
Table 4.2.	Best compromised output with lead compensator DR in ALFC for 1% load variation in area-1.	68
Table 4.3.	Comparison of several performance indices and maximum overshoot with tuned controller gain.	71
Table 4.4.	Comparison of performance indices and MDR with and without different DR controllers in LFC of a Hydrothermal inter connected power system.	74
Table 4.5.	Comparison of several performance indices and maximum overshoot with tuned controller gain.	75
Table 5.1.	Comparison of different performance indices with and without BESS/DR in ALFC with inertia controller in wind.	98
Table 5.2.	Eigenvalue representation with different controllers.	108
Table 5.3.	System performance indices and MDR with variation in system parameters.	109
Table 6.1.	Microgrid parameter values [68].	113
Table 6.2.	Observation of different performance indices for system parameter variations.	128
Table 6.3.	Comparison of performance index with different controllers for ALFC.	132

CHAPTER 1

INTRODUCTION

1.1. General Introduction

Demand side management (DSM) is a demand-control approach used by electric utilities to encourage customers to change their electricity usage patterns and levels. DSM is a strategy-based tool designed to control demand from electricity utilities by encouraging the consumers through a suitable payment structure. Through this program, consumers change their level and pattern of electricity usage according to the requirement of the power system. The electricity customers, electric utilities and grid operators receive a variety of financial and operational benefits from DSM. The introduction of DSM in power system is beneficial for environment in terms of lower emission as it reduces the requirement of additional fossil fuel units in the power system. Hence, it is also said that DSM saves the earth's limited resources and lower the cost of energy. There are mainly three types of DSM programs or techniques such as: i) energy efficiency ii) demand response (DR) and iii) strategic load growth.

DR is the most advantage on among all DSM techniques as it directly affects the load or demand. Any techniques to reduce or shift demand are included in demand response (DR) technique category. Demand response programs not only help to defer high supply costs by reducing peak consumption, but they also help to change the net load structure (which is the total load minus wind and solar power generation) while integrating renewable energy sources. DR refers to all changes made to a utility customer's electricity consumption patterns with the intent of altering the timing, total power consumption, or intensity of spontaneous demand. DR techniques include a variety of activities taken by the client at the electric meter during high charges or network congestion during peak periods. So, DR programs are becoming a more attractive resource alternative in the electric power market, as grid modernization activities expand their capabilities and potential. These programs also have the potential to save money for electricity providers by reducing peak demand and deferring the development of new power plants and power distribution networks, particularly those used during peak periods.

Generally, Demand Response techniques are of two types such as: 1. Price based DR and 2. Incentive based DR. Each DR type has some scheme to execute the technique. Incentive based DR

program gives emphasize on maximizing the benefits of retailer by involving the utility and elasticity of consumers. This technique is generally used to curtail load from demand side. In this technique of DR program, customers who participate in demand adjustment during scheduled or unscheduled system disruptions receive rate savings or bill credits. Customers who agree to follow the contract but do not reduce their consumption during the outage hours will be punished according to the terms of contact. Large industrial loads are the target consumers for this type of incentive DR projects.

To demonstrate the idea of Demand Response, a supply and demand curve is presented in Fig. 1.1. Since most customers are not directly affected by changes in spot prices, their short-term demand is idealized as a vertical line with no elasticity, representing the fact that most consumers are not responsive to spot pricing. A reduction in quantity demanded, from Q' to Q'' , is how load curtailment is represented in Fig. 1.1. This reduction of demand indicates how the price decreases from P' to P'' . Fig. 1.1, implies that a small reduction in demand will result in a big reduction in generation cost and, in turn, a reduction in electricity price. Demand response is studied using demand-price elasticity.

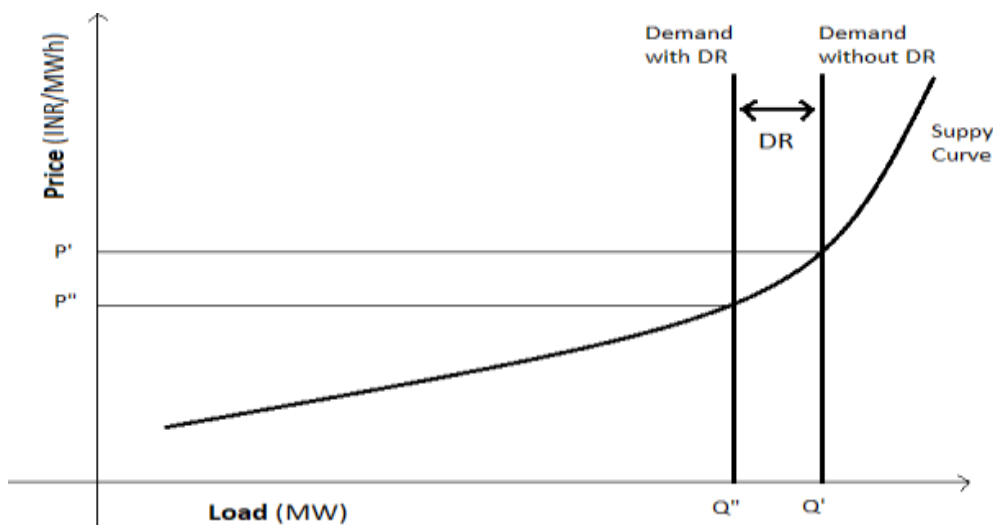


Fig. 1.1. A conceptual representation of Demand response considering Inelastic Demand.

Over the last few decades, the electricity consumption is increased tremendously. This increase in demand ultimately exerts severe stress on the balance between supply and demand. Supply of and demand for electricity in a power system must be maintained in balance in real time. Grid conditions can change significantly from day-to-day and even within moments. Mismatches in supply and demand arising from uncertainties in grid conditions can pressurize the integrity of the grid over very large areas within seconds. Such challenges posed by these

uncertainties make demand side management extremely important. Grid operators like independent system operators (ISOs), regional transmission organizations (RTOs) or utilities can use DSM to curtail or shift loads instead of, increasing generation as traditionally followed. Hence DSM can be incorporated in the load frequency control (LFC) for better dynamic performance in cost effective way.

In recent years, battery energy storage system (BESS) is found to be a promising device for different applications for power system such as load leveling, peak shaving, spinning reserve, uninterruptible power supply (UPS), voltage sag correction, area regulation, flicker compensation etc. The main characteristic of BESS is its static nature which enables the system to give quick dynamic response compared to the generators in the load frequency control problem for sudden load change. So, BESS is very effective for frequency regulation application in power system. The BESS contributes power to the grid when demand exceed supply and it absorbs the power from grid when demand falls below the supply during frequency regulation process.

As both DSM and BESS are promising tools for load frequency control problem, their effect in frequency regulation of power system is investigated in presence of renewable energy sources in various power system from different perspectives.

1.2. Literature Survey

1.2.1. Frequency Regulation

Over the last few years, it is being observed that the electricity demand is changing more hastily and unpredictably, causing frequent and abrupt mismatch between supply and demand. This mismatch power between supply and demand ultimately causes frequency fluctuation. ALFC problem is one of the most vital issues of power system operation. The key reason of power system blackout is mismatch power between generation and demand. Maintaining balance between generation and load together with system losses is essential for maintaining the frequency in a power system [1,2]. This important issue in power system can be resolved by frequency regulation. The frequency regulation can be achieved by balancing supply and demand including system losses [3]. Moreover, ALFC is the pivotal feature of the power system to maintain frequency and the tie-line power flow at the specific scheduled levels irrespective of load change [1-2]. In conventional method of frequency control, ALFC carries the sole responsibility of maintaining the balance.

Traditionally frequency regulation is achieved by balancing generation and demand through load following [4-8]. All types of generations present in an interconnected power system are not suitable for automatic generation control (AGC). For example, nuclear power generator provides maximum output which is considered as base load and therefore, do not participate in automatic generation control (AGC). Similarly, gas turbine plant operates during peak demands only and has very poor significant role in AGC. So, either thermal or hydro unit is the natural choice of generation for AGC in any power system. Even though thermal power generations are the most widely used resource around the world, still they have several drawbacks such as burning fossil fuel releases harmful emissions into the atmosphere and at the same time it consumes Earth's limited resources. Hence it can be said that conventional power generations not only affect environment but also increase the cost of generation dramatically because of extra transportation cost [9]. Because of various technical, economic, social and environmental factors, in many cases it is not viable and desirable now a days to augment traditional fossil-based generation [10].

The frequency regulation performance for a hydro-power system also analyzed in this thesis. Hydro system has two types of governors i.e., (1) Mechanical (2) Electrical. Electrical governor is helpful in comparison to mechanical governor for better dynamic performance of the power system [11,12]. Literature survey shows significant research on AGC for interconnected thermal system, but a few has been reported for interconnected hydrothermal power system [13]. The traditional power system has mechanical governor and modern hydro power systems are designed with electric governor [14]. Researchers have found that electric governor is better for frequency regulation in comparison to mechanical governor [11,12,15]. Extensive research work is available on automatic demand and frequency regulation for interconnected power system consisting of both hydro and thermal generation along with spinning and non-spinning reserve.

In order to prevent the global warming, the renewable energy resources (RES) have been integrated in present day power system. Researchers have considered presence of distributed generations (DGs) comprising of RES in ALFC problem [12,16]. This thesis analyses the frequency regulation performance of RES integrated power system. The analysis proceeds with the introduction of RES in interconnected power system and microgrid (MG). Renewable energy-based generation provides more cost effective and environment friendly options. Though renewable energy sources are good choice for restructuring of modern power

system but their intermittency in nature makes operation and control of the system more challenging. These sources are highly volatile and depend on atmospheric and climate condition which might cause unavailability at the time of demand in the power system.

Though RES have many advantages, it causes some problems like fluctuation in their output power due to uncertainties of weather conditions [17]. This causes system frequency fluctuation and ultimately affects the dynamic performance of the system. Also, because of this nature of the renewable sources, high penetration of these sources in the system is making the ALFC problem more complex day by day. Hence only integration of RES is not the solution for blackout of power system.

RES like wind energy source is the most suitable energy generation to overcome the load fluctuation in modern power system in the next decades [18,19]. Power system faces many instability issues due to uncertainties in integrated RES. Wind integrated power system also faces some inertia issues due to introduction of power electronic devices in the grid connected wind generators [12,20,21]. While the PI-controller of DFIG mainly provides fast recovery of the turbine speed during transient period, the PD controller is more sensitive for providing inertia support for frequency regulation [20,22]. Due to this PD controller of DFIG is of main interest when load frequency control is concern.

The ALFC problem turn out to be intricate for isolated micro grid (MG) due to the amassed use of RES and its isolation nature from main grid in the power system [23]. The main issues with the renewable energy integrated isolated MG are its low inertia. Moreover, when the microgrid is connected to the main grid through tie line, it follows the frequency of the main grid. In that case it is needed to take care of magnitude and quality of voltage and power only and it is not required to bother about the frequency. However, when the micro grid is separated from the main grid in the event of failure in main grid or when there is maintenance schedule in the main grid, the MG become autonomous and it needs to take care of frequency along with the magnitude and quality of voltage and power. If it fails to regulate the power supply characteristics, it loses stability and consumers will have to suffer from power supply discontinuity.

The renewable energy sources such as solar and wind are generally considered as RESs in the power system. This thesis has given more emphasis on wind contribution in case of interconnected power system for frequency regulation. Moreover, both wind and solar power

contribution are analysed when the frequency regulation performance tested for isolated microgrid as it mainly depends on RES.

To overcome the load frequency control problem, many controllers have been proposed for interconnected conventional power system in literature. In [24-26], researchers use different control techniques to improve ALFC problem of inter-connected conventional power system. In [24], the load frequency control problem of two-area thermal power system is solved by using a non-dominated sorting genetic algorithm-II (NSGA-II) technique. The efficient optimization technique NSGA-II is used in the above work to tune the proportional integral derivative (PID) controller placed in the secondary control loop of ALFC of two-area power system. The load frequency control problem of a hydrothermal two-area power system is solved through optimal control strategy by using a new performance index that avoids the need for a load demand estimator in [25]. In [26], the ALFC problem is solved by setting suitable hydro-governor parameters and integral controller gain of secondary control loop using a suitable algorithm for a two-area hydrothermal power system.

In recent literature the frequency regulation study further looks forward for RES integrated power system. In [12,21,22,27], the renewable energy source like wind energy system is integrated in two-area thermal system and analyze the frequency control concerns for betterment of frequency regulation. In each of the above-mentioned work doubly fed induction generator (DFIG) is used from the wind energy source and researchers proposed some modified inertia control scheme in DFIG that uses frequency deviation from the system to provide fast active power injection that arrests the fall in frequency during transient conditions and improves system dynamics. Again in [20], researchers given emphasis on inertia issue from wind and proposed an inertia controller in the wind generator. The proposed inertia controller enhances frequency regulation by considering an additional power reference signal. Additionally, this inertia controller of DFIG allows a fraction of the kinetic energy stored in rotational masses to be released in order to provide earlier frequency support at the time of load fluctuation. Similarly, the various impact and issues regarding the integration of wind in modern power system that represent the security of the power system, power quality and the power system stability are presented in [28]. This study reveals that at low wind penetration level, the impacts of inertia issues is minimal but inertia impact on power system increases with increase in wind penetration. The work in [29], proposes an additional dynamic demand control strategy in coordination with DFIG controller to provide adequate inertial response with guaranteed rotor security. This proposed controller from wind generator side mitigates the

potential of the secondary frequency dip and improves the performance of primary frequency control. In [30], a wide-area synthetic inertia control strategy is designed in DFIG to avoid inertia issues from wind integrated power system and finally the proposed controller in DFIG could able to improve primary frequency control. In [31], the inertia control based DFIG controller in a two-area hydrothermal power system is applied for better frequency regulation. A multi-objective optimization technique is used to find the best values of inertia control parameters of DFIG and automatic generation control (AGC) parameters of power system for smooth frequency control.

In [32],[33] researchers have emphasized on the gain scheduling of conventional proportional integral (PI) controller by the help of fuzzy logic control in ALFC to improve the frequency control problem of microgrid. In [32], the instability issue due to high level of penetration of RES is reduced by the application of optimal coordination control strategy between diesel engine generators (DEGs) and superconducting magnetic energy storage (SMES) system for MG frequency control. This coordination strategy is controlled by the fuzzy logic-based PI controller. In [33], a novel mixed algorithm based on grey wolf optimizer and cuckoo search is implemented for optimal tuning of fuzzy PI controller gains for smoothing the frequency fluctuation in an autonomous microgrid due to highly intermittent energy from RES and load fluctuation.

1.2.2. Demand Side Management

Demand side management (DSM) is a paragon of decision situation from demand side. In this regard, DSM may be incorporated in modern power system to get better frequency regulation in cost effective way. Demand side management (DSM) manages the load from demand side through a well-designed program. The DSM program modifies power demand by providing some benefits to customer [34-36]. Demand side management is indispensable in modern power system for low carbon future. It has the ability to control and manipulate load from demand side to turn them on/off or change their consumption pattern according to the grid condition by taking into consideration of technical and economical constraints [37]. DSM can control and manage the sudden change in load demand through a program by educating consumer and can provide considerable economical and reliable power system [38]. DSM has various technique to manage energy or load from demand side. Demand response (DR) is one technique of DSM. DR involves a short-term load manipulation program to influence load consumption pattern by the consumer through incentive payment design when the system is at off nominal condition [37]. DR provides an additional opportunity for balancing the generation

and demand from demand side by dropping or shifting consumers' electricity usage. Demand response was first introduced in 1980 to offer better reliability and security compare to traditional control system in terms of balancing generation and load [39]. DR is the change in load/demand with respect to change in price from demand side. It has many applications and one of them is managing demand-supply balance. DR manages the supply-demand in an automated load frequency control (ALFC) loop in cost effective way. Hence it is very much important to explore the dynamic response of modern power system including demand side management (DSM). In most of the previous research work, the impact of DSM is explored for conventional power system. Demand response is introduced in conventional LFC to check the effectiveness of DSM/DR for frequency regulation of one area power system [17]. Moreover, recent studies prove that DR is a suitable choice for economic way of frequency regulation [40,41].

The collaboration of DR in ALFC increases the stability margin of the system and improves the system dynamic [17]. DR can act in conjunction with the conventional ALFC in a coordinated manner to enhance the frequency control mechanism of the system. DR participate in the frequency regulation process by sending switching signals to the controllable loads from demand side. Though DR is beneficial for frequency regulation but it cannot provide frequency control at required speed because of communication delay in the DR process arising from demand side [42,43]. This delay produces phase lag between input and output of the DR loop due to which switching on or off of the load cannot take place fast enough for frequency regulation. This leads to overshoot, instability and oscillation in system dynamic performances [17,43]. The presence of current harmonics in any induction heating system also deteriorates the system stability [44]. Lead compensator is therefore required to be introduced in DR control loop to overcome these problems.

Applications of delay compensators for different power system issues can be found in the literature. In [45], an adaptive delay compensator (ADC) is used for robust wide area damping controller design of power system. Engagement of wide area measurement system (WAMS) is considered for mitigation of low- frequency inter- area oscillations caused by time delay [46]. Some works in the literature, designed the delay compensator like wide area measurement system (WAMS) in [47]. In [48,49]), conventional lead- lag compensator has been designed to compensate the phase lag produced at output of the control loop caused by remote signal delays, but none of these studies are related to DR loop in ALFC process.

However, it is observed from the above works that the presence of communication delay in control loop adversely affects the system performance and even leads to the system instability.

A few works have been reported on the influence of communication delay in DR control loop for frequency regulation. These have considered a constant delay in the DR loop. In [17], DR is introduced in LFC model for frequency regulation. In this study more emphasis has been given to the design of DR control loop in traditional LFC but no compensation for the delay in the DR loop is considered. This study is also limited to the application of DR in LFC for single area power system. In [50], fuzzy based DR is incorporated in LFC for frequency regulation in a multiarea power system but delay issues in DR is not compensated separately by using any compensator. In [51], delay issues in DR control loop have been overcome by an ADC for a single area power system.

1.2.3. Battery Management for Frequency Regulation

Battery energy storage system (BESS) are often used as power support in case of unavailability of renewable energy sources. The application of BESS in ALFC problem shows greater improvement in system dynamics because of its very fast dynamic response [52]. Specific control strategy for BESS is developed in [53,54,55] for frequency regulation. In [56], battery capacity is optimized in order to achieve highest expected profitability of the device while participating in frequency regulation. So, searching out a suitable strategy for taking care of battery life while participating of BESS in ALFC of power system is a promising research area in power system operation and control.

The RES alone is not capable to solve ALFC problem due to its inconsistency power supply nature. The static characteristic of battery energy storage system (BESS) enables it to participate in frequency control process of any power system compare to other generator in the power system for quick dynamic response in the frequency control process. So, BESS is a suitable choice to smooth out power balance between generation and demand in a RES introduced low inertia isolated MG [57]. But battery has also some limits to support power to some extent as it needs a regulated charging and discharging operation to maintain good battery life [58]. So, researchers have studied the BESS for frequency regulation in isolated MG in different prospective. In [59], the frequency regulation is achieved by the application of μ -synthesis based dc link voltage regulator in BESS for MG. Researchers discussed the use of BESS in coordination with wind farms for ancillary services[60]. Literature verifies that some arrangements must be done along with BESS or within BESS model for smooth frequency regulation and provide better battery life. Hence, in order to guarantee the service continuity of

BESS for frequency regulation in isolated MG, some state of charge (SOC) strategy must be implemented in BESS.

In the few works in literature, BESS and DR are individually applied for frequency regulation and both found promising for the purpose. It is now essential to check the frequency regulation performance when DR and BESS are participated in ALFC in coordinated manner. Participation of BESS in ALFC may deteriorate battery life at the time of high load change. So, special preventive measure should be developed in addition with battery participation for frequency regulation. In [61], a special incremental battery model is used to improve the performance of ALFC for conventional power system but researchers did not emphasize on battery SOC for load following which is very important for saving battery life.

1.2.4. Model Predictive Controller (MPC)

Model predictive controller (MPC) provides online optimization scheme to control the load frequency control problem. The MPC modelling for power system control specially depends on states space equations of the power system [62]. Researchers have designed the requisite MPC for different power system to solve the control issues accompanied with various type of generation in the power system [63]-[65]. Moreover, the performance of MPC application can be improved by tuning its parameters with different evolutionary algorithms that associated with the cost function of MPC online optimization [66],[67]. The recent research findings discovered that the MPC tuning parameters associated with cost function of MPC is fuzzified with fuzzy logic controller for smooth frequency regulation of power system [68]. Furthermore, bat inspired algorithm in [69] and particle swarm optimization (PSO) in [70] are applied to tune the MPC tuning parameters for its online optimization scheme to solve ALFC problem.

Moreover, introduction of another state-of-the-art technology like DR in the ALFC function for frequency regulation has made the control further complex. So, restructuring of modern power system must include ALFC with DR to get enhanced frequency regulation in cost effective way.

So, the futuristic power system is now bound to introduce more sophisticated and robust controllers to face various challenges like uncertainties and inertia issues from renewable energy sources, sudden unpredicted load variation, communication issues from demand side load management while participating in ALFC. So, choosing a most robust controller for ALFC

is a challenging task for modern power system. In recent literature, some of the rigorous control techniques such as fuzzy logic control (FLC) [71], μ -synthesis scheme [72], H_∞ and μ -synthesis approach [73], FLC with PSO algorithm implementation [74], sliding mode control (SMC) [75] are used for ALFC.

Apart from the above-mentioned controllers, the model predictive controller (MPC) is one of the highly recognized and widely used controllers to solve ALFC problem of modern power systems. The MPC predicts the system trajectories by using state-space model of the given system [76]. The MPC becomes a suitable candidate to the control complex systems due to its online optimization scheme that is capable to treat the system constraints at each sampling time. The current state of the art of implementation of MPC for ALFC problem in power system is worked out with different configuration of power system like wind turbine included conventional power system [77], hybrid power sources [78], multi-area power system [79,80], micro grid [68,81,82], battery integrated power system [83,84,85] etc. In [77], ALFC problem has been solved for a wind integrated multi-area power system by employing a MPC that designed by concerning all the wind turbine parameters along with the system parameters. A MPC is designed for a simplified Nordic power system for load frequency control problem [78]. To enhance the ALFC performance a distributed MPC scheme with discrete-time Laguerre functions is incorporated in multi-area power systems [79]. In [80], MPC is designed for frequency control of an electric vehicles and inertia control-based wind generator integrated isolated three area power system. A fuzzy based parameter driven MPC is designed for ALFC problem of an isolated micro grid [68]. A PSO optimized MPC is used to regulate the frequency of an isolated power system [81]. MPC-based control framework in ALFC is developed for the secondary control of microgrid by considering cyber-attack from different communication issues in microgrid [82]. In [83], a MPC frame work is developed to simultaneously optimize frequency regulation market participation while mitigating capacity diminishing problem using high-fidelity battery models. Furthermore, a two-layer MPC in ALFC is designed by considering the battery constraint in a battery included power system where BESS participate for frequency regulation task by maintaining SOC level [84]. In [85], a novel adaptive intelligent model predictive control (AIMPC) scheme is developed in ALFC to stabilize the frequency of microgrid by considering the SOC control of the battery of electric vehicles. From reported study, it is found that the application of MPC is limited to the power system of limited power sources. As MPC is a robust control method, it must be applied in ALFC of the modern

power system having renewable energy resources and other modern techniques like DR in it.

Now the recent trends of MPC application for load frequency control solution, the studies emphasize on operational life of battery and to improve system reliability in long run [84,85]. A SOC based BESS model is used for frequency regulation of an interconnected power system [86]. Moreover, in [87,88], the performance of DR and BESS allied in ALFC of a microgrid is analysed and found suitable for the system performances. In [87] an intelligent share-based controller is proposed among DR, BESS and supplementary control of ALFC for better frequency regulation, but in this work battery operational life is not considered for frequency regulation. A SOC strategy-based BESS participation in ALFC in co-ordination with DR is considered for frequency regulation [89]. But the above work neither applied for interconnected power system nor the battery used as a special full order converter included incremental BESS model. Moreover, the above works are analysed only with a PI/PID based controller in ALFC of power system having only thermal power system and not included renewable energy sources. Similarly, the performance of MPC in ALFC is examined in presence of BESS and renewable energy sources (RES) in ALFC for power system [84,85]. However, the performance of MPC is not analysed in presence of BESS, DR and RES control. Earlier in the literature, researchers have given more attention to the inertia issues due to participation of wind energy sources in the conventional power system with conventional PI/PID controller in ALFC. Those issues have been overcome by the application of different controller in the wind generator [22,12] in co-ordination with integral controller in ALFC which makes the system more complicated.

By keeping in mind of current state of art of frequency regulation and its limitation, the thesis has decided to proceed with the introduction of DSM/DR and BESS in ALFC of different type of power system and analyse frequency regulation performances. Moreover, a sophisticated controller is required to implement in ALFC as the introduction of DR makes the system more complicated due to communication effect. Additionally, BESS should be designed with a suitable SOC controller in it by keeping the maximum and minimum value of SOC for power delivery from battery for frequency regulation.

1.3. Objectives of the Thesis

The objective of the thesis has been set according to the gap in the literature for smooth frequency regulation of power system.

1. To introduce DR in ALFC of a wind integrated two-area thermal power system for checking the role of DSM in ALFC.
2. To study the role of DSM/DR on dynamic response of a hydrothermal system.
3. To design the DR control loop to compensate the delay issues in DR for smooth frequency control in an inter-connected power system.
4. To implement a new SOC based strategy for the incremental BESS model in co-ordination with DR in ALFC of each area of a wind integrated two- area thermal power system for smooth frequency regulation.
5. To propose a new state space based MPC concerning all the variables in the incremental BESS model.
6. To analyse specially the proposed MPC based ALFC for inertia issues from wind in absence of separate inertia controller in wind generator.
7. To examine the saving of battery life when DR is presented in the proposed MPC based ALFC.
8. To compare the MPC based ALFC with a robust PSO optimized integral controller based ALFC in co-ordination with PD controller from wind for inertia issues to confirm the effectiveness of the proposed MPC controller for the studied power system.
9. To implement the delay compensator in DR loop in the isolated MG.
10. To formulate MPC for the studied isolated MG.
11. To tune the input parameter R_w associated with cost function of MPC in collaboration with PI controller gain parameters in delay compensator in DR by PSO.
12. To verify the frequency control scheme having simple BESS with a strategy-based SOC controller in BESS.
13. To validate the proposed PSO tuned MPC in collaboration with lead compensator-based DR and BESS for frequency control in the studied isolated MG through OPAL-RT OP5600 with RT lab version of 19.3.0.228.

1.4. Contributions of the Thesis

The thirteen objectives mentioned in the above section is fulfilled in the thesis by the five different contributions of the thesis. The contribution of the thesis is summarised as below:

1. The ALFC model of a two- area power system has been developed to check the role of DSM in ALFC of power system. Each area consists of a thermal unit and a WECS. Then DR is introduced in the system and the performance of the ALFC system in terms of frequency regulation is observed and analyzed.
2. Further the role of DSM is investigated for hydrothermal power system. This investigation is done to check the role of DSM/DR in different situation in power system. Due to high inertia property of hydro energy system, any sudden change in load does not affect the system turbine immediately. For this phenomenon, hydro generating turbine is superior to steam turbine for frequency regulation due to load change. Hence this paper attempts to study the role of DSM/DR on dynamic response of a hydrothermal system.
3. An attempt has been taken to design the DR control loop to compensate the delay issues for smooth frequency control in an inter-connected power system. A new lead compensator is proposed in this work for mitigation of the delay problem in DR loop. The compensator consists of a washout filter, a lead compensator followed by a PI controller. All the parameters of the ALFC controller including the DR loop and also the PD controller of DFIG are tuned by using PSO. The performance of the proposed delay compensator in DR loop is examined by considering two different two-area power system, a wind integrated two-area thermal system and a two-area hydrothermal power system.
4. A new SOC based strategy has been implemented for the incremental BESS model in co-ordination with DR in ALFC of each area of a wind integrated two-area thermal power system for smooth frequency regulation. It has proposed a new state space model for MPC concerning all the variables in the incremental BESS model. The proposed MPC based ALFC is analyzed specially for inertia issues from wind in absence of separate inertia controller in wind generator. The saving of battery life is examined when DR is present in the proposed MPC based ALFC. Finally, the MPC based ALFC is compared with a robust PSO optimized integral controller based ALFC in co-ordination with PD controller for inertia

issues to confirm the effectiveness of the proposed MPC controller for the studied power system.

5. The delay compensator in DR loop in the isolated MG is implemented. The MPC formulation for the studied isolated MG is developed. The tuning of the input parameter associated with cost function of MPC in collaboration with PI controller gain parameters in delay compensator in DR is done by using particle swarm optimization (PSO). The verification of the proposed frequency control with a strategy-based SOC in BESS is done through OPAL-RT OP5600 with RT lab version of 19.3.0.228.

1.5. Organization of the Thesis

This thesis is organised in seven chapters as follows:

Chapter 1

This chapter presents a brief introduction to the problems of frequency regulation, application of DSM and BESS for frequency regulation of power system. The literature survey is carried out on frequency regulation, demand side management, battery management for frequency regulation and model predictive controller application for load frequency control problem. The limitation of the existing methods identified through the survey have been the driving force to set the objectives of the research. The contribution of the research is also highlighted.

Chapter 2

The different modelling of power system is described in this chapter. The modelling creates a computer model of the power grid including all its components and their features to perform the study easily. The different models considered are conventional and renewable generation units, battery storage unit and different modern technological equipment for power system control. These components have impedances, time constants, gains, power ratings, capacities, start-up time etc, which all are need to be input into the computer model for simulation study. In view of the above information, this research uses different components of power system for frequency regulation analysis.

Chapter 3

This chapter introduces DR in ALFC of two-area power system. The two-area power system in which DSM/ DR introduced in ALFC to investigate the role of DSM/DR for

frequency regulation are 1) Wind integrated two-area thermal power system, 2) Hydrothermal two-area power system. The frequency regulation performance with introduction of DSM/DR in ALFC of above-mentioned test system is observed and analyzed. The introduction of DR is found to be promising for load frequency control problem.

Chapter 4

A new lead compensator is proposed in this chapter for mitigation of the delay problem in DR loop. The compensator consists of a washout filter, a lead compensator followed by a PI controller. All the parameters of the ALFC controller including the DR loop and also the PD controller of DFIG are tuned by using PSO to get overall smooth frequency regulation.

Chapter 5

The chapter has taken a challenge to design a MPC for ALFC of two-area, wind integrated thermal power system equipped with BESS and DR for frequency regulation task. Primarily, the incremental BESS model employs a new state of charge (SOC) based strategy to regulate the power from battery for saving battery life. Then DR, along with the SOC based BESS, is employed in ALFC for frequency regulation. A modified state space model of MPC incorporating all BESS variables is developed and employed in ALFC of the studied power system. The performance of the designed MPC is examined for inertia issues arising from wind in the conventional two-area power system. Furthermore, the capability of BESS for frequency regulation and effect on the life of BESS with the proposed control strategy is measured through MPC based ALFC and results compared with system performance when integral controller in ALFC and inertia controller from wind are present. In addition to DR and BESS in ALFC, double fed induction generator (DFIG) based proportional derivative (PD) inertia controller also contributes in the power system for frequency support from wind energy section to avoid inertia issues. So, all the controllers of the test power system such as integral controller in ALFC and PD controller in wind are tuned concurrently for smooth frequency control. However, performance of MPC is tested for smooth frequency regulation by tuning PD controller gain of wind only while keeping MPC gain parameters as available in literature. particle swarm optimization (PSO) is used to tune the integral controller gain of ALFC for the studied power system to compare the results with MPC based ALFC.

Chapter 6

This chapter proposes a PSO based MPC for ALFC of microgrid. The generalized state space analysis is considered to model the MPC including all controllable and uncontrollable

generation units. The proposed MPC is used in the MG for frequency regulation as a single input multi-output system. The MPC is considered as parameter driven controller whose input parameter R_w is tuned with widely used robust PSO technique to get better frequency control. Moreover, the proposed MPC is collaborated with DR which has been accompanied by a proportional integral (PI) controller with lead compensator-based delay compensator to avoid the delay issue persist in DR. So, the input parameter R_w of MPC for its online optimization and PI controller gain parameters of DR are tuned by minimizing the performance index like integral time square error (ITSE) to get smooth frequency regulation for an isolated MG. To evaluate the effectiveness of the proposed scheme of frequency regulation, an isolated MG equipped with conventional diesel unit, fuel cell, wind energy, solar energy, battery cell is taken as test system. The effectiveness of the proposed scheme for frequency control is evaluated and compared with a robust fuzzy adaptive MPC. Finally, the results prove the efficacy of the proposed scheme through various case studies. In view of practical validation, the proposed frequency control scheme for the studied isolated MG is realized in real time through OPAL-RT OP5600 with RT lab version of 19.3.0.228.

CHAPTER 2

TEST MODELS FOR THE STUDY

2.1. Introduction

Modelling of power system is an important task for the analysis of power system for any given purpose. The modelling creates a computer model of the power grid including all its components and their features to perform the study. The different components that are modeled include conventional and renewable generation units, battery storage unit and different modern equipment's for power system control. These components have impedances, time constants, gains, power ratings, capacities, start -up time etc, all of which are to be inputted into the computer model for simulation study. In view of the above information, this research uses different components of power system for frequency regulation analysis. The most common components/test models commonly used in different parts of this research work are as follows:

1. Model of Hydro-Electric Governing System
2. Model of DFIG based Wind generator
3. Model of DR for ALFC
4. Model of BESS

2.2. Modelling of Hydro-Electric Governing System

The hydraulic governor is mainly used to control the speed and load for a hydraulic unit. The output characteristics of the hydro turbine depends on the amount of the water fed to the turbine. In hydro turbine, the change in turbine output power ΔP_m and change in gate opening (ΔG) are mathematically related as [11]:

$$\frac{\Delta P_m}{\Delta G} = \frac{1 - sT_w}{1 + 0.5sT_w} \quad (2.1)$$

Where, T_w is the starting time of water required by a head to speed up the flow of water in the penstock. Electric governor is more beneficial in regards to dead bands and time lags as

compared to mechanical governor. So, in the present study, electric governor is modelled in the Hydro-power system. The adjustment in dynamic behavior of electric governor should be similar to those of mechanical hydraulic governor [11,12]. Three tuned controllers with proportional-integral-derivatives (PID) action are provided with the electro hydraulic governor which is shown in Fig. 2.1 [12].

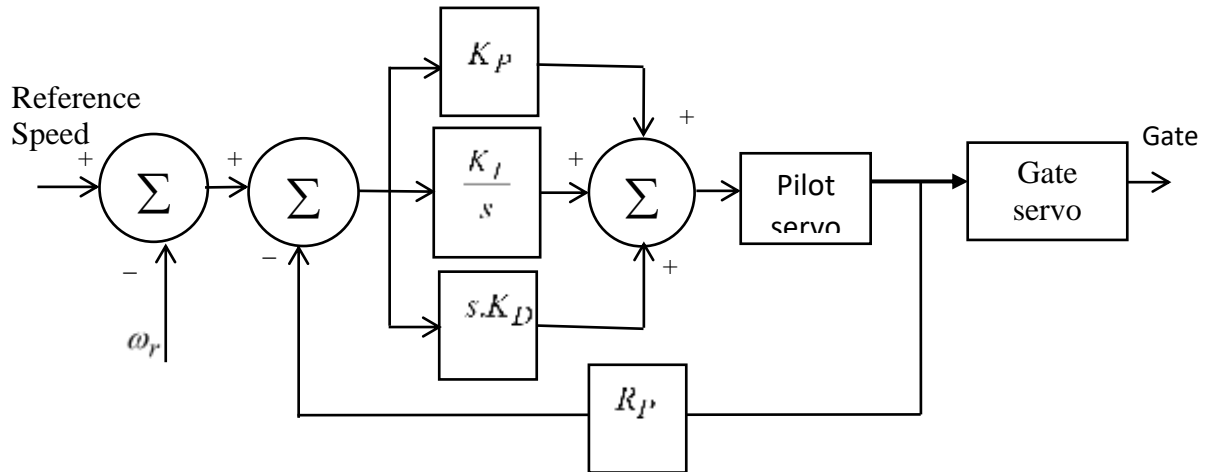


Fig. 2.1. Electro-hydraulic governors with PID action.

In the Fig.2.1, K_P =proportional gain, K_I =integral gain, K_D =derivative gain, R_P = Hydraulic governor permanent droop. Hydraulic governor has a relatively large temporary droop and long wash out time. As a result, the hydro system is sluggish in nature as compare to thermal system. Hence any abrupt change in load/generation does not affect the system instantly. Hydro system has inertia constant, self-regulation (or load damping), governor speed droop as similar to thermal system. In addition to that, it specifies a temporary (or transient) droop, washout time constant of the speed governor and higher inertia constant due to water. Therefore, the study has taken attempt to examine the frequency regulation performance of a hydro system cooperating with thermal power system as explained in chapter-3.

2.3. Modelling of DFIG based Wind generator

Generally, the Doubly Fed Induction Generator (DFIG) based wind energy conversion system (WECS) is used to utilize the maximum power available from the wind energy. It is an asynchronous generator. For the purpose of frequency regulation, DFIG based wind generator is able to participate in system frequency support while its speed remains decoupled from grid frequency. As the inertial response of DFIG based wind energy system and thermal system are different, an additional controller along with DFIG is required to restore the inertial response capability of the system. DFIG plays an important role in the dynamic performance analysis of the power system by keeping balance between change in tie line power and frequency [28-30].

20% frequency support from the DFIG based wind power resources is assumed to be integrated with thermal system for improvement of frequency regulation in presence of PD controller in it [12].

This section elaborates about the inertia control method of grid connected DFIG. The DFIG based wind turbine connected in the system is not capable to control the inertia effect automatically, as it is uncoupled from grid by the grid side converter. Therefore, additional controllers are used to make the DFIG capable to give further signal while providing the active power from the wind energy source for the frequency support. Fig. 2.2 shows the inertia control DFIG. The inertia control of DFIG provides an additional power signal ΔP^* to the nonconventional generator along with the reference power signal. This additional signal is expressed in (2.2) [12]. The nonconventional DFIG based wind generator system measures the frequency deviation by the transducer and passes it through a high pass washout filter to the additionally used inertia controller.

$$\Delta P^* = -K_{df} \frac{d\Delta f_0'}{dt} - K_{pf} \Delta f_0' \quad (2.2)$$

Where, K_{pf} and K_{df} are the control parameter of the frequency deviation and the gain parameter of the derivative of frequency deviation respectively. The value of these parameters affects the inertia of the system.

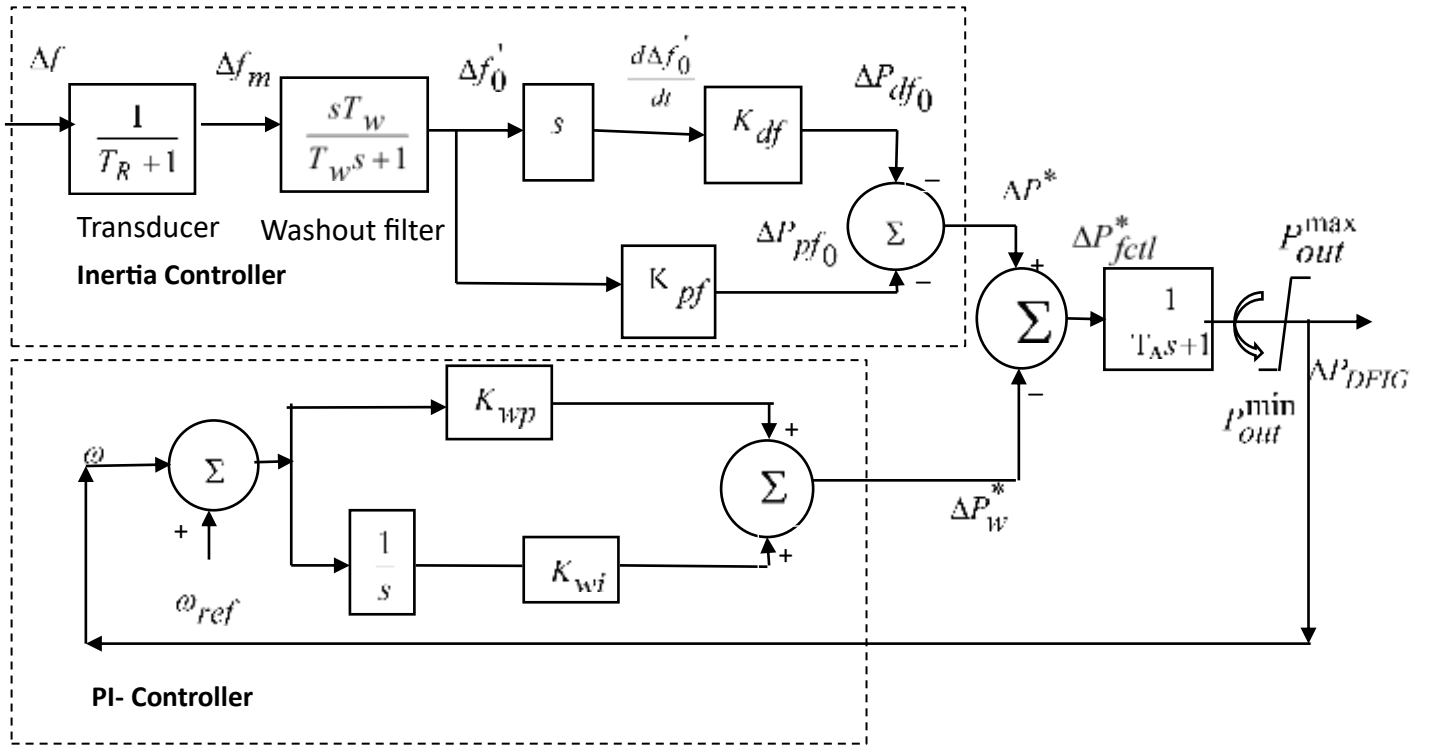


Fig. 2.2. Transfer function model of DFIG controller.

The PI controller present in the DFIG system helps fast speed recovery after the transient period is over. This controller is a low inertia controller whose parameters do not vary significantly for optimization [22]. The proportional gain constraint K_{wp} and integral gain constraint K_{wi} of PI- controller of DFIG are chosen from [22]. The reference power (ΔP_w^*) computed by the PI controller which takes the input as the speed variation ($\omega - \omega_{ref}$) as shown in Fig. 2.2 is expressed in equation (2.3) [21].

$$\Delta P_w^* = (\omega - \omega_{ref})K_{wp} + K_{wi} \int (\omega - \omega_{ref}) dt \quad (2.3)$$

So, the total controlled active power (ΔP_{fctl}^*) inserted to doubly fed induction generator can be written as follows [27]:

$$\Delta P_{fctl}^* = \Delta P^* - \Delta P_w^* \quad (2.4)$$

Where,

ΔP_{ctl}^* = Net change in controlled active power provided to non conventional generator,

ΔP^* = Change in controlled power provided by PD controller;

ΔP_w^* = Change in power provided by relatively slow PI controller

As the transient period ends within few seconds, the reference power signal from PI controller may be considered as constant and $\Delta P_w^* = 0$, hence the net output power injected from DFIG to either area of the power system may be expressed as [23]:

$$\Delta P_{DFIG_i} = \Delta P^* \quad (2.5)$$

2.4. DR Modelling for ALFC

A small reduction in demand will result in a big reduction in generation cost and, in turn, a reduction in electricity price [35]. Demand response is studied using demand-price elasticity. It introduces a negative slope on the original demand curve as shown in Fig. 2.3. The demand-price elasticity could be defined as the relative slope (α) of demand-price curve [35]. The mathematical expression of slope of DR is expressed as in (2.6). where Δd and $\Delta \rho$ are respective changes in demand and price; d_0 and ρ_0 are respectively the base demand and price of a given equilibrium point.

$$\alpha = \frac{\Delta d / d_0}{\Delta \rho / \rho_0} \quad (2.6)$$

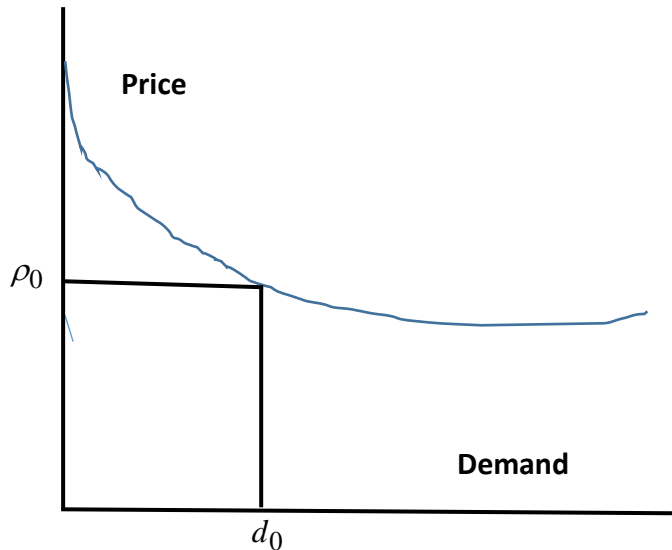


Fig. 2.3. Demand Price curve.

DR program for short term load manipulation by keeping in mind to influence energy consumption pattern. DR is defined as “the changes in electricity uses by end-users (consumers) from their normal consumption pattern in response to incentive payment designed to include lower electricity used at times of high whole sale prices or when system reliability is jeopardized” [90,91]. DR is the most advantageous among all DSM techniques as it affects directly the load or demand. Hence all DSM techniques are gradually being replaced by DR program in the new electricity market. It is important to know the pattern of DR in load frequency control to investigate the improvement of dynamic response of the power system. But with employment of DR in the secondary loop, the control effort can be split between two control loops based on their cost at real time electricity market. DR loop is included in the secondary loop of ALFC through a well-designed program based on slope of demand-price curve (α) mentioned in (2.6). The value of α is between 0 and 1. This concept of DR modelling is incorporated in different test model of power system for the purpose of getting better frequency response.

2.5. Modelling of BESS

Battery energy storage systems are the suitable choice for load frequency control problem, so different battery models are used for LFC problem. In this study an incremental model of lead acid battery connected with a converter is considered in a two-area wind integrated power system for frequency control problem. DR is also introduced in the ALFC in co-ordination with BESS. In this section only BESS modelling is elaborated. A new state of charge (SOC) strategy-based model is developed in the incremental BESS model for better battery life while providing smooth frequency regulation. This SOC strategy has been discussed in chapter-5.

In the present study, the battery storage power block includes a 12-pulse bridge converter along with star/delta-star power transformer, a control scheme and a parallel series connected cells. The whole arrangement of the BESS plant and the equivalent circuit of BESS are shown in Fig. 2.4 and Fig. 2.5 respectively [61].

In Fig. 2.5, E_{do} = 12 pulse converter ideal voltage [61], E_t = r.m.s voltage (line to neutral) and

$$A = \frac{6\sqrt{6}}{\pi} \text{ and } E_{do} = A.E_t$$

From Fig. 2.5 battery terminal voltage E_{bt} can be obtained as,

$$E_{bt} = E_{do} \cos \alpha - \frac{6}{\pi} X_{co} I_{BESS} \quad (2.7)$$

Where α is firing angle of converter, X_{co} = commutating reactance and I_{BESS} = d.c. current flowing into battery. The various parameters in the equivalent battery model are as follows [61],

R_{bt} = connecting resistance, R_{bs} = internal resistance, R_b = over voltage resistance, C_b = over voltage capacitance, C_{bp} = battery capacitance, E_{boc} = open circuit voltage of battery, R_{bp} = self-discharge resistance, E_b = battery over voltage

The I_{BESS} in the equivalent battery circuit is expressed as in (2.8).

$$I_{BESS} = \frac{E_{bt} - E_{boc} - E_b}{R_{bt} + R_{bs}} \quad (2.8)$$

The battery absorbs active power (P_{BESS}) and reactive power (Q_{BESS}) based on converter circuit analysis [61]. There are two control strategies for BESS i.e, (i) P-Q modulation and (ii) P-modulation. In ALFC study, only incremental real power is considered for analysis. Hence, in this study, real power absorbed by the battery is considered only for P-modulation calculation by keeping reactive power absorbed by battery as zero. Therefore, the active and reactive power absorb by battery considered for the study are expressed in (2.9) and (2.10) respectively.

$$P_{BESS} = A.E_t.I_{BESS} \cdot \cos \alpha^\bullet = (E_{do} \cos \alpha)I_{BESS} = E_{CO}.I_{BESS} \quad (2.9)$$

$$Q_{BESS} = 0 \quad (2.10)$$

Where $E_{co} = E_{do} \cos \alpha$ = dc voltage without overlap.

By linearizing equation (2.9), the incremental real power is expressed as in (2.11).

$$\Delta P_{BESS} = E_{co}^0 \Delta I_{BESS} + I_{BESS}^0 \Delta E_{co} \quad (2.11)$$

Constant current operating mode is most suitable procedure for load frequency control problem [20]. As we know, the frequency regulation is associated with two general term power deviation (between generation and demand) and system disturbance in the power system. So, in the current study the voltage ΔE_{co} , which is responsible for battery output power is assumed to be decompose into two parts as shown in (2.12).

$$\Delta E_{co} = \Delta E_{cof} + \Delta E_{cod} \quad (2.12)$$

Where, ΔE_{cof} = Voltage responsible to care power deviation and ΔE_{cod} = Voltage responsible to care system disturbance.

By combining (2.11) and (2.12), we get

$$\Delta P_{BESS} = E_{co}^0 \Delta I_{BESS} + I_{BESS}^0 \Delta E_{cof} + I_{BESS}^0 \Delta E_{cod} \quad (2.13)$$

According to our assumption of constant current operating mode, the 1st term of power in (2.13) may be neglected for frequency regulation problem. Also, 2nd term may be neglected as this term of power is associated with voltage ΔE_{cof} that not responsible for system disturbances. The third term of power deviation respond to the system disturbances [61]. hence this term is only considered as incremental power from BESS for the ALFC problem. Moreover, in the current study, battery is operating according to system disturbances only. Hence, summation of 1st and 2nd term of equation (2.13) are assumed to be zero for the present study which results in equation (2.14).

$$E_{co}^0 \Delta I_{BESS} + I_{BESS}^0 \Delta E_{cof} = 0 \quad (2.14)$$

So, we obtain

$$\Delta P_{BESS} = I_{BESS}^0 \Delta E_{cod} \quad (2.15) \text{ This}$$

damping signal ΔE_{cod} in (2.15) is considered as deviation from power system which analyses further for BESS participation for ALFC study. The damping signal ΔE_{cod} is mathematically expressed as in (2.16).

$$\Delta E_{cod} = \frac{K_{BESS}}{1 + ST_{BESS}} \Delta Signal \quad (2.16)$$

Where K_{BESS} and T_{BESS} are control loop gain and measurement device time constant respectively.

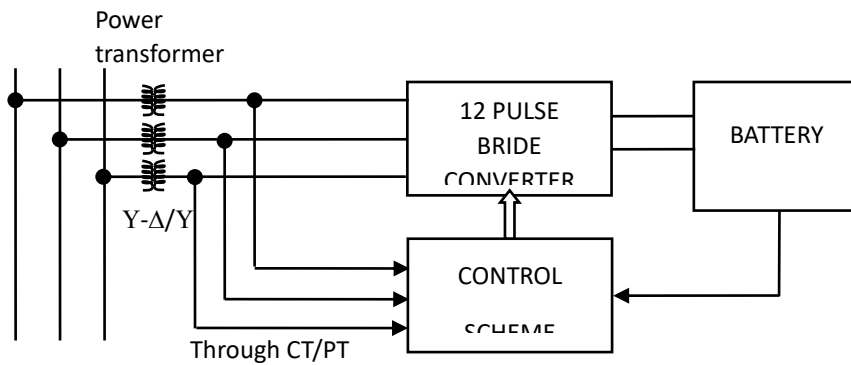


Fig. 2.4. Schematic description of a BESS plant.

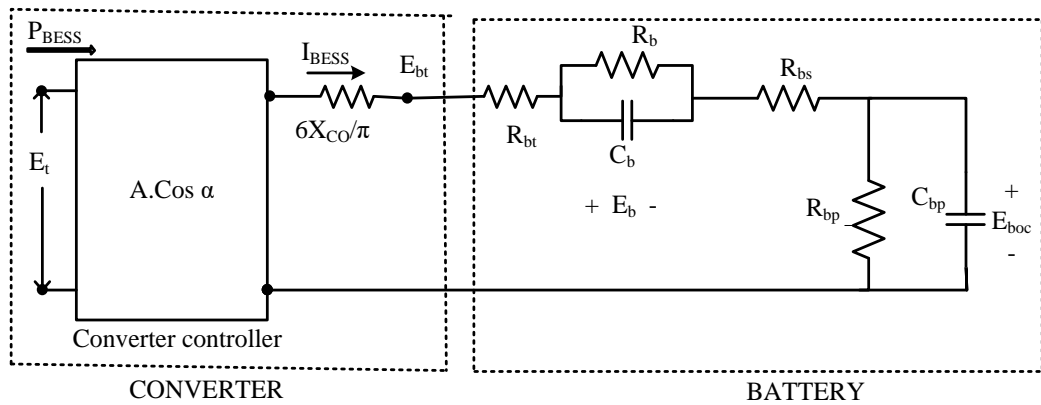


Fig. 2.5. Equivalent circuit of BESS.

The damping effect from the power system is injected to the control loop through the useful feedback signal in Fig. 2.6 as ΔSignal . So, the operation of battery output power ΔP_{BESS} directly depends on power system disturbances. The useful signal ΔSignal provides the system disturbance like frequency deviation /area control error signal to the control loop of BESS that graphically presented in Fig. 2.6.

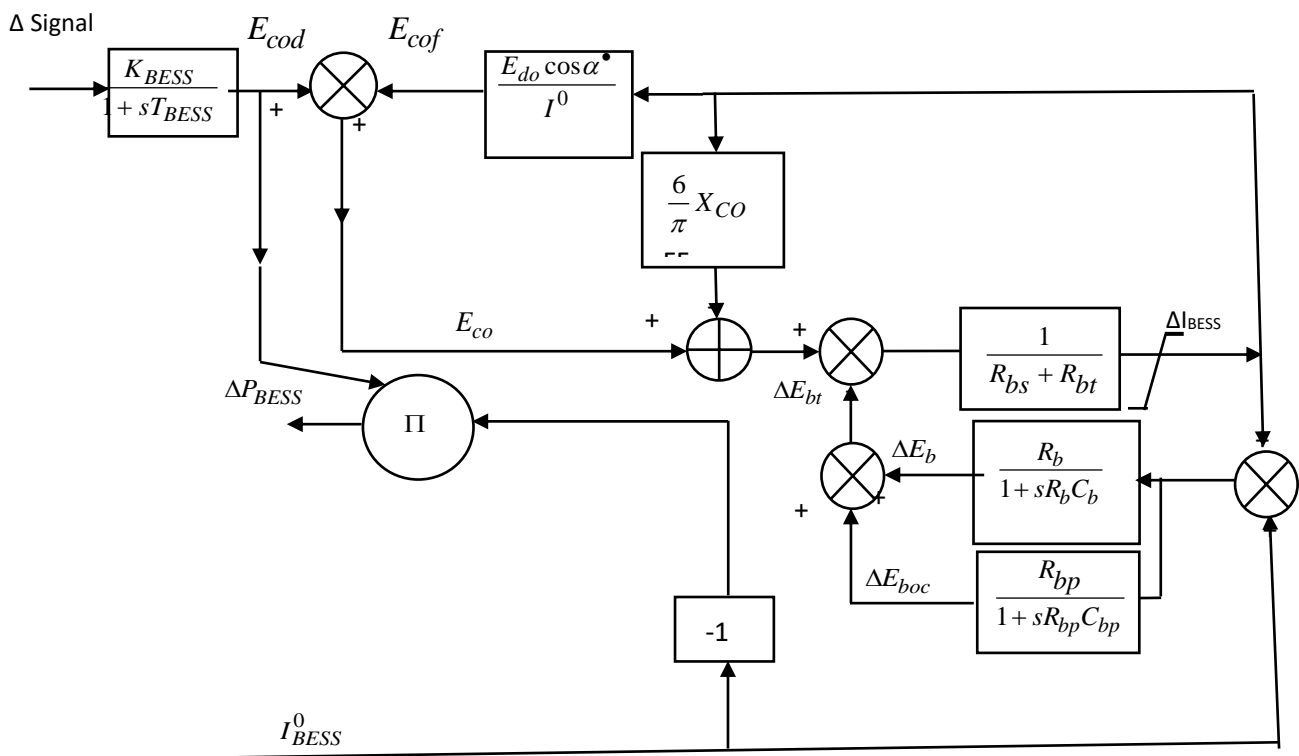


Fig. 2.6. Transfer function model of BESS.

The various parameters of the battery are taken from [61] and are presented in Table 2.1. The parameters of the two-area power system where battery is applied for frequency regulation are presented in Table. 2.2. The battery parameters are converted into per unit values for their application in the present study.

Table 2.1. Actual values of BESS parameters.

BESS Parameters		
Battery voltages = 1755 – 2925V DC	$C_{bp} = 52597F$	$K_{BESS} = 100kv / pu.mw$
$R_{bs} = 0.013\Omega$	$X_{CO} = 0.0274\Omega$	$\alpha^\circ = 15^\circ$
$R_{bt} = 0.0167\Omega$	$I_{BESS}^0 = 4.426KA$	Base voltage = 10KV, Base current = 200KA
$R_b = 0.001\Omega$	$R_{bp} = 10k\Omega$	$C = 40MWh$
$C_b = 1F$	$T_{BESS} = 0.026sec$	$SOC_{ref} = 0.5$

Table 2.2. Power System parameters where BESS is applied.

Power System parameters (Base power = 2000MW)											
Area no.	K_P (Hz/pu.MW)	K_r	T_r (sec)	T_p (sec.)	f (Hz)	T_g (sec)	T_i (sec)	R (Hz/pu.MW)	H	D (pu.MW/Hz)	B (pu.MW/Hz)
1	120	0.5	10	20	60	0.08	0.3	3	4.7104	8.33×10^{-3}	0.3417
2	120	0.5	10	20	60	0.08	0.3	3	4.7104	8.33×10^{-3}	0.3417

The per unit conversion is performed by the following calculation.

Per unit conversion of BESS parameters:

The base values for the calculation are considered according to power system base values where battery applied for load frequency control problem. The assumed base values are: Base value of voltage= 10 kV and Base value of current= 200 kA and Base impedance (Z_{Base})= 0.05 Ω ,

The following BESS parameters are determined by the subsequent calculations:

i) Per unit value calculation for (X_{CO})

The base impedance (Z_{Base}) can be mathematically related to (X_{CO}) as:

$$Z_{Base} = \text{Base value of } X_{CO}$$

$$\text{Per unit of } X_{CO} = \frac{\text{Actual value of } X_{CO}}{\text{Base value of } X_{CO}} = \frac{0.0274\Omega}{0.05\Omega} = 0.548 \text{ pu.}$$

ii) Per unit value calculation for (R_{bs})

$$Z_{Base} = \text{Base value of } R_{bs}$$

$$\text{Per unit of } R_{bs} = \frac{\text{Actual value of } R_{bs}}{\text{Base value of } R_{bs}} = \frac{0.013\Omega}{0.05\Omega} = 0.26 \text{ pu.}$$

iii) Per unit value calculation for (R_{bt})

$$Z_{Base} = \text{Base value of } R_{bt}$$

$$\text{Per unit of } R_{bt} = \frac{\text{Actual value of } R_{bt}}{\text{Base value of } R_{bt}} = \frac{0.0167\Omega}{0.05\Omega} = 0.334 \text{ pu.}$$

iv) Per unit value calculation for (R_b)

$$Z_{Base} = \text{Base value of } R_b$$

$$\text{Per unit of } R_b = \frac{\text{Actual value of } R_b}{\text{Base value of } R_b} = \frac{0.001\Omega}{0.05\Omega} = 0.02 \text{ pu.}$$

v) Per unit value calculation for (R_{bp})

$$Z_{Base} = \text{Base value of } R_{bp}$$

$$\text{Per unit of } R_{bp} = \frac{\text{Actual value of } R_{bp}}{\text{Base value of } R_{bp}} = \frac{10000\Omega}{0.05\Omega} = 200,000 \text{ pu.}$$

vi) Per unit value calculation for (C_b)

$$Z_{Base} = \text{Base value of reactive capacitance of } C_b$$

$$\text{Let, Base value of } C_b = C_{bBase}$$

$$\text{So, } Z_{Base} = \frac{1}{2 \times \pi \times f \times C_{bBase}}$$

$$\Rightarrow C_{bBase} = \frac{1}{2 \times \pi \times f \times Z_{Base}} = \frac{1}{2 \times \pi \times 60 \times 0.05} = 0.05307\text{F}$$

$$\text{Per unit of } C_b = \frac{\text{Actual value of } C_b}{\text{Base value of } C_b} = \frac{1\text{F}}{0.05307\text{F}} = 18.84 \text{ pu.}$$

vii) Per unit value calculation for (I_{BESS}^0)

$$\text{Base value of } I_{BESS}^0 = \frac{\text{Base Power}}{\text{Base Voltage}} = \frac{2000 \times 10^6 \text{ Watt}}{10 \times 10^3 \text{ Volt}} = 200\text{KA}$$

$$\text{Per unit value of } I_{BESS}^0 = \frac{\text{Actual value of } I_{BESS}^0}{\text{Base value of } I_{BESS}^0} = \frac{4.426 \text{ KA}}{200 \text{ KA}} = 0.02213\text{pu.}$$

2.6. PSO Optimization Technique

Particle swarm optimization (PSO) technique is a robust stochastic method of optimization introduced in 1995 [92]. This optimization technique gives the solution to a particular problem based on the movement and intelligence of swarms. Moreover, the solution of the problem depends on the concept of social interaction. The number of particles that constitute a swarm move around in space for searching of the best solution in space. This research applied the PSO to tune the control parameters of power system for load frequency control problem.

The general solution of PSO optimization technique depends on the dimension of the problem, population size of particles over a series of time steps. The response of population of swarm to give the optimum solution depends on the quality factor of gbest and pbest values. The allocation of responses between pbest and gbest ensures a diversity of response. Each particle of population adapted its position in accordance with gbest change, adhering to the principle of stability. Each particle updates the gbest and pbest for the optimum solution with updated values of velocity and position. Both of them are updated as follows:

$$V_j(t+1) = V_j(t) + c_1 r_1 (p_j - x_j(t)) + c_2 r_2 (p_g - x_j(t))$$

$$x_j(t+1) = x_j(t) + v_j(t+1)$$

Where, $v_j(t)$ = velocity vector of j^{th} particle at time t , $x_j(t)$ = position vector of j^{th} particle at time t . Vector p_j is the memory of particle j at current generation, and vector p_g is the best location found by the whole swarm. Cognitive coefficient c_1 and social coefficient c_2 are known as acceleration coefficients. r_1 and r_2 are two random number with uniform distribution. With all the above theoretical consideration, the application of PSO for the current research study has followed the below computational steps:

Step-1: Read the system data and select the gain parameters to be optimized.

Step-2: No. of trials to be executed, p_{max} and set trial count $p = 0$.

Step-3: Specify maximum iteration allowed, Itr_{max} .

Step-4: Generate a population of particles with random velocity, position and fitness value.

Step-5: Initiate iteration count $Itr = 0$.

Step-6: Compute the value of objective for all particles.

Step-7: Calculate pbest and gbest [92,93] for present condition.

Step-8: Increase iteration count by 1, $Itr = Itr + 1$.

Step-9: Go to step 11, if maximum iteration count is reached

Step-10: Calculate velocity and position of each particle and go to step-6.

Step-11: Gain parameters are obtained for p^{th} trial.

Step-12: Update trial count, $p \leftarrow p+1$.

Step-13: If $p < p_{\text{max}}$, then jump to step-4.

Step-14: Stop.

ROLE OF DEMAND SIDE MANAGEMENT FOR FREQUENCY REGULATION

3.1. Introduction

Automatic load frequency control (ALFC) is the pivotal feature of power system to maintain frequency and the tie-line power flow at the specific scheduled levels irrespective of load change in an inter-connected power system. Moreover, all types of generations present in an interconnected power system are not suitable for automatic generation control (AGC). For example, nuclear power generator provides maximum output which is considered as base load and therefore, do not participate in automatic generation control (AGC). Similarly, gas turbine plant operates during peak demands only and has an insignificant role in AGC. So, either thermal or hydro unit is the natural choice of generation for AGC in any power system. Over the last few decades, the traditional grid is experiencing many challenges because of tremendous increase in electricity demand. To fill the gap between generation and demand renewable based generation is being deployed because of its advantages over traditional generation [10]. However, renewable energy resources cause some problems like fluctuation in their output power due to uncertainties of weather conditions. This leads to fluctuation in system frequency and ultimately affects the dynamic performance of the system. One of the most important issues in power system is frequency regulation. However, introduction of renewable energy sources has made the problem more challenging. In this regard, demand side management (DSM) may be incorporated in ALFC to get better frequency regulation in cost effective way.

In view of the above investigation, this chapter introduces DR/DSM in ALFC of two-area power system. The two-area power systems considered to investigate the role of DSM/DR for frequency regulation are as follows:

1. Wind integrated two-area thermal power system
2. Hydro thermal two-area power system

The frequency regulation performance with introduction of DSM/DR in ALFC of above-mentioned test system is observed and analyzed as discussed in the following sections.

3.2. ALFC Modelling with DR for Different Power System

DR is incorporated in the automatic load frequency control (ALFC) of different inter-connected power system through a well-designed program. The program manipulates load in short-term to influence supply demand balance. DR is the most advantageous DSM technique [94]. In the present work DR is included in the secondary loop of the ALFC.

The control strategy of secondary loop of ALFC is shared between two control paths depending on the DR price in the electricity market. The DR program is designed on the basis of slope of demand-price curve (α). Mathematically, $\alpha = (\Delta d / d_0) / (\Delta \rho / \rho_0)$ where Δd and $\Delta \rho$ are change in demand and change in price respectively and d_0 is base demand, ρ_0 is base price [35]. ‘ α ’ is a positive decimal number with maximum value of one. In this present study, the role of DR is investigated for two types of interconnected power system such as wind integrated two-area thermal power system and hydro thermal two-area power system. All the parameters taken for these two different power system models for simulation are mentioned in Table. 3.1 and Table. 3.2. Table. 3.1 represent the system parameters of wind integrated two area thermal system and Table 3.2 shows the system parameters of two-area hydrothermal power system. The characteristics of ALFC in terms of frequency regulation in presence of DR for the above power system is analyzed and observed in the following subsections.

Table 3.1. Nominal Parameters of two area wind integrated thermal Power System Model.

Area no.	K_P (Hz/pu.MW)	K_r	T_r (sec)	T_p (sec.)	f (Hz)	T_g (sec)	T_t (sec)	R (Hz/pu.MW)	H	D (pu.MW/Hz)	B (pu.MW/Hz)
1	120	0.5	10	20	60	0.08	0.3	3	4.7104	8.33×10^{-3}	0.3417
2	120	0.5	10	20	60	0.08	0.3	3	4.7104	8.33×10^{-3}	0.3417

Table 3.2. Parameters taken for the hydrothermal System Model [2].

Area no.	K_P (Hz/pu.MW)	K_r	T_r (sec)	T_p (sec.)	f (Hz)	T_g (sec)	T_t (sec)	R (Hz/pu.MW)	H (s)	D (pu.MW/Hz)	B (pu.MW/Hz)
1	120	0.5	10	20	60	0.08	0.3	2.4	5	8.33×10^{-3}	0.425
2	120	0.5	10	20	60	0.08	0.3	2.4	5	8.33×10^{-3}	0.425

3.2.1. Wind integrated two-area thermal power system

Fig. 3.1 shows the wind integrated two-area thermal power system in which DR is introduced in each area of the two-area power system to investigate the role of DR for frequency regulation. The performance of the ALFC with DR in terms of frequency regulation is observed through power balance analysis of the studied power system.

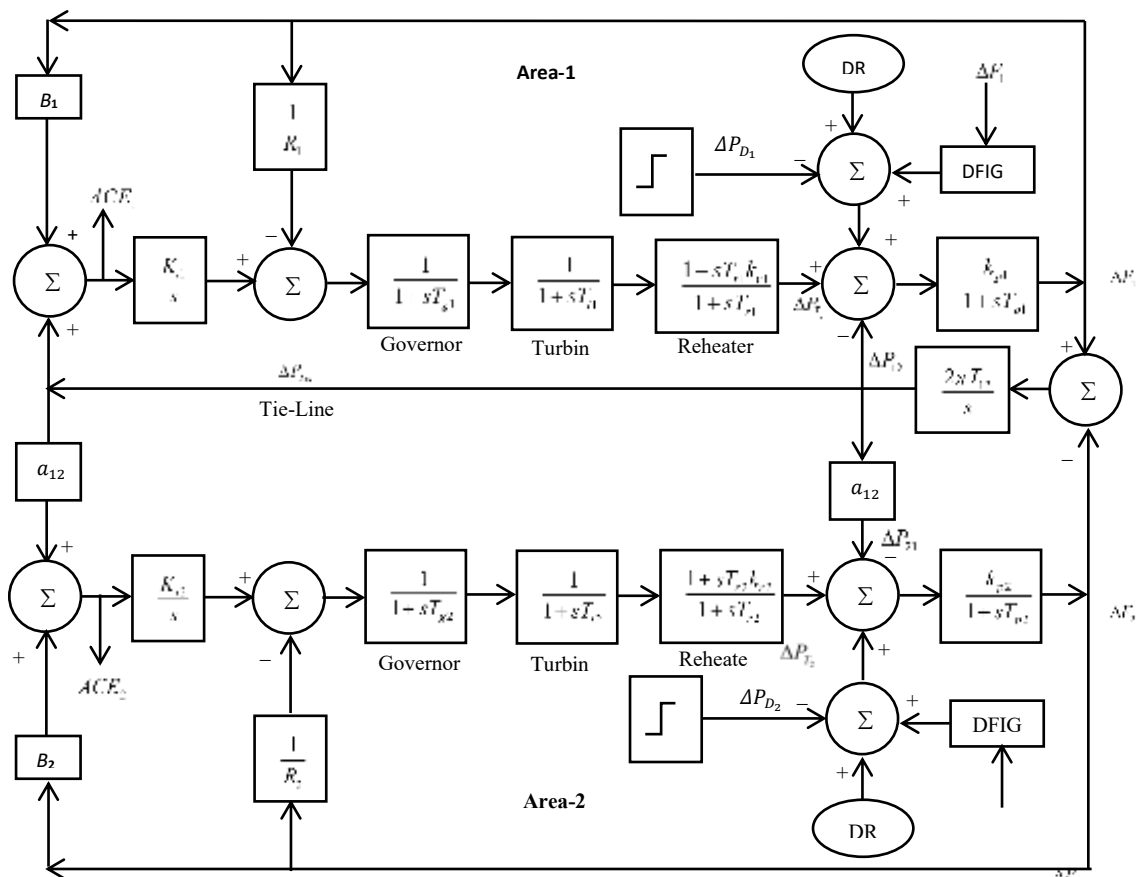


Fig.3.1. The ALFC model of two-area interconnected power system in presence of DR and DFIG.

3.2.2. Hydro thermal two-area power system

In the present study a linear transfer function model of a thermal system integrated with a hydro system is considered for simulation [12]. The power output of both the areas are 2000MW. DR is incorporated within the hydrothermal system to analyze dynamic behavior and is shown in Fig. 3.2.

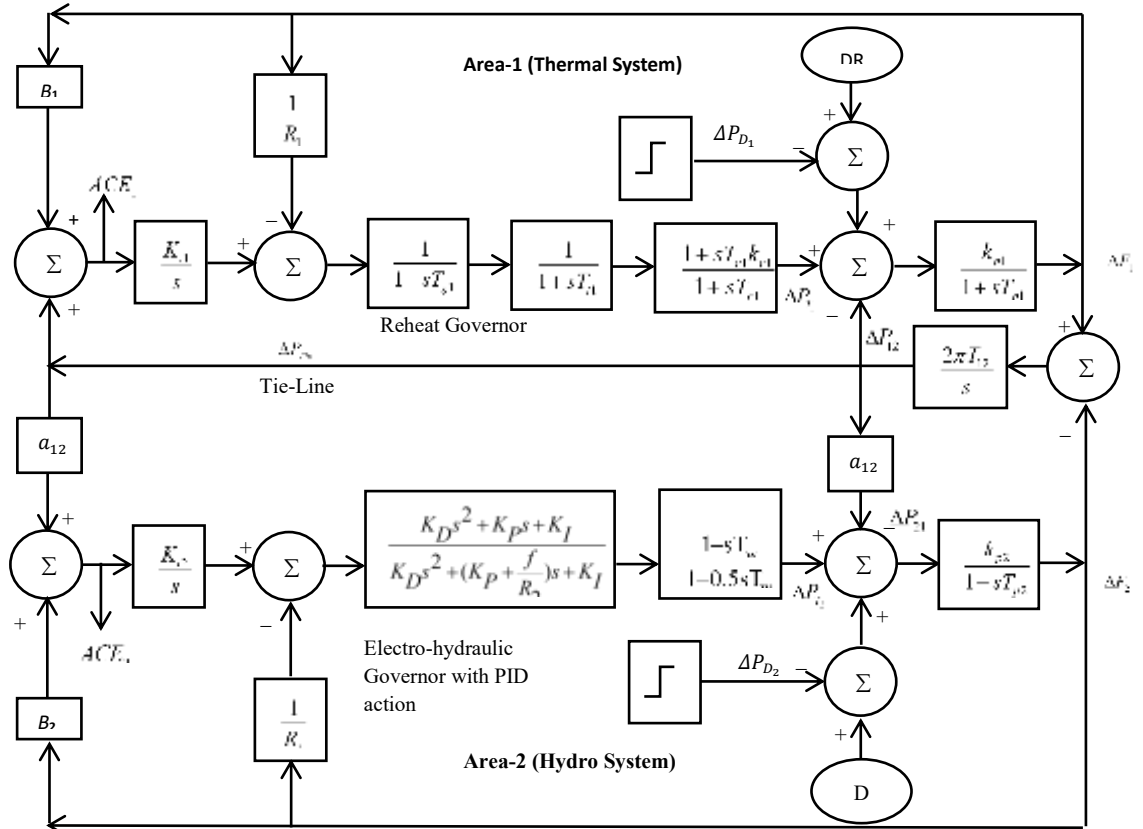


Fig. 3.2. The ALFC model of the hydro-thermal test system.

3.2.3. Power balance equations

The general power balance equation for any single area power system [1], is given by

$$\Delta P_T(s) - \Delta P_D(s) = 2Hs\Delta f(s) + D\Delta f(s) \quad (3.1)$$

where, $\Delta P_T(s)$ =incremental change in turbine power

$\Delta P_D(s)$ =incremental change in demand

H =inertia constant, Δf =frequency deviation

and $D = \Delta P_D / \Delta f$

The area control error (ACE), which in addition to frequency error (Δf) contains the errors in the interconnected tie-line powers. So, the Power balance equation of i^{th} area for the conventional two area power system is expressed as:

$$\Delta P_{T_i}(s) - \Delta P_{D_i}(s) \pm \Delta P_{Tie,i}(s) = 2H_i s \Delta f_i(s) + D_i \Delta f_i(s) \quad (3.2)$$

The Power balance equation after including the wind energy conversion system (WECS) in the conventional two area power system is modified as:

$$\Delta P_{T_i}(s) - \Delta P_{D_i}(s) \pm \Delta P_{Tie,i}(s) + \Delta P_{DFIG,i}(s) = 2H_i s \Delta f_i(s) + D_i \Delta f_i(s) \quad (3.3)$$

Since demand response (DR) performs like spinning reserve in magnitude and power flow direction, i.e., once frequency deviation is negative (or, positive), it is required to turn OFF (or, ON) a portion of the responsive loads (i.e., DR). Hence power balance equation can be simply modified for the proposed model in two area wind integrated thermal system as follows in presence of DR:

$$\Delta P_{T_i}(s) - \Delta P_{D_i}(s) \pm \Delta P_{Tie,i}(s) + \Delta P_{DFIG,i}(s) + \Delta P_{DR_i}(s) = 2H_i s \Delta f_i(s) + D_i \Delta f_i(s) \quad (3.4)$$

Similarly, the Power balance equation for i^{th} area of a two-area hydro-thermal network will be same as (3.2). And power balance equation of hydrothermal power system in presence of DR becomes as in (3.5),

$$\Delta P_{T_i}(s) - \Delta P_{D_i}(s) \pm \Delta P_{Tie,i}(s) + \Delta P_{DR_i}(s) = 2H_i s \Delta f_i(s) + D_i \Delta f_i(s) \quad (3.5)$$

where, ΔP_{DR_i} is the incremental change in DR of i^{th} area, $\Delta P_{DFIG,i}$ is the incremental change in DFIG output of i^{th} area. $\Delta P_{Tie,i}$ is the change power of the tie line. $\Delta P_{Tie,i}$ will be negative if area- i is sending power to the tie line and vice-versa.

3.3. Proposed Methodology of tuning of AGC parameters for two-area system

The primary objective of this research is to get better dynamic response with participation of DR in the ALFC loop. Tuning of control parameters of the power system for ALFC study is a must to get better frequency regulation. Hence, the respective control parameters of the studied two-area power system are tuned by considering the objective of minimizing the settling time of dynamic performances of the power system w. r. t load change in either area. Particle swarm optimization (PSO) is a robust optimization tool and therefore is adopted here to tune the gain only. The optimization problem is solved for both the test system with the help of PSO following flowchart shown in Fig. 3.3.

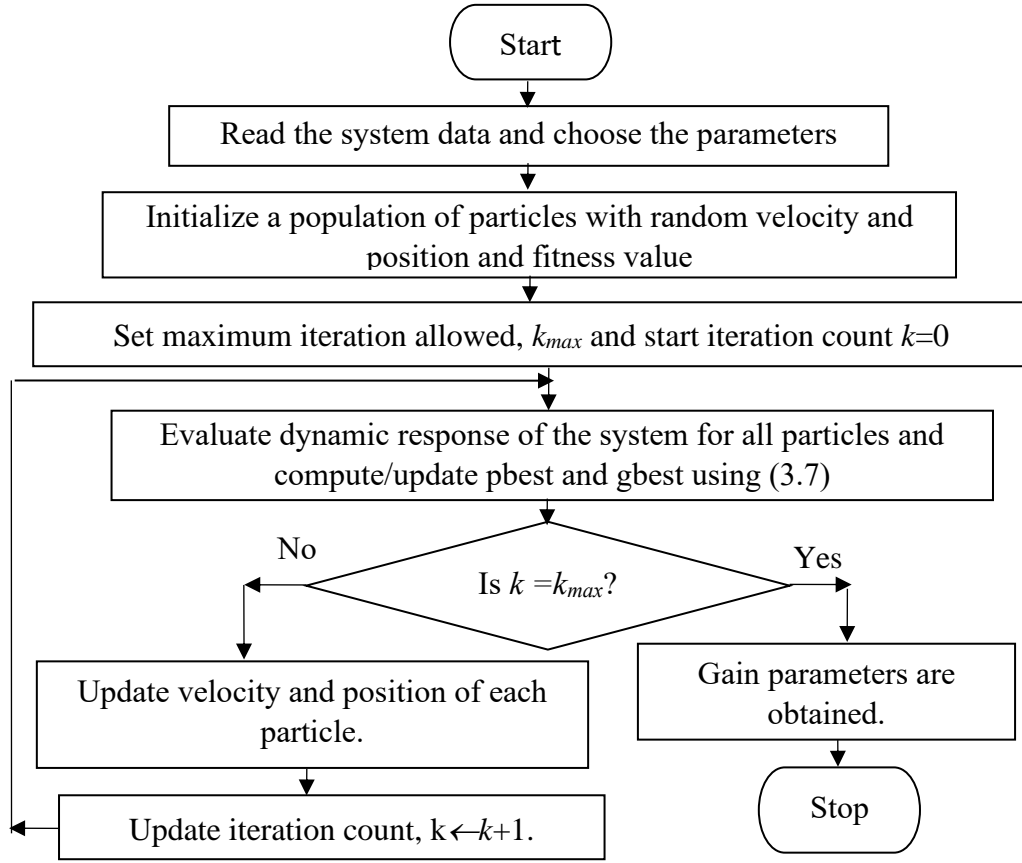


Fig. 3.3. The flowchart to obtain gain parameters.

3.3.1. PSO algorithm for Wind integrated two-area thermal power system

To know the role of demand side management, the gain parameter of the DR loop is kept constant. The suitable tuning of gain parameter of both conventional integral controller and DFIG controller (K_{pf} , K_{df}) are required for better frequency regulation, hence it is necessary to tune them. A set of most suitable gain parameters are to be selected for the domain of optimization introduced PSO. The design of objective function is important for success of any optimization process. Hence objective function is designed on the basis of certain specification of automatic generation control (AGC). It is formulated as minimization of function expressed by:

$$J = T_{s\Delta f_1} + T_{s\Delta f_2} + T_{s\Delta P_{Tie}} \quad (3.6)$$

Where, $T_{s\Delta f_1}$, $T_{s\Delta f_2}$ and $T_{s\Delta P_{Tie}}$ are the settling time of frequency deviations in area-1, area-2 and tie line power deviation respectively.

3.3.2. PSO algorithm for Hydro thermal two-area power system

Present work aims to explore the dynamic response of a hydrothermal system with the existence of demand response as well as to achieve better angle stability via optimization. The objective function is designed with the aid of some specifications of AGC provided in [3]. Present optimization problem goals to optimize the value of integral controller parameters/ (K_{i1} and K_{i2}) of the two-area system to obtain minimum overall settling time of the system

response using particle swarm optimization (PSO) technique [92,93]. The key feature of this research to present the role of DSM in ALFC and for that purpose, one optimization technique is required to tune the controller gain. PSO is a robust optimization tool and therefore is adopted here to tune the gain only. There is no aim to present the efficacy of any optimization technique and therefore no other optimization technique is presented or compared with PSO. Rather the objective function (T) is adopted as:

$$T = T_1 + T_2 + T_{Tie} \quad (3.7)$$

In aforesaid equation T is the global settling time of the system and T_1 and T_2 settling time of frequency deviation in area-1 and area-2 respectively, and T_{Tie} is the time required to settle down the tie line power deviation.

3.4. Simulation and Results

The simulation has been done by taking nominal values of system parameters for the respective power system from Table. 3.1 and Table. 3.2. The performance of the system has been observed with variation of step load and the controller parameter are optimized by using PSO [92,93] to minimize the summation of settling time of frequencies in area-1, area-2 and in the tie line.

3.4.1. Comparative Analysis with and without DR

The simulation has been carried out for dynamic performances of the above two type of inter-connected power system by considering different case studies. The case studies are basically depending on the load change in different areas. So, depending on the case studies the performances of the DR for frequency regulation is analyzed for wind integrated thermal power system and Hydro thermal two-area power system. The details comparative studies are described in the below subsections.

3.4.1.1. Wind integrated two-area thermal power system

The performance of the wind integrated thermal power system has been observed with variation of step load and the controller parameter are optimized by using Particle Swarm Optimization (PSO) to minimize the summation of settling time of frequencies in area-1, area-2 and in the tie line. The Table 3.3 shows different tuned control parameter along with the settling time for grid frequency deviation and deviation in the tie line power for 1% load change in the area-1 in absence of DR in both the areas. The results are shown for five trials of PSO. K_i is integral controller gain in the automatic generation control (AGC) loop. K_{pf} and K_{df} respectively, are the proportional and derivative controller gains in the DFIG [3,12].

The simulation has been carried out for dynamic performance of the same power system condition, but in presence of demand response (DR) with the K -parameters obtained in Table 3.3. The Table 3.4 presents the settling time for grid frequency deviations and deviation in the tie line power corresponding to control parameter used from Table 3.3. Table 3.4 shows lower settling times in all frequency deviation and tie line power deviation as compared with Table 3.3. So, it has been observed that demand side management (DSM) can be considered for better frequency regulation of power system.

The Table 3.5 shows the results with PSO for 2% load change in the area-2 in absence of DR in both the areas. The Table 3.6 shows the results corresponding to controller parameters of Table 3.5 but in presence DR in both the areas. Results obtained in Table 3.6 confirm the improvement in dynamic response of the power system in presence of DR.

The Table 3.7 shows the results with PSO for 2% load change in the area-1 and 1% load change in area-2 simultaneously in absence of DR in both the areas.

Table 3.3. Tuned controller parameters and settling time of frequency deviations and tie line power deviation for load change in the area-1 in absence of DR.

Controller Parameters			Settling Time in sec.			Total Settling Time (T_s) in Sec.
K_i	K_{pf}	K_{df}	ΔF_1	ΔF_2	ΔP_{Tie}	
0.41588	0.29852	0.12664	28.35	29.54	24.73	82.62
0.42469	0.2946	0.12131	28.25	29.39	24.48	82.12
0.46145	0.28792	0.11316	28	28.93	23.15	80.08
0.56342	0.30313	0.10398	27.77	26.91	20.41	70.09
0.42343	0.29578	0.12396	28.26	29.41	24.51	82.18

Table 3.4. Controller parameters and settling time of frequency deviations and tie line power deviation for load change in the area-1 in presence of DR.

Controller Parameters			Settling Time in sec.			Total Settling Time (T_s) in Sec.
K_i	K_{pf}	K_{df}	ΔF_1	ΔF_2	ΔP_{tie}	
0.41588	0.29852	0.12664	21.16	18.24	9.28	48.67
0.42469	0.2946	0.12131	21.59	18.57	9.17	49.33
0.46145	0.28792	0.11316	19.78	16.72	8.38	44.88
0.56342	0.30313	0.10398	12.730	12.970	6.87	32.57
0.42343	0.29578	0.12396	20.81	17.93	9.18	47.87

Table 3.5. Tuned controller parameters and settling time of frequency deviations and tie line power deviation for load change in the area-2 in absence of DR.

Controller Parameters			Settling Time in sec.			Total Settling Time (T_s) in Sec.
K_i	K_{pf}	K_{df}	ΔF_1	ΔF_2	ΔP_{tie}	
0.44206	0.29928	0.12351	33.45	30.47	26.27	90.19
0.40179	0.33428	0.022125	34.12	30.91	27.38	92.41
0.41597	0.29527	0.12227	33.78	30.64	26.95	91.37
0.3800	0.28874	0.1247	34.98	30.97	28.42	94.37
0.35081	0.32727	0.15618	36.04	32.45	36.04	98.05

Table 3.6. Controller parameters and settling time of frequency deviations and tie line power deviation for load change in the area-2 in presence of DR.

Controller Parameters			Settling Time in sec.			Total Settling Time (T_s) in Sec.
K_i	K_{pf}	K_{df}	ΔF_1	ΔF_2	ΔP_{tie}	
0.44206	0.29928	0.12351	31.74	28.77	9.72	70.23
0.40179	0.33428	0.022125	31.58	28.68	10.95	71.15
0.41597	0.29527	0.12227	30.75	29.6	10.35	70.70
0.3800	0.28874	0.1247	33.26	32.11	11.91	77.28
0.35081	0.32727	0.15618	34.68	33.41	12.13	80.22

The Table 3.8 shows the results corresponding controller parameter of Table 3.7 but in presence DR in both the areas. Results obtained in Table 3.8 confirm the improvement in dynamic response of the power system in presence of DR.

Table 3.7. Tuned controller parameters and settling time of frequency deviations and tie line power deviation for load changes in the area-1 and area-2 simultaneously in absence of DR.

Controller Parameters			Settling Time in sec.			Total Settling Time (T_s) in Sec.
K_i	K_{pf}	K_{df}	ΔF_1	ΔF_2	ΔP_{tie}	
0.46266	0.29185	0.11655	34.48	33.44	23.08	91.00
0.42657	0.29611	0.12243	34.95	34.01	24.45	93.41
0.52807	0.29328	0.10701	32.73	31.70	21.89	86.32
0.47346	0.29653	0.11459	34.39	33.33	22.78	90.50
0.48088	0.29187	0.11522	34.29	33.21	22.62	90.12

Table 3.8. Controller parameters and settling time of frequency deviations and tie line power deviation for load change in both the areas in presence of DR.

Controller Parameters			Settling time in sec.			Total Settling Time (T_s) in Sec.
K_i	K_{pf}	K_{df}	ΔF_1	ΔF_2	ΔP_{tie}	
0.46266	0.29185	0.11655	30.56	27.54	8.50	66.60
0.42657	0.29611	0.12243	31.99	29.09	9.10	70.18
0.52807	0.29328	0.10701	32.32	27.33	7.26	66.91
0.47346	0.29653	0.11459	31.22	28.16	8.04	67.43
0.48088	0.29187	0.11522	34.39	31.25	8.30	73.94

3.4.1.2. Hydro thermal two-area power system

Next, a two-area hydrothermal power network where hydro unit is furnished with electric governor is considered [12]. To investigate the role of demand side management for frequency regulation of the proposed system, DR is introduced in the secondary loop of ALFC in both the areas which is shown in Fig. 3.2. Specifications for the network investigated are mentioned in Table. 3.2. The system performance of the test network has been obtained with optimum integral controller gains for step variation of load in the two areas. The simulations are carried out with DR as well as without DR for three trials of PSO in each case.

The Table 3.9 shows the values of optimal controller gain i.e, K_{i1} & K_{i2} present in area-1 and area-2 respectively and the corresponding settling time of frequency deviations of both the areas and tie line power deviation for 1% step load variation in area-1 in absence of DR. Table 3.10 presents the results for the same system scenario but in presence of DR. Table 3.10 displays improvement in settling times for all type of deviations in the network as compared with Table 3.9.

The Table 3.11 shows the tuned parameters for 1% step load variation in the area-2 without DR. However, Table 3.12 displays the corresponding outcomes in presence of DR in the system for 1% step load variation in area-2. Table 3.10 and Table 3.12 shows the upgrading in dynamic responses of the hydro-thermal power structure in presence of DR in comparison with Table 3.9 and Table 3.11 respectively. The Table 3.13 exhibits the result for comparison of several performance indices of the system when the selected controllers gain tuned with PSO for step load change in either area with and without DR in ALFC of the hydrothermal system.

Table 3.9. Optimal controller gains and corresponding settling times for 1% SLP in the area-1 without DR.

Controller gain		Settling time in sec.			Total Settling Time (<i>T</i>) in Sec.
K_{i1}	K_{i2}	ΔF_1	ΔF_2	ΔP_{tie}	
-2.0873	-0.094789	25.51	24.83	19.55	69.89
-2.2066	-0.094208	24.91	23.67	19.34	67.92
-2.1453	-0.093728	25.23	24.62	19.40	69.25

Here the performance indices taken for the comparison are Integral of time multiple of absolute error (ITAE), integral time square error (ITSE), integral absolute error (IAE) and integral square error (ISE) and Minimum damping ratio (MDR). These are common performance indices taken into prime consideration during tuning of any controller parameters of AGC.

Table 3.10. Optimal controller gains and corresponding settling times for 1% SLP in the area-1 with the aid of DR.

Controller gain		Settling time in sec.			Total Settling Time (<i>T</i>) in Sec.
K_{i1}	K_{i2}	ΔF_1	ΔF_2	ΔP_{tie}	
-0.8206	-0.013155	21.44	19.50	12.92	53.86
-0.8206	-0.011689	19.22	19.52	12.94	51.68
-0.81334	-0.013155	19.24	19.52	12.95	51.71

Table 3.11. Optimal controller gains and corresponding settling times for 1% SLP in the area-2 without DR.

Controller gain		Settling time in sec.			Total Settling Time (<i>T</i>) in Sec.
K_{i1}	K_{i2}	ΔF_1	ΔF_2	ΔP_{tie}	
-2.2824	-0.0973	16.74	29.53	16.41	62.68
-2.1921	-0.094903	18.64	20.57	17.96	57.17
-2.2791	-0.094703	18.75	20.26	18.27	57.28

Table 3.12. Optimal controller gains and corresponding settling times for 1% SLP in the area-2 with the aid of DR.

Controller gain		Settling time in sec.			Total Settling Time (<i>T</i>) in Sec.
K_{i1}	K_{i2}	ΔF_1	ΔF_2	ΔP_{tie}	
-0.045902	-0.41089	11.9800	19.3200	16.8100	48.11
-0.047891	-0.40457	12.14	19.35	16.84	48.33
-0.045364	-0.41117	11.98	19.32	16.82	48.12

Table 3.13. Comparison of various performance indices with and without DR in ALFC.

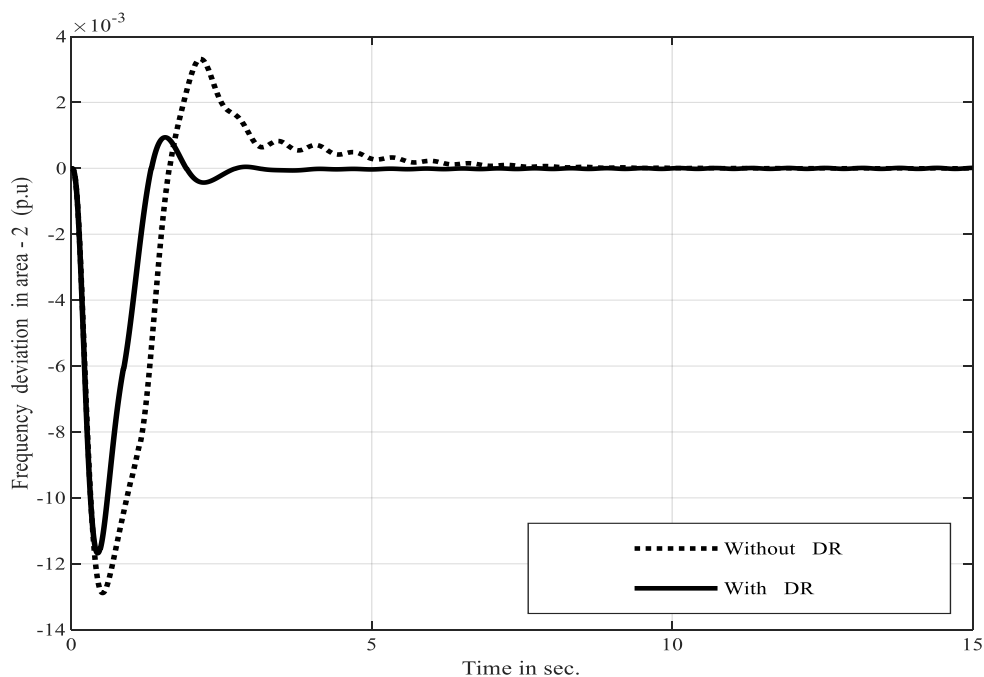
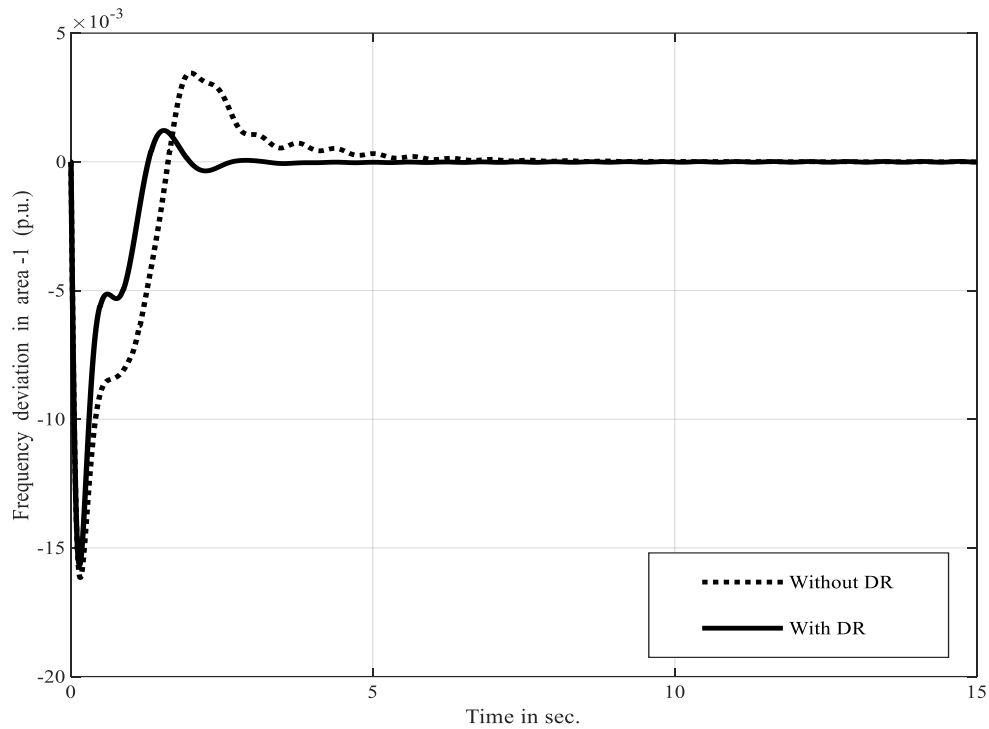
Performance indices	For 1% SLP in area-1		For 1% SLP in area-2	
	<i>In presence of DR</i>	<i>In absence of DR</i>	<i>In presence of DR</i>	<i>In absence of DR</i>
<i>ITSE</i>	0.0028	0.0039	0.0040	0.0135
<i>ISE</i>	0.0015	0.0019	0.0024	0.0060
<i>ITAE</i>	0.3467	0.4227	0.4202	0.7826
<i>IAE</i>	0.1048	0.1236	0.1187	0.1972
<i>MDR</i>	0.0999	0.1258	0.0977	0.1131
<i>T (in sec.)</i>	51.71	69.25	48.11	62.68

3.4.2. Overall Frequency Regulation with DR

This subsection describes the dynamic responses with the best tuned controller parameters chosen from results presented in Section-3.4.1.1 and Section-3.4.1.1 for wind integrated thermal power system and Hydro thermal two-area power system respectively on the basis of getting least settling time. The corresponding results are presented in following subsections.

3.4.2.1. Wind Integrated two area thermal Power System

The dynamic responses of frequencies ΔF_1 , ΔF_2 of the two areas and ΔP_{tie} , the tie line power deviations are provided in Fig. 3.4, Fig. 3.5 and Fig. 3.6 for the simulation studies performed. All of these figures support that of DR improves dynamic responses of power system.



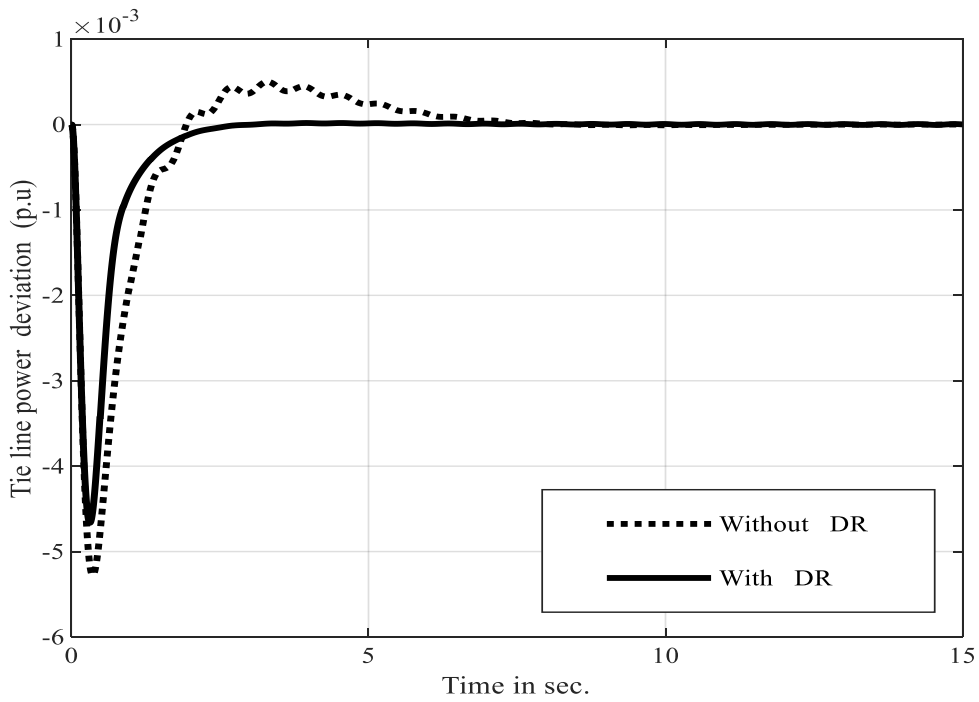
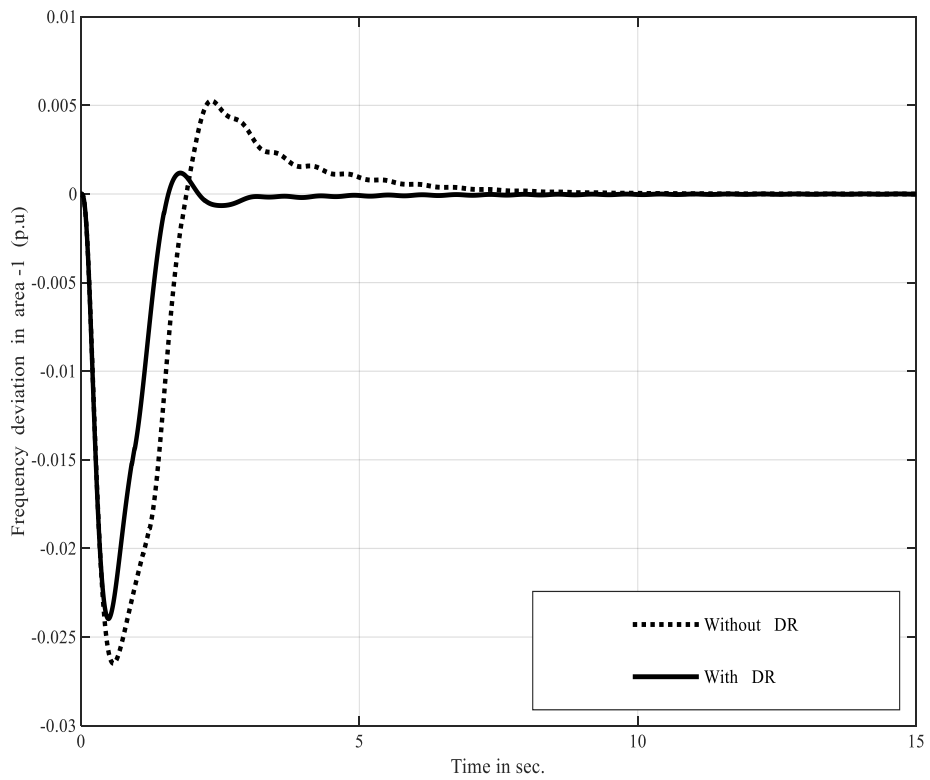


Fig. 3.4. The system frequency and tie line power deviations for 1% load change in area-1 with and without DR.



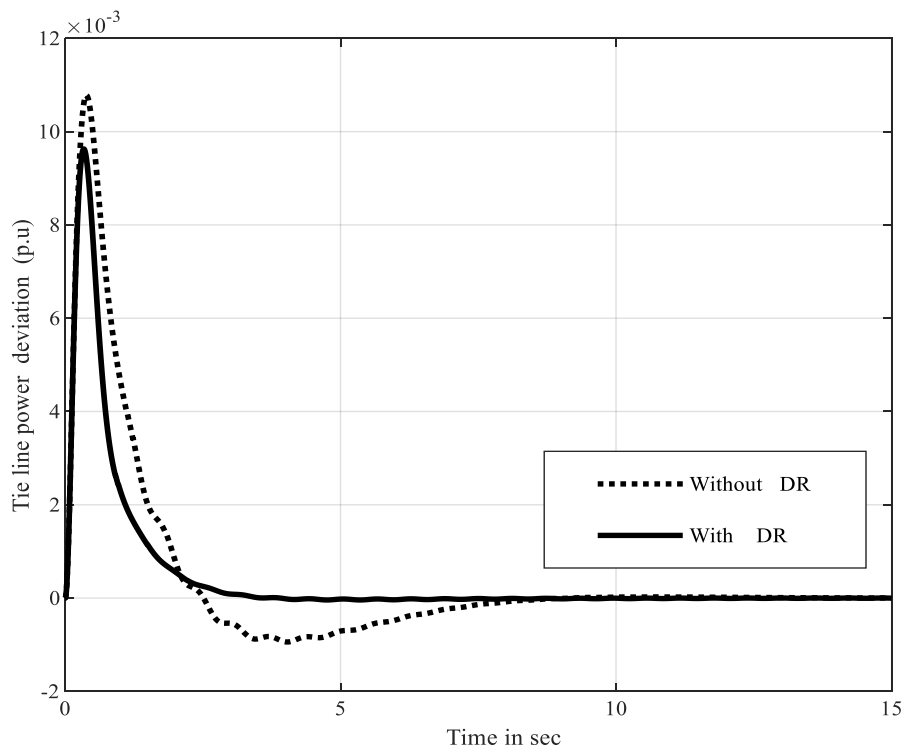
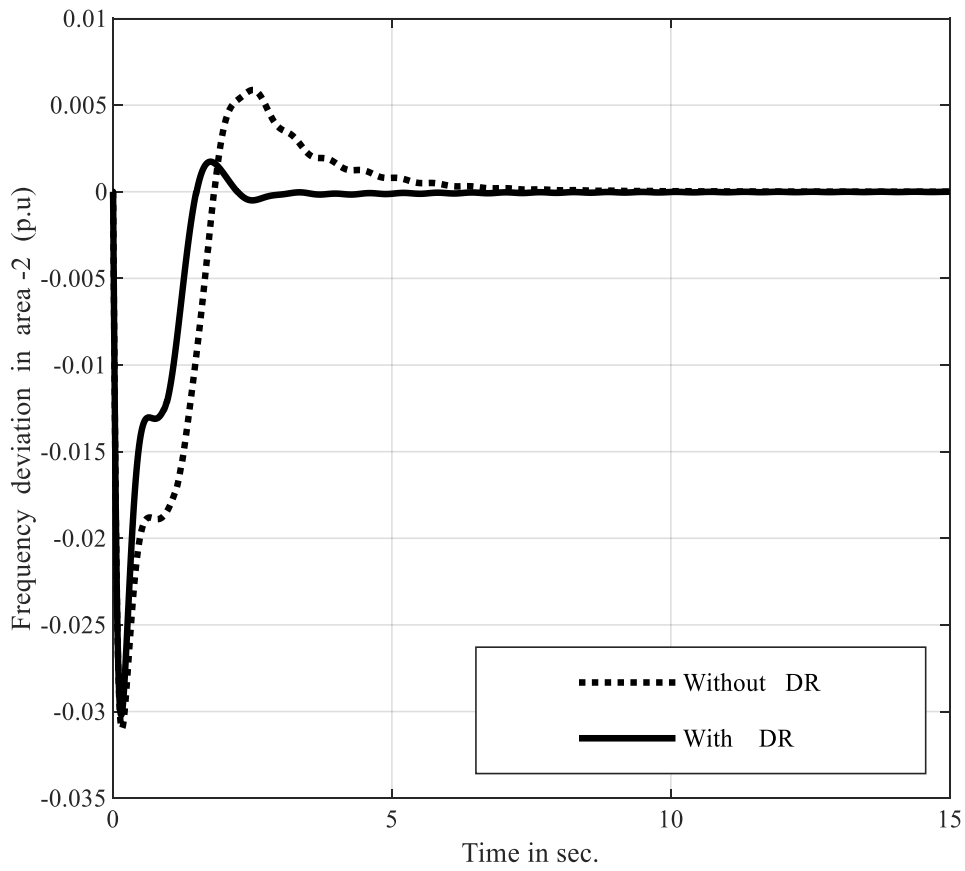
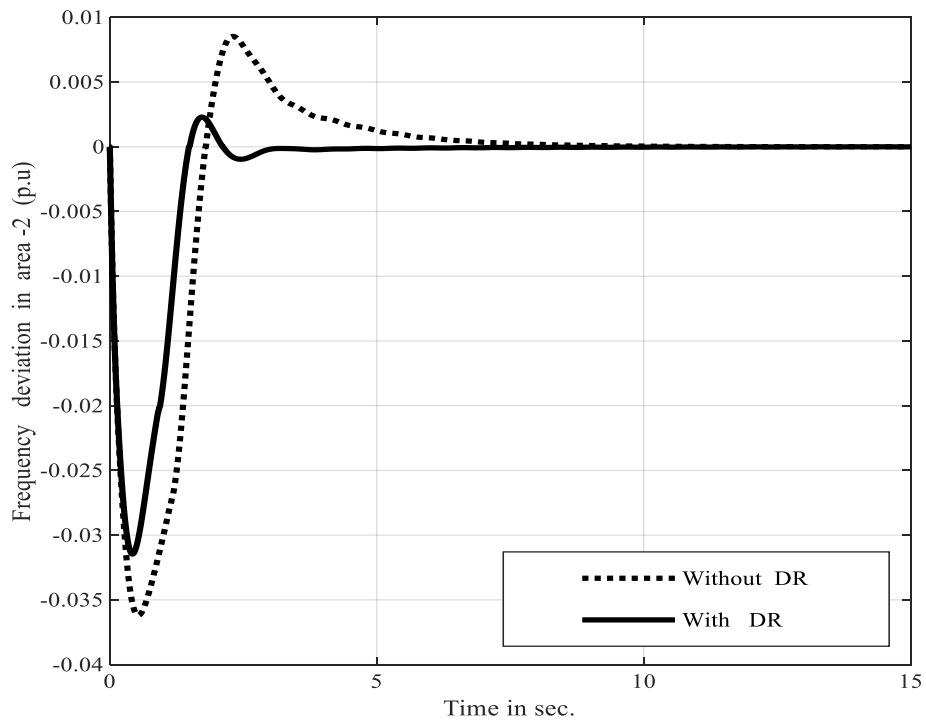
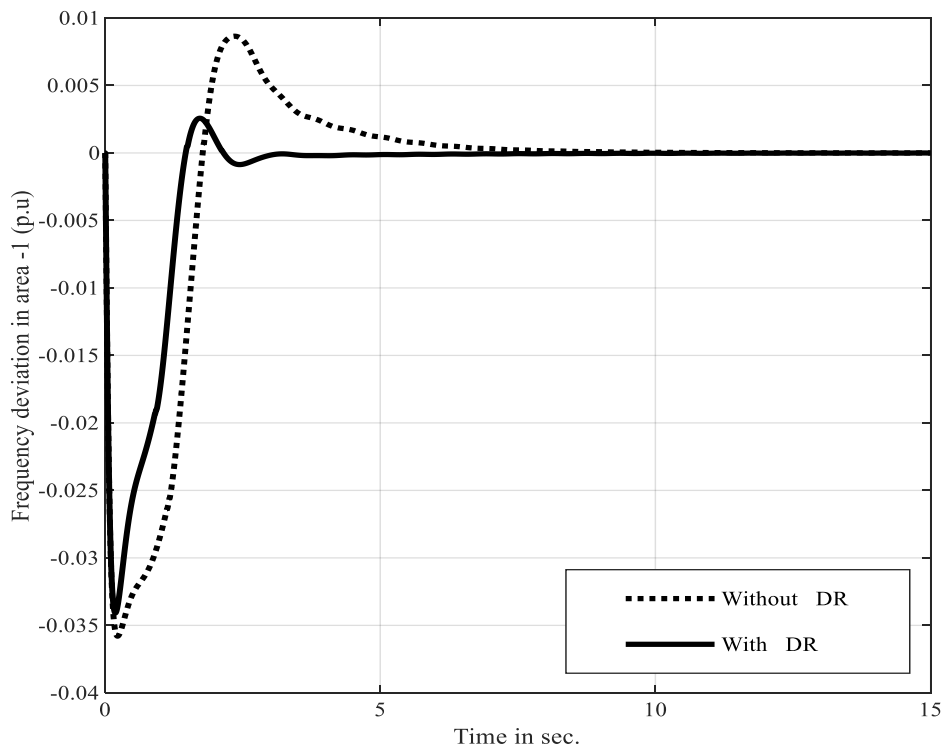


Fig. 3.5. The system frequency and tie line power deviations for 2% load change in area-2.



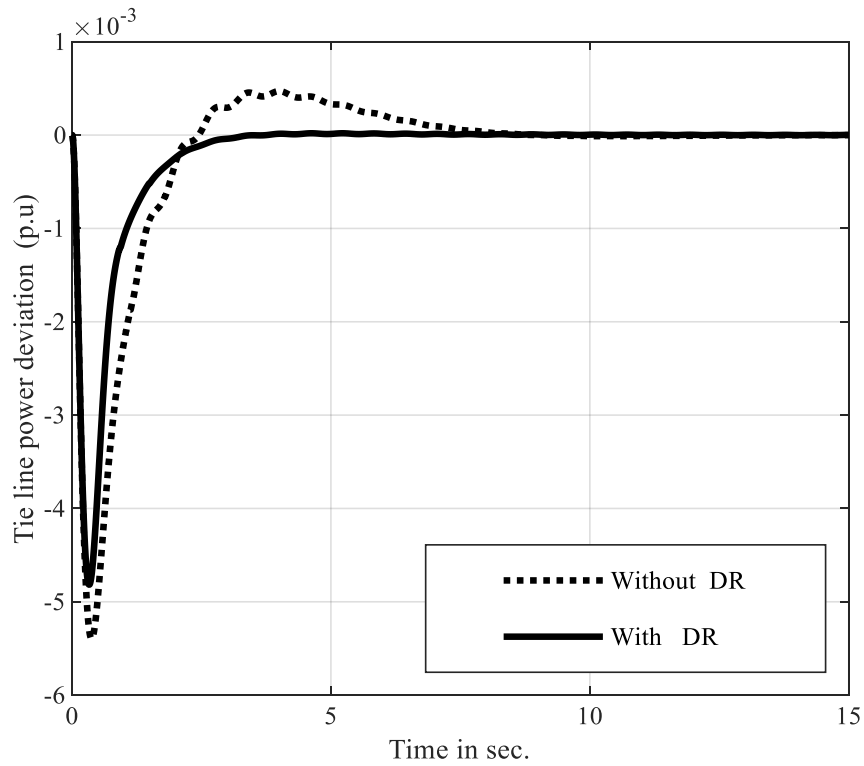
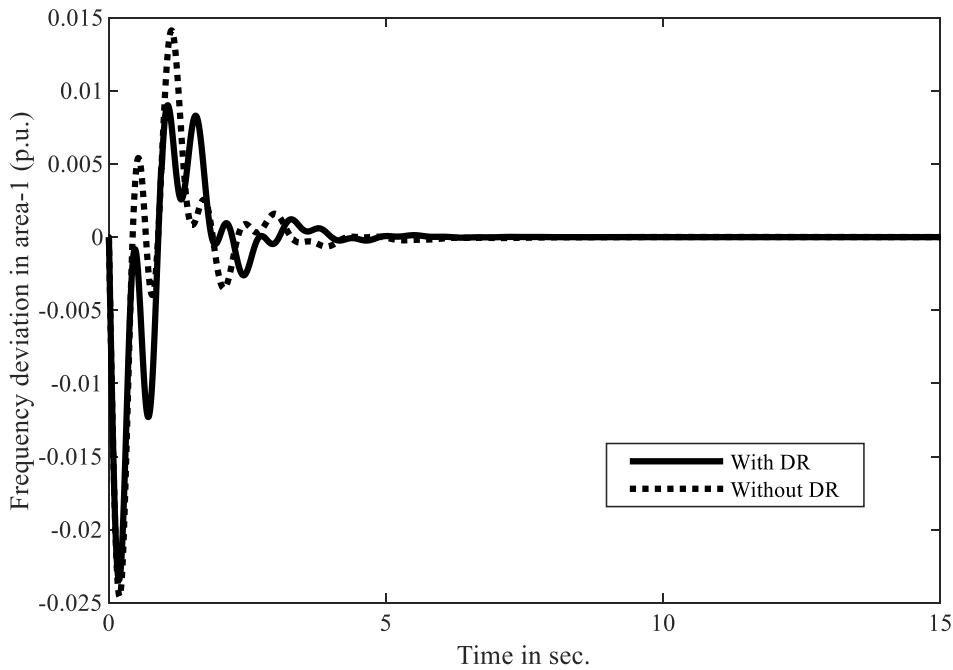


Fig. 3.6. The system frequency and tie line power deviations for 2% load change in area-1 and 1% load change in area-2 simultaneously and with without DR.

3.4.2.2. Hydro thermal two-area power system

The best tuned controller parameters are chosen from Table 3.10 and Table 3.12 on



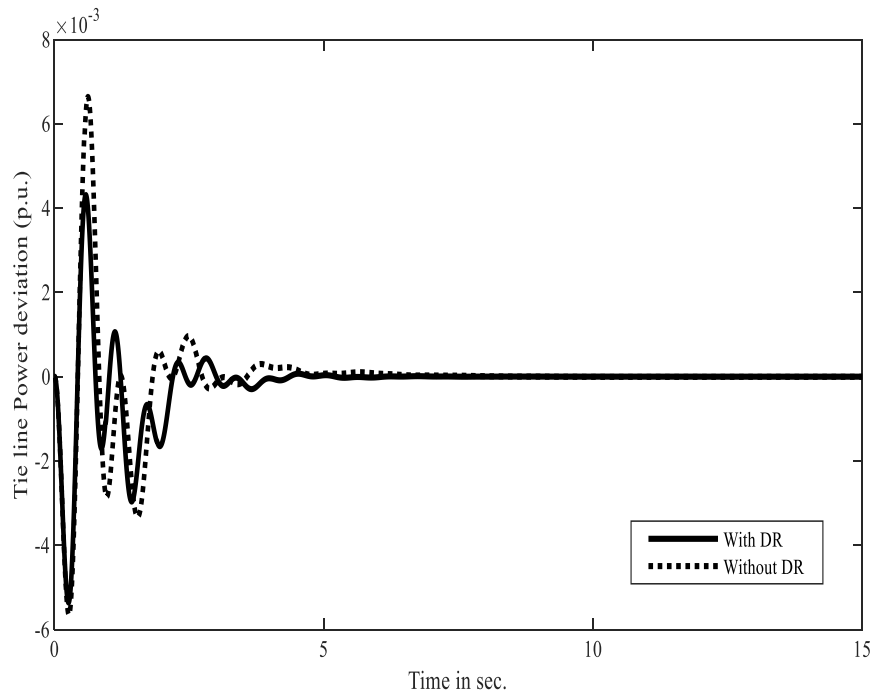
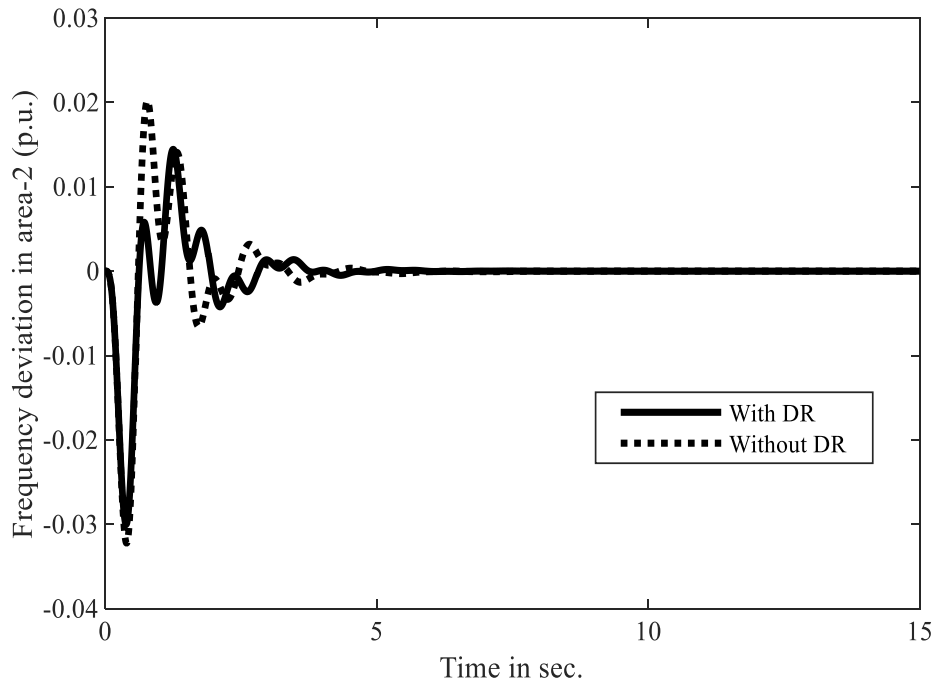


Fig. 3.7. Deviations in frequencies and tie line power for load change in area-1.

the basis of getting least settling time and then dynamic responses is obtained as in Fig. 3.7 and Fig. 3.8. The variation in frequency deviations ΔF_1 , ΔF_2 of the two areas and the tie line power deviations ΔP_{Tie} are displayed in Fig. 3.7 and Fig. 3.8 for 1% SLP in area-1 and area-2

respectively. The improvement in the system dynamic response in presence DR is noticeable in both the figures as compared to recently reported results in [12].

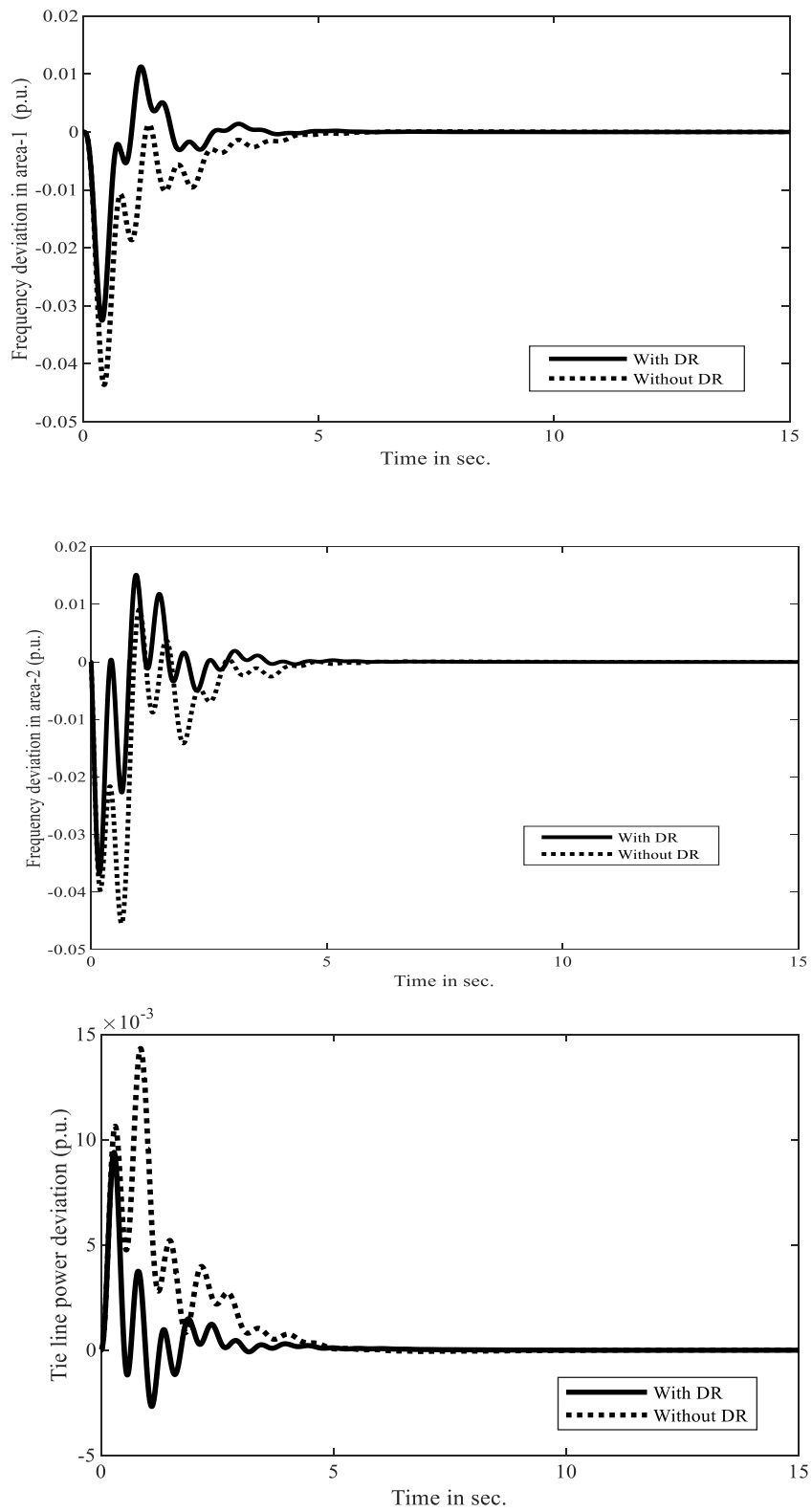


Fig. 3.8. Deviations in frequencies and tie line power for load change in area-2.

3.5. Conclusion

Demand side management (DSM) has a significant role in maintaining power balance from the customer side. In this paper, the ALFC model of a two-area power system consisting of a thermal and a DFIG unit and integrated with DSM is developed. Furthermore, DR is introduced in the automatic load frequency control (ALFC) model of a two-area hydrothermal power network to study the efficacy of DSM in respect of dynamic stability of a power network. PSO is implemented to tune the control parameters. Here, the selected controller gains of both the areas are optimized using PSO to minimize total settling time i.e, summation of settling times for frequency deviations of the two areas and tie line power deviation. The role of demand side management in terms of DR in dynamic response of present power system is studied. It has been observed that demand side management is able to improve the settling time for all type of frequency deviations. Also, the simulation results show that DR plays a key role in enhancement of dynamic stability of power network. The performance indices to assess dynamic stability of power system such as ITAE, IAE, ITSE, ISE are computed and their values proved that DSM definitely improves dynamic stability of power system.

3.6. Publication from This Work

Conference Publication

- [1] **Swetalina Bhuyan**, Sunita Halder nee Dey, Subrata Paul, 'Role of demand side management in automatic load frequency control', The first international conference on Emerging Frontiers in electrical and electronic Technologies (ICEFEET-2020), NIT, Patna 10-11th July, 2020.
- [2] **Swetalina Bhuyan**, Sunita Halder nee Dey, Subrata Paul, Sabita Chaine, 'Analysis of Frequency Regulation for a Hydro-Thermal System with ALFC-DR Model', International Conference on Power Electronics and Energy (ICPEE-2021), KIIT Deemed to be University, Bhubaneswar, Odisha, 2-3 January 2021.

CHAPTER 4

MODIFIED DELAY COMPENSATION IN DEMAND RESPONSE FOR FREQUENCY REGULATION OF INTERCONNECTED POWER SYSTEMS INTEGRATED WITH RENEWABLE ENERGY SOURCES.

4.1. Introduction

Demand Response (DR) provides an additional opportunity for balancing the generation and demand from demand side by dropping or shifting consumers' electricity usage. Demand response was first introduced by Shweppe et al. in 1980 to offer better reliability and security compare to traditional control system in terms of balancing generation and load [39]. DR is the change in load/demand with respect to change in price from demand side. The collaboration of demand response in ALFC increases the stability margin of the system and improves the system dynamic performance [17]. Though DR is beneficial for frequency regulation but it cannot provide frequency control at required speed [42,43] because of communication delay in the DR process arising from demand side. This delay produces phase lag between input and output of the DR loop due to which switching on or off of the load cannot take place fast enough for frequency regulation. This leads to overshoot, instability and oscillation in system dynamic performances [17,43]. Hence, this chapter has taken an attempt to design the DR control loop to compensate the delay issues for smooth frequency control in an inter connected power system. A new lead compensator is proposed in this work for mitigation of the delay problem in DR loop. The performance of the proposed delay compensator in DR loop is examined by considering two different two area power system, a wind integrated two-area thermal system and a two-area hydrothermal power system. The optimal power share between DR and the supplementary control are measured according to the PJM regional ISO/RTO real-time electricity market [97].

4.2. Frequency response modelling

4.2.1. ALFC Modelling of Two-Area Power System

The concept of the study is analyzed by considering a two area first order linear transfer function model of power system. The parameters taken for the two-area system for simulation are mentioned in the Appendix. Each area of the power system is having a thermal and wind energy generation unit. A grid connected DFIG is considered for WECS. The main motto of this work is to get smooth frequency control. So, DR is introduced in the traditional ALFC of the two-area power system. The delay in the system is considered as time varying delay whose value is taken in the range of 0-0.1sec for simulation. To compensate the communication delay present in the DR process, which jeopardize the system stability, a two stage lead compensator-based PI-controller is designed in the DR control path of ALFC. The study is analyzed by simulating a two area inter connected power which shown in Fig. 4.1. The proposed delay compensated DR control loop is presented in Fig. 4.2.

The DFIG based wind power sources are supplying real power to both the areas via the stator and rotor of the induction generator. Moreover, two end-to-end power electronics converters are connected with a DC link to build an interface between rotor and stator. This converter is capable to track wind energy over a wide range by using the principle of Maximum Power Point Tracking (MPPT) [12,20]. The penetration of wind energy at the time of load perturbation makes the system lower inertia due to the existence of power electronics converter in DFIG. This power electronics converter affects the natural dynamics of frequency change ΔF with respect to real power change ΔP in conventional generators. Ultimately, it averts from retorting change in system frequency. This inertia effect can be overcome through the grid side DFIG controller connected in wind energy conversion system [20].

In Fig. 4.1, capacity of each area is 2000MW in which conventional generator is generating 80% of total and rest 20% frequency support from Wind energy conversion system. So, real power generation in each area- i (1 and 2) by conventional and non-conventional generator are ΔP_{T_i} and ΔP_{DFIG_i} respectively which are added in the system. DR-control loop provides additional adjustment of real power from demand side to each area of the system during the load perturbation. The DR power is added to both the area as ΔP_{DR_i} . The only real

power is subtracted from the system is load deviation power ΔP_{D_i} . As the system is interconnected power system, so tie line power deviation $\Delta P_{Tie,i}$ does exist in the system and it will be adding to the particular area of the system if the area is being paid power from the tie line or else it will be subtracted.

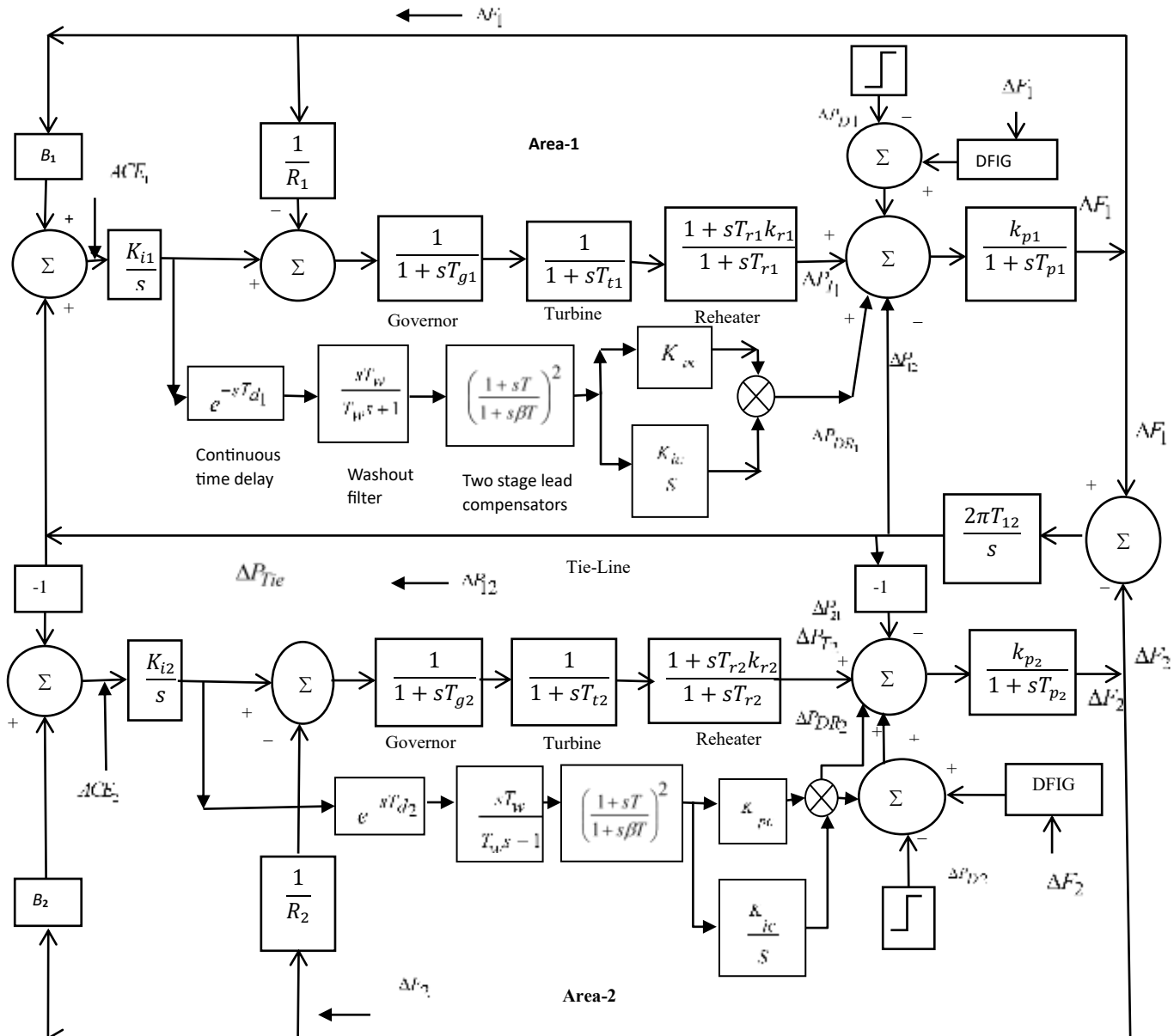


Fig. 4.1 Transfer function model of the test system with proposed DR.

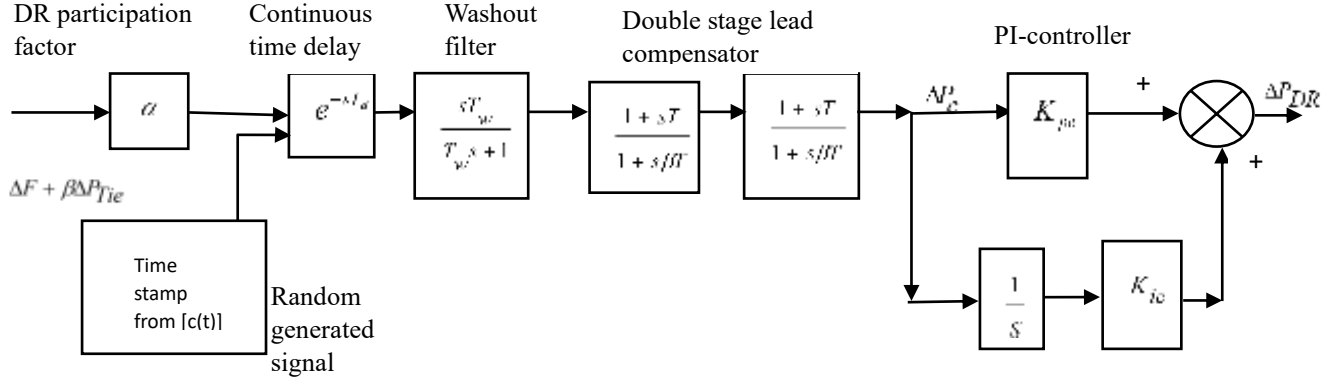


Fig. 4.2 Proposed controller for delay compensation in DR loop.

When the load perturbation occurs in either area of the system the generation and demand side power changes immediately to match the new load in each area. At steady state the power balance equation for any area- i can be expressed as:

$$[\Delta P_{T_i} + \Delta P_{DFIG_i} + \Delta P_{DR_i} \pm \Delta P_{Tie,i} - \Delta P_{D_i}] * \frac{K_{P_i}}{1 + sT_{P_i}} = \Delta F_i \quad (4.1)$$

where, $K_{P_i} = \frac{1}{D_i}$ Hz/p.u.MW, $T_{P_i} = \frac{2H_i}{fD_i}$ second.

K_{P_i} is power system gain, D_i is damping constant and T_{P_i} is power system time constant, H_i inertia constant of area- i and f is the nominal frequency of the system in Hz.

So, frequency aberration of area- i due to load perturbation can be derived from (4.1) as:

$$\frac{2H_i}{f} \Delta F_i \cdot s + D_i \Delta F_i = [\Delta P_{T_i} + \Delta P_{DFIG_i} + \Delta P_{DR_i} \pm \Delta P_{Tie,i} - \Delta P_{D_i}] \quad (4.2)$$

$$\Rightarrow \Delta F_i = \frac{1}{2.H_i \cdot s + D_i} * [\Delta P_{T_i} + \Delta P_{DFIG_i} + \Delta P_{DR_i} \pm \Delta P_{Tie,i} - \Delta P_{D_i}] \quad (4.3)$$

Note that in (4.3) all the real power deviations and frequency deviation are in s-domain and are in per unit value for the analysis.

4.2.2. Inertia control DFIG

The detail modelling of DFIG controller with its mathematical expressions are well explained in chapter-2. To analyze the effect of inertia control on the frequency regulation, the derived power balance equation in (4.3) is used for the analysis. By considering (2.2) & (2.5) in chapter-2 and applying in (4.3), we get the time domain power balance equation as below:

$$\Delta P_{T_i} - \Delta P_{D_i} \pm \Delta P_{Tie,i} + (-K_{df} \frac{d\Delta f_i}{dt} - K_{pf} \Delta f_i) + \Delta P_{DR_i} = 2H_i \frac{d\Delta f_i}{dt} + D_i \Delta f_i \quad (4.4)$$

(Note: for area-i it is assumed that $\Delta f_0' = \Delta f_i'$)

$$\Rightarrow (2H_i + K_{df}) \frac{d\Delta f_i}{dt} = \Delta P_{T_i} - \Delta P_{D_i} \pm \Delta P_{Tie,i} - (K_{pf} + D_i) \Delta f_i + \Delta P_{DR_i} \quad (4.5)$$

The s-domain representation of (4.5) is expressed in (4.6).

$$\Delta F_i(s) = \frac{1}{2H_i^* s + D_i^*} * [\Delta P_{T_i} + \Delta P_{DR_i} \pm \Delta P_{Tie,i} - \Delta P_{D_i}] \quad (4.6)$$

$$\text{where, } 2H_i^* = 2H_i + K_{df}, D_i^* = D_i + K_{pf} \quad (4.7)$$

The new inertia constant H_i^* is obtained by arbitrarily varying the controller gain K_{df} . The system inertia increases with +ve value of K_{df} and this is possible within a feasible margin. Similarly, the damping constant D_i of the system is increased with +ve value of K_{pf} . So larger value of K_{pf} can provide better frequency damping.

Therefore, it proves that inertia control of DFIG is capable to increase the inertia of the system while supporting for frequency control of a wind integrated power system. So, the value of DFIG controller parameters K_{pf} and K_{df} are optimized in this work when DR is familiarized in conventional ALFC of the test model. The controller gains are tuned on the basis of getting smooth frequency regulation with lesser transient error and settling time with the help of PSO.

4.2.3. Mathematical Background with DR

The introduction of DR in ALFC enhances the frequency regulation process by balancing additional load between the DR control loop and the secondary LFC loop itself. This can be mathematically expressed as follows:

$$\Delta P_{D_i} = \Delta P_{S_i} + \Delta P_{DR_i} \quad (4.8)$$

where, $(\Delta P_{S_i}, \Delta P_{DR_i})$ are the power sharing from supplementary and DR control in i^{th} control area of the power system respectively.

The frequency deviation due to load perturbation in any area- i is analyzed through power balance equation in (4.6). The proposed DR control loop shares additional power which is shown in Fig. 4.2. The work included the modified DR control loop for smooth frequency control. The transfer function of the forward DR control path is mentioned in Section 4.3.3.

The steady state frequency deviation for the test system has been derived in (4.6) to examine the role of DR in frequency control process in which load is assumed to be disturbed in either area. In Fig. 4.3, $(G_i(s) = \exp(-T_{d_i}s))$ and T_{d_i} = delay time in i^{th} control area.

$$\Delta P_{DR_i} \cong G_i(s)\Delta P_{DR_i} \quad (4.9)$$

From (4.6),

$$\Delta F_i(s) = \frac{1}{2.H_i^*.s + D_i^*} * [M_i(s).[\Delta P_{S_i}(s) - \frac{1}{R_i}\Delta F_i(s)] - \Delta P_{D_i}(s) \pm \Delta P_{Tie,i} + G(s).\Delta P_{DR}(s)] \quad (4.10)$$

$$\Rightarrow (2.H_i^*.s + D_i^*).\Delta F_i(s) + \frac{M_i(s)}{R_i}.\Delta F_i(s)$$

$$= M_i(s).\Delta P_{S_i} - \Delta P_{D_i}(s) \pm \Delta P_{Tie,i} + G(s).\Delta P_{DR_i} \quad (4.11)$$

$$\Rightarrow \Delta F_i(s) = \frac{1}{\varphi_i(s)}.[M_i(s).\Delta P_{S_i}(s) + G_i(s).\Delta P_{DR_i}(s) \pm \Delta P_{Tie,i}(s)] - \frac{1}{\varphi_i(s)}.[\Delta P_{D_i}(s)] \quad (4.12)$$

$$\text{where, } \varphi_i(s) = 2.H_i^*.s + D_i^* + \frac{M_i(s)}{R_i} \quad (4.13)$$

As ΔP_{D_i} is step load change and it is a constant term in the system. So, the transfer function of the step load variation can be considered as:

$$\Delta P_{D_i}(s) = \frac{\Delta P_{D_i}}{s} \quad (4.14)$$

After considering (4.14) in (4.13), the frequency deviation at steady state can be uttered based on final value theorem as below:

$$\Delta F_{i,ss} = \lim_{s \rightarrow 0} s.\Delta F_i(s) = \frac{\Delta P_{S_{i,ss}} + \Delta P_{DR_{i,ss}} - \Delta P_{D_i}}{\varphi_i(0)} \quad (4.15)$$

The tie line power $\Delta P_{Tie,i}$ is assumed to be zero at steady state.

where,

$$\Delta P_{S_i,SS} = \lim_{s \rightarrow 0} s.M_i(s).\Delta P_{S_i}(s) \quad (4.16)$$

$$\Delta P_{DR_i,SS} = \lim_{s \rightarrow 0} s.\Delta P_{Tie,i}(s) = 0 \quad (4.17)$$

$$\Delta P_{Tie,i,SS} = \lim_{s \rightarrow 0} s.\Delta P_{Tie,i}(s) = 0 \quad (4.18)$$

$$\varphi_i(0) = 2.H_i^*.s + D_i^* + \frac{M_i(0)}{R_i} = D_i^* + \frac{1}{R_i} \approx B_i \quad (4.19)$$

In (4.19) the expression $\varphi_i(0)$ is the frequency bias of the system i.e., (B) So, after including $\varphi_i(0)$ in (4.15), the steady state frequency deviation can be expressed as:

$$\Delta F_{i,ss} = \lim_{s \rightarrow 0} s.\Delta F_i(s) = \frac{\Delta P_{S_{i,ss}} + \Delta P_{DR_{i,ss}} - \Delta P_{D_i}}{D_i^* + \frac{1}{R_i}} \quad (4.20)$$

It can be concluded from (4.20) that if load trouble size meets with the combined control power contributed from supplementary control and DR- control loop, the frequency deviation can verge to zero at steady state. So only supplementary control is not sufficient to force the system having zero frequency deviation at steady state. In addition, DR control gives more freedom to neutralize the frequency aberration at steady state as it complements the supplementary control in LFC. So, introduction of DR in LFC could able to regulate the frequency in more reliable way. Also, it helps independent system operator (ISO)/ regional transmission organization (RTO) for economic power system operation. In order to achieve good frequency regulation at steady state the control effort in LFC is splitted between the supplementary and DR control loop.

4.3. The Proposed controller

4.3.1. Stability Analysis with Proposed Controller

The stability of the dynamic interconnected power system can be easily analyzed through small signal stability study. The present study investigated through system modelling and state-space representation. Here the two-area wind-integrated DR-LFC model is

represented with its first order transfer function approach. The formulation of state-space equation for the proposed model highly depends of the general form of equation represented in (4.21) [2,95].

$$\Delta \dot{x} = A\Delta x + Bk \quad (4.21)$$

$$\Delta y = C\Delta x \quad (4.22)$$

$$|\lambda I - A| = 0 \quad (4.23)$$

Where, $\Delta x, k$ are state variable and control variable vectors respectively. The matrices A, B, C are the constant matrices and its dimension depends on the system problem. Referring to those above general form of state equation, the state variable vector for the proposed system is represented as tails:

$$\Delta x = [\Delta F_1, \Delta F_2, \Delta P_{12}, \Delta P_{T_1}, \Delta P_{T_2}, \Delta P_{DR_1}, \Delta P_{DR_2}, \Delta P_{S_1}, \Delta P_{S_2}, \Delta P_{DFIG_1}, \Delta P_{DFIG_2}]$$

$$k = [K_i, K_{pf}, K_{df}, K_{pc}, K_{ic}]$$

Mainly the stability test for the present study is analyzed through the damping factor and eigen values calculation. The higher values of the damping ratio indicate more degree of stability of the system and vice versa.

Hence, proper selection of all controller gains ($K_i, K_{pf}, K_{df}, K_{pc}, K_{ic}$) are required for complete progress in performance of the system.

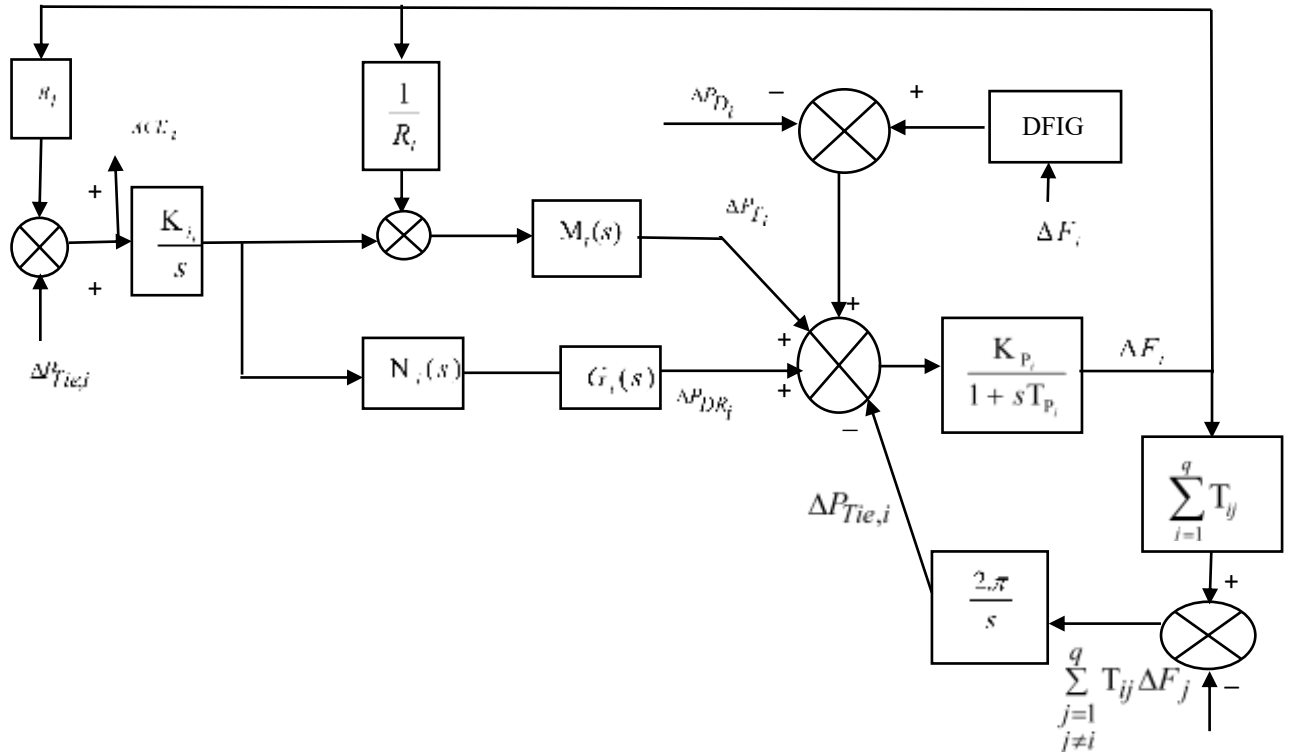


Fig. 4.3. Modified i^{th} area wind integrated power system model with delay compensated DR model in frequency control loop.

4.3.2. Synthesis of Lead Compensator

Though DR is a challenging process for frequency regulation of modern power system but, DR delay produced phase lag which causes the system unstable and oscillatory. The present issue may be solved by the use of lead compensator in the DR control path, as lead compensator is capable to decrease overshoot. Also, it speeds up the system performance. Therefore, lead compensator has been coupled with a PI based DR controller to improve the system overshoot.

The lead compensator circuit shown in Fig. 4.4 is capable of producing phase lead output signal when phase lag input is applied to it. The transfer function of the compensator network can be expressed based on the general transfer function as:

$$G_c(s) = \frac{s + z}{s + p} \quad (4.24)$$

Where Z is zero and P is pole of the system. In the present work, lead compensator is placed in the DR loop in both the areas. The input to the compensator is area control error (ACE)

which accomplished with time delay. The output of compensator (P_c) as shown in Fig. 4.2 again passes through a PI controller to provide smooth DR output. Hence, the gain of the lead compensator in DR loop can be derived referring to (4.24) as below:

$$\text{Let } z = \frac{1}{T}, \quad P = \frac{1}{\beta T} \quad (4.25)$$

From (4.24),

$$G_c(s) = \frac{E_0(s)}{E_i(s)} = \frac{s + \frac{1}{T}}{s + \frac{1}{\beta T}} = \beta * \frac{sT + 1}{1 + s\beta T} \quad (4.26)$$

where, $\beta = \frac{R_2}{R_1 + R_2}$, $\beta < 1$, $T = R_1 C$,

$$E_i(s) = ACE = B\Delta F + \Delta P_{Tie}, \quad E_0(s) = P_c$$

Where (B) is frequency bias. To get frequency response we put, $s = j\omega$. So, (4.26) is expressed in frequency domain as:

$$G_c(\omega) = \beta \left(\frac{1 + j\omega T}{1 + j\omega\beta T} \right) \quad (4.27)$$

Phase response of the frequency response can be derived as below:

$$\angle G_c(j\omega) = \tan \theta = \tan^{-1}(\omega T) - \tan^{-1}(\omega\beta T) \approx \theta \quad (4.28)$$

The basic condition for maximum compensation is $\frac{d\theta}{d\omega} = 0$, $\omega = \omega_m$

$$\omega_m = \sqrt{(\omega_{c1} \cdot \omega_{c2})} = \sqrt{\left(\frac{1}{T} \cdot \frac{1}{\beta T} \right)} = \frac{1}{T\sqrt{\beta}} \quad (4.29)$$

where, $\omega_{c1} = \frac{1}{T}$, $\omega_{c2} = \frac{1}{\beta T}$

This, (T) is the design parameter to build a lead compensator. This can be obtained by tuning the parameter for the better performance of the system or can be obtained by analyzing the system stability in presence of lead compensator and any stability criterion like Bode Plot criterion, Nyquist stability criterion may be used to get the compensator parameters. In this study (T) & (βT) are chosen for better phase compensation of system and whose values are generally specified in [46].

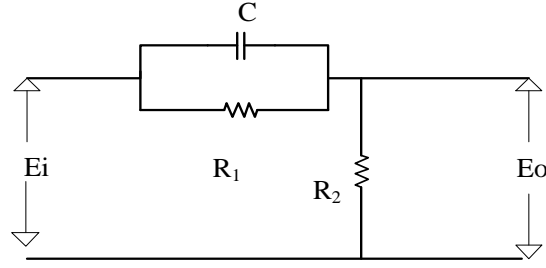


Fig. 4.4. Phase Lead network.

4.3.3. The Structure of Two Stage Lead Compensator Plus PI-Based DR Delay Controller

The structure of double lead plus PI based DR controller is implemented with conventional ALFC to reduce the influence of communication delay on DR loop for frequency control which is shown in Fig. 4.2. Though DR-controller can provide the cost-effective way of frequency control but the existence of delay in DR loop leads the system into phase lag. The controller structure consists of a participation factor, a washout filter, two-stage lead compensator and a PI controller. The participation factor provides the information to the DR about the quantity of sharing power to be adjusted from demand side. The washout filter serves like a high pass filter with time constant, whose value for the study is taken as 6 seconds [2]. The lead compensator is used to reduce the overshoot created in the processing signal in DR loop due to the existence of delay in it. The output of the lead compensator block (ΔPc) passes through a PI controller block to get smooth frequency regulation for the overall system. The overall transfer function of the proposed DR controller is stated as

$$N(s) = \alpha \left(\frac{sT_w}{1 + sT_w} \right) \left(\frac{1 + sT}{1 + s\beta T} \right)^2 \left(K_{pc} + \frac{K_{ic}}{s} \right) \quad (4.30)$$

Where, $N(s)$ is transfer function of the projected controller model and α is DR participation factor. K_{pc} is proportional gain parameter, K_{ic} integral parameter of PI controller in DR loop.

4.3.4. Problem Formulation

Frequency regulation is the vital aspect of the power system. The problem associated with the frequency control of power system are frequency deviation, occurrence of damping

and delaying in settling time of the dynamic response of the system. In the present study, DR is participated in frequency control process. Though the participation of DR enhances the frequency control process but it badly effects the system damping and ultimately affect the stability because of presence of delay in DR loop. In addition to the DR controller, inertia control DFIG is used for frequency support from WECS. So that the damping effect in DR loop and inertia effect in wind energy sources are reflected in frequency deviation and overall settling time of the dynamic response. And hence, the objective of the study is to minimize either any one from frequency deviation and total settling time or minimize both. So, in this contest the generally used performance indices like Integral of Time Multiple of Absolute Error (ITAE), Integral Time Square Error (ITSE), Integral Absolute Error (IAE) and Integral Square Error (ISE) are tested for better performance of the system. Then, ITAE is considered as one of the objective functions for tuning controller gain, because it contributes more reduction in settling time and overshoot of the system. The second objective function is considered as overall settling time of the two-area power system. Hence the multi objective optimization problem is formulated as [96]:

$$J = w_1 \left[\frac{T_s - T_{s_{\min}}}{T_{s_{\max}} - T_{s_{\min}}} \right] + w_2 \left[\frac{ITAE - ITAE_{\min}}{ITAE_{\max} - ITAE_{\min}} \right] \quad (4.31)$$

where, T_s is total settling time which is the summation of settling time of frequency deviation in area-1, settling time of frequency deviation in area-2, and settling time of tie-line power deviation.

$T_{s_{\min}}$, $ITAE_{\max}$ are obtained by optimizing T_s individually.

$ITAE_{\min}$, $T_{s_{\max}}$ are obtained by optimizing $ITAE$ individually.

The optimization problem is considered as minimization problem subjected to

$$\begin{aligned} K_i^{\min} < K_i < K_i^{\max}, K_{pf}^{\min} < K_{pf} < K_{pf}^{\max} \\ K_{df}^{\min} < K_{df} < K_{df}^{\max}, K_{ic}^{\min} < K_{ic} < K_{ic}^{\max} \\ K_{pc}^{\min} < K_{pc} < K_{pc}^{\max}, K_{i1}^{\min} < K_{i1} < K_{i1}^{\max}, K_{i2}^{\min} < K_{i2} < K_{i2}^{\max} \end{aligned}$$

The PSO is used to tune the above five controller parameters to get minimum settling time and frequency deviation ($ITAE$). The optimization problem has been solved by PSO algorithm shown in Fig. 4.5. Then the stability test has been carried out by using eigen value analysis.

4.4. Simulation and Results

The integration of non-conventional energy sources like hydro, solar, wind etc. into the modern power system is gaining more and more reputation. Hence, hydro and wind are integrated into thermal system in a two-area power system in separate simulation model for the present study. Then, the proposed delay compensated DR loop is introduced in LFC of both the simulation model and frequency analysis for the two-area system is performed. The MATLAB and SIMULATION TOOLBOX is used to simulate the proposed models. At first the proposed controller is examined with a wind integrated two-area thermal power system which is shown in Fig. 4.1. Additionally, the same proposed controller is tested for a hydro-thermal two-area power system that referred from [12]. The capacity of each area of both the test model are assumed as equal in capacity i.e 2000 MW. Wherever, in the first test model, the contribution of frequency support from DFIG based WECS is same in both the area i.e 20% of total capacity of the area. The system performances are observed by considering 1% step load variation in area-1. To concise the paper, the system performances are analyzed only for 30% DR contribution in LFC. The controller gains for each test models are tuned by using PSO [26]. All the results for each test models are narrated in the following sub-sections.

4.4.1. Study on Wind Integrated Two-Area Thermal Power System

In this section, the system model is simulated for Fig. 4.1 whose parameters are given

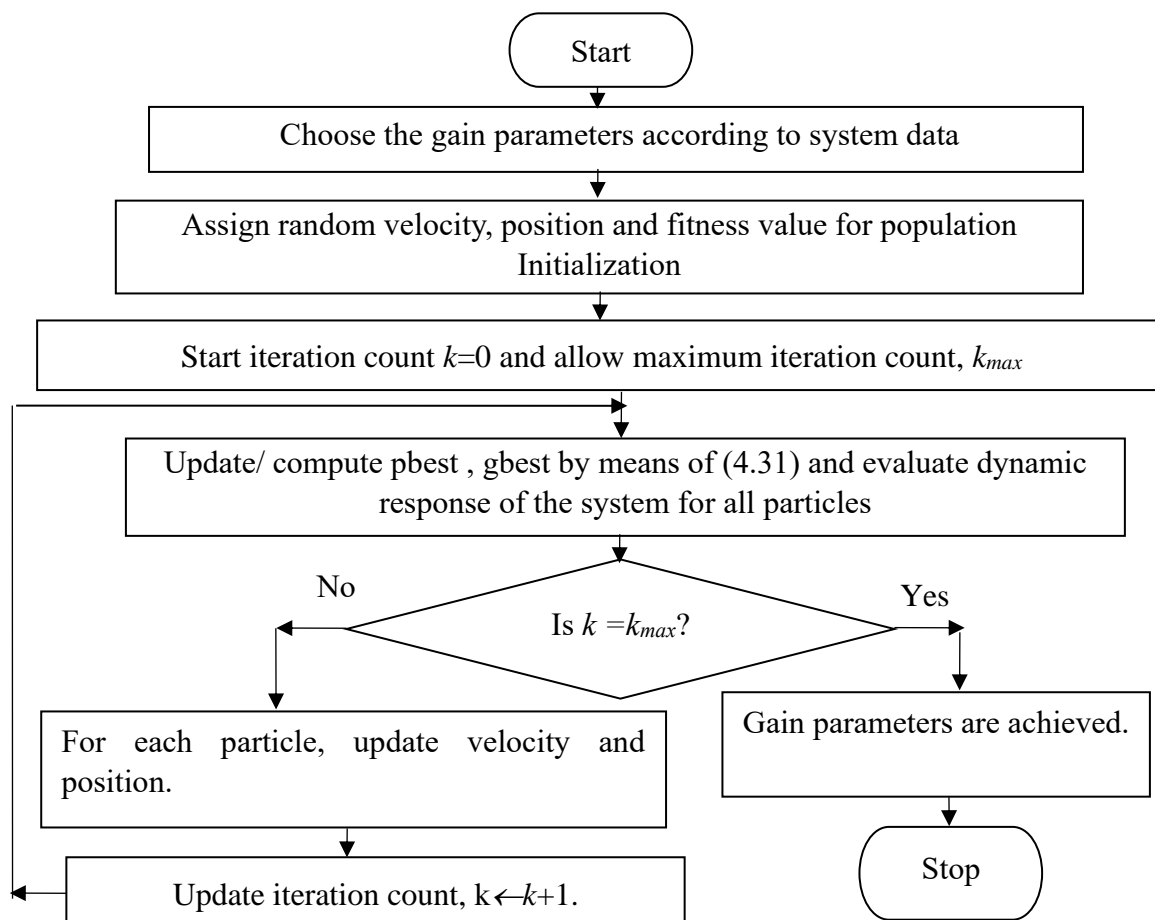


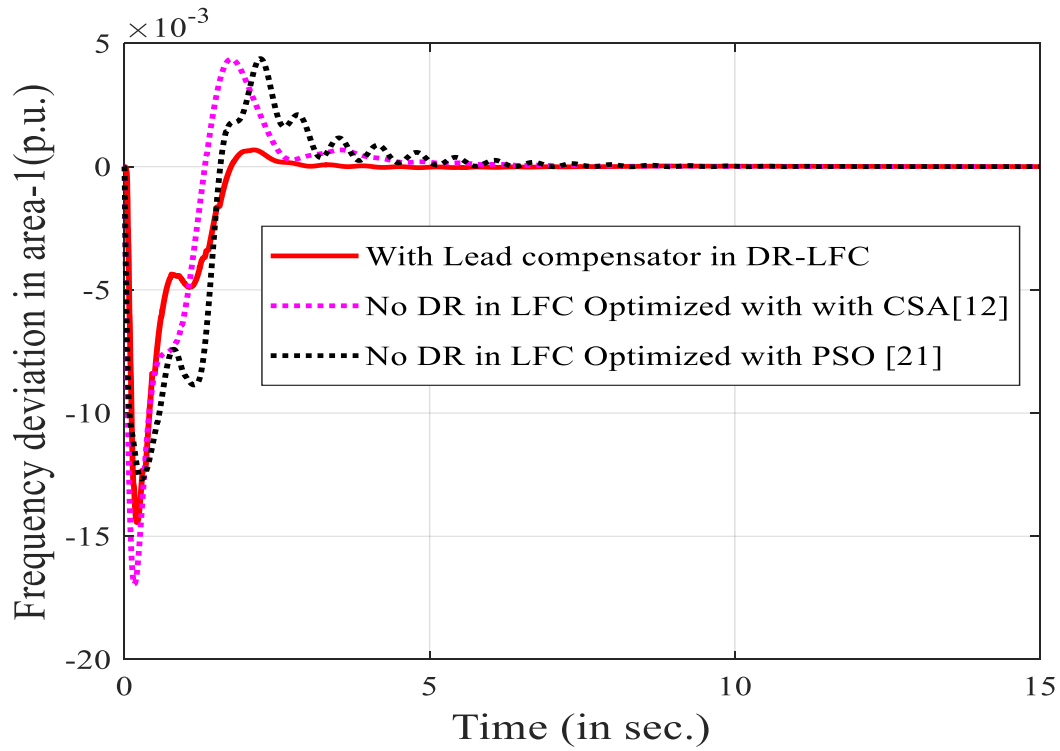
Fig. 4.5 PSO flow chart to tune control parameters.

in appendix. The capacity, the contribution of frequency support from DFIG and contribution of DR in LFC of each area of the systems are assumed identical for the study. Hence, the values of the controller parameters are optimized and supposed to be equal in both the areas.

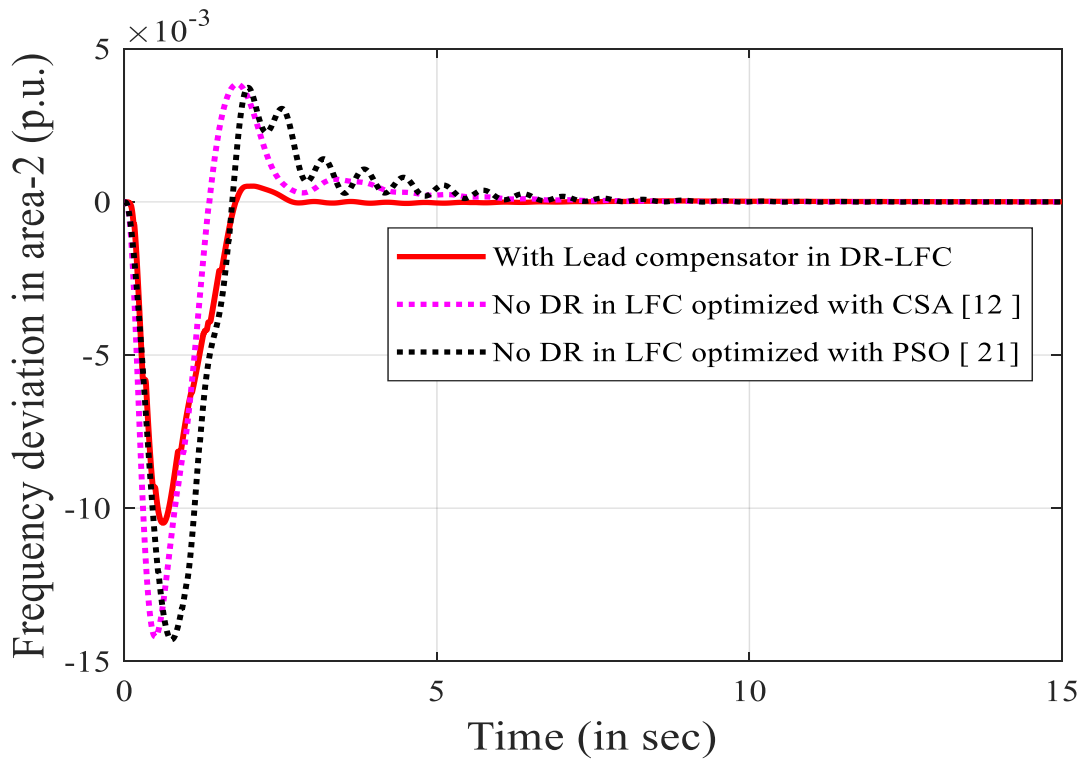
4.4.1.1. Comparative study of Proposed Delay Control DR in with Other Controllers in ALFC

The proposed method has considered the limitation and technical issues in [12,21] and enhances the system performance by implementing the modified DR controller in LFC of the system. Then the proposed controller is tuned with PSO along with the existing controller in [21], in coordinated manner considering objective function in (4.31). Then with the help of those tuned controller parameters, system dynamic performances are analyzed and are compared with existing controller in [12,21] which are shown in Fig. 4.6. The dynamic time

domain responses of frequency deviations in two areas i.e, $\Delta F_1, \Delta F_2$ and tie line power deviation ΔP_{Tie} are obtained for 1% step load change in area-1.



(a)



(b)

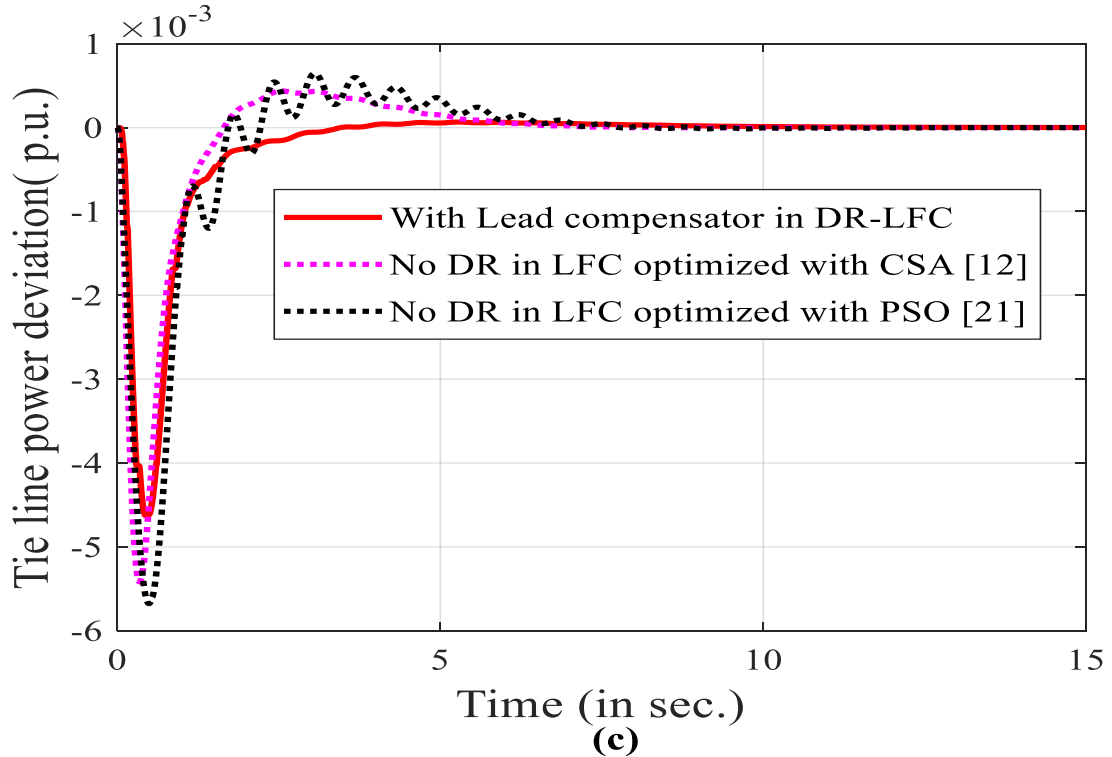


Fig. 4.6. The tie line power deviation and area frequency deviations for 1% load change in area-1 for different schemes of controllers.

Further, with the proposed optimized controller parameters, several performance indices which has not been optimized in the objective function are also evaluated and compared the performance with other existing controller for LFC problem. Corresponding parameters are tabulated in Table 4.1. The Table 4.1 shows lower values of settling time, ITAE and higher value of minimum damping ratio (MDR) with proposed controller in LFC of the test system. Results confirm the better performance with proposed controller.

For proper visualization of enhancement in system execution in terms of speed and stability with proposed delay compensated DR in LFC as compare to other existing controller in LFC [12,21], settling time and different performance indices like MDR are compared through bar diagram representation shown in Fig.4.7, Fig. 4.8 respectively. The result shows improved performances with proposed controller as compared to the existing controller for LFC problem in literature [12,21].

Table 4.1. Comparison of performance indices and MDR with different controllers in LFC by considering 20% frequency support from DFIG.

Different type of controller	Controller parameters					Settling time (in sec.)			(T_s) in Sec	Minimum damping ratio (MDR)	ITAE
	K_i	K_{pf}	K_{df}	K_{pc}	K_{ic}	ΔF_1	ΔF_2	ΔP_{Tie}			
Lead compensator-based DR in LFC (Proposed)	0.4158	0.29852	0.1266	2.9266	0.3497	12.47	9.27	9.9	31.63	0.5500	0.1714
without DR in LFC [12]	0.7218	0.2512	0.0975	-	-	24.53	25.56	20.81	70.90	0.2963	0.8994
without DR in LFC [21]	0.5412	0.2723	0.2902	-	-	31.10	30.06	21.34	82.50	0.2857	1.2773

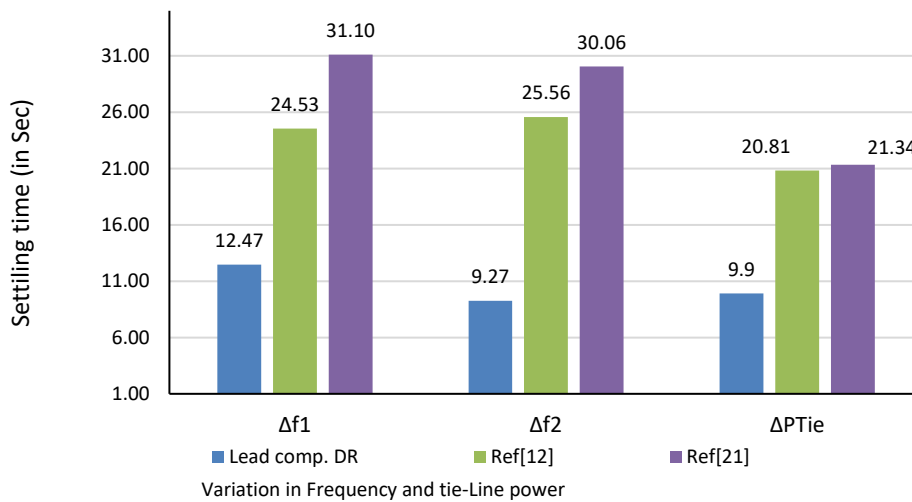


Fig. 4.7. Verdict of settling time with different controllers.

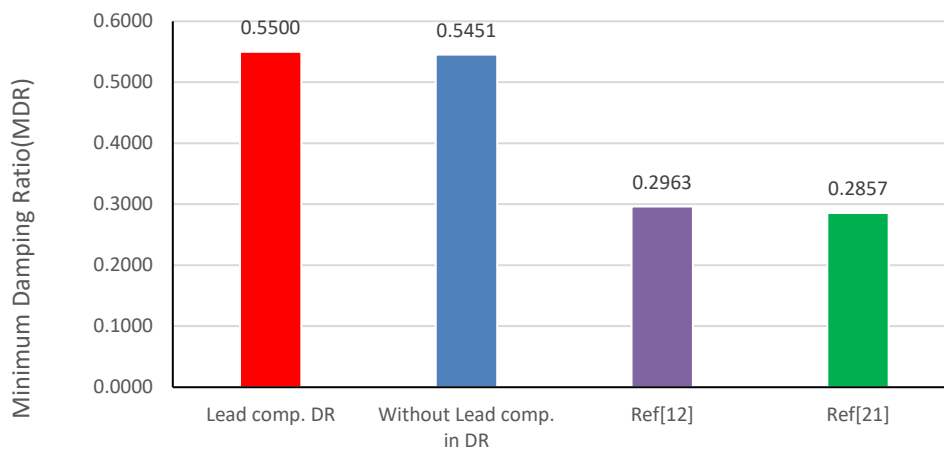


Fig. 4.8. Comparison of MDR with different controllers.

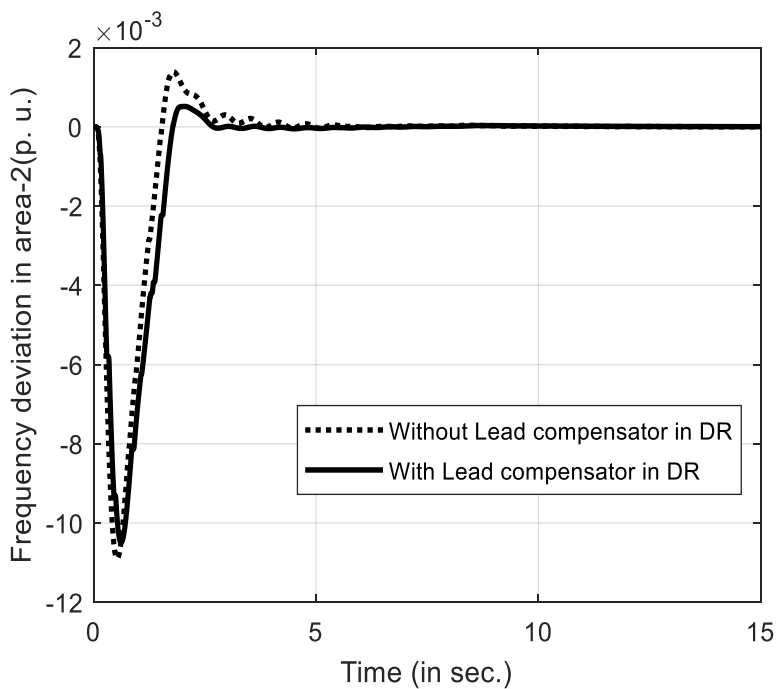
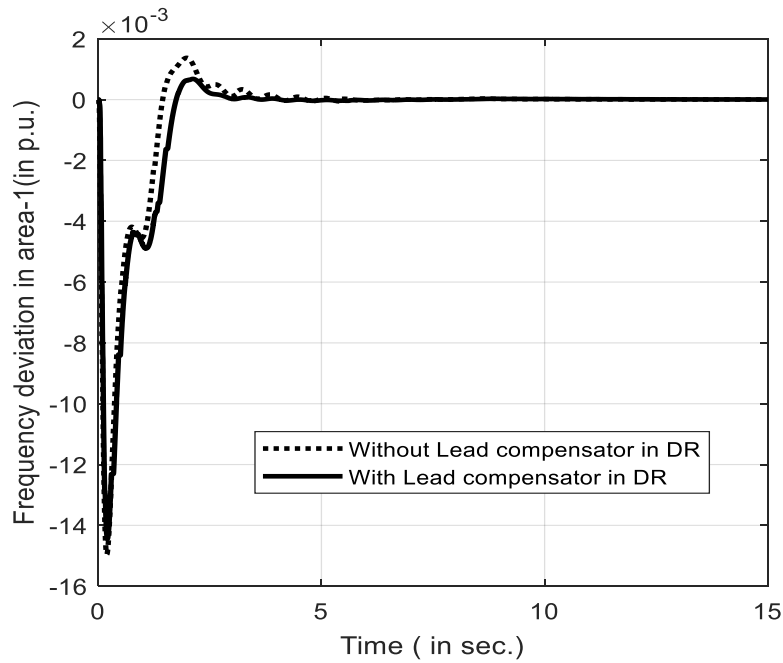
4.4.1.2. Comparative study Between Lead Compensator in DR and Without Lead Compensator in DR Controller

In the proposed study, lead compensator has taken major role to mitigate time delay effect in the DR control loop. So, the DR controller parameters and the inertia control parameters of DFIG are tuned in synchronized way for different objective functions. The best compromise results are obtained when the objective function is formulated as weighted sum normalized form of multi objective optimization considering as single objective problem as mentioned in equation (4.31). Corresponding results are presented in the Table 4.2. Further, the stability of the power system is verified in occurrence of the proposed controller by Eigen value calculation. Table 4.3 shows the comparison results of several performance indices and eigenvalues obtained with tuned controller parameters in presence of lead compensator in DR-LFC and in absence of lead compensator in DR-LFC. The result shows that lead compensator can improve the overshoot of the system and proposed controller does not affect the stability of the system, moreover it can able to improve the oscillation of the system as minimum damping ratio is improving.

Table 4.2. Best compromised output with lead compensator DR in ALFC for 1% load variation in area-1.

Output variables	Different objective functions used with 30% DR contribution in LFC		
	T_s (Total settling time in sec.)	$ITAE$	Objective function of equation (4.31) (Best compromise solution)
T_s (sec.)	31.0100	119.15	31.63
ITAE	0.176495	0.128709	0.1714
Multi-objective Function	31.0100	0.128709	0.174370
ITSE	7.5777e-04	4.4566e-04	7.3248e-04
IAE	0.0688	0.0514	0.0677
ISE	4.7902e-	3.2405e-04	4.6872e-04

The time domain performances of tie-line power deviation ΔP_{Tie} and frequency deviations in both the areas i.e, $\Delta F_1, \Delta F_2$ are obtained for the best compromise solution with and without lead compensation in DR loop. Fig. 4.9 shows corresponding time domain responses of the test system. For proper visualization of improvement in overshoot with lead compensator has been represented by bar diagram shown in Fig. 4.10.



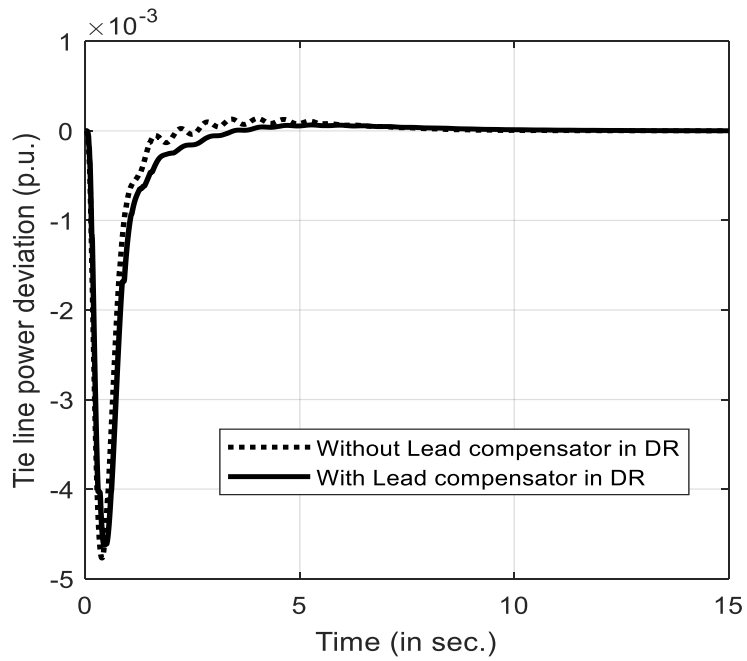


Fig. 4.9. The tie line power deviation and area frequency deviations for 1% load variation in area-1 with lead compensator in DR and without lead compensator in DR.

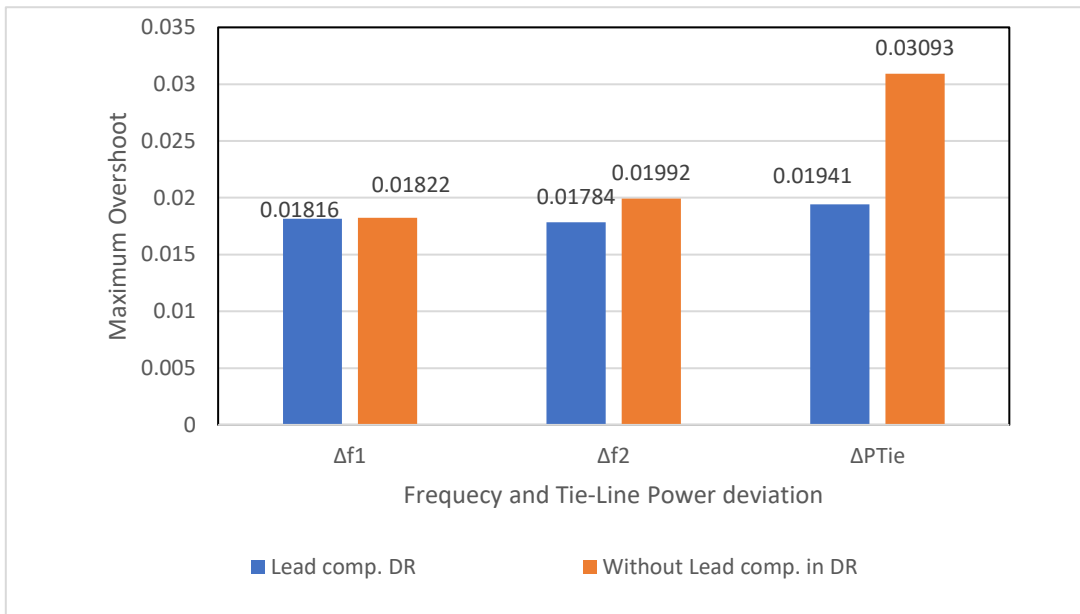


Fig. 4.10. Judgement of maximum overshoot with and without lead compensator in DR controller.

The multi objective optimization is carried out by considering the objective function in equation (4.31) with and without lead compensator in DR loop and the results are shown in Table 4.3. The result in the Table 4.3 shows lower values of settling time, *ITAE*, maximum overshoot and higher values of *MDR* when lead compensator introduced in DR loop. These results verify the effectiveness of lead compensator for improvement in system performance indices like maximum overshoot, settling time, *ITAE* and *MDR*.

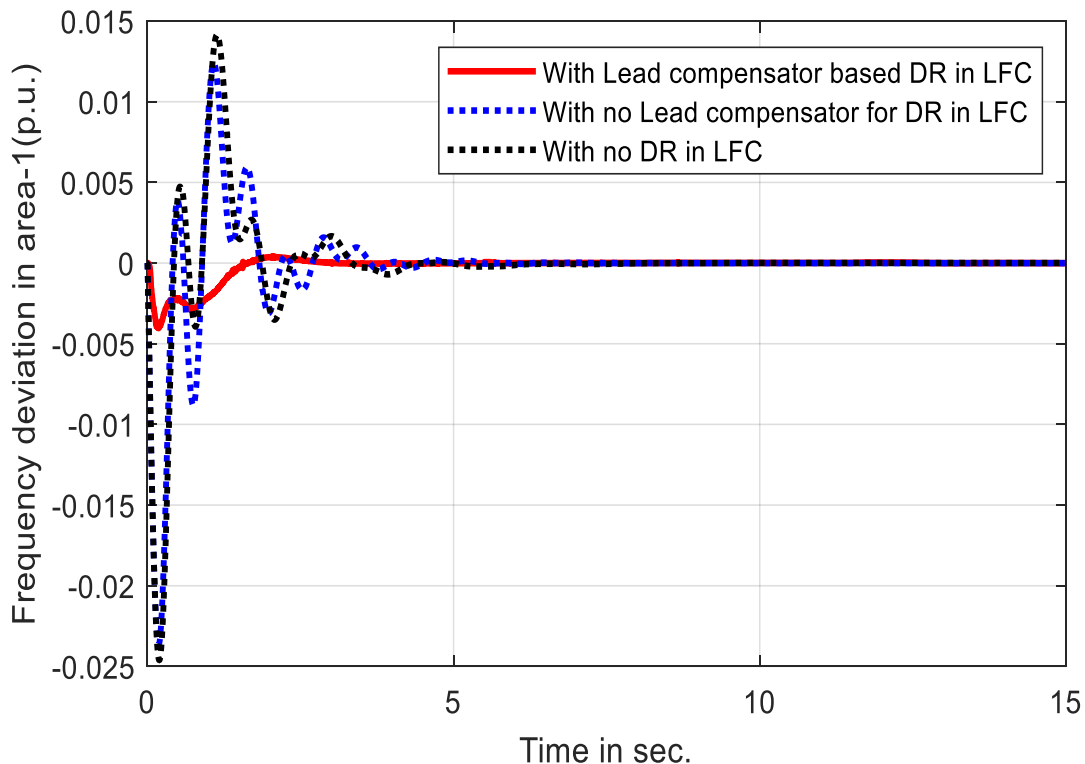
Table 4.3. Comparison of several performance indices and maximum overshoot with tuned controller gain.

Output variables		Best compromised solution	
		Without Lead compensator in DR	With Lead compensator in DR
T_s		54.29	31.36
ITAE		0.2174	0.1714
Maximum overshoot	ΔF_1	0.01822	0.01816
	ΔF_2	0.01992	0.01784
	ΔP_{Tie}	0.03093	0.01941
MDR		0.5451	0.5500
Eigenvalues		1.0e+02 *	1.0e+02 *
		-1.0045 + 0.0000i	-0.7728 + 0.0280i
		-1.0045 + 0.0000i	-0.7728 - 0.0280i
		-0.1263 + 0.0000i	-1.0046 + 0.0000i
		-0.0586 + 0.0478i	-1.0046 + 0.0000i
		-0.0586 - 0.0478i	-0.7728 + 0.0286i
		-0.1263+0.0000i	-0.7728-0.0286i

4.4.2. Study on Wind Integrated Two-Area Hydrothermal Power System

The contest with the hydrothermal system is the difference between their governor characteristics of individual hydro and thermal unit [27]. Due to high water inertia in hydro system, it arrests the frequency deviation earlier than thermal system. Hence overall system performance may vary from merely thermal two area power system. In this section of approach, the hydrothermal system is tested [6]. In the model each area of the power system is having capacity of 2000MW. The area-1 is having a thermal system of same nominal parameter as thermal system in Fig. 4.1. The area -2 is having a hydro unit whose nominal parameters are taken from [6]. The LFC integral controller parameters (K_{i1} =integral gain of thermal unit, K_{i2} = integral gain of thermal unit) and proposed DR controller are optimized in coordinated

manner with PSO by considering the objective function in equation (4.31) to get better dynamic performances of the system. The system behavior is analyzed and controller gain are tuned by assuming 1% load variation in thermal (area-1) unit. Several performance indices of the system like ITAE, IAE, ITSE, ISE and MDR are obtained with the tuned controller which are shown in Table. 4.4. To verify the effectiveness of the proposed DR controller in LFC of hydrothermal system, the time domain performances like frequency deviation in both the area $\Delta F_1, \Delta F_2$ and tie line power deviation ΔP_{Tie} are obtained for 1% step load change in area-1. Moreover, the same performances are compared with the performances of the hydrothermal system when DR present in the system without any delay compensation and in absence of DR in LFC which are shown in Fig. 4.11. Fig. 4.11 shows better dynamic performances with lead compensator-based DR controller in LFC. Also, it can be cleared from the Fig. 4.11, the lead compensator in DR loop improves the stability and reduces the peak over shoot in system dynamic performances. The reduction in values of time errors and increase in MDR value obtained in Table. 4.4 indicates effective contribution of lead compensated DR controller in LFC towards more degree of stability compared to other form of LFC techniques mentioned. Additionally, Fig. 4.11 elucidates, only including DR in LFC of hydrothermal system can able to reduce the settling time error but the lead compensator-based DR controller in LFC can capable to reduce the damping and peak overshoot along with reduced settling time.



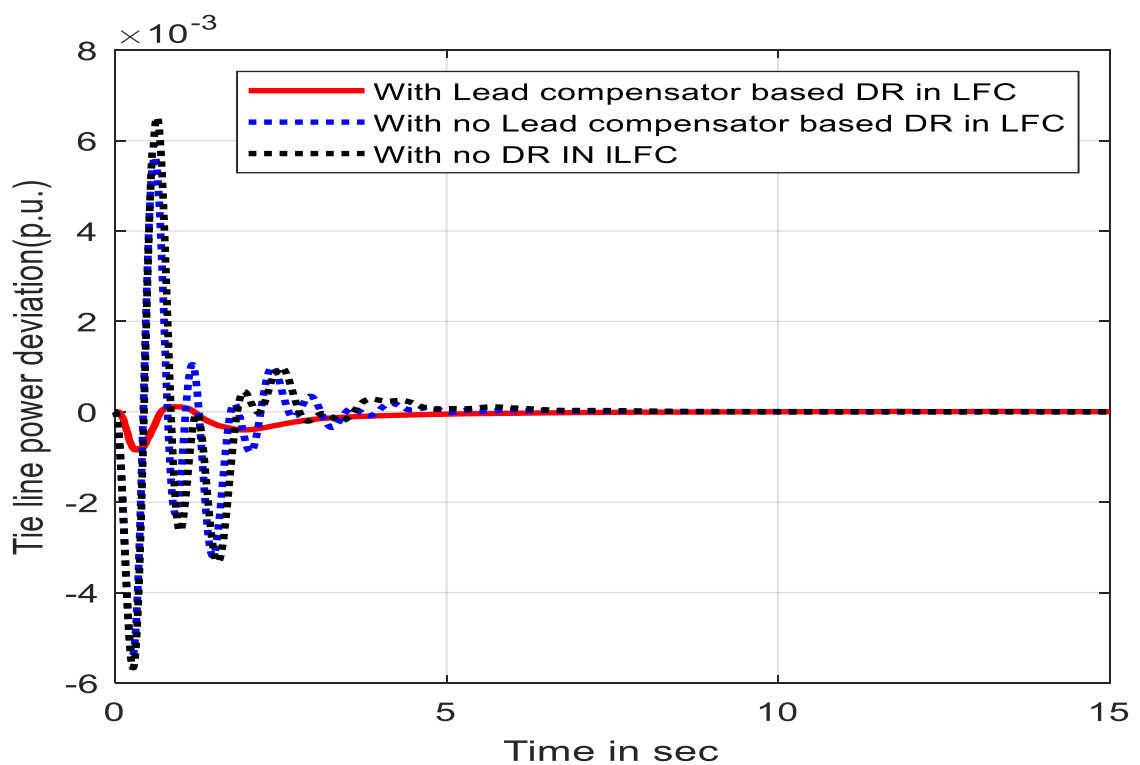
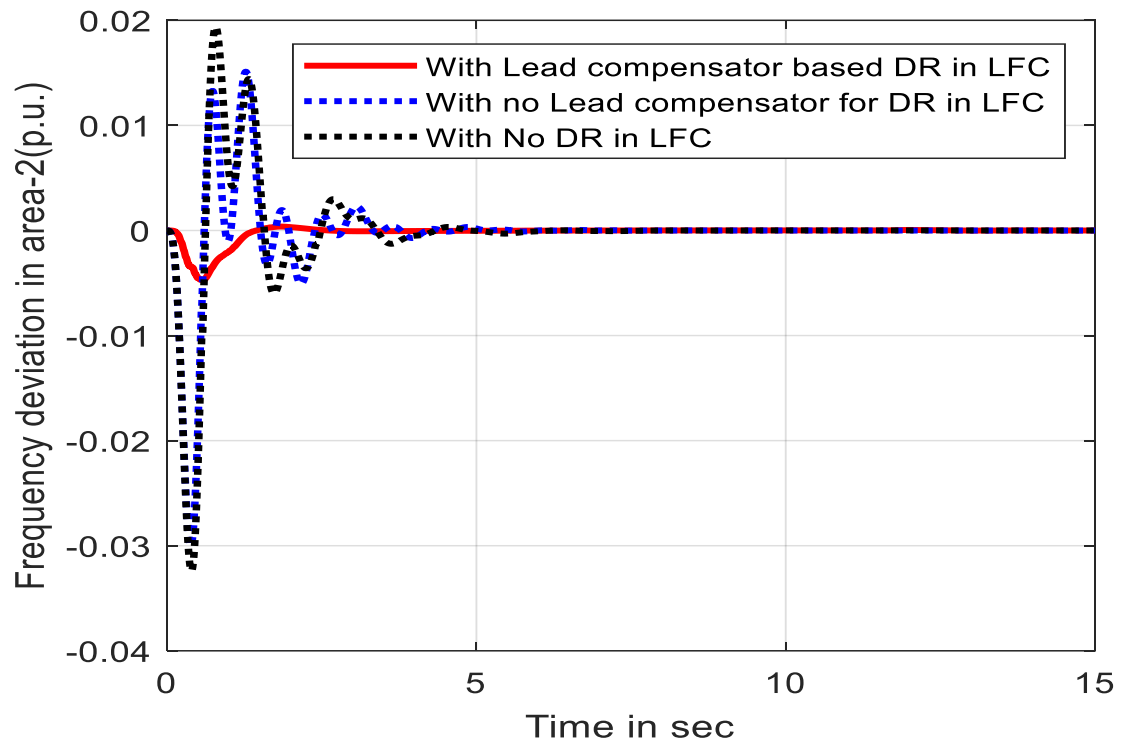


Fig. 4.11. The tie line power deviation and area frequency deviations for 1% load change in area-1 with and without different DR controller for hydrothermal system.

Table 4.4. Comparison of performance indices and MDR with and without different DR controllers in LFC of a Hydrothermal inter connected power system.

Different type of controller in LFC	Controller parameters				(T_s) in Sec	Minimum damping ratio (MDR)	ITAE	ITSE	ISE	IAE
	K_{i1}	K_{i2}	K_{pc}	K_{ic}						
Delay Compensation based DR	-2.2467	0.0093	5.3888	3.0671	32.68	0.2191	0.0737	7.5576e-05	4.9362e-05	0.0204
Without Delay Compensation for DR	-1.5638	0.01244	0	0	47.73	0.1027	0.2967	0.0030	0.0015	0.0944
In absence of DR	-2.0873	-0.0947	0	0	58.470	0.1308	0.4396	0.0039	0.0019	0.1259

4.5. Sensitivity Analysis with The Proposed Controller

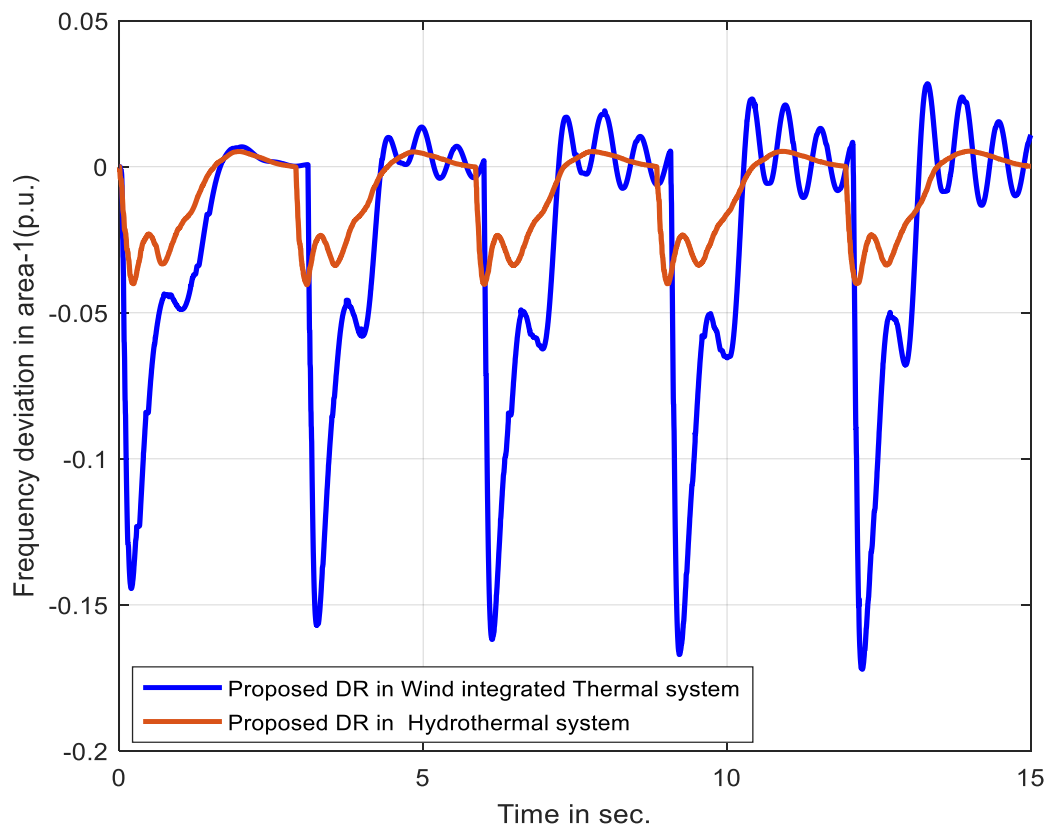
To study the robustness of the proposed controller for the approached systems, the system parameters and operating conditions are varied. At first, the system parameters like washout filter time constant in DR loop T_w , WECS time constant T_A , Equivalent WECS inertia H_e for wind integrated thermal system in the range of +50% to -50%. in step of 25%. This sensitivity test has been done with PSO tuned controller parameter for proposed DR controller in LFC of wind integrated thermal system when 1% load change in area-1. Furthermore, the system performance indices such as ITAE, MDR and settling time for $\Delta F_1, \Delta F_2, \Delta P_{Tie}$ are obtained with corresponding system parameter variations which are shown in Table. 4.5. The results in Table. 4.5 proves that the variation in system parameters have not degraded the system performances and are merely changed for $\pm 50\%$ of parameters change.

Further to compare the robustness between the hydrothermal system and wind integrated thermal system in presence of proposed controller, a continuous operating load change has been assumed in the range of 0% to 50% in a step of 10% in area-1 for total simulation time. The sensitivity test has been done when PSO tuned controller parameters are used in the systems. The dynamic responses like $\Delta F_1, \Delta F_2$ and ΔP_{Tie} are obtained for both the test systems with continuous load change which are shown in Fig. 4.12. Fig. 4.12 reveals that even for continuous load change, the system is hardly degraded their performances. Additionally, result shows

hydrothermal system is more robust with proposed controller for the continuous variation of operating load as compared to the wind integrated thermal system due to its higher inertia.

Table 4.5. Comparison of several performance indices and maximum overshoot with tuned controller gain.

Parameter Change	% Change	Wind integrated Thermal System				
		ITAE	Settling Time			MDR
			ΔF_1	ΔF_2	ΔP_{Tie}	
Nominal	0	0.1714	12.47	9.27	9.9	0.5500
T_g	+50	0.1713	15.20	16.12	10.11	0.5419
	+25	0.1711	13.54	17.41	10.57	0.3467
	-25	0.1719	13.80	10.32	10.69	0.5506
	-50	0.1726	20.13	9.620	9.90	0.3896
WECS time constant (T_A)	+50	0.1728	17.52	13.56	11.42	0.5967
	+25	0.1715	14.34	13.190	10.72	0.6012
	-25	0.1751	15.00	11.990	10.64	0.4759
	-50	0.1799	19.71	13.90	19.31	0.4145
Equivalent WECS inertia (H_e)	+50	0.1744	18.05	14.20	11.51	0.5469
	+25	0.1731	16.95	11.640	9.64	0.5485
	-25	0.1721	14.82	12.86	10.63	0.5493
	-50	0.1771	15.93	14.89	12.27	0.5273



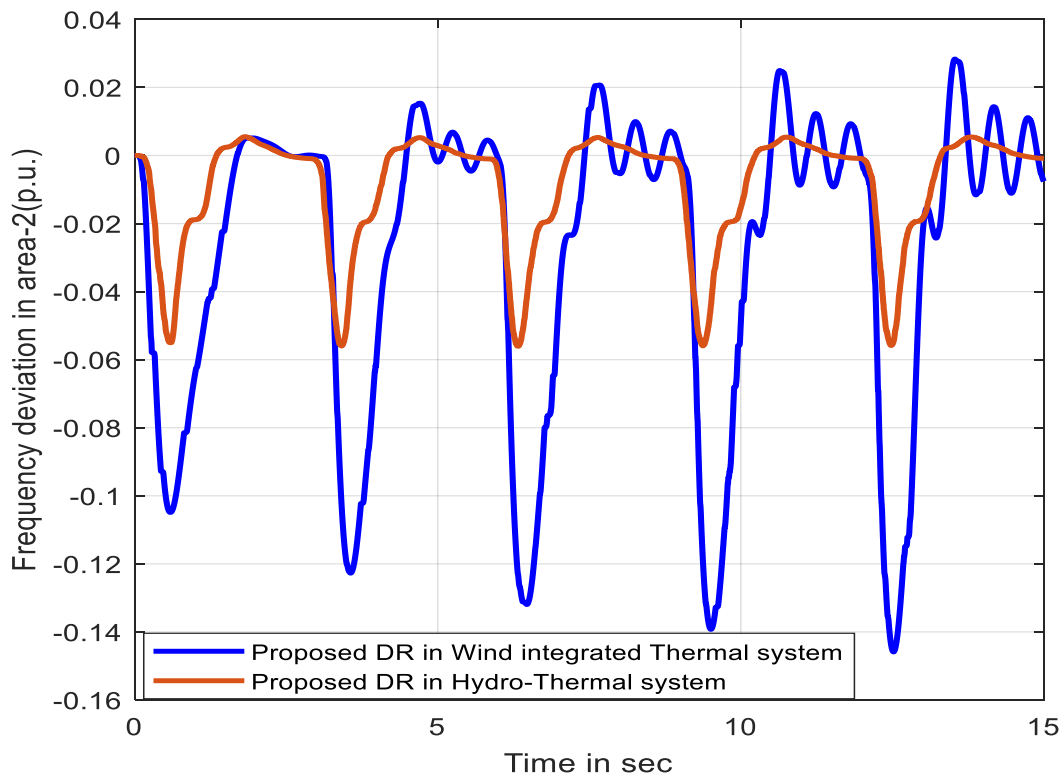
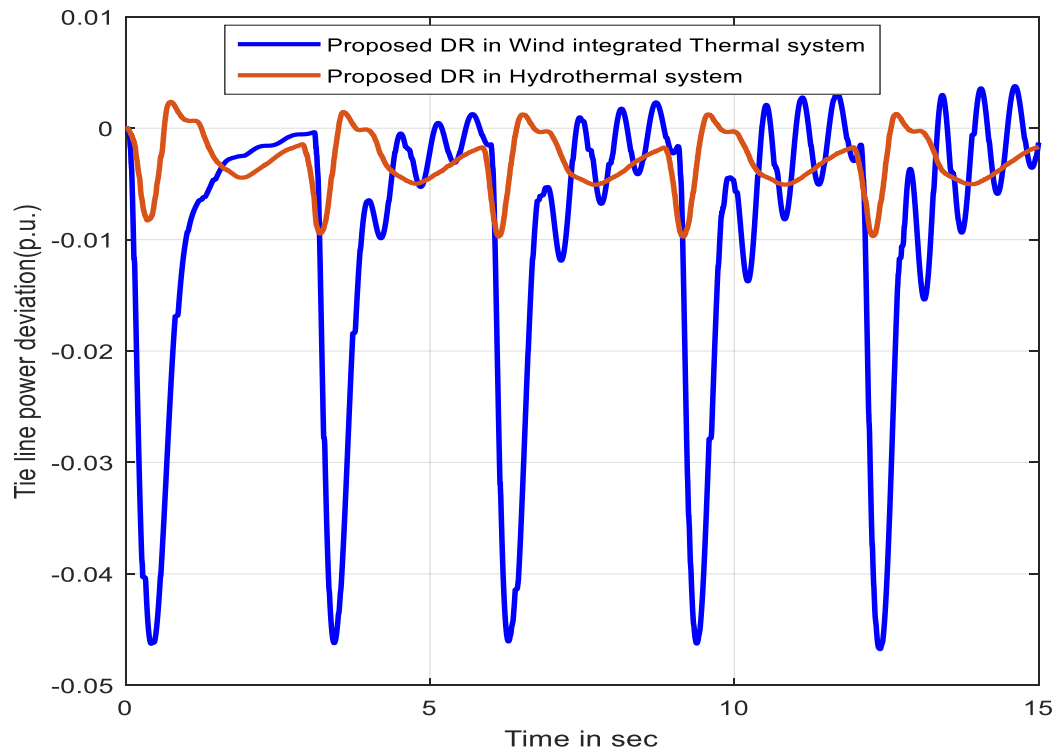


Fig. 4.12. ΔF_1 , ΔF_2 and ΔP_{Tie} of different power system for continuous load change (from 0% to 50%) in area-1 with proposed DR in ALFC.

4.6. Discussion

In this section, the main outcomes, comparisons with other past studies and research carried out, implications and other critical analysis of the outcomes, strengths and weaknesses of the present studies are described as follows:

- The improvement of this DR control scheme for frequency regulation over other published research work is the modified delay compensator in DR loop, which comparatively enhances the performance of the power system.
- The results presented in the simulation and result Section demonstrate that the proposed delay compensated DR controller is efficient for effective frequency regulation in a delay-introduced demand side frequency regulation scheme. This proposed delay compensator is working flawlessly for both wind-integrated thermal system and hydrothermal system. Especially, due to the addition of modified lead compensator-based PI controller in DR loop collaborated with AGC, the overshoot, settling time, frequency deviation and tie-line power deviation are decreasing. Also, the system oscillations die out drastically faster thereby improving the system stability.
- Though DR is a good solution for frequency regulation itself, but with the addition of modified delay compensator in DR, dynamic performances further improve the earlier improvement of the power system performances in terms of overshoot, settling time, frequency deviations and tie-line power deviation. The simulation results for the wind integrated two area thermal test system reveals that, DR reduces the settling time of 23% while lead compensator-based DR could able to reduce the settling time of 56%. Similarly, while DR reduces the ITAE of 75%, the proposed controller in DR could be able to reduce it of 81%. Simulation results for two area hydrothermal test system reveal that, while DR reduces the settling time of 12%, lead compensator-based DR could able to more reduce the settling time of 44%. Similarly, while DR reduces the ITAE of 38%, the proposed controller in DR could be able to reduce it of 83%. Furthermore, it has been observed that damping ratio increases in the dynamic performances of both the test system with proposed delay compensated DR in ALFC. The damping ratios are mentioned in Table-4.3 and Table-4.4 for wind integrated two area power system and two area hydrothermal system respectively. This proves that stability increases with addition of proposed delay compensator in DR. Also, the robustness of the proposed controller is scrutinized for both the test system for various

parameters variation in the range of $\pm 50\%$ and continuous load variation in the range of 0-50% of its nominal values. The results show that system performances are changing negligibly with the above load and parameter variations. Also, it has been observed that the proposed controller shows more robustness for hydrothermal system as compared to wind integrated thermal system.

- The present study is limited to the application of the proposed modified delay compensator based DR controller to the two-area hydrothermal power system and two-area wind integrated thermal system. In future, it can be examined for widely spread integrated modern power system having conventional and many non-conventional power generations along with storage devices to check the effectiveness of the proposed controller. The uncertainty of wind is not envisaged in this model, whereas only 20% frequency support is considered from wind. Hence, in future the uncertainty issue can be considered for any renewable energy integrated in the system for frequency regulation in presence of proposed delay compensated DR controller. The participation factor for DR contribution in ALFC is considered fixed in this study; it may be optimized in future.

4.7. Conclusion

To summarize, this extensive study analyzes the frequency regulation in ALFC of a DR collaborated power system. The significant shortcoming in DR is communication delay that appears in the system during sending commands from the control center to controllable loads for balancing the system and receiving response. Therefore, in the present study, a modified delay compensator is envisaged to enhance the effectiveness of DR for frequency regulation. The modified delay compensator is a lead compensator-based PI controller in DR loop. The performance of the proposed controller is examined by considering two different two area power system i.e, hydrothermal and wind integrated thermal system as test systems. For the wind integrated thermal system, DFIG based wind is considered for frequency support. In addition, the inertia effect on thermal system due to the integration of DFIG is taken care in the study by considering a PD-inertia controller in it. The performance analysis is done by simulating the transfer function model of the test systems in MATLAB Toolbox. The simulation results are examined with tuned values of all controller along with the modified DR controller for frequency regulation. A normalized form of weighted sum PSO multi objective optimization is used to tune the controller parameters designed in the above test systems for smooth frequency regulation. The stability and robustness of these systems with the proposed controller are analyzed through eigen value calculation. The result exhibits better efficiency

with proposed controller. Furthermore, the dynamic performances of the test systems show better results than earlier works in literature. Finally, the sensitivity analysis of the proposed controller for two area wind integrated thermal system and hydrothermal system shows negligible difference in system performances even with parameter variation in the range of $\pm 50\%$ and continuous load variation in the range of 0% to 50% of its nominal values. However, the study to check the performance of proposed delay compensator is limited to some selected power system. Future work will further investigate the performance of proposed controller for different power system integrated with renewable energy sources and storage devices.

4.7. Publication from This Work

Journal publication

- [1] **Swetalina Bhuyan**, Sunita Halder Nee Dey, and Subrata Paul. "Modified delay compensation in demand response for frequency regulation of interconnected power systems integrated with renewable energy sources." Cogent Engineering, Taylor & Francis, vol 9(1) (2022): 2065899.

CHAPTER 5

ROLE OF DR IN PRESENCE OF BATTERY MANAGEMENT SYSTEM IN A MPC BASED ALFC STUDY

5.1. Introduction

In view of hike in electricity demand, the infrastructure of power system is changing day by day to maintain equilibrium between generation and demand. A major part of these changes involves augmentation of generation capacity of the system. Because of various technical, economic, social and environmental factors, in many cases it is not viable and desirable nowadays to augment traditional fossil-based generation [1]. Renewable energy-based generation provides more cost effective and environment friendly options. Though renewable energy sources are good choice for restructuring of modern power system but their intermittency in nature makes operation and control of the system more challenging. These sources are highly volatile and depend on atmospheric and climate condition which might cause unavailability at the time of demand in the power system. Because of this nature of the renewable sources, high penetration of these sources in the system is making the automatic load frequency control (ALFC) problem more complex day by day.

Battery energy storage system (BESS) are often used as power support in case of unavailability of renewable energy sources. The application of BESS in ALFC problem shows greater improvement in system dynamics because of its very fast dynamic response [2]. In order to achieve highest expected profitability of the device, battery capacity is optimized while participating in frequency regulation in [6]. So, searching out a suitable strategy for taking care of battery life while participating of BESS in ALFC of power system is a promising research area in power system operation and control.

Moreover, recent studies prove that another state-of-the-art technology like demand response (DR) is a suitable choice for economic way of frequency regulation [10,11]. The introduction of DR in the ALFC function for frequency regulation has made the control further complex. So, the futuristic power system is now bound to introduce more sophisticated and robust controllers to face various challenges like uncertainties and inertia issues from

renewable energy sources, sudden unpredicted load variation, communication issues from demand side load management while participating in ALFC.

In view of the above analysis, this chapter contribution is made as follows:

1. First of all, this paper has implemented a SOC based strategy for the incremental BESS model in co-ordination with DR in ALFC of each area of a wind integrated two- area thermal power system for smooth frequency regulation.
2. It has proposed a new state space based MPC concerning all the variables in the incremental BESS model.
3. The proposed MPC based ALFC is analysed specially for inertia issues from wind in absence of separate inertia controller in wind generator,
4. The saving of battery life is examined when DR is present in the proposed MPC based ALFC.
5. Finally, the MPC based ALFC is compared with a robust PSO optimized integral controller based ALFC in co-ordination with PD controller for inertia issues to confirm the effectiveness of the proposed MPC controller for the studied power system.

5.2. ALFC Modelling with BESS, DR and DFIG

A transfer function model of two area wind integrated thermal power system is simulated in this study for the purpose of frequency regulation. Then DR and BESS are introduced in each area to analyse the performance of the system for frequency regulation. The specification for two area power system and wind energy source are referred from [22]. The BESS modelling for frequency regulation is presented in chapter-2 and its parameters referred from [61]. Similarly, DR modelling referred from [17]. The capacity of each area is 2000 MW out of which 20% contribution are considered from wind in each area. The inertia controller based DFIG is included in the system for frequency support whereas DR and BESS are strategically included in the ALFC of both the area of studied power system to meet the frequency regulation purpose. The whole arrangement for the studied two area power system including incremental BESS and DR is shown in Fig. 5.1. The BESS model receives Δ signal as area control error (ACE) after being controlled by MPC. In order to check frequency deviation with respect to load change, power balance equation of the power system is obtained.

The power balance equation of the i^{th} area of the two-area power system is expressed in equation (5.1). All the term in (5.1) ΔP_{Tie} are expressed in per unit for analysis.

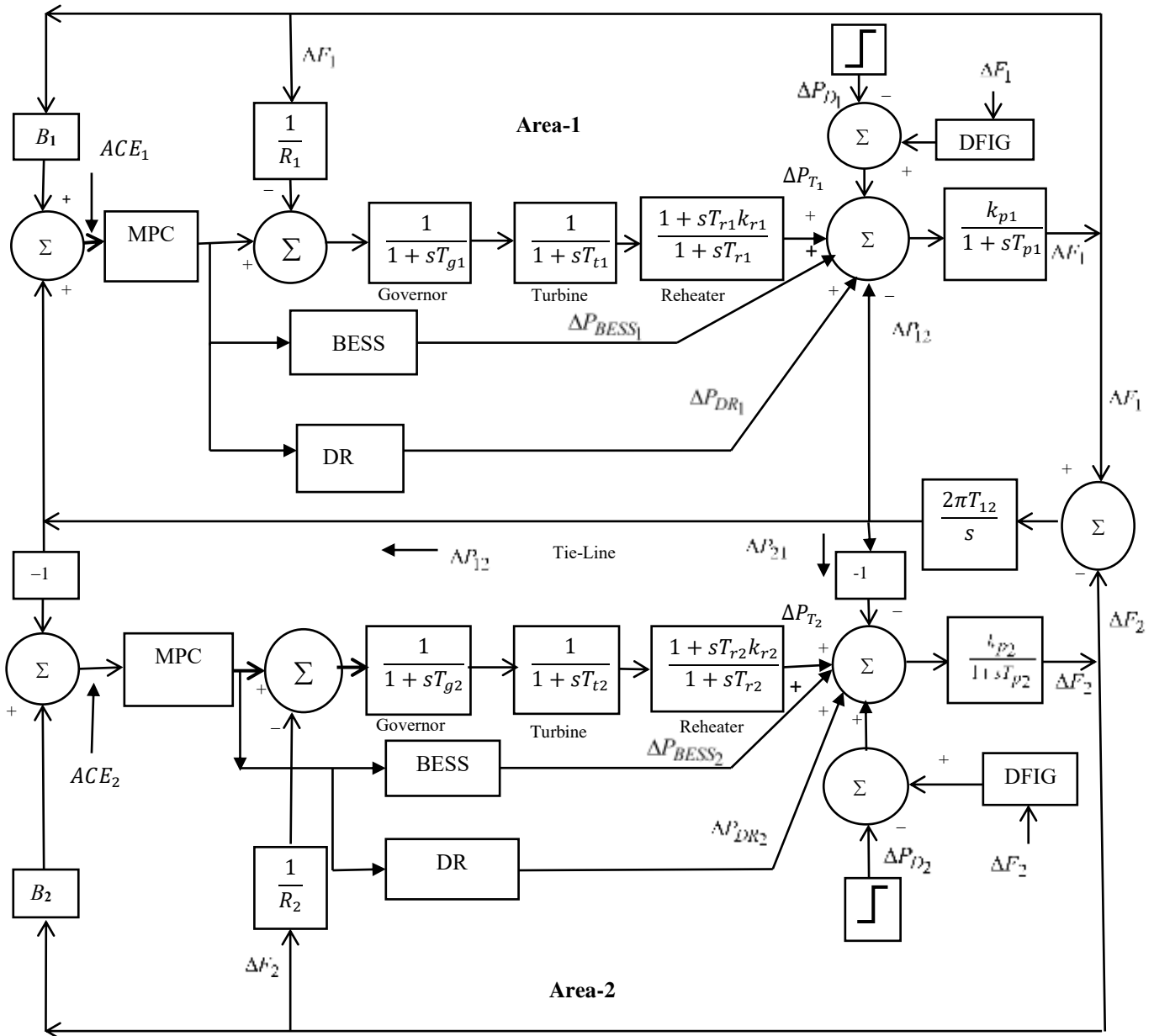


Fig. 5.1. Transfer function model of studied two area power system.

$$[\Delta P_{T_i} + \Delta P_{DFIG_i} + \Delta P_{DR_i} + \Delta P_{BESS_i} \pm \Delta P_{Tie,i} - \Delta P_{D_i}] * \frac{K_{P_i}}{1 + sT_{P_i}} = \Delta F_i \quad (5.1)$$

Where $K_{P_i} = \frac{1}{D_i^*} \text{Hz/pu.MW}$, $T_{P_i} = \frac{2H_i^*}{fD_i^*}$ second.

K_{P_i} = gain of power system, D_i^* = new damping constant of power system with inertia controller from wind in area-i and T_{P_i} = power system time constant, H_i^* = new inertia constant of power system with inertia controller from wind in area-i and f = nominal frequency of power system in Hz.

So, frequency deviation of area-i due to load perturbation can be derived from (5.1) as:

$$\frac{2H_i^*}{f} \cdot \Delta F_i \cdot s + D_i^* \cdot \Delta F_i = [\Delta P_{T_i} + \Delta P_{DFIG_i} + \Delta P_{DR_i} + \Delta P_{BESS_i} \pm \Delta P_{Tie_i} - \Delta P_{D_i}] \quad (5.2)$$

$$\Rightarrow \Delta F_i(s) = \frac{1}{2 \cdot \frac{H_i^*}{f} \cdot s + D_i^*} * [\Delta P_{T_i} + \Delta P_{DFIG_i} + \Delta P_{DR_i} + \Delta P_{BESS_i} \pm \Delta P_{Tie_i} - \Delta P_{D_i}]$$

(5.3)

5.3. Mathematical Analysis of ALFC

In the present study DR and BESS are co-ordinately participated in the ALFC loop of each area of the power system for smooth frequency regulation. The sharing of power from BESS and DR are assumed to be constant in the study. The control share allocation in the ALFC loop of each area of the test system is considered as in equation (5.4).

$$\alpha_{sup_i} + \alpha_{DR_i} + \alpha_{BESS_i} = 1 \quad (5.4)$$

Where, α_{sup_i} , α_{DR_i} and α_{BESS_i} are participation factor for thermal generation control of ALFC, participation factor for DR in ALFC and participation factor for BESS in ALFC respectively in area-i. In general, the ' α_{DR_i} ' is a variable and its value may be chosen based on price of DR [17]. In [17], it has been proved that DR is a good choice for frequency regulation. Also, it is tested that higher the DR participation in the secondary control loop, better in the dynamic performances for frequency regulation. So, this study has not given more emphasis on participation factor for each units rather for the shake of simulation study for the proposed methodology, it is supposed to consider the participation factors are as follows $\alpha_{DR_i} = 0.2$, $\alpha_{sup_i} = 0.7$, $\alpha_{BESS_i} = 0.1$.

According to the present concept the additional power in each area of power system will be compensated by DR, BESS and thermal generation of power system. This can be mathematically expressed as in (5.5).

$$\Delta P_{D_i} = \alpha_{\text{sup}} \Delta P_{S_i} + \alpha_{DR} \Delta P_{DR_i} + \alpha_{BESS} \Delta P_{BESS} \quad (5.5)$$

Where, ΔP_{D_i} = incremental load change, ΔP_{S_i} = power drive from thermal generation,

ΔP_{DR_i} = power drive from DR loop, ΔP_{BESS_i} = power drive from BESS in i^{th} area of power system. Equation (5.3) express the change in frequency due to load change in area-i. The frequency deviation at steady state in presence of DR in ALFC is derived in chapter-4 and expressed in (5.6). So, in the present study the steady state frequency deviation for BESS and DR introduced ALFC is expressed in (5.7).

$$\Delta F_{i,ss} = \lim_{s \rightarrow 0} s \Delta F_i(s) = \frac{\Delta P_{S_{i,ss}} + \Delta P_{DR_{i,ss}} - \Delta P_{D_i}}{\varphi_i(0)} \quad (5.6)$$

$$\Delta F_{i,ss} = \lim_{s \rightarrow 0} s \Delta F_i(s) = \frac{\Delta P_{S_{i,ss}} + \Delta P_{BESS_{i,ss}} + \Delta P_{DR_{i,ss}} - \Delta P_{D_i}}{\varphi_i(0)} \quad (5.7)$$

$$\text{where, } \varphi_i(0) = 2.H_i^* .s + D_i^* + \frac{M_i(0)}{R_i} = D_i^* + \frac{1}{R_i} \approx B_i \quad (5.8)$$

$$\Delta P_{S_{i,ss}} = \lim_{s \rightarrow 0} s M_i(s) . \Delta P_{S_i}(s) \quad (5.9)$$

From Fig. 5.1 [17],

$$M_i(s) = \frac{1}{1 + sT_{gi}} \cdot \frac{1}{1 + sT_{ti}} \cdot \frac{1 + sT_{ri} k_{ri}}{1 + sT_{ri}} \quad (5.10)$$

$$\Delta P_{DR_{i,ss}} = \lim_{s \rightarrow 0} s \Delta P_{DR_i}(s) = 0 \quad (5.11)$$

$$\Delta P_{BESS_{i,ss}} = \lim_{s \rightarrow 0} s \Delta P_{BESS_i}(s) = 0 \quad (5.12)$$

Equation (5.7), mathematically proves that BESS and DR with supplementary control can be capable to provide frequency deviation of zero at steady state. Furthermore, with the accessibility of DR and BESS will give more degree of freedom for frequency control. The mathematical expression in (5.7) demonstrates that even if the supplementary control not able to access the power, still DR and BESS can give assurance for Zero frequency deviation at steady state.

5.4. Proposed Approach

To get the better frequency regulation for a wind integrated conventional two area interconnected power system, a robust MPC is designed in the ALFC collaborating with BESS and DR of each area of power system. The proposed MPC drives the power of thermal generator, battery and DR in each area when there is a frequency and tie line power change in the power system. The proposed MPC design has given more emphasis on battery variables in the BESS model. The battery used in the test system is an incremental battery model presented in chapter-2 in Fig. 2.10 [61]. The BESS model includes various variables that may affect the system performance in terms of stability. So, to avoid those issues the proposed MPC is designed by considering all state variables of BESS. Apart from the Proposed MPC design, the present work also proposes a SOC based strategy for BESS operation condition / participation to save battery life during the course of system frequency regulation. The derived mathematical expression in (5.7) proves that, the combination of BESS and DR can stretch oath for zero frequency deviation at steady state. Moreover, with the proposed SOC based strategy of BESS, the present study also measures the impact of DR participation to save battery life. With all these considerations, the present study proceeds with a model predictive based ALFC and compare the results with integral controller based ALFC in the same wind integrated two area power system having BESS and DR in the ALFC. PSO is used only to tune the controller parameters of integral controller based ALFC and PD controller (used for frequency support) in wind concurrently. The details of the SOC based strategy of BESS and MPC implementation for the studied power system are explained in the following subsections. The procedure of tuning integral controller based ALFC controller is also described briefly in the following subsection.

Generally, SOC_{ref} is not fixed for all battery operation and its value varies as 0.5 or 0.7 [99, 100, 104]. In this study SOC_{ref} is considered as 0.5. According to the calculated SOC, the battery is set to give conditional output as described in (5.14).

$$\left. \begin{aligned} \Delta P_{BESS} &= \alpha_{BESS} P_{ref} \text{ if } SOC_{min} \leq SOC_{cal} \text{ or } SOC_{cal} \leq SOC_{max} \\ &= 0 \text{ if } SOC_{max} \leq SOC_{cal} \text{ or } SOC_{cal} \leq SOC_{min} \end{aligned} \right\} \quad (5.14)$$

where, P_{ref} is the change in power between supply and demand. SOC_{min} = lower bound of SOC, SOC_{max} = upper bound of SOC. The minimum and maximum value of SOC assumed for the study are 0.3 and 0.7 respectively.

5.4.2. Implementation of MPC for ALFC

5.4.2.1. Basic of MPC for ALFC Study

In this study, the test system is a two-area power system with identical capacity in each area. So, two identical MPC are designed in each area based on the MPC modelling procedure followed from [76]. In each area, conventional generator, BESS and DR are taken part in ALFC resolution. The MPC design depends on the discrete state space model representation of the studied power system. The general discrete state space model representation is expressed in (5.15) and in (25.16) of [101].

$$\dot{X} = AX + BU + EU \quad (5.15)$$

$$Y = CX + DU \quad (5.16)$$

Where A, B, C, D, E are the state space variable matrices needed to build the MPC. These state space matrices (A, B, C, D, E) are to be determined for the power system for the application of MPC in ALFC study.

So, the dynamics of the studied two area power system shown in Fig. 5.1, is defined with its state variables to design the MPC for the studied power system that shown in underneath equations.

$$\dot{\Delta F}_1 = -\frac{1}{T_{P1}} \Delta F_1 + \frac{K_{P1}}{T_{P1}} [\Delta P_{DFIG} + \Delta P_{T1} + \Delta P_{BESS1} + \Delta P_{DR1} + \Delta P_{12} - \Delta P_{D1}] \quad (5.17)$$

$$\dot{\Delta P}_{T_1} = -\frac{1}{T_{t_1}} \Delta P_{T_1} + \frac{1}{T_{t_1}} \Delta P_{g_1} \quad (5.18)$$

$$\dot{\Delta P}_{g_1} = -\frac{1}{T_{g_1}} \Delta P_{g_1} - \frac{1}{R_1 T_{g_1}} \Delta F_1 - \frac{1}{T_{g_1}} \Delta P_{CT_1} \quad (5.19)$$

$$\dot{\Delta P}_{DFIG_1} = -\frac{1}{T_{A_1}} \Delta P_{DFIG_1} + \frac{1}{T_{A_1}} \Delta F_1 \quad (5.20)$$

$$\dot{\Delta P}_{BESS_1} = -\frac{1}{T_{b_1}} \Delta P_{BESS_1} + \frac{1}{T_{b_1}} \Delta P_{CB_1} \quad (5.21)$$

$$\dot{\Delta P}_{12} = 2\pi T_{12} \Delta F_2 - 2\pi T_{12} \Delta F_2 \quad (5.22)$$

$$\dot{\Delta F}_2 = -\frac{1}{T_{P_2}} \Delta F_2 + \frac{K_{P_2}}{T_{P_2}} \left[\Delta P_{T_2} + \Delta P_{BESS_2} + \Delta P_{DR_2} + \Delta P_{DFIG_2} - \Delta P_{12} - \Delta P_{D_2} \right] \quad (5.23)$$

$$\dot{\Delta P}_{T_2} = -\frac{1}{T_{t_2}} \Delta P_{T_2} + \frac{1}{T_{t_2}} \Delta P_{g_2} \quad (5.24)$$

$$\dot{\Delta P}_{g_2} = -\frac{1}{T_{g_2}} \Delta P_{g_2} - \frac{1}{T_{g_2}} \Delta P_{CT_2} - \frac{1}{R_2 T_{g_2}} \Delta F_2 \quad (5.25)$$

$$\dot{\Delta P}_{DFIG_2} = -\frac{1}{T_{A_2}} \Delta P_{DFIG_2} + \frac{1}{T_{A_2}} \Delta F_2 \quad (5.26)$$

$$\dot{\Delta P}_{BESS_2} = -\frac{1}{T_{b_2}} \Delta P_{BESS_2} + \frac{1}{T_{b_2}} \Delta P_{CB_2} \quad (5.27)$$

These above eleven state space equations are derived for wind, battery and DR integrated two area power system. To make the text concise, the other state space variables in the studied power system for DR and battery variables like $(\Delta V_S, \Delta I_{BESS})$ associated with BESS are not presented here but taken into consideration for MPC design. These variables directly produce variables matrices. The state space modelling for DR and BESS are done by referring transfer function modelling from [17,61]. Then the state space matrices like A, B, C, D, E are formed from all the derived state space equations of the two--matrices are used to model the proposed MPC but the special care is taken for battery variables while modelling the MPC.

5.4.2.2. MPC formulation for its adaptive optimization

MPC is a novel model-based control approach which employs on adaptive optimization procedure at each sampling time over prediction horizon to calculate the optimal control action. The basic configuration of MPC implementation with its optimization scheme for each area of the studied two area power system is shown in Fig. 5.3. At the time of disturbances, MPC measures the area control error (ACE) of respective area and compared with reference value of ACE ($ACE^{ref} = 0$) at each sampling instant (k). The proposed MPC calculates the control input at each sampling time represented by k . At sampling instant k , the MPC calculates sequence of N_C number of control inputs $\{u(k+i-1), i= 1,2,3... N_C\}$ for the plant at the time of disturbances. This sequence of control input consists of present control input $u(k)$ and $(N_C - 1)$ nos of control inputs in the future. Here sequence of N_C control inputs is calculated such that N_P number of predicted outputs $\{y(k+i), i = 1, 2, 3... N_P\}$, at sampling instant k , are as close as possible to desired output. Where N_P = prediction horizon and N_C = control horizon. In other words, the control sequence $\{u(k+i-1), i= 1,2,3... N_C\}$ is calculated such that the area control error (ACE) between predicted output and desired output over a prediction horizon N_P , is as minimum as possible using an optimization technique in built with MPC.

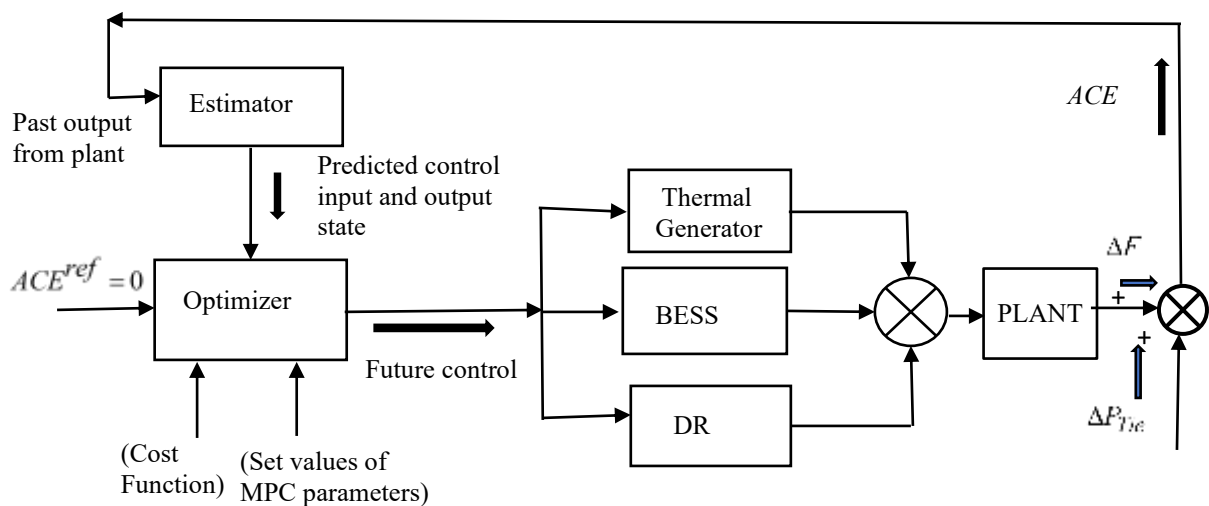


Fig. 5.3. Configuration of MPC for ALFC for the test system.

5.4.2.3. MPC stability and optimization algorithm execution time

The MPC application depends on receding horizon approach in presence of constraints [101]. This receding horizon approach makes the system as a nonlinear feedback control system. This may make the system unstable. But the robust MPC is a stable controller whose performance specifications are met for specified range of system model variations in terms of system parameters variation or operating load variation. So, for the purpose of stability, while formulating the MPC, the cost function of MPC must be formulated as a LYAPUNOV function and formulating a terminal set constraint [101]. Whereas the formulation of cost function is not needed if MPC formulation done in popular commercial tool like MATLAB program by the MATHWORKS [101]. The proposed MPC design uses MATLAB program by the MATHWORKS for the application of frequency regulation in each area of the two-area power system and hence cost function formulation is not needed separately. Furthermore, the execution time for online optimization of MPC is an important point of discussion for today's perspective as it is still an issue of MPC [101]. It is observed that the execution time for optimization by MPC for frequency regulation is about $1.16 \mu s$ in present study. On average the proposed MPC reduces the optimization algorithm execution time by 22% maintaining the same output quality as conventional PI controller. Furthermore, the stability/robustness of the proposed MPC for the present study of frequency regulation is examined by the application of eigen value analysis and simulation-based approaches that is presented in Section-V.

5.4.2.4. Objective function of MPC

In the present study, the frequency control is achieved through the combination of power drive from thermal generator, BESS and DR simultaneously. The formulation of cost function for adaptive control of MPC for ALFC is described as in (5.28). In this study the adaptive optimization scheme of MPC optimizes the *ACE* through its optimizer with a set of MPC parameters like prediction horizon, control horizon, weights on manipulated variables, weights on manipulated variable rates, weight on output signals. These MPC parameters are referred from literature and mentioned in Appendix. The mathematical formulation of cost function for MPC is considered as in (5.28).

$$O = (ACE^{ref} - ACE^{pred}).(ACE^{ref} - ACE^{pred})^T \quad (5.28)$$

Where,

ACE^{ref} = Reference of system output as Area control error

ACE^{pred} = predicted output of the system as Area control error

In this study, MPC predicts the future performance of the system by minimizing ACE, where

$$ACE_i = B_i \Delta F_i + \Delta P_{Tie_i}, \quad i=1, 2 \text{ and } B_i = \text{frequency bias in } i^{th} \text{ area.}$$

Moreover, the algorithm used to process the MPC for studied ALFC of the power system is explained in Fig. 5.4.

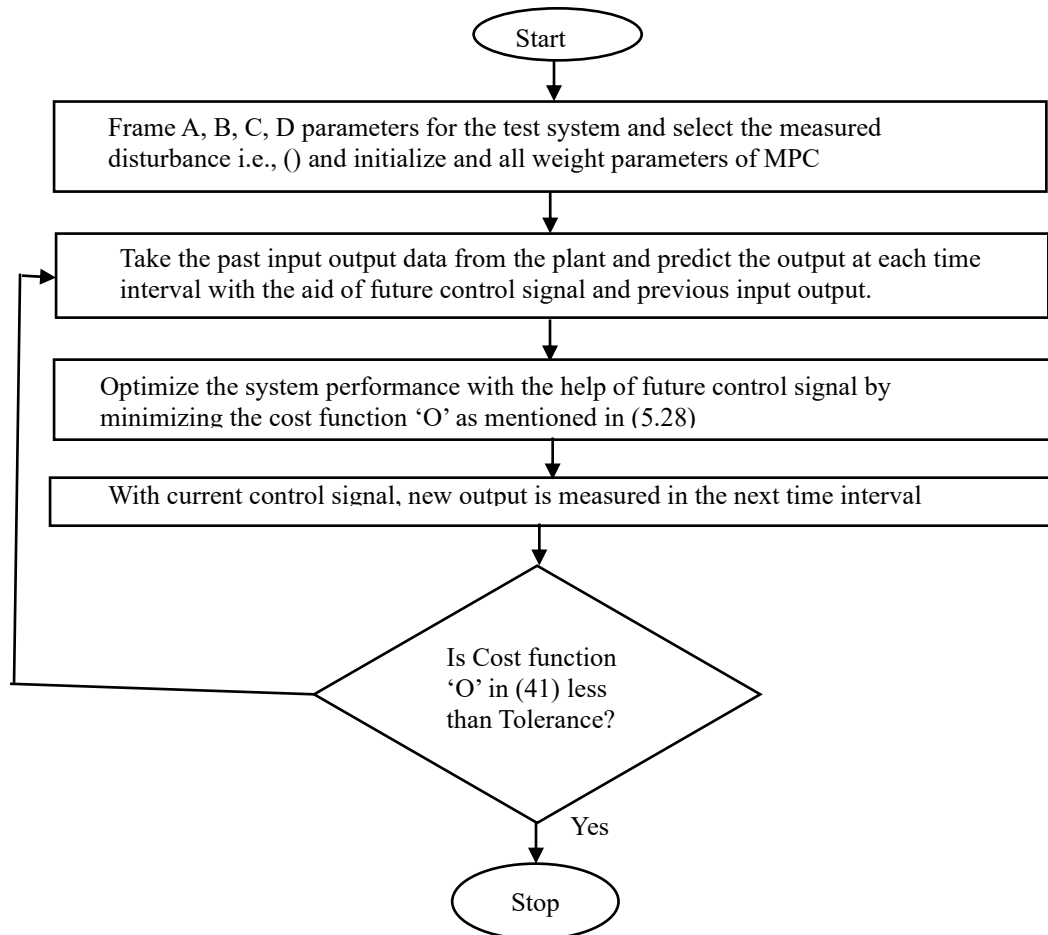


Fig. 5.4. Flow chart for MPC in ALFC of the two -area power system.

5.4.2.5. Problem Formulation

Basically, this problem formulation is done for ALFC having integral controller. In the current study, the test system consists of BESS, DR, DFIG in both the area of power system. The dynamic performance of the power system mainly depends on tuning of controller present in the system. In the present test system, the integral control gain (K_i) of ALFC and PD-controller parameters (K_{pf}, K_{df}) for inertia control of DFIG in both the areas of power system are considered for tuning to get smooth frequency control of power system. Particle swarm

optimization is a widely used robust optimization technique to tune controller parameters [93]. So, this optimization method is used for the purpose of the current study. The above-mentioned gain parameters are tuned by using PSO. The PSO parameters details for tuning the controller parameters are given in Appendix. Moreover, optimization technique needs a suitable objective function for a particular problem to tune any control parameters. The generally used four performance indices like Integral of time multiple of absolute error (ITAE), integral time square error (ITSE), integral absolute error (IAE) and integral square error (ISE) are optimized individually to tune the controller gain to get smooth dynamic performance of the power system. Among those four sets of individual optimizations of performance indices, the tuned controller gain obtained by optimizing ITAE independently gives better dynamic performances in terms of settling time, over shoot and undershoot. So, ITAE has been taken as one of the objective functions of this optimization methodology as it considered in chapter-4. Similarly, settling time is also taken as another objective function for tuning the control parameters. So, to formulate the problem of current study a multi objective function is formulated as follows [96]:

$$J = w_1 \left[\frac{T_s - T_{s_{\min}}}{T_{s_{\max}} - T_{s_{\min}}} \right] + w_2 \left[\frac{ITAE - ITAE_{\min}}{ITAE_{\max} - ITAE_{\min}} \right] \quad (5.29)$$

where, T_s = algebraic sum of settling time of frequency deviation in area-1, settling time of frequency deviation in area-2 and settling time of tie-line power deviation.

$$\text{and } ITAE = \int_0^{t_{sim}} t \cdot [|(\Delta f_1)| + |(\Delta f_2)| + |(\Delta P_{Tie})|] \cdot dt \quad (5.30)$$

where t_{sim} = simulation time, ΔP_{Tie} = tie line power deviation, $\Delta f_1, \Delta f_2$ are frequency deviation in area-1 and area-2 respectively.

$T_{s_{\min}}, ITAE_{\max}$ are gained by optimizing T_s separately.

$ITAE_{\min}, T_{s_{\max}}$ are gained by optimizing $ITAE$ separately.

Here the optimization problem is minimization problem subjected to the following boundaries:

$$K_i^{\min} < K_i < K_i^{\max}, K_{pf}^{\min} < K_{pf} < K_{pf}^{\max}$$

$$K_{df}^{\min} < K_{df} < K_{df}^{\max}$$

5.5. Simulation and Results

5.5.1 Simulation Procedure for Frequency Regulation

Before examining the effectiveness of MPC in ALFC, it is required to test the effectiveness of BESS for the studied power system with conventional integral controller in ALFC. The present study proceeds with transfer function model of a wind integrated two area power system for frequency regulation. In, [17], it is proved that DR is a superior way out for frequency regulation for the wind integrated two-area thermal power system. So, at the beginning of this simulation study, BESS performance is measured by taking different case studies. A new SOC conservation strategy is employed in the BESS to save the battery life while participating for frequency regulation of the studied power system. Finally, the study carried out with performance of MPC in ALFC in presence of wind, BESS, DR in the test power system and also checks the improvement in battery life. The MATLAB and SIMULATION TOOLBOX is used to simulate the proposed models. The efficiency of the proposed work is analysed with different case studies which are as follows:

5.5.2. Impact of DFIG Controller in Presence of BESS

The penetration of wind into the conventional system decreases the system inertia [22]. So, in this case study the impact of DFIG controller for frequency support from wind is examined in presence of BESS. In this regard three separate scenarios are considered to investigate relative performance of wind power over thermal power in terms of their abilities in providing frequency regulation in a battery integrated power system. A PD-controller is considered as inertia controller in wind power source and shown in Fig. 2.2 in chapter-2. The inertia controller parameters (K_{pf}, K_{df}) are tuned along with automatic generation control (AGC) parameter (K_i) to get system frequency regulation performances while considering frequency support from wind. In absence of frequency support from wind this PD-controller is not considered for frequency regulation performances of the system. The two scenarios are tested in this case study as follows:

- First case, no wind penetration in the thermal system.
- 20% wind power with inertia controller.

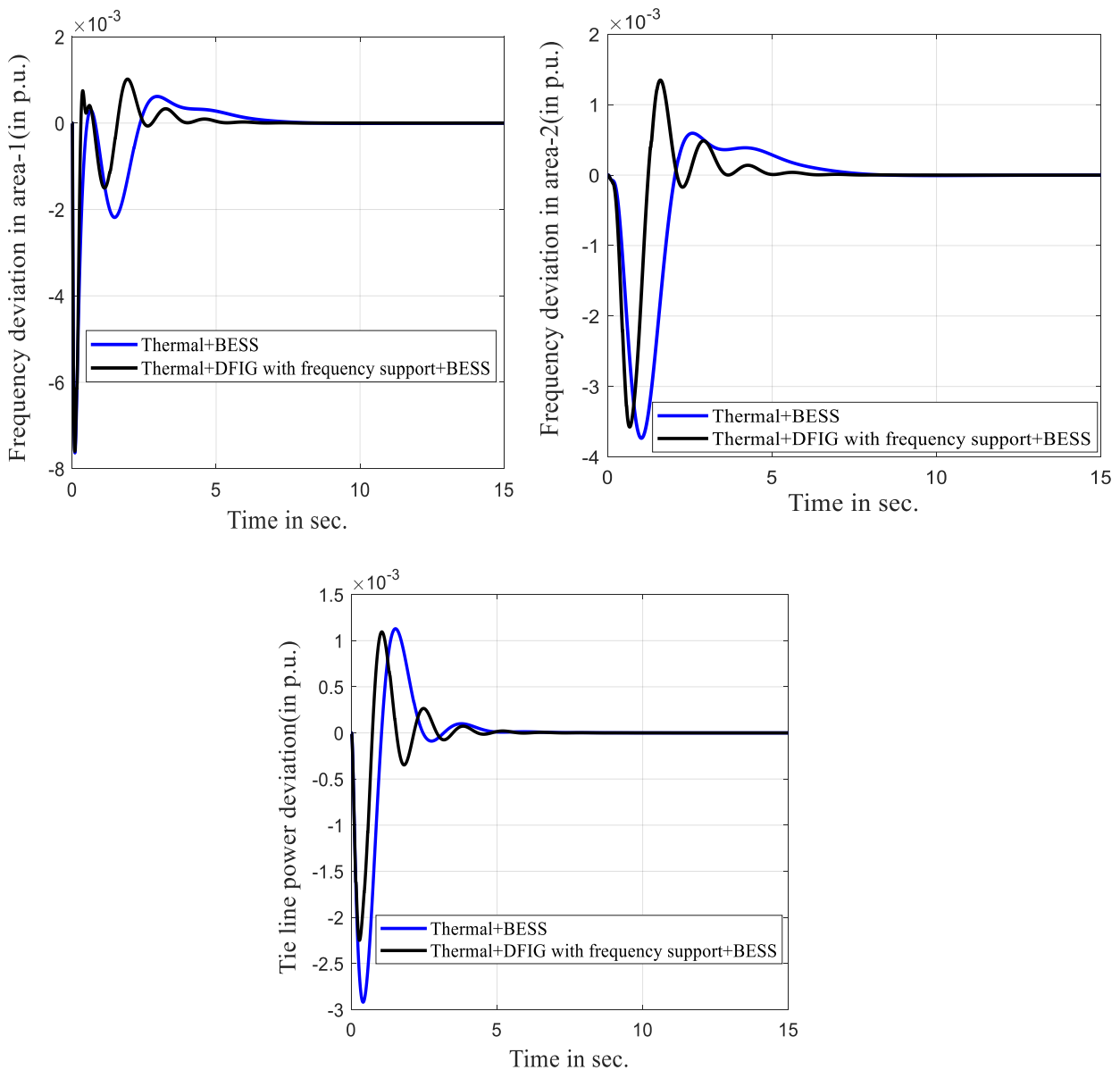


Fig. 5.5. Frequency deviation in each area and tie line power deviation when BESS collaborated with ALFC.

In both the above trials, BESS is participated in the ALFC and the controller parameters in each scenario are carried out by using PSO. The above test has been done for 1% load change in area-1. The behavior of the frequency deviation and tie line power deviation for the above scenarios are shown in Fig. 5.5. From results, it has been found that in second case i.e, when inertia controller is considered from wind, the system gives best dynamic performances in terms of frequency deviations in area-1 & 2 and tie line power deviation. Hence, while analyzing system performance with proposed SOC based BESS and delay compensated DR participated in ALFC, the wind participation must be included with inertia controller for smooth frequency regulation.

5.5.3. Impact of SOC based BESS and DR in ALFC

In the beginning of this case study several load participation factor like 0.1,0.2,0.3,0.4 and 0.5 for BESS in ALFC is tested to get smooth power output from battery. The battery participation factor implies the percentage of power share from battery in ALFC. In this study, the battery responses in discharging mode for frequency support is obtained for different participation factors which shown in Fig.5.6. From Fig. 5.6, it has been noticed that with 10% BESS contribution / for participation factor 0.1 in ALFC, battery is showing better performance in terms of quickly balancing the power at steady state. So, while tuning the controller parameters for improved system performance, it has been supposed that 10% of system load support is available from BESS. Then DR contribution in the ALFC is assumed as 70% and rest 20% control effort are measured from supplementary control.

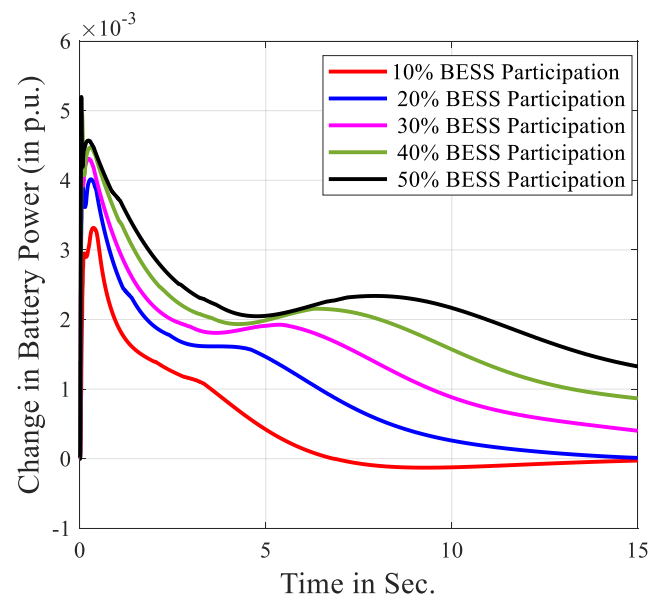


Fig. 5.6. Responses of BESS under discharging mode in area-1 for 1% load change in area-1.

Far ahead of this case study, AGC control parameter (K_i) and DFIG control parameters (K_{pf}, K_{df}) of both the areas are tuned only in presence of BESS in ALFC and when both BESS and DR present in ALFC to get improved dynamic performances for 1% load change in area-1. Also, for the same load change in area-1, those gain parameters are tuned when BESS and DR individually present in the ALFC to compare the performance of the system with BESS and DR separately. The controller parameters are tuned by using PSO by considering objective function as in (5.29). Also, the system performance is analyzed when both BESS and DR absent in the system by referring the CSA tuned controller parameters in [12]. The different system

performance indices are obtained with those tuned control parameters which has been displayed in Table. 5.1. This table also shows that by optimizing ITAE independently, others errors like ITAE, ISE, IAE, ITSE are also reducing drastically. The dynamic responses of power system with the tuned controller are obtained in terms of frequency deviation of both the areas and tie line power deviation with and without BESS, and are shown in Fig. 5.7. The obtained results prove the better performances with SOC based BESS in ALFC in terms of settling time, time error. Moreover, the best results are obtained when both SOC based BESS and DR present in ALFC.

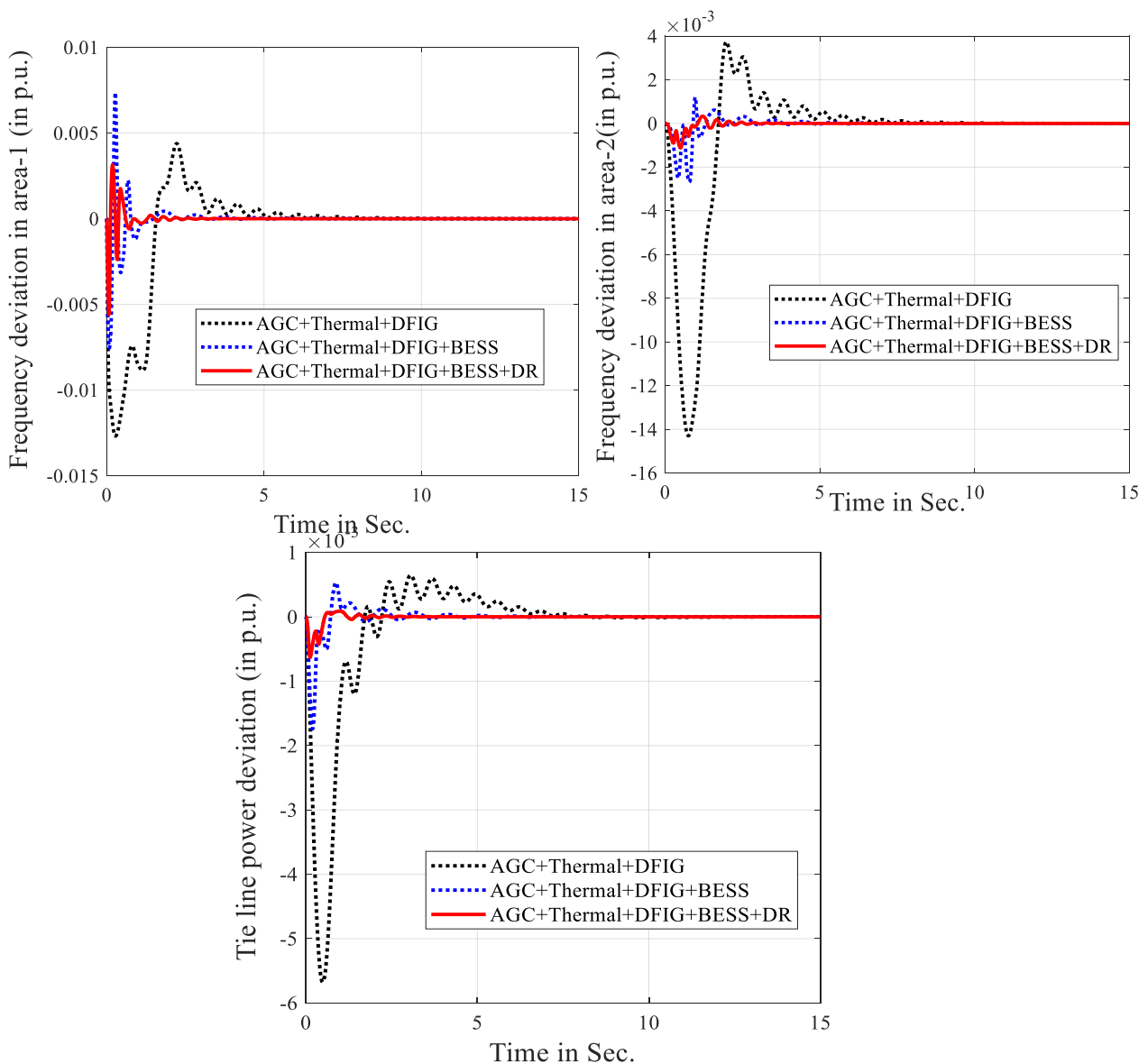


Fig. 5.7. Frequency and Tie line power deviation when both BESS and DR collaborated in ALFC for 1% load change in area-1.

5.5.4. Impact of MPC in ALFC

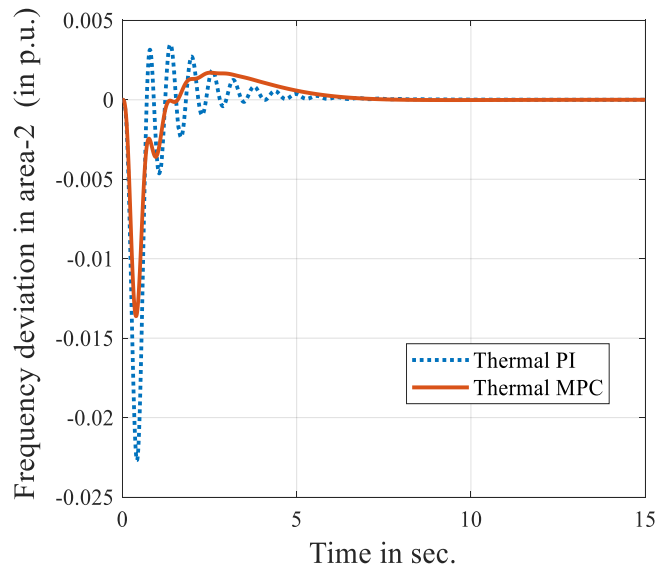
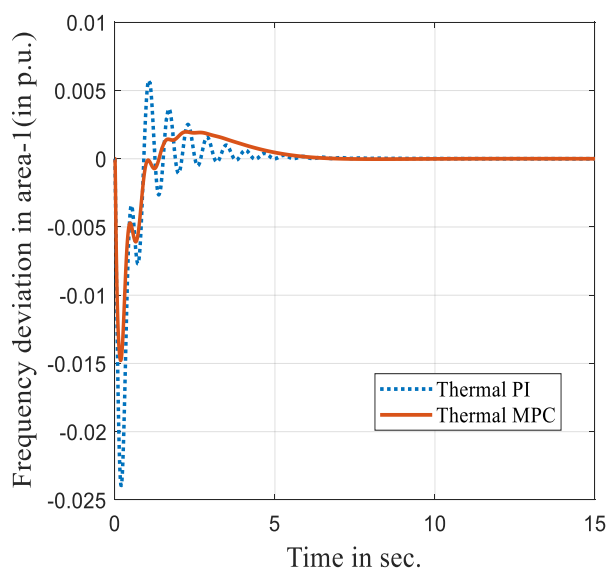
To evaluate the performance of MPC in a multi-source integrated power system for frequency regulation, a transfer function model of two area power system is simulated in the present study. First of all, the performances of MPC in ALFC are examined for a two-area power system for load frequency control problem. The MPC is designed by concerning BESS parameters and its performances compared with conventional MPC without considering the BESS parameters for ALFC study. At the beginning, the designed MPC is applied for a BESS integrated two-area thermal power system. Furthermore, the same BESS parameters based MPC design is tested for a wind and battery integrated two area power system. Four numbers of case studies are done to check the performance of the BESS parameters concerning MPC by considering different source of frequency support in each area of the two-area power system. The results are analysed by comparing the dynamic performance of the system in presence of MPC and integral control individually in the secondary control loop of the two-area power system. The study is inspected with 1% step load variation in area-1 only. The integral controller gain is tuned with the help of particle swarm optimization wherever in case of MPC, parameters like prediction horizon, control horizon, weight on manipulated variable, weight on manipulated variable rates, weight on output signals are considered on trial-and-error basis in the analysis. The sampling time for frequency regulation analysis with MPC in simulation is set as 0.01second in the present study and with that value of sampling time MPC optimization algorithm execution time found about 1.16 μ second. Finally, it proves that MPC is the better choice for load frequency control problem for all type of generation in each area of the power system. Also, it is found that MPC design based on parameters of BESS can able to avail better dynamic performance for the battery integrated power system. The efficiency of the proposed work is analysed with four different sub-case studies which are as follows:

5.5.4.1. MPC for Two-Area Thermal Power System

Fig. 5.8 shows the dynamic behaviour of the studied two area power system with each area having thermal generation unit of 2000MW only for conventional integral controller and proposed MPC controller. The dynamic behaviour in terms of area frequency deviations and tie line power deviation are observed in presence of PI and MPC controller in ALFC separately. The results from this case study found that MPC is performing better then PI controller in ALFC for load frequency control problem.

Table 5.1. Comparison of different performance indices with and without BESS/DR in ALFC with inertia controller in wind.

Type of controller in ALFC	Gain parameters of controller			Settling time (in sec.)			(T_s) in Sec	(ITAE)	(ITSE)	(IAE)	(ISE)
	K_i	K_{pf}	K_{df}	ΔF_1	ΔF_2	ΔP_{Tie}					
With both BESS & DR in ALFC (Proposed)	12.1703	1.74768	0.11288	5.33	5.33	2.59	13.25	0.0067	4.8145e-06	0.0040	9.3584e-06
Only with BESS in ALFC	8.867	0.974	-0.41653	16.56	18.47	7.90	42.93	0.0390	4.9398e-05	0.0135	4.9215e-05
Only with DR in ALFC	0.5634	0.30313	0.1039	12.73	12.970	6.87	32.57	0.1400	6.8988e-04	0.0656	4.8762e-04
No BESS & DR support in ALFC [12]	0.5412	0.2723	0.2902	31.10	30.06	21.34	82.50	1.2773	0.0027	0.1373	9.9607e-04



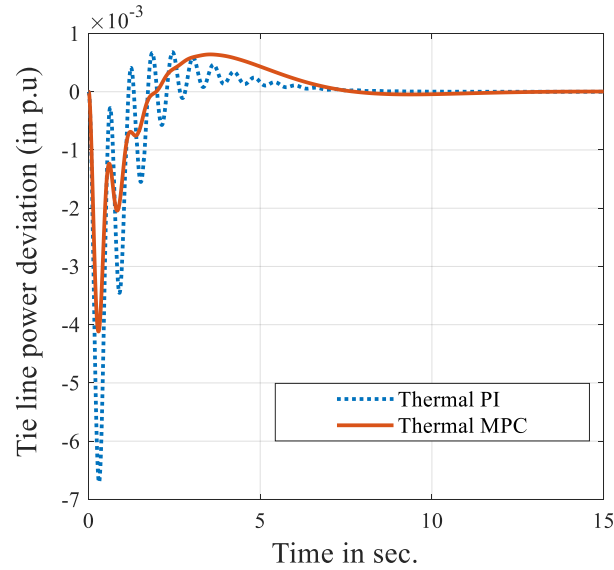


Fig. 5.8. Comparison of dynamic performances in terms of tie line power deviation and area frequency deviations for 1% load variation in area-1 with different controller in ALFC.

5.5.4.2. MPC for Battery (BESS)Integrated Two Area Thermal Power System

In this study an incremental SOC controlled based battery energy system model is included in both the area to accompany the thermal system for load frequency equilibrium. A new set of state variables are built to design the MPC which concern the battery energy system variables. Fig. 5.9 shows the comparison of dynamic behaviours of the test power system in terms of area frequency deviations and tie line power deviation between integral controller and proposed MPC controller in ALFC. The results from this case study found that MPC concerning on battery energy system variables are performing better than integral controller in ALFC for load frequency control problem in terms of settling time and peak over shoot.

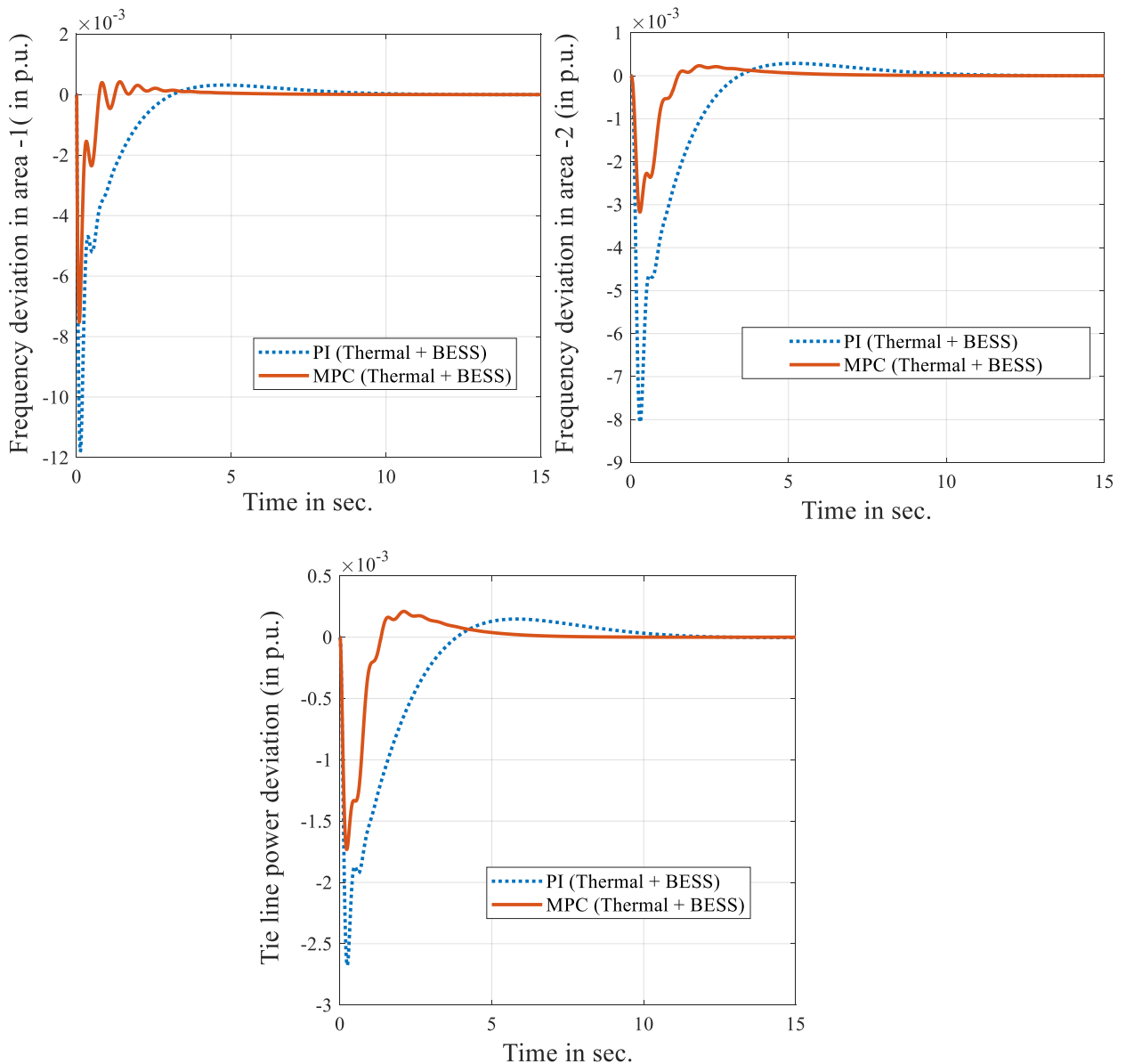


Fig. 5.9. Comparison of dynamic performances in terms of tie line power deviation and area frequency deviations for 1% load variation in area-1 with different controller in ALFC in presence of BESS.

Fig. 5.10 shows the consequence of battery SOC with the application of different type of controller in ALFC in each area of the battery integrated two-area thermal power system. The different type of controller used in ALFC for the test system are as usual conventional PI controller, MPC without concerning BESS variables and MPC with concerning BESS variables. Outcomes prove that change in SOC is least when MPC designed on the basis of BESS variables in a battery integrated thermal power system. This implies that energy exchange between BESS and power grid is comparatively small, when a better controller

designed for ALFC. This ultimately save the battery life as fluctuation of SOC reduces the battery life.

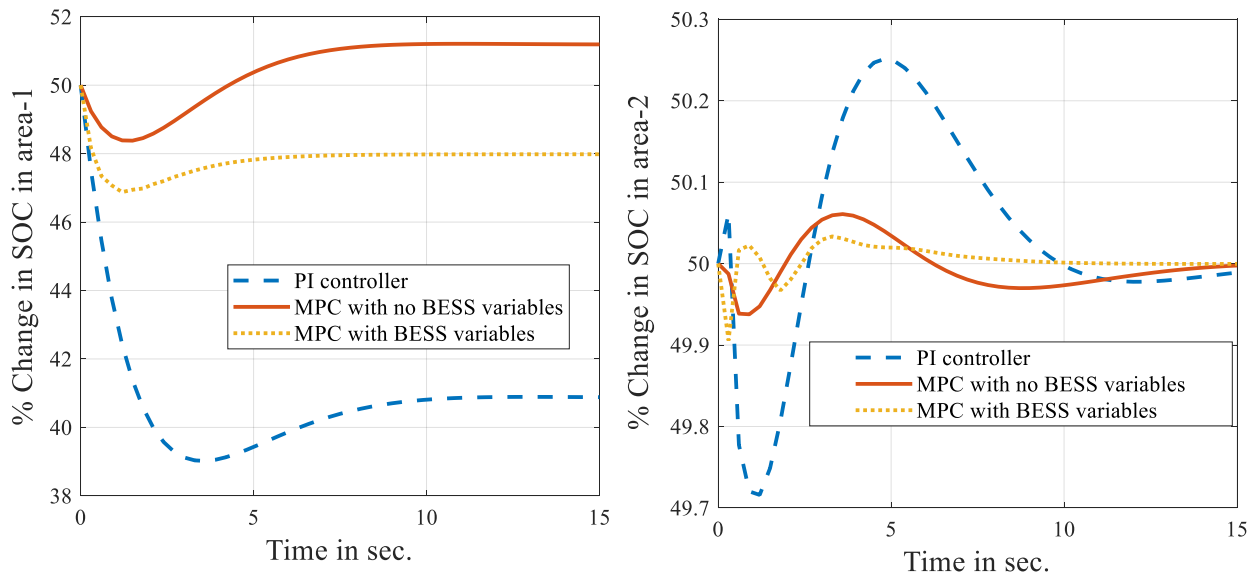


Fig. 5.10. Simulation results of SOC variation for 1% step load variation in area-1 with different controller in ALFC.

Fig. 5.10 shows the consequence of battery SOC with the application of different type of controller in ALFC in each area of the battery integrated two-area thermal power system. The different type of controller used in ALFC for the test are as usual conventional PI controller, MPC without concerning BESS variables and MPC with concerning BESS variables. Outcomes prove that change in SOC is least when MPC designed on the basis of BESS variables in a battery integrated thermal power system. This implies that energy exchange between BESS and power grid is comparatively small, when a better controller designed for ALFC. This ultimately can save the battery life.

5.5.4.3. MPC for Wind and Battery (BESS) Integrated Two Area Thermal Power System

In this case study the performance of BESS parameters concerning MPC is applied in the ALFC of a wind and battery integrated two-area thermal power system. Then the performance of model predictive control is compared with conventional PI controller for load frequency control problem. The specialty of this case study is the integration of DFIG based wind energy generation which adversely affects the inertia of the system. The overall inertia of the power system reduces due to participation of high DFIG based wind farm. So, the design of inertia control is a must to improve the inertia issue and alternatively improve frequency regulation

of the inter connected system without interfering with the performance of automatic generation control adversely.

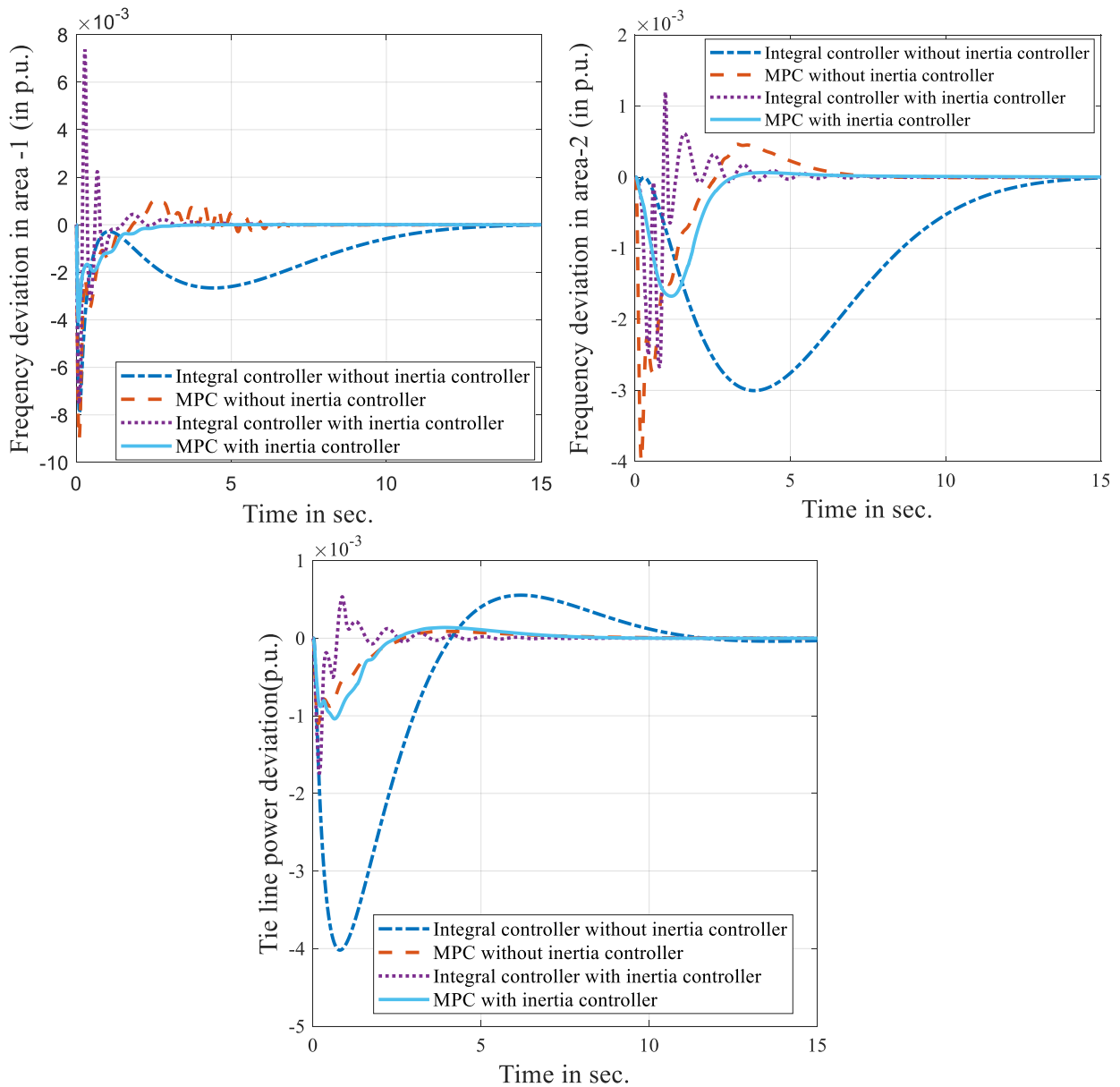


Fig. 5.11. Comparison of dynamic performances in terms of tie line power deviation and area frequency deviations for 1% load variation in area-1 with different controller in ALFC and DFIG.

Fig. 5.11 shows the comparison between MPC controller and conventional integral controller in ALFC as well as with and without inertia controller in DFIG in order to get better dynamic performance of the test system. Looking into the past research inertia control design in [22,12], it has been observed that the designed inertia control (PD control) in wind energy source can improve the frequency regulation without affecting the automatic generation control power system. The integration of wind energy source without inertia controller badly effects the system frequency regulation, when power system having integral controller in ALFC but

MPC controller in ALFC even without inertia control from wind can improve the overall frequency regulation in terms of overshoot and settling time which is graphically proved in Fig. 5.11. So, it can be concluded that proposed MPC in ALFC can able to reduce the number of controllers present in the power system. Moreover, the study proves graphically in Fig. 5.11 that power system with inertia controller from wind generator and proposed MPC in ALFC can able to provide better frequency regulation in terms of over shoot, settling time and damping out of oscillation. This shows the effectiveness of the proposed MPC in comparison to integral controller in ALFC.

Fig. 5.12 shows the consequence of battery SOC with the application of different type of controller in ALFC in a wind and battery integrated two-area thermal power system. The different type of controller used in ALFC for the test are as usual conventional PI controller, MPC with concerning BESS variables. Outcomes prove that change in SOC is least when MPC designed on the basis of BESS variables in a wind and battery integrated thermal power system. This implies that energy exchange between BESS and power grid is comparatively small, when a better controller designed for ALFC. This ultimately can save the battery life.

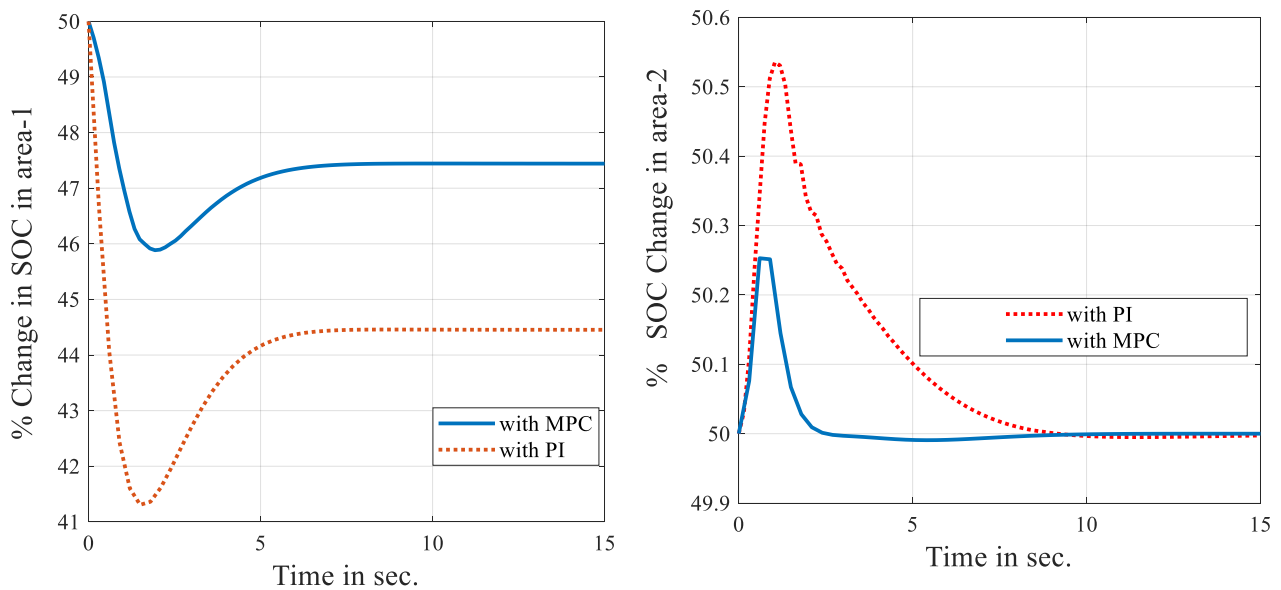


Fig.5.12. Simulation results of SOC variation for 1% step load variation in area-1 with different controller in ALFC.

Fig. 5.13 shows the comparison between cost function of MPC concerning on BESS variables and without concerning BESS variables in ALFC of a wind and BESS integrated power system. Results show that MPC design concerning on BESS variables can provide minimum error for the step load variation. So, BESS concerning MPC may be the suitable choice for ALFC to get healthier frequency regulation for a wind and battery integrated thermal power system which is very common in modern power system.

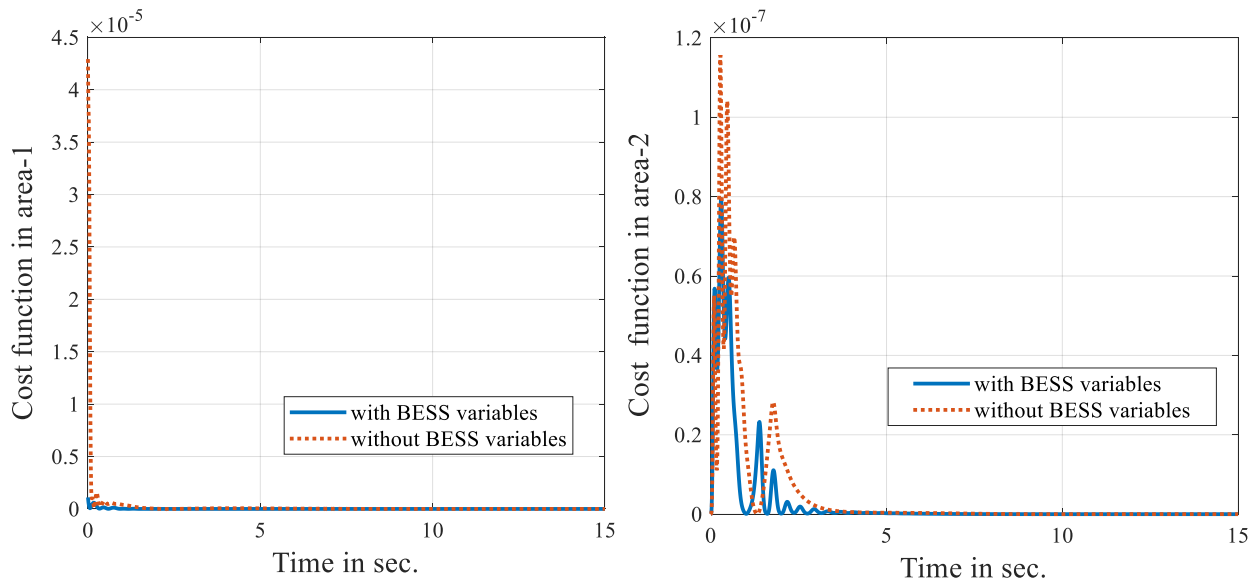


Fig. 5.13. Comparison of responses of Cost functions of different MPC design over simulation period.

5.5.5. Impact of DR in MPC Based ALFC for SOC Change in BESS

From all the above case study it is found that MPC based ALFC can able to provide better dynamic performances in comparison to integral control based ALFC irrespective of type of active power sources present in the power system for 1% load perturbation in area -1. Also, in the Section-B of the simulation study, it is proved that DR along with BESS in ALFC can able to provide comparatively better frequency regulation. So, in this case study, the change in SOC is obtained for participated BESS in an inertia control-based wind integrated power system. To check the effectiveness of DR in MPC based ALFC for battery SOC change, the simulation study is done for the following two area power system. All the systems are obviously associated with BESS.

- (i) wind integrated thermal system without DR in PI controller based ALFC,
- (ii) wind integrated thermal system without DR in MPC based ALFC
- (iii) wind integrated thermal system with DR in MPC based ALFC

The results obtained for change in SOC in each area is shown in Fig. 5.14. Outcomes prove that change in SOC is least when BESS participated in MPC based ALFC in coordination with DR. This implies that energy exchange between BESS and power grid is very small, when BESS is cordially participated with DR in MPC based ALFC which can also save the battery life by protecting SOC.

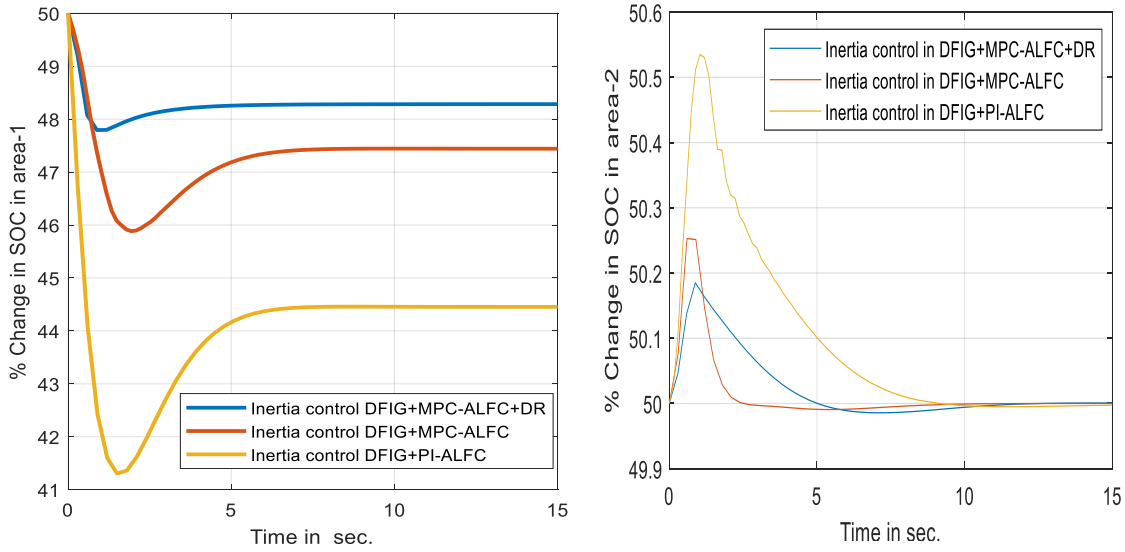


Fig. 5.14. SOC variation for 1% step load variation in area-1 for different type of controller.

5.6. Discussion

This section describes the overall performance of the MPC based ALFC and its main outcomes, comparison with other controller in this field, research carried out, application and other critical analysis of the outcomes, strength and weakness of the present study.

The implementation of MPC in a multi-source environment can able to provide overall frequency regulation performance of the power system. Moreover, MPC based ALFC also can able to save the battery life more effectively as compared to Integral based ALFC. Furthermore, MPC based ALFC with DR as control unit in addition to BESS can capable to improve the battery life while providing better frequency regulation.

In addition to provide comparatively smooth frequency regulation, MPC can also suppress the inertia issues due to presence of DFIG to some extent which was not possible by integral control in ALFC. This has been tested by simulation study and shown in Fig. 5.11. Also, the performance of MPC controller is compared with integral controller in ALFC when additional inertia controller presents in wind for frequency support. This assessment is done in presence of BESS as control unit in ALFC and Fig. 5.11 shows the truthfulness of MPC controller for improved frequency regulation.

To investigate the stability of the proposed MPC, the Eigen values are obtained for the two-area thermal power system with proposed MPC in ALFC with BESS and compared those values for the same system without BESS having conventional MPC in ALFC. The compared

results are presented in Table. 5.2. From Table. 5.2, it is found that the proposed MPC providing better stability in comparison to conventional MPC used in [41], as it provides higher negative real values in the Eigenvalue calculations.

In addition, the stability of the proposed controller is analysed from the minimum damping ratio value point of view. Fig. 5.15 shows the comparison bar diagram for minimum damping ratio between proposed MPC controller and conventional integral controller used in ALFC of wind integrated thermal power system in [22,12]. In [22] and [12], integral controller parameters of ALFC are tuned with the help of PSO and cuckoo search algorithm (CSA) respectively. Results prove that the proposed MPC controller is most suitable for die outing of oscillations from system dynamics due to its least minimum damping ration (MDR). The results prove that the proposed MPC controller can give more stability to the power system.

Moreover, the stability /robustness of proposed MPC is also examined for variation in the system parameters and the operating conditions. First of all to test robustness of the proposed controller, various system parameters like wind energy source time constant (T_A), equivalent inertia constant of wind energy source (H_e) and governor time constant (T_g) are varied in the range of -50% to $+50\%$ from their respective nominal values. The observation of the system performance indices with the variation of the above-mentioned parameters of the studied power system with proposed controller and controller used in chapter-4 are presented in Table. 5.3. It is observed from Table. 5.3 that the system performance indices of the system have not been changed so far and are nearly change for $\pm 50\%$ of parameter change. Moreover, Table. 5.3 shows higher damping ratio with proposed MPC controller which proves the comparative more stability with the proposed controller.

To check the robustness of the system from operating point of view, a continuous operating load change has been assumed in the range of 0-5% in a step of 1% in area-1 for total simulation time. The load variation for different time interval is shown in Fig. 5.16. The system performances in terms of frequency deviations in both areas and tie-line power deviation are obtained for continuous load variation with proposed MPC. Then the above dynamic performances are compared with a robust controller applied in ALFC in chapter-4 for same load operation and that shown in Fig. 5.17. The Fig. 5.17 proves that proposed MPC

controller gives more robustness to the system even with continuous load change as compared to the controller used in chapter-4.

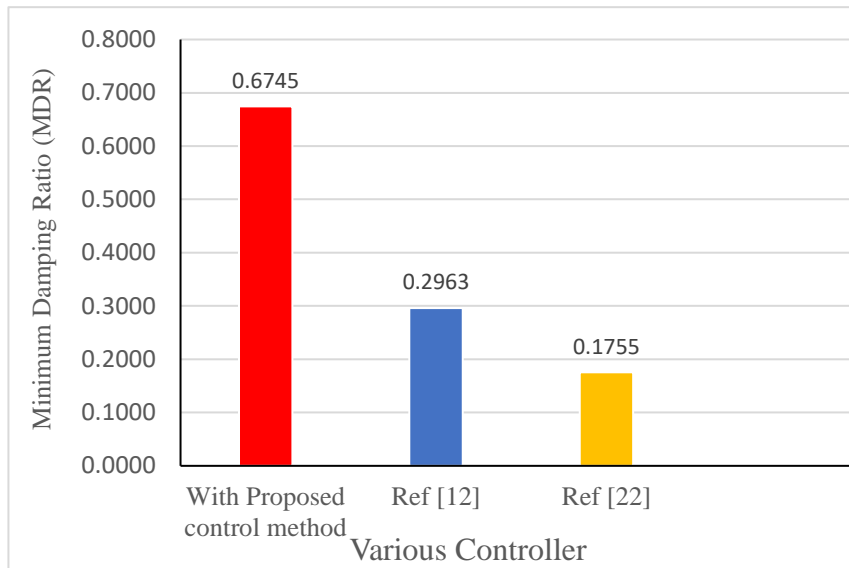


Fig.5.15. Damping ratio with different controllers in ALFC.

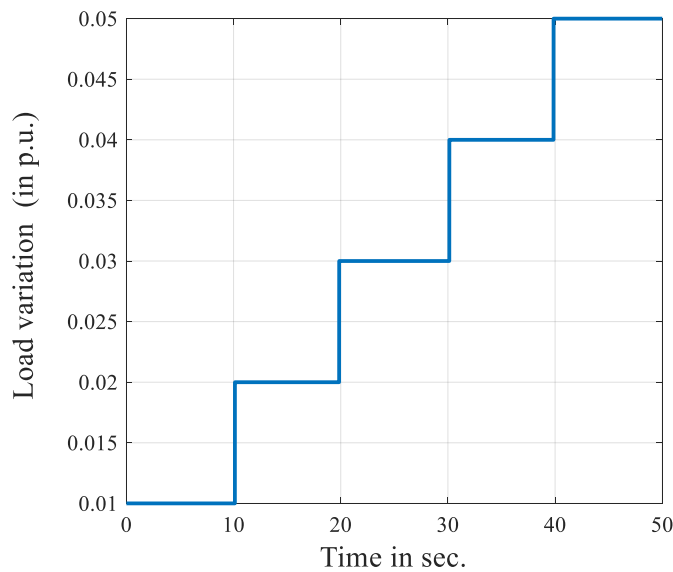


Fig. 5.16. Pattern of step load change.

In future, the various parameters of MPC like prediction horizon, control horizon can have optimized for its adaptive optimization process to get more smooth frequency regulation of the power system. Moreover, the proposed control scheme may be applied to multi area power system to verify the effectiveness of the control method in wide range.

Table 5.2. Eigenvalue representation with different controllers.

With conventional MPC [102]	With Proposed MPC
-2.5000 + 0.0000i	-13.4082+0.0000i
-0.1297 + 0.0000i	-1.0988+2.4968i
-0.0990 + 0.0000i	-1.0988-2.4968i
-2.7200 + 2.7377i	-9.5190+0.0000i
-2.7200 - 2.7377i	-5.1542+1.8913i
-2.1412 + 0.0000i	-5.1542-1.8913i

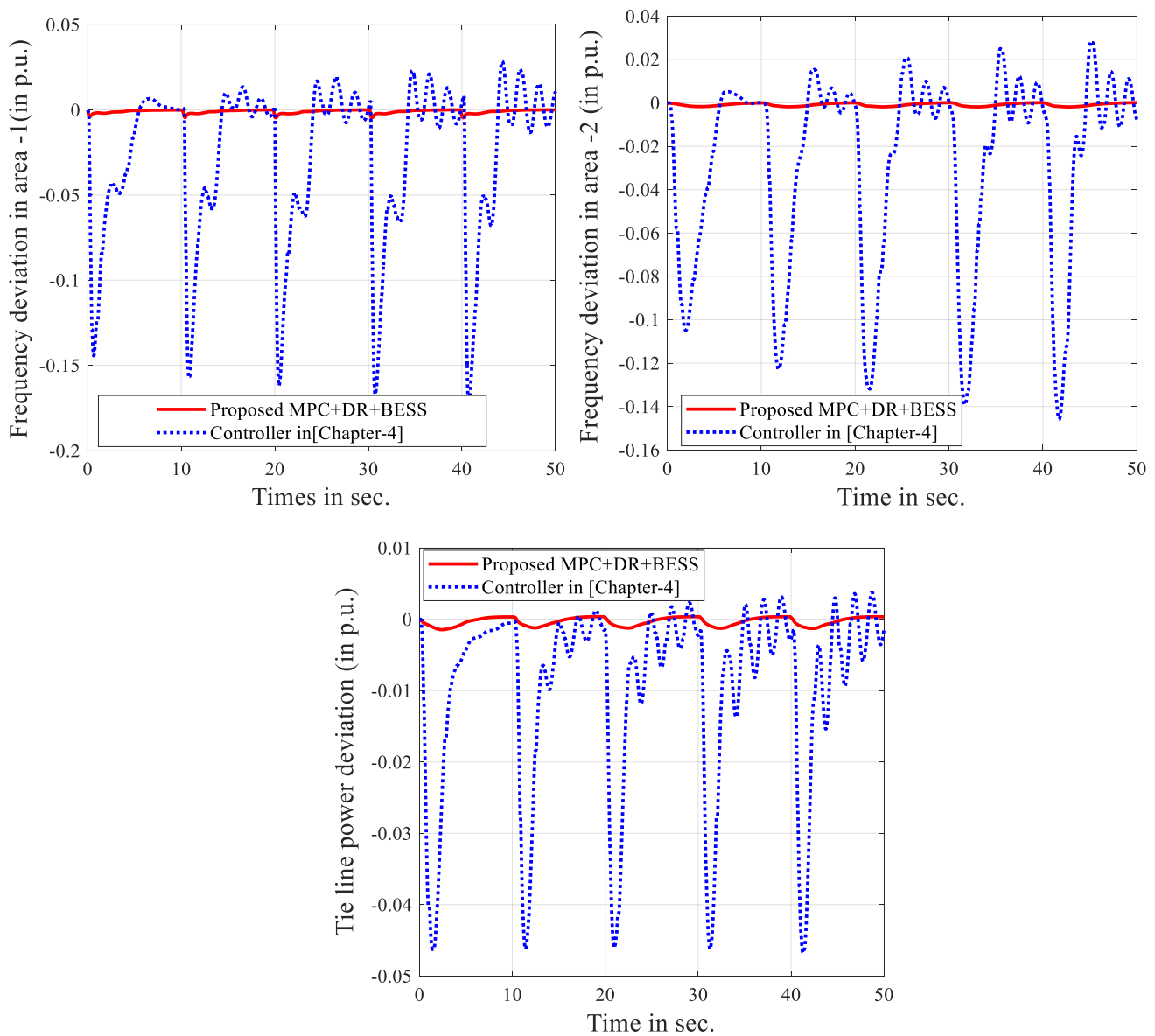


Fig. 5.17. Frequency deviations and tie line power deviation for continuous load change.

Table 5.3. System performance indices and MDR with variation in system parameters

Parameter Change	% Change	ITAE [chapter-4]	ITAE (Proposed MPC)	Settling Time							MDR [chapter-4]	MDR (Proposed MPC)
				ΔF_1 [chapter-4]	ΔF_1 (Proposed MPC)	ΔF_2 [chapter-4]	ΔF_2 (Proposed MPC)	ΔP_{Tie} [chapter-4]	ΔP_{Tie} (Proposed MPC)			
Nominal	0 Nominal	0.1714	0.004153	12.47	4.89	9.27	4.01	9.9	2.05	0.5500	0.6745	
T_g	+50	0.1713	0.005512	15.20	6.02	16.12	5.00	10.11	3.23	0.5419	0.6112	
	+25	0.1711	0.004751	13.54	5.23	17.41	4.35	10.57	3.1	0.3467	0.6437	
	-25	0.1719	0.004431	13.80	5.07	10.32	4.98	10.69	2.99	0.5506	0.6342	
	-50	0.1726	0.005171	20.13	6.91	9.620	5.43	9.90	3.43	0.3896	0.5748	
	+50	0.1728	0.006213	17.52	5.28	13.56	4.91	11.42	3.45	0.5967	0.5984	
T_A	+25	0.1715	0.004923	14.34	5.00	13.19	4.48	10.72	2.89	0.6012	0.6002	
	-25	0.1751	0.004394	15.00	4.98	11.99	5.1	10.64	3.11	0.4759	0.6234	
	-50	0.1799	0.006293	19.71	6.12	13.90	5.23	19.31	3.54	0.4145	0.5725	
	+50	0.1744	0.005728	18.05	5.02	14.20	5.76	11.51	3.55	0.5469	0.5528	
	+25	0.1731	0.004658	16.95	4.98	11.64	4.95	9.64	2.97	0.5485	0.6243	
H_e	-25	0.1721	0.004952	14.82	4.97	12.86	5.11	10.63	3.01	0.5493	0.6575	
	-50	0.1771	0.006257	15.93	5.20	14.89	5.23	12.27	3.72	0.5273	0.5967	

5.7. Conclusion

To summarize the extension method for frequency regulation, it is found that MPC based ALFC is a robust control method for the modern power system. The performance of the MPC is examined in this study in presence of renewable energy sources, battery and the new form of technology like demand side management for frequency regulation. Furthermore, the collaboration of DR along with BESS in conventional ALFC gives more degree of solution for frequency regulation in terms of stability, error reduction and settling time that shown in Table. 5.1. The SOC strategy-based BESS could able to save the battery life as it operates within the SOC limit while participating in ALFC for frequency control. Also, it has been observed that change in SOC is least when BESS collaboratively participated with DR in MPC based ALFC. That implies that the exchange of power between BESS and power grid will be less when BESS and DR co-cordially participated in the proposed MPC based ALFC which can save battery life too. The simulation results proved that the most effective way to improve the system dynamic behavior is obtained when both SOC based BESS and DR present in the proposed MPC based ALFC with frequency support from wind. Finally, all the results with the present method of control action designed for ALFC are compared in terms of their system performance indices like ITAE and settling time with other results present in [34], which having conventional method of control action in ALFC for smooth frequency regulation. Results prove the effectiveness of proposed control action for ALFC.

5.8. Publication from This Work

Journal publication

- [1] **Swetalina Bhuyan**, Sunita Halder nee Dey, Subrata Paul, “A robust MPC design concerning on battery variables for frequency regulation and saving battery life collaborating with demand response for a multi-source integrated power system”. Electrical Engineering, Springer Nature (2023), <https://doi.org/10.1007/s00202-023-01924-1>.

CHAPTER 6

REAL TIME PERFORMANCE ANALYSIS OF DR AND MODEL PREDICTIVE CONTROL FOR ALFC STUDY IN MG

6.1. Introduction

The automatic load frequency control (ALFC) problem turn out to be intricate for isolated microgrid (MG) due to the increasing use of renewable energy resources (RES) and its isolation from main grid in the power system [1]. The main issues with the renewable energy integrated isolated MG are its low inertia. Moreover, when the microgrid is connected to the main grid through tie line, it follows the frequency of the main grid. In that case it is needed to take care of magnitude and quality of voltage and power only, and it is not required to bother about the frequency. However, when the micro grid is separated from the main grid in the event of failure in main grid or when there is maintenance schedule in the main grid, the MG become autonomous and it needs to take care of magnitude and quality of voltage, frequency and power. However, model predictive control (MPC) provides online optimization scheme to control the output of a power system. The MPC modelling for power system control specially depends on states space equations of the power system [18]. Furthermore, the delay issue in demand response (DR) has not been analysed when MPC is used for DR introduced ALFC solution of a MG. To fill up the gap in the literature, the present work has designed the MPC incorporating DR for ALFC of an isolated MG and its application is verified with the help of real time experimental set up in OPAL-RT. The following considerations are taken into account while performing the frequency regulation with proposed MPC in ALFC collaborating with DR and BESS in RES integrated MG:

- i. Implementing the delay compensator in DR loop in the isolated MG.
- ii. Formulating MPC for the studied isolated MG.

Table 6.1. Microgrid parameter values [68].

Parameter	Value	Parameter	Value
D (p. u. MW/Hz)	0.015	$T_g(s)$	0.08
$2H(s)$	0.1667	$T_t(s)$	0.4
$T_{fc}(s)$	0.26	$T_b(s)$	0.1
$T_{inv}(s)$	0.04	R (Hz/p. u MW)	3
$T_{filt}(s)$	0.004	-	-

6.3. MPC formulation for Micro-Grid

MPC is a feedforward as well as feedback control algorithm that uses model of the process/plant to predict the future outputs. It is a multi-input multi-output control technique that uses the explicit model of process or plant, to calculate sequence of control input and predict outputs into the future. It uses an optimizer to calculate these control inputs, such that the plant output follows the desired set point. MPC uses the notion of horizon, instead of making the error between set point and predicted output zero instantly to achieve stabilization. It looks the error over a period of time into the future. It calculates the current control action such that the error between set point and predicted output in the future is as minimum as possible.

The general formulation of MPC for a particular power system depends on state space representation of the power system [62]. The universal state space equations for single input single output discrete time state space model of a plant given below.

$$x_1(k+1) = A_1x_1(k) + B_1u(k) + E_1w(k) \tag{6.1}$$

$$y(k) = C_1x(k) + D_1u(k) \tag{6.2}$$

Where, u is control input, y is plant output, x_1 is state variable vector with dimensions of $n_1 \times n_1$ and n_1 is a finite number.

To analyze the MPC formulation, it is assumed that at time instant $k, k > 0$, the state variable vector $x(k)$ is available. The state variable vector at k gives the plant information at k . The sequence of control input to the plant is denoted by,

$$\Delta u(k), \Delta u(k+1), \Delta u(k+2), \Delta u(k+3) \dots \Delta u(k+N_C-1)$$

where, N_C is the control horizon, gives the information that how many future control inputs that are assigned to calculate. The input is constant after N_C numbers of control inputs. Here sequence of N_C control inputs is calculated such that ΔP_{Tie} number of predicted outputs $\{y(k+1), i = 1, 2, 3 \dots N_P\}$, at sampling instant k , are as close as possible to desired output. In otherwords, the control sequence $\{u(k+i-1), i=1,2,3 \dots N_C\}$ is calculated such that the sum of squared error between predicted output and desired output over a prediction horizon ΔP_{Tie} , is as minimum as possible using an optimization technique. For the adaptive optimization of MPC, the value of ΔP_{Tie} and N_C are considered as 10 and 2 respectively for the present study.

With the use of current state vector $x(k)$ at k , the future state variable vectors for N_P number of time instants are determined. where, N_P is prediction horizon. The future state variable vectors are denoted by,

$$x(k+1), x(k+2), x(k+3) \dots x(k+\Delta P_{Tie})$$

For the current study, the number of control horizon N_C , is selected such that it is less than

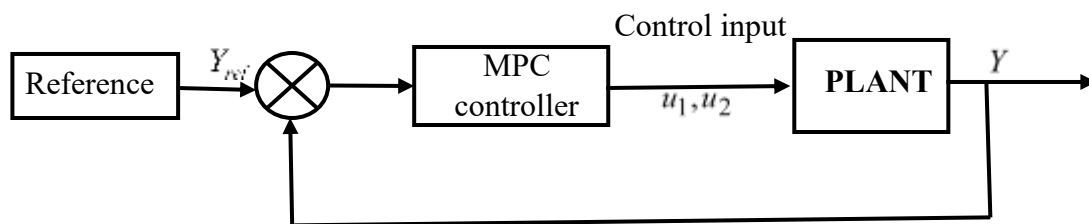


Fig.6. 2. Basic structure of a Model predictive controller-based plant.

prediction horizon, ΔP_{Tie} . The basic configuration of MPC implemented plant (present microgrid) is described in the Fig. 6.2. The main function of MPC is to give a optimized control signal to the plant such that the performance of the plant reaches at its desired output level.

As intensive studies are presented in the literature about the general procedure to formulate objective function of MPC [101], so here only the basic optimization formulation are explained. Considering all the above mentioned constraints, the objective function to determine sequence of control input ΔU is as trails,

$$O = (Y - Y_{ref})^T (Y - Y_{ref}) + \Delta U^T \bar{R} \Delta U \quad (6.3)$$

Where, Y = set of predicted output, Y_{ref} = set point or reference vector, ΔU is sequence of control input rate vector,

$$Y_{ref} = [1 \ 1 \ 1 \ 1 \ \dots \ 1]^T * r(k) \quad (6.4)$$

The dimension of Y_{ref} matrix is $(\Delta P_{Tie} \times 1)$ and $r(k)$ is reference value at k^{th} sampling instant.

\bar{R} is control input rate weight matrix, $\bar{R} = R_w * I_{N_C \times N_C}$, R_w is any real positive number, ($R_w \geq 0$), I is a unit identity matrix of the dimensions $N_C \times N_C$, $r(k)$ is reference value.

In the objective function shown in (6.3), the first term is related to minimize the error between the predicted output and reference, the second term is related to minimizing the size of control input ΔU , when the objective function ‘ O ’ is optimized. The term R_w is tuned to get desired closed loop performance of the plant. $R_w = 0$, means that the size for control inputs has not been cared that how large it would be or how minimum it would be.

6.4. Proposed Scheme for Frequency Regulation

6.4.1. Model Predictive Control implementation in ALFC of MG

The MPC implementation of the microgrid for frequency regulation is presented in Fig. 6.1. The most common controllable energy unit in MG are diesel unit and fuel cell unit. So, in the studied MG, both conventional diesel unit and fuel cell unit are considered as controllable unit in connection with MPC to stabilize the load frequency in the event of fluctuation in demand or renewable generation like wind and PV. In short, when there is any fluctuation either from renewable energy sources or from load demand, MPC automatically drives the power from these two control units by giving the appropriate control signal according to the state of the microgrid. Meanwhile, DR and BESS can be participated in frequency regulation process to stabilize the micro grid. Moreover, lead compensator is used in DR to provide more degree of stability while regulating the frequency for the microgrid. The lead compensated DR has a separate PI controller in its loop to control the delay issue persist in the DR loop. Depending on the system configuration, both BESS and DR may work together at a particular time or one of them may disconnected or both are disconnected from frequency regulation process. Thus, diesel unit, fuel cell, BESS and DR are included for frequency regulation process while only diesel unit and fuel cell are participated in the secondary control of frequency regulation of microgrid. Moreover, all units are included for modelling of MPC except DR. So, the demand response is separately controlled with a conventional PI controller whose parameters are tuned in co-ordination with MPC input tuning parameter (R_w) to get

smooth and stabilize frequency regulation. PSO is used to tune the above considered control parameters of PI in lead compensated DR and R_w in MPC. A linear stochastic state space function is presented here for the proposed micro grid as trails:

$$\begin{aligned} \dot{x} &= Ax + Bu + Ew \\ y &= Cx + Du \end{aligned} \quad (6.5)$$

Where each of the state space function in (6.5) for the MG are presented as follows:

$$x = [\Delta F \ \Delta P_{PV_INT} \ \Delta P_{PV_FLT} \ \Delta P_{GD} \ \Delta P_{TD} \ \Delta P_{FC} \ \Delta P_{FC_INV} \ \Delta P_{FC_FLT} \ \Delta P_{BESS}]^T \quad (6.6)$$

$$y = \Delta F \quad (6.7)$$

$$u = [\Delta u_1 \ \Delta u_2]^T \quad (6.8)$$

$$A = \begin{bmatrix} -\frac{D}{2H} & 0 & \frac{1}{2H} & 0 & \frac{1}{2H} & 0 & 0 & \frac{1}{2H} & -\frac{1}{2H} \\ 0 & -\frac{1}{T_{inv}} & 0 & 0 & 0 & 0 & 0 & 0 & 0 \\ 0 & \frac{1}{T_{filt}} & -\frac{1}{T_{filt}} & 0 & 0 & 0 & 0 & 0 & 0 \\ -\frac{1}{RT_g} & 0 & 0 & -\frac{1}{T_g} & 0 & 0 & 0 & 0 & 0 \\ 0 & 0 & 0 & \frac{1}{T_t} & -\frac{1}{T_t} & 0 & 0 & 0 & 0 \\ -\frac{1}{T_{fc}} & 0 & 0 & 0 & 0 & -\frac{1}{T_{fc}} & 0 & 0 & 0 \\ 0 & 0 & 0 & 0 & 0 & \frac{1}{T_{inv}} & -\frac{1}{T_{inv}} & 0 & 0 \\ 0 & 0 & 0 & 0 & 0 & 0 & \frac{1}{T_{filt}} & -\frac{1}{T_{filt}} & 0 \\ \frac{1}{T_b} & 0 & 0 & 0 & 0 & 0 & 0 & 0 & -\frac{1}{T_b} \end{bmatrix}$$

$$B = \begin{bmatrix} 0 & 0 \\ 0 & 0 \\ 0 & 0 \\ \frac{1}{T_g} & 0 \\ 0 & 0 \\ 0 & \frac{1}{T_{fc}} \\ 0 & 0 \\ 0 & 0 \\ 0 & 0 \end{bmatrix}, \quad E = \begin{bmatrix} -\frac{1}{2H} & \frac{1}{2H} & 0 \\ 0 & 0 & \frac{1}{T_{inv}} \\ 0 & 0 & 0 \\ 0 & 0 & 0 \\ 0 & 0 & 0 \\ 0 & 0 & 0 \\ 0 & 0 & 0 \\ 0 & 0 & 0 \\ 0 & 0 & 0 \end{bmatrix}, \quad C = [1 \ 0 \ 0 \ 0 \ 0 \ 0 \ 0 \ 0 \ 0 \ 0]$$

$$D = 0, \quad u = [u_1 \ u_2], \quad w = [\Delta P_L \ \Delta P_W \ \Delta P_{PV}]^T$$

The different variables used in the state space analysis of the MG are presented below:

ΔF = frequency fluctuation in the load,

R = droop in load frequency,

D = damping coefficient of the microgrid,

H = inertia constant of rotating parts in microgrid,

ΔP_L = load disturbance,

T_{fc} = time constant of fuel unit,

T_t = time constant of turbine,

T_g = time constant of governor,

T_{filt} = time constant of filter unit,

T_{inv} = time constant of inverter unit,

T_b = time constant of battery energy storage system,

ΔP_{TD} = change in turbine mechanical power output from the diesel unit

ΔP_W = disturbance in wind power,

ΔP_{PV} = disturbance in solar power,

ΔP_{PV_INV} = change in power outputs from inverter circuit of solar unit,

ΔP_{PV_FLT} = change in power outputs of filter circuit of solar unit,

ΔP_{GD} = power fluctuation in governor of diesel unit,

ΔP_{FC} = fuel cell unit power output fluctuation,

ΔP_{FC_INV} = power fluctuation in inverter unit of fuel cell,

ΔP_{FC_FLT} = power fluctuation in filter unit of fuel cell,

u_1 = input to the diesel unit from MPC,

u_2 = input to the fuel cell unit from MPC,

ΔP_{BESS} = battery unit power output fluctuation,

As MPC realization depends on system discrete signal, so the continuous state space function present in (6.5) for MG is represented in discrete form in (6.9).

$$\begin{cases} x(k+1) = A_{dis}x(k) + B_{dis}u(k) + E_{dis}w(k+1) \\ y(k) = C_{dis}x(k) + D_{dis}u(k) \end{cases} \quad (6.9)$$

Where all the discrete form of state matrices in (6.9) are related to continuous form of state equation in (6.5) are as follows [103]:

$$A_{dis} = e^{AT_s}; B_{dis} = (A_{dis} - I)A^{-1}B \text{ and the condition is valid when } A \text{ is invertible;} \\ E_{dis} = E, C_{dis} = C.$$

And the discrete form of state matrix for modelling of MPC is presented in (6.10).

$$x(k) = [\Delta F(k) \ \Delta P_{PV_INT}(k) \ \Delta P_{PV_FLT}(k) \ \Delta P_{GD}(k) \ \Delta P_{TD}(k) \ \Delta P_{FC}(k) \ \Delta P_{FC_INV}(k) \\ \Delta P_{FC_FLT}(k) \ \Delta P_{BESS}(k)]^T \quad (6.10)$$

6.4.2. Lead Compensator based DR for Frequency Regulation in MG

A conventional PI controller-based lead compensator DR as shown in Fig. 4.2 in Chapter-4 is added in the microgrid in addition to proposed PSO based MPC in secondary control loop of MG for smooth frequency control. The details description of conventional PI controller-based lead compensator DR can be referred from Chapter-3. This delay compensated DR is having two controller gain like K_{pc} , K_{ic} . As the DR controller is not considered for MPC design in in this Chapter for frequency regulation, so K_{pc} , K_{ic} are tuned together along with MPC input tuning parameter using PSO to get smooth frequency control.

6.4.3. BESS Modelling for Frequency Regulation

This section describes the different type of BESS modelling for frequency regulation of the isolated MG. Initially, a simple BESS model is used to test the frequency regulation performances with the proposed scheme of control technique in ALFC in presence of DR. The application of simple BESS modelling for frequency regulation of MG is shown in Fig. 6.1. As SOC control-based BESS is a suitable choice for frequency regulation as proved in Chapter-5, in the present section the SOC control-based BESS is applied in MG to compare the frequency regulation performance w.r.t. simple BESS model keeping the same proposed control scheme in ALFC of MG. The Proposed SOC controller in Chapter-5 is implemented

on a suitable incremental BESS model used in [61]. The SOC control-based BESS is shown in Fig. 5.2 in Chapter-5. The different parameters of the SOC control-based BESS model are presented as bellow and its values are referred from Appendix.

K_{BESS} = battery controller gain,	T_{BESS} = battery time constant,
α = converter's firing angle,	X_{co} = commutating reactance,
I_{BESS} = battery current flowing,	R_{bt} = connecting resistance,
R_{bs} = internal resistance,	R_b = over voltage resistance,
C_b = battery over voltage capacitance,	C_{bp} = capacitance of battery,
E_{boc} = battery open circuit voltage,	R_{bp} = self-release resistance,
E_b = battery over voltage,	E_{bt} = battery terminal voltage,
E_{do} = 12 pulse converter's ideal voltage,	ΔE_{cof} = power deviation-based Voltage
ΔE_{cod} = system disturbance-based Voltage	$\Delta E_{co} = \Delta E_{cof} + \Delta E_{cod}$ = dc voltage without overlap

The effectiveness of the SOC based BESS model is compared with simple BESS model for proposed frequency control scheme in simulation and result Section.

In Section-6.5.4, the frequency regulation is analysed with SOC control-based BESS. The SOC control-based BESS participated in ALFC of MG by considering the disturbance of microgrid in terms of frequency regulation as a defined signal ‘ Δ signal’ graphically presented in Fig. 5.2 in Chapter-5. The SOC control strategy of BESS depends on its mathematical calculation of SOC that presented in equation (5.14) in Chapter-5.

6.4.4. PSO Optimization to Tune R_w , K_{pc} , K_{ic} for Overall Frequency Control

PSO is a widely used robust optimization technique [93]. This technique is used in this study for tuning of different control parameters in the study. MPC has many parameters like input tuning parameter (R_w), prediction horizon (N_P), control horizon (N_C) and sampling time (T_s), that are directly linked with the performance of power system. From the simulation study it has been found that R_w of MPC greatly affects the dynamic performance of the studied power system. So, for the proposed MPC scheme, the input tuning parameter R_w is chosen to be tuned for MPC online optimization process for frequency regulation of MG. However, the conventional PI controller parameters like K_{pc} , K_{ic} of DR loop are also tuned in collaboration

with R_w to acquire smooth frequency control. Here, in the study integral time square error (ITSE) is measured as the objective function for tuning the gain parameters for better frequency control. Moreover, the objective function for MPC is expressed in equation (6.3). In (6.3), the plant output Y and Y_{ref} refers to frequency deviation (ΔF) and reference value of frequency deviation (ΔF_{ref}) of MG respectively. The input rate weight matrix \bar{R} in (6.3) is inter related to R_w which tuned by PSO to get minimum ITSE. So, here the problem formulation is a minimization problem. The details algorithm to tune R_w, K_{pc}, K_{ic} by PSO to get minimum error in terms of ITSE is presented in Fig. 6.3. The mathematical expression of ITSE which is to be minimized using PSO is presented in equation (6.11).

$$ITSE = \int_0^{t_{sim}} t. [\Delta f^2]. dt \quad (6.11)$$

PSO have been used to tune the three numbers of chosen parameters R_w, K_{pc}, K_{ic} as the dimension of the problem. In this Chapter, the other different parameters of the PSO are set as: number of particles =20, acceleration factors (c1& c2) considered as equal i.e, 2, maximum and minimum inertia weight as 0.9 and 0.4 respectively.

6.5. Simulation and Results

This section examines the effectiveness of the proposed PSO tuned MPC in presence of delay compensated DR for frequency regulation of MG. The studied MG with proposed scheme of frequency regulation technique that shown in Fig. 6.1 is built in MATLAB/Simulink for analysis. The total simulation time is considered 10 second and sampling time is set as 0.01 second. The present frequency regulation analysis is established for certain values of load and generation variations. In the analysis, from Section-6.5.1 to Section-6.5.3, the load variation, solar power variation and wind power variation are sets as 0.02 p.u,0.2p.u,0.25 p.u respectively. The implementation of MPC for ALFC considered all the load and generation variations for its online optimization process to provide smooth frequency control. The various case studies are done to test the effectiveness of the proposed load frequency control scheme.

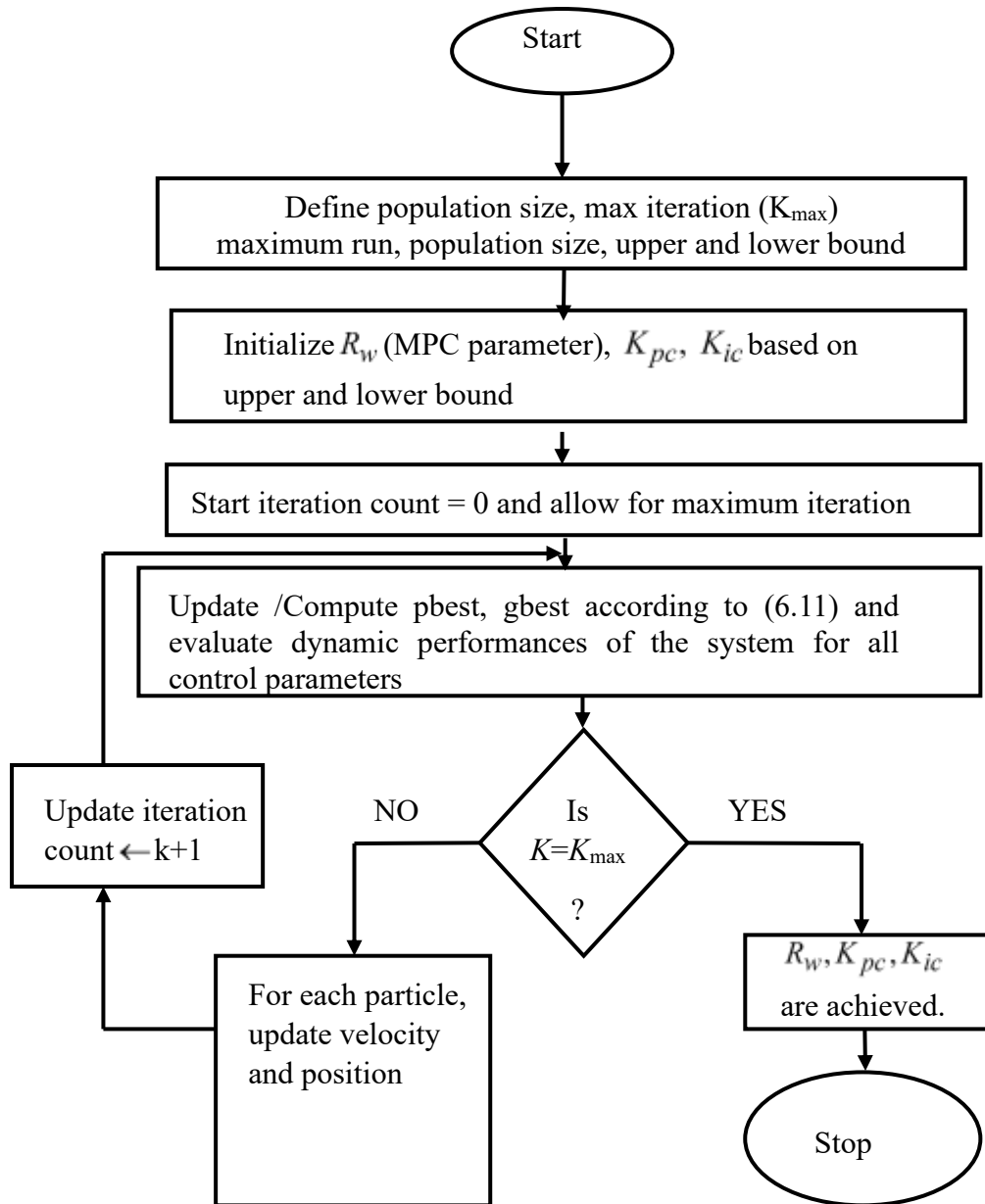
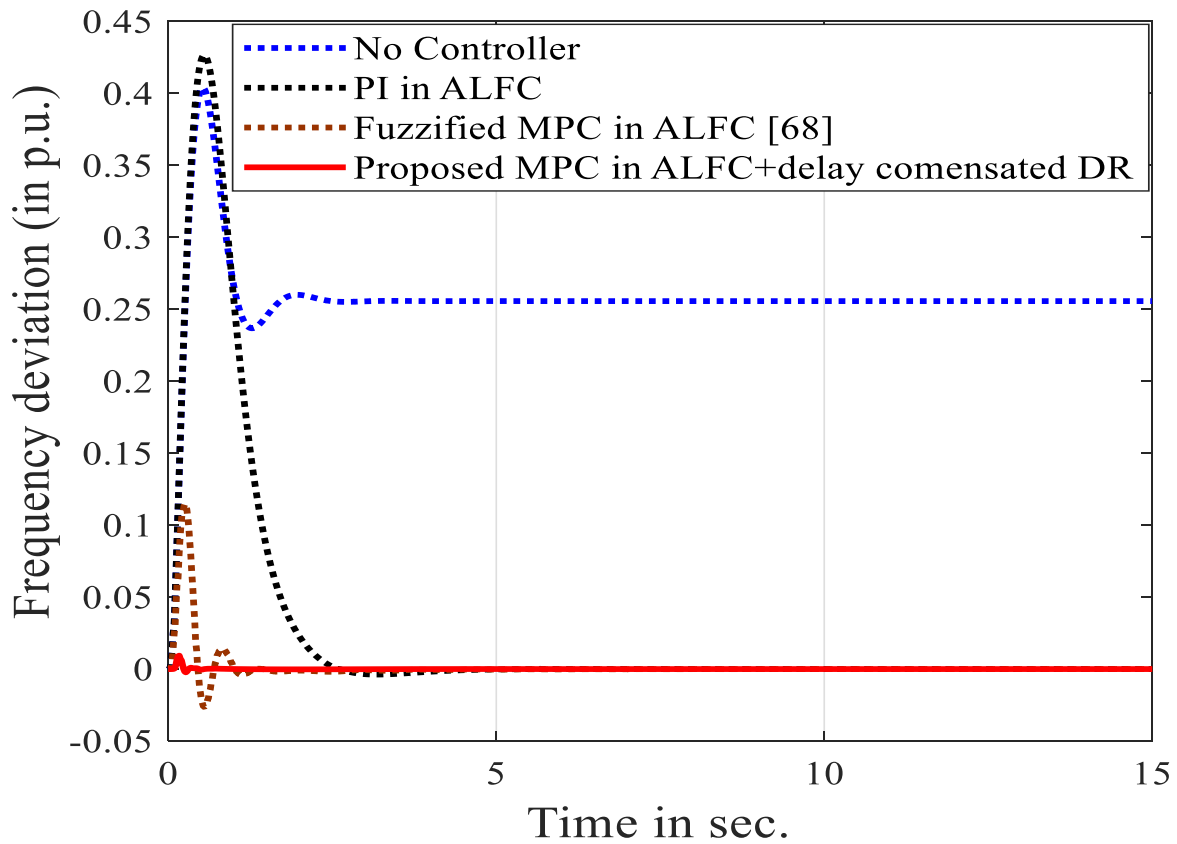


Fig. 6.3. PSO algorithm to tune R_w, K_{pc}, K_{ic} .

6.5.1. Performance Analysis of Proposed Frequency Control Scheme Compared to Others Existing Control Scheme for ALFC in MG.

This section studies the performance of proposed PSO tuned MPC in collaboration with DR and simple BESS model for frequency regulation. The arrangement of proposed frequency regulation scheme is shown in Fig. 6.1. For the set values of load and generation variation, MPC input parameter R_w , PI gain parameters (K_{pc} , K_{ic}) in delay compensated DR are tuned to get better frequency regulation in MG. Then the dynamic performance of MG in terms of frequency deviation is obtained with those tuned values of gain parameters along with tuned MPC online optimization scheme in ALFC. Furthermore, the obtained frequency deviation with the proposed scheme is compared with fuzzified adaptive MPC [68] and other conventional controller in ALFC of MG. The comparison of dynamic responses in terms of frequency regulation and cost function of proposed MPC is obtained and shown in Fig. 6.4 (a) and Fig. 6.4 (b) respectively. The tuned gain values are $R_w = 0.74603$, $K_{pc} = -0.5437$ and $K_{ic} = 0.4911$.



(a)

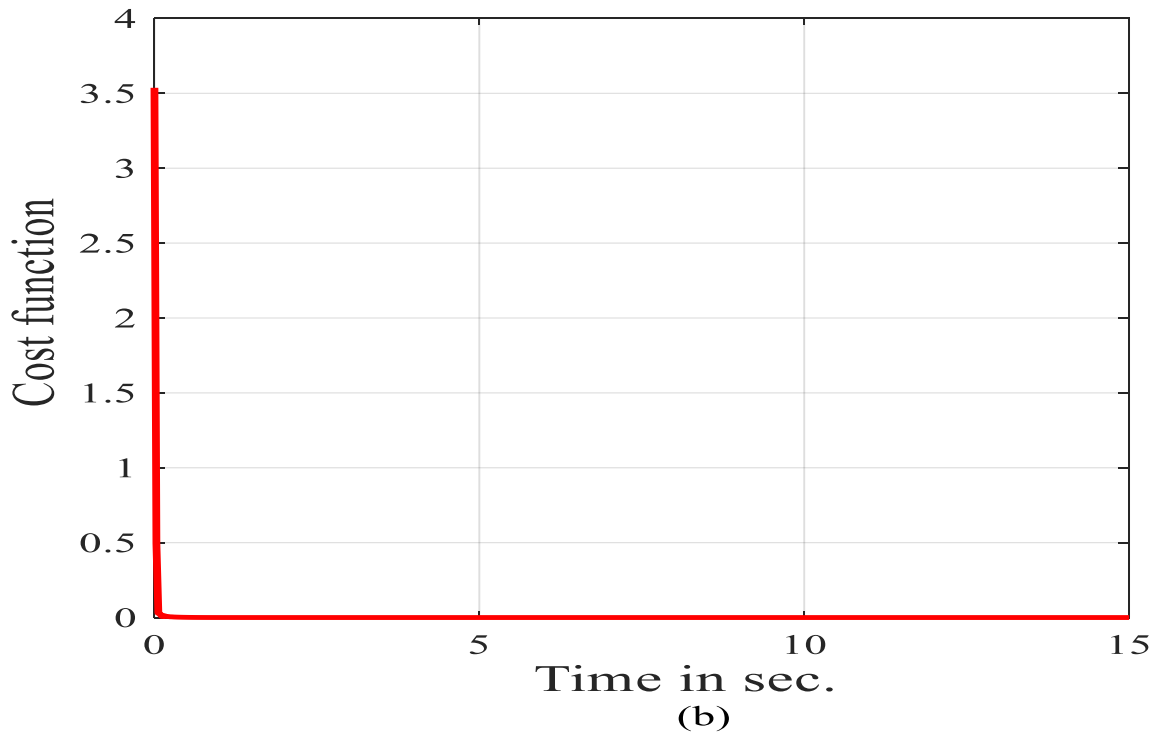


Fig. 6.4 Responses from case A in terms of a) comparison of frequency deviations of MG b) cost function of proposed MPC.

The results shown in Fig. 6.4. (a) proves better frequency control in terms of settling time, overshoot and undershoot, die out of oscillations.

6.5.2. Proposed MPC Combined with and without Lead Compensator in DR Loop.

In this section, the delay compensator in DR is examined for the frequency control performance in collaboration with simple BESS model and proposed PSO tuned MPC in ALFC of MG. The input parameter of MPC is tuned with and without delay compensator in MG. The dynamic performance in terms of frequency regulation is obtained with only tuned value of MPC in case of without delay compensator in DR of MG. Similarly, with tuned value of K_p and PI gain parameters of delay compensator DR loop are applied to find frequency deviation of MG when delay compensated DR collaborated with PSO tuned MPC for frequency control process. Then the frequency control performance is compared with the proposed scheme of frequency control technique with and without delay compensator in DR loop of studied MG and that shows in Fig. 6.5. Fig. 6.5 proves that delay compensator in DR can able to reduce the over shoot and under shoot from system dynamics in MG.

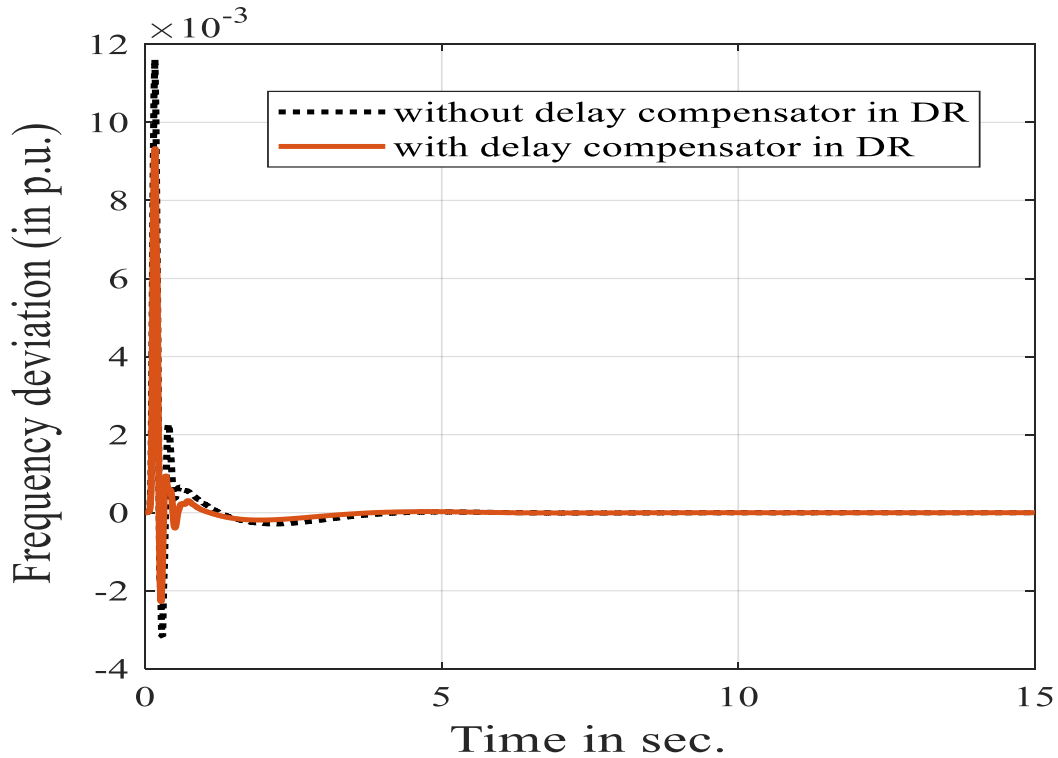
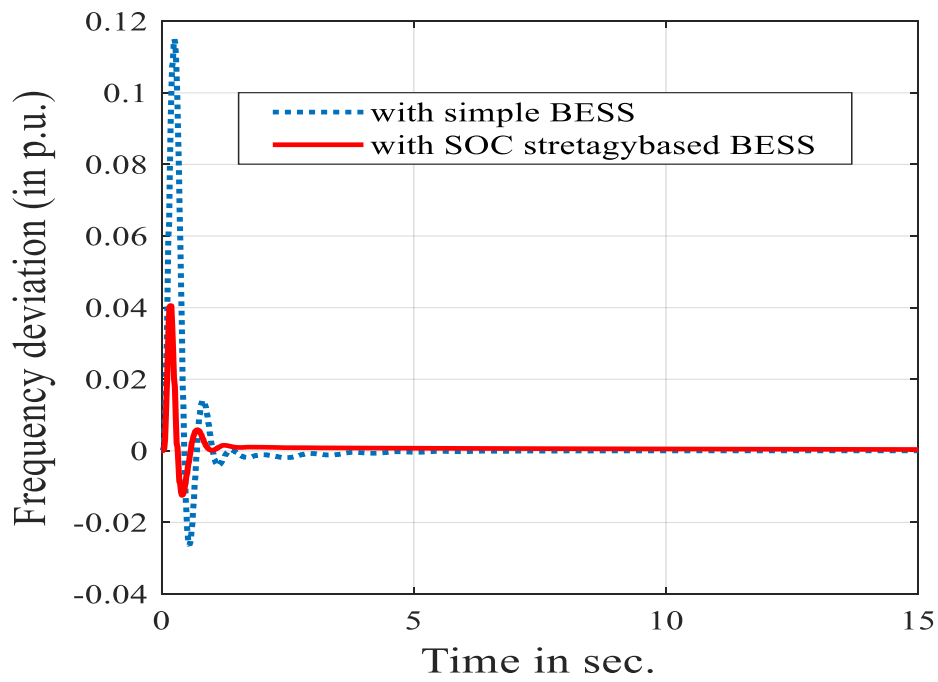


Fig. 6.5. Comparison of frequency deviation of the MG with and without delay compensator in DR.

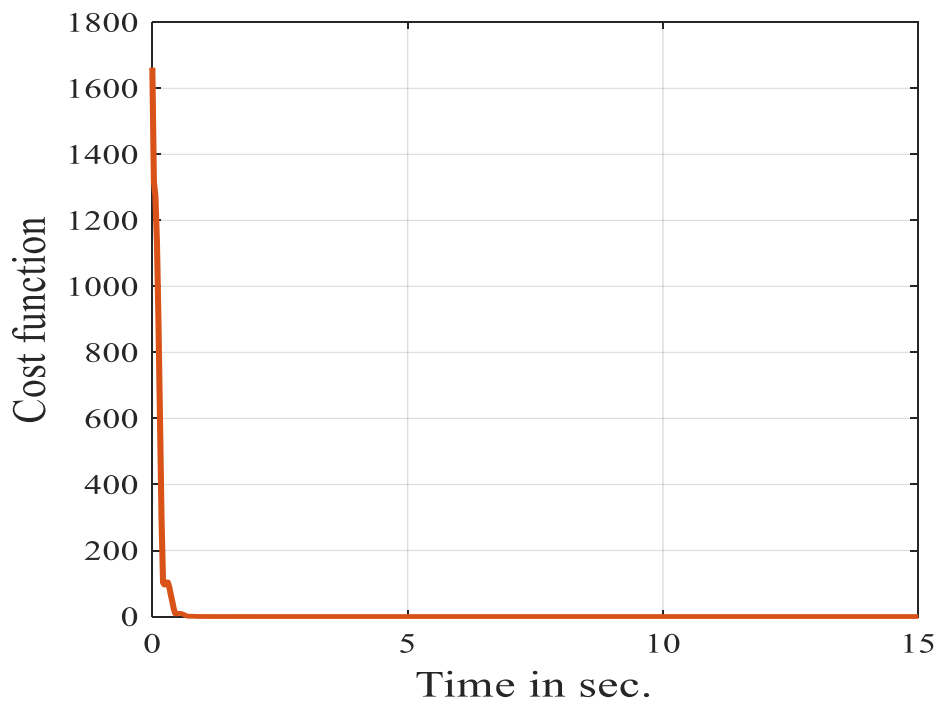
6.5.3. Comparison of SOC Control Based BESS and Simple BESS Model for Frequency Regulation in MG.

From Section-6.5.2, it is verified that lead compensator DR is a good choice for frequency regulation. So, this section has considered the lead compensator-based DR along with a SOC control strategy-based BESS model for frequency regulation in presence of proposed PSO based MPC in ALFC of the studied MG. So, in the present study, the MG is having the power sources such as diesel unit, fuel cell, wind energy, solar energy, SOC control strategy-based BESS and lead compensator-based DR. To solve the ALFC problem of the MG, MPC is designed in ALFC which drives the power of the diesel and fuel cell unit at the time of load and generation mismatch. Meanwhile, BESS and DR participate in frequency regulation task according to system configuration. In short, the BESS and DR both are connected at the same time to the MG to solve ALFC problem depending on the system power requirements. As the battery modelling is modified from simple BESS model to SOC strategy-based BESS model as in Section IV C by keeping all other arrangement same as in Fig. 6.1 for frequency regulation analysis. The results compared the frequency control performances for the different BESS modelling in ALFC of MG. The system performance of the MG in terms of frequency

deviation for simple BESS model and SOC control strategy-based BESS model is shown in Fig. 6.6(a).



(a)



(b)

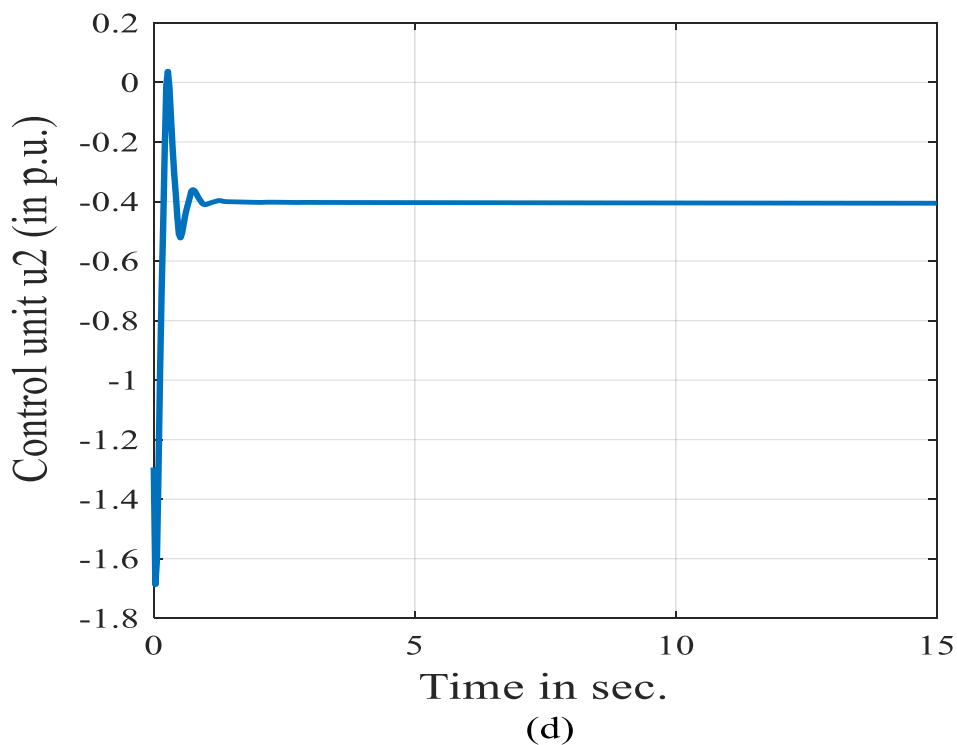
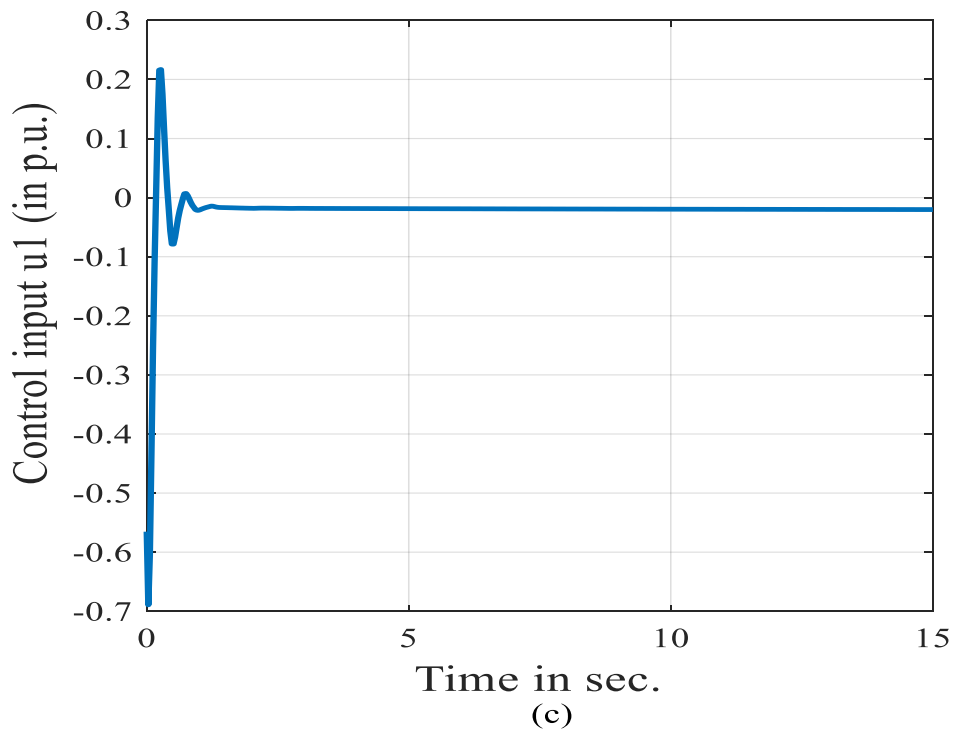


Fig. 6.6. Responses from Section 6.5.3 in terms of a) comparison of frequency deviations of MG b) cost function of proposed MPC c) control input to diesel cell d) control input to fuel cell.

Fig. 6.6(a) proves that the introduction of SOC based BESS model in the proposed frequency control scheme in ALFC of MG gives better dynamic frequency regulation in comparison with the introduction of simple BESS model in the ALFC scheme of MG in terms of settling time,

maximum overshoot. Hence, with the introduction of SOC based BESS model in the proposed frequency control scheme, the respective cost function and the control input to diesel cell u_1 and control input to fuel cell u_2 from proposed MPC are obtained and are shown in Fig. 6.6(b), Fig. 6.6(c) and Fig. 6.6(d) respectively.

6.5.4. Sensitivity Analysis with the Proposed Frequency Control Scheme.

This section provides the robustness test of the proposed frequency regulation scheme which contains PSO tuned MPC in ALFC in collaboration with delay compensated DR and BESS. The robustness issue is very important criteria for control system modelling in any system. Moreover, the introduction of MPC in power system needs to be analysed for stability as it depends on receding horizon approach in presence of constraints that might make the system unstable [101]. In overall, the formulation of cost function for MPC is not an issue if MPC designed in a commercial tool like MATLAB program by the MATHWORKS [101]. In the present work, the MPC formulation is made in MATLAB. Apart from MPC in ALFC, other conventional controller like PI controller is also present in DR loop. So, a simulation-based approach is used in this section to check the stability of the isolated MG in presence of all set of controllers in the system. In this simulation approach three numbers of selected system parameters are varied from -50% to $+50\%$ of its nominal values in a step of 25% . The three system parameters that are chosen in the study to vary are battery time constant (T_b), governor time constant (T_g) and damping coefficient (D). Then the performance of the system is observed in terms of performance indices like ITAE and minimum damping ration (MDR) for each step of parameter variation with the proposed scheme of controller ALFC of MG and obtained results presented in Table. 6.2. The outcomes of Table. 6.2 reveals that system performance indices are not changed so far for system parameter variation and is merely changes for $\pm 50\%$ of parameter variation.

Furthermore, the robustness of the proposed frequency control scheme also checked from load operating point of analysis. In this analysis, the system load has set as continuous step load change of 0-5% in a step of 1% in the MG for total simulation time of 50 second. The operating load pattern for continuous load change is presented in Fig. 6.7. The system performance in terms of frequency deviation is obtained for continuous load variation with proposed frequency regulation scheme. Then the obtained frequency deviation is compared with the frequency deviation obtained from same MG with a robust MPC controller used for frequency regulation task in [68]. The comparison results are presented in Fig. 6.8. The Fig. 6.8 shows that the overshoot and undershoot are less with proposed PSO based MPC in

comparison with fuzzy adaptive MPC used for ALFC for continuous load change in the MG. So, the degree of stability is more with proposed scheme of frequency regulation over controller used in [68].

Table 6.2. Observation of different performance indices for system parameter variations.

Parameter Change	% Change	ITSE	MDR
Nominal	0	0.000069	0.5243
T_g	+50	0.000012	0.4112
	+25	0.000051	0.5037
	-25	0.000031	0.5042
	-50	0.000071	0.4748
T_b	+50	0.000113	0.4984
	+25	0.000023	0.5002
	-25	0.000024	0.5234
	-50	0.000093	0.4725
D	+50	0.000128	0.4828
	+25	0.000088	0.5203
	-25	0.000082	0.5075
	-50	0.000117	0.4967

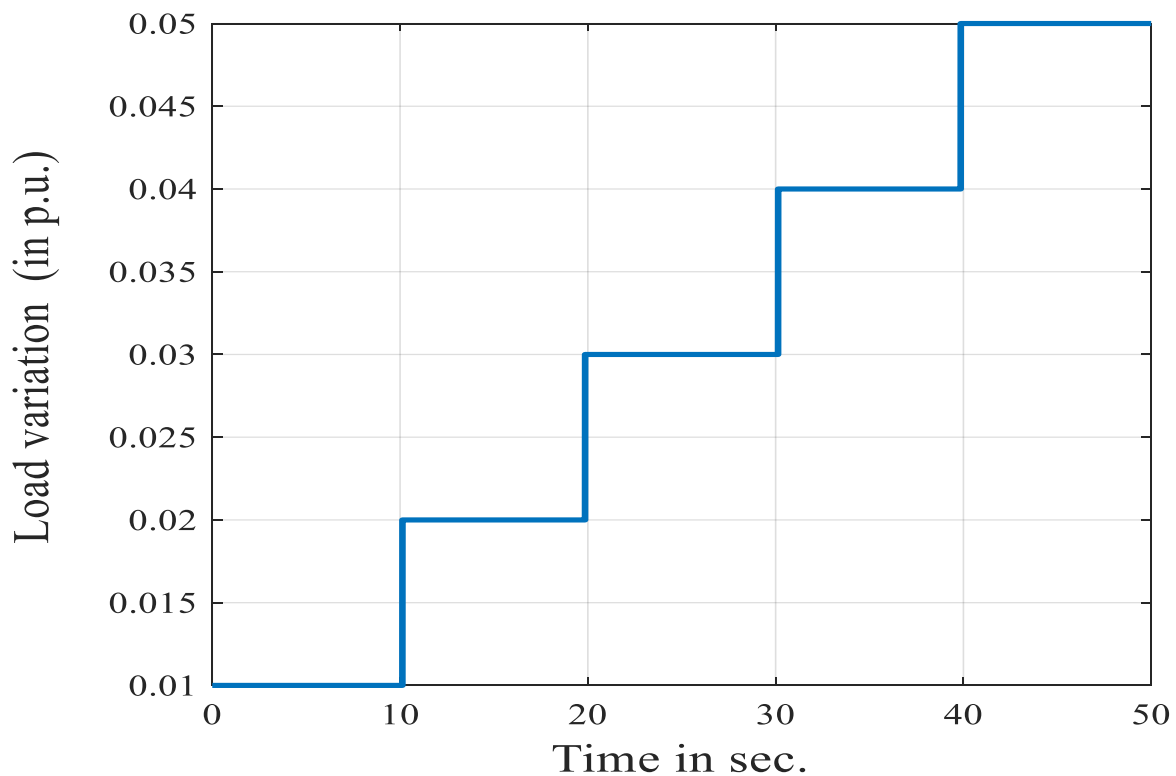


Fig. 6.7. Pattern of step load change

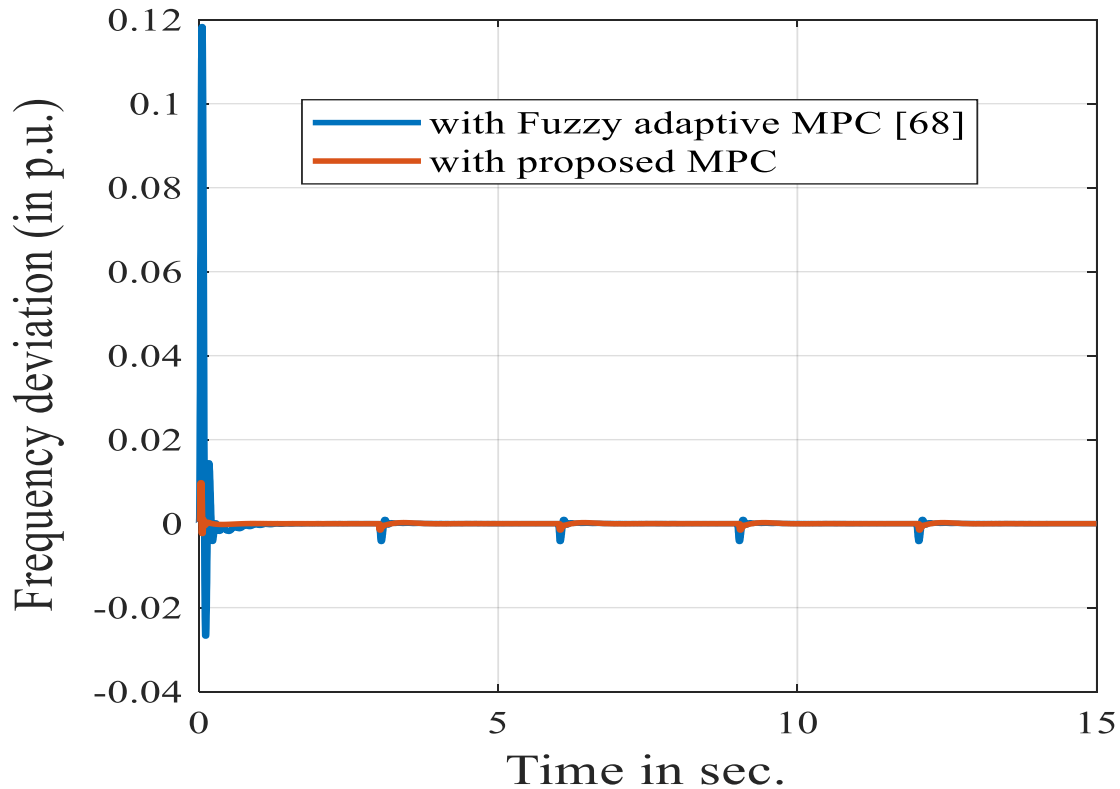


Fig. 6.8. Comparison of frequency deviation with different controller for continuous load variation.

6.6. Experimental Test Analysis

In view of practical validation of proposed frequency control scheme, the performance of proposed frequency control scheme for studied MG is realized with real time analysis through OPAL-RT OP5600 with RT lab version of 19.3.0.228. The studied MG model with proposed frequency control scheme in presence of BESS and lead compensator-based DR in ALFC is modelled in real time simulator in the RT lab of the target platform (hardware synchronized real time simulator) by considering fixed step size of 0.01second. The PF511127S01 hardware with 12 cores has been used. The number of steps without overruns is consider as 10 for the real time simulation study in OPAL-RT. The experimental set up for current study with OP5600 at power system and simulation lab in Electrical engineering department, Jadavpur University is shown in Fig. 6.9.

The real time dynamic performance with proposed frequency control scheme in presence of BESS and lead compensator based DR in ALFC for load variation of 0.02 p.u in presence of solar power and wind power contribution of 0.2p.u and 0.25 p.u respectively is shown

in Fig. 6.10.

Similarly, to check the robustness of the proposed control scheme in real time the frequency deviation is obtained for the load variation in the range of 0-5% in a step of 1% for first 50 second as done in simulation in Section-VD and the result is shown in Fig. 6.11.



Fig. 6.9. OP5600 Set-up for real time application of the proposed control scheme.

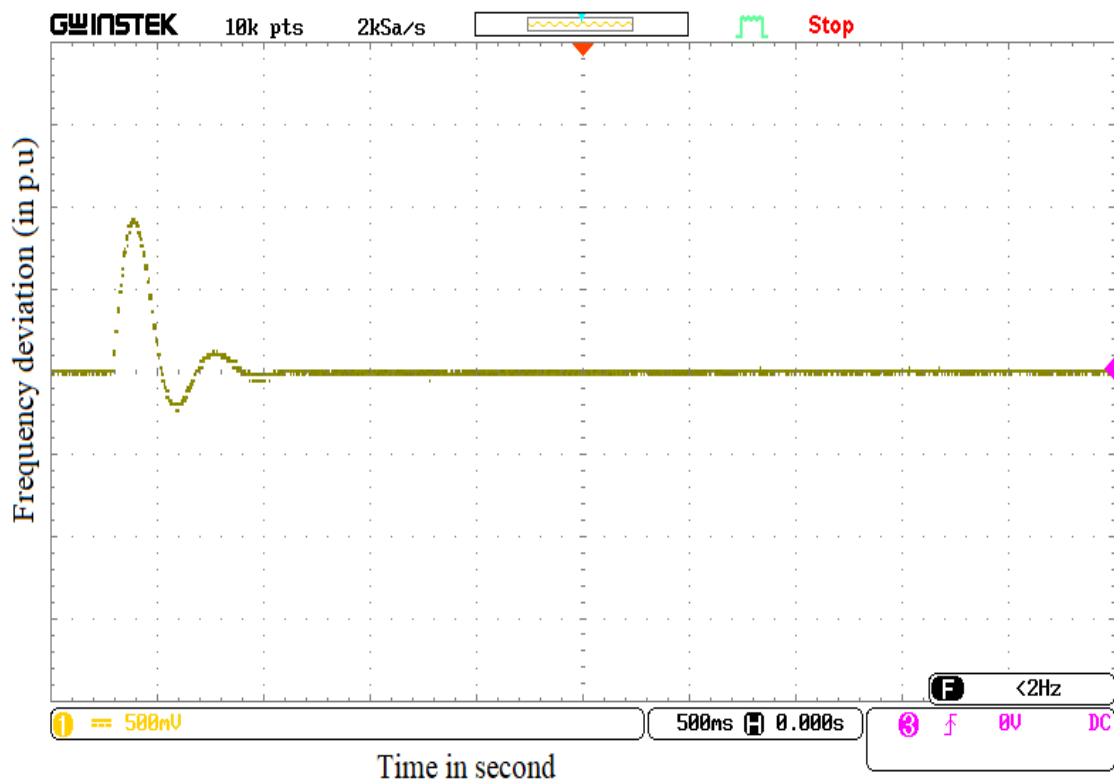


Fig. 6.10. Real time response in OPAL-RT of MG with proposed scheme for frequency regulation.

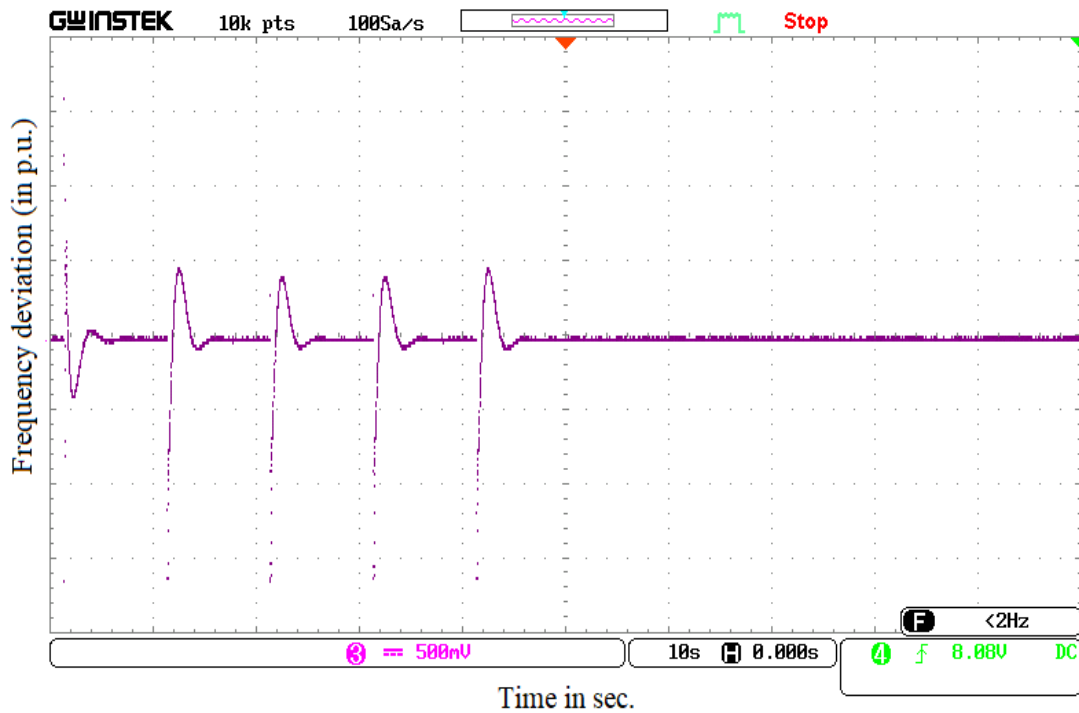


Fig. 6.11. Real time response in OPAL-RT of MG for continuous load variation in the range of 0-5% in a step of 1% for first 50 second.

6.7. Discussion

This section describes the overall outcomes for the application of proposed frequency control scheme for ALFC problem in isolated MG. Furthermore, compare the optimization execution time with the proposed set of controllers in ALFC with another recent robust controller used in ALFC of MG [68]. Also, discusses the effectiveness of proposed scheme of frequency control in real time application. At the end of this section, the future scope of the present study is presented.

The execution of proposed frequency control scheme in MG can able to afford overall improved frequency control performances in terms of performance index like ITAE compared to existing controller used in MG applied for same purpose in literature. This comparison in ITAE for different controller for ALFC including the proposed frequency control scheme is presented in Table. 6.3.

Table. 6.3. Comparison of performance index with different controllers for ALFC.

Existence of controller in ALFC	ITSE
Proposed MPC along with SOC control-based BESS model and lead compensator-based DR	0.000069
Proposed MPC along with simple BESS model and lead compensator-based DR	0.002974
Fuzzy Adaptive MPC [68]	0.009268
PI Controller	0.02872
No Controller	0.3472

In addition to PSO tuned MPC in ALFC, the additional delay compensator in DR for frequency regulation scheme can able to reduce the overshoot and undershoot from the system dynamic performances that specially arose in the system due to the communication loop from the advanced frequency regulation technique like DR. This has been graphically proved in Fig. 6.5. Moreover, the proposed frequency control scheme together with lead compensator-based DR and BESS in ALFC is found robust for frequency regulation study of the studied isolated MG. This robustness is concluded from simulation-based results shown in Fig. 6.8. Same observation is found in real time application as shown in Fig. 6.11.

Another important part of discussion is the execution time for online optimization of adaptive optimization scheme of MPC implemented in ALFC of MG. The proposed PSO based MPC in collaboration with lead compensator-based DR and BESS in ALFC takes an execution time of $1.01 \mu s$ for its adaptive optimization. It is observed that the proposed PSO based MPC reduces the optimization algorithm execution time by 25% maintaining the quality of output of the system compared to a robust fuzzified MPC applied to solve ALFC problem in[24].

In future, along with input tuning parameter R_w , the other several parameters such as prediction horizon, control horizon of MPC can have optimized for its adaptive optimization process to get more smooth frequency regulation of the MG. Moreover, the proposed control scheme may be applied to multi-area power system to verify the effectiveness of the control method in wide range.

6.8. Conclusion

The proposed scheme of frequency control method can improve the dynamic performance of the system in terms of ITSE, overshoot and undershoot. Moreover, the introduction of lead compensator-based delay compensator in DR is exclusively responsible to reduce the overshoot and undershoot from the dynamic response of the system. Furthermore, the effectiveness of SOC control-based BESS model shown in Fig. 4 is tested in the proposed frequency control scheme by replacing the simple BESS model from the MG with the SOC control-based BESS model. The dynamic performance of MG is found more promising in terms of reduction in settling time, overshoot and undershoot. The overall results prove the effectiveness of the proposed PSO tuned MPC in collaboration with delay compensated DR and BESS for ALFC. Additionally, results of real time simulation in OPAL-RT validate the real time application of proposed control strategy for MG.

6.9. Publication from This Work

Journal publication

- [1] **Swetalina Bhuyan**, Sunita Halder Nee Dey, and Subrata Paul. " Experimental Assessment of Parameter Driven MPC for frequency regulation in Collaboration with Delay Compensated Demand Response of an Isolated Micro grid." (Communicated).

CHAPTER 7

CONCLUSION

This chapter presents conclusion of the thesis in general based on the results analyzed in the previous chapters. The future scope of the present work is also presented.

7.1. General Conclusion

The conclusion of the thesis is summarized below:

1. The ALFC model of a two-area power system consisting of a thermal and a DFIG unit as well as integrated with DSM model of a power system is developed. PSO is implemented to tune control parameter to minimize total settling time of frequency for step change in load in any area. The role of demand side management in terms of DR in dynamic response of present power system is studied. It has been observed that demand side management is able to improve the settling time for all type of frequency deviations.
2. Demand side management has a significant role in maintaining power balance from the customer side. In this work, DR is introduced in the ALFC model of a two-area hydrothermal power network to study the efficacy of DSM in dynamic stability of a power network. Here, the selected controllers gain of both the areas are optimized using PSO to minimize total settling time i.e, summation of settling time for frequency deviations of the two areas and tie line power deviation. Simulation result shows that DR plays a key role in enhancement in dynamic stability of power network. The performance indices to assess dynamic stability of power system; like ITAE, IAE, ITSE, ISE are computed and their values proved that DSM definitely improves dynamic stability of power system.
3. This extensive study analyzes the frequency regulation in ALFC of a DR collaborated power system. The significant shortcoming in DR is communication delay that appears in the system during sending commands from the control center to controllable loads for balancing the system and receiving response. Therefore, in the

present study, a modified delay compensator is envisaged to enhance the effectiveness of DR for frequency regulation. The modified delay compensator is a lead compensator-based PI controller in DR loop. The performance of the proposed controller is examined by considering two different two area power system i.e, hydro-thermal and wind integrated thermal system as test systems. For the wind integrated thermal system, DFIG based wind is considered for frequency support. In addition, the inertia effect on thermal system due to the integration of DFIG is taken care in the study by considering a PD-inertia controller in it. The performance analysis is done by simulating the transfer function model of the test systems in MATLAB Toolbox. The simulation results are examined with tuned values of all controller along with the modified DR controller for frequency regulation. A normalized form of PSO based weighted sum multi objective optimization is used to tune the controller parameters designed in the above test systems for smooth frequency regulation. The stability and robustness of these systems with the proposed controller are analysed through eigenvalue calculation. The result exhibits better efficiency with proposed controller. Furthermore, the dynamic performances of the test systems show better results than earlier works in literature. Finally, the sensitivity analysis of the proposed controller for two area wind integrated thermal system and Hydrothermal system shows negligible difference in system performances even with parameter variation in the range of $\pm 50\%$ and continuous load variation in the range of 0% to 50% of its nominal values. However, the study to check the performance of proposed delay compensator is limited to some selected power system. Future work will further investigate the performance of proposed controller for different power system integrated with renewable energy sources and storage devices.

4. To summarize the extension method for frequency regulation, it is found that MPC based ALFC is a robust control method for the modern power system. The performance of the MPC is examined in this study in presence of renewable energy sources, battery and the new form of technology like demand side management for frequency regulation. Furthermore, the collaboration of DR along with BESS in conventional ALFC gives more degree of solution for frequency regulation in terms of stability, error reduction and settling time. The SOC strategy-based BESS could able to save the battery life as it operates within the SOC limit while participating in ALFC for frequency control. Also, it has been observed that change in SOC is least when BESS collaboratively participated with DR in MPC based ALFC. That implies

that the exchange of power between BESS and power grid will be less when BESS and DR co-cordially participated in the proposed MPC based ALFC which can save battery life too. The simulation results proved that the most effective way to improve the system dynamic behaviour is obtained when both SOC based BESS and DR present in the proposed MPC based ALFC with frequency support from wind. Finally, all the results with the present method of control action designed for ALFC are compared in terms of their system performance indices like ITAE and settling time with other results present in [12], which having conventional method of control action in ALFC for smooth frequency regulation. Results prove the effectiveness of proposed control action for ALFC.

5. A new PSO tuned MPC in collaboration with delay compensated DR and SOC control-based BESS for ALFC study for microgrid is developed. The proposed scheme of frequency control method can improve the dynamic performance of the system in terms of ITSE, overshoot and undershoot. Moreover, the introduction of lead compensator-based delay compensator in DR is exclusively responsible to reduce the overshoot and undershoot from the dynamic response of the system. Furthermore, the effectiveness of SOC control-based BESS model is tested in the proposed frequency control scheme by replacing the simple BESS model from the MG with the SOC control-based BESS model. The dynamic performance of MG is found more promising in terms of reduction in settling time, overshoot and undershoot. The overall results prove the effectiveness of the proposed PSO tuned MPC in collaboration with delay compensated DR and BESS for ALFC. Additionally, results of real time simulation in OPAL-RT validate the real time application of proposed control strategy for MG.

7.2. Future Scope of Work

Based on the extensive investigations carried out in this work, the following possible areas for future work seem to be worth pursuing:

1. In future, the various parameters of MPC like prediction horizon, control horizon can have optimized for its adaptive optimization process to get more smooth frequency regulation of the hybrid power system.

2. Moreover, the proposed control scheme may be applied to multi area power system to verify the effectiveness of the control method in wide range.
3. Real time verification of the performance of all developed control strategy in ALFC for multi area power system can be done using OPAL-RT.

REFERENCES

1. P. Kundur, Power system Stability and Control. New York, NY, USA: McGraw-Hill, 1994.
2. A. Chakrabarti and S. Halder, Power system analysis: operation and control, 3rd Edition. PHI Learning Pvt. Ltd., 2010.
3. O.I. Elgerd, Electric energy systems theory: an introduction, 2nd Edition. McGraw-Hill, 2005 [25th Reprint].
4. R. Doherty and M. O'Malley, "A new approach to quantify reserve demand in systems with significant wind installed capacity," IEEE Transaction on power systems, vol. 20, no. 2, pp. 587–595, May 2005.
5. H. Huang and F. Li, "Sensitivity analysis of load-damping characteristic in power system frequency regulation," IEEE Transaction on power systems, vol. 28, no. 2, pp. 1324–1335, May 2013.
6. Ibraheem, P. Kumar, and D. P. Kothari, "Recent philosophies of automatic generation control strategies in power systems," IEEE Transaction on power systems, vol. 20, no. 1, pp. 346–357, February, 2005.
7. H. Bevrani, Robust Power System Frequency Control. New York, NY, USA: Springer, 2009.
8. C.C. Wu, W.J. Lee, C.L. Cheng and H.W. Lan, "Role and value of pumped storage units in an ancillary services market for isolated power system-simulation in the Taiwan power system," IEEE Transaction Ind. Appl., vol. 44, no. 6, pp. 1924–1929, Nov./Dec. 2008.
9. P.A. Stott, M.A. Mueller, "Modeling fully variable speed hybrid wind diesel systems", In Proceedings of the 41st International Universities Power Engineering Conference, Newcastle upon Tyne, UK, 6–8 September, 2006.
10. Nguyen, Nga, et al. "Frequency response in the presence of renewable generation: Challenges and opportunities." IEEE open access journal of power and energy 8 (2021): 543-556.
11. J. Nanda, A. Mangla, and S. Suri, "Some new findings on automatic generation control of an interconnected hydrothermal system with conventional controllers," IEEE Transactions on energy conversion, vol.21, no.1, pp.187-194, 2006
12. S. Chaine, and M. Tripathy, "Performance of CSA optimized controllers of DFIGs and AGC to improve frequency regulation of a wind integrated hydrothermal power

- system,” Alexandria Engineering Journal, vol.58, no.2, pp.579-590, 2019.
13. M. L. Kothari, J. Nanda, and P. S. Satsangi, “Automatic generation control of hydrothermal system considering generation rate constraint,” J. Inst. Eng. India, vol. 63, pp. 289–297, Jun. 1983.
 14. M. Leum, "The development and field experience of a transistor electric governor for hydro turbines," IEEE Transactions on Power Apparatus and Systems, vol. 4, pp. 393-402, 1966.
 15. M. L. Kothari, and J. Nanda, "Application of optimal control strategy to automatic generation control of a hydrothermal system," IEE Proceedings D (Control Theory and Applications). Vol. 135, no. 4. IET Digital Library, 1988.
 16. P. Bhatt, R. Roy, and S. P. Ghoshal. "Dynamic participation of doubly fed induction generator in automatic generation control," Renewable energy vol.36, no.4, pp. 1203-1213, 2011.
 17. S. A. Pourmousavi and M. H. Nehrir, “Introducing dynamic demand response in the LFC model.” IEEE Transactions on Power Systems, vol. 29, no. 4, pp.1562-1572, 2014.
 18. F.A. Hassan, M. Mahmoud, O.A.M. Almohammed, “Analysis of the Generated Output Energy by Different Types of Wind Turbines,” Journal of Human, Earth, and Future, vol.1, no. 4, pp.181-187,2020.
 19. F.A. Hassan, “Multi-criteria approach and wind farm site selection analysis for improving power efficiency,” Journal of Human, Earth, and Future, vol.1, no.2, pp.60-70, 2020.
 20. J.M. Mauricio, A. Marano, A. Gómez-Expósito, J.L. M. Ramos, “Frequency regulation contribution through variable-speed wind energy conversion systems,” IEEE Transactions on Power Systems. Vol. 24, no. 1, pp.173–180, 2009.
 21. S. Chaine, M. Tripathy, and D. Jain, “Nondominated Cuckoo search algorithm optimized controllers to improve the frequency regulation characteristics of wind thermal power system,” Engineering science and technology, an international journal, vol. 20, no. 3, pp. 1092-1105, 2017.
 22. S. Chaine, M. Tripathy, and S. Satpathy, “NSGA-II based optimal control scheme of wind thermal power system for improvement of frequency regulation characteristics”, Ain Shams Engineering Journal, vol. 6, no. 3, pp. 851-863,2015.
 23. Z. Yi, Y. Xu, W. Gu, and Z. Fei, “Secondary Frequency Regulation for a Microgrid,” vol. 12, no. 2, pp. 1078–1089, 2021.
 24. S. Panda, Yegireddy NK. “Automatic generation control of multi-area power system

- using multi-objective non-dominated sorting genetic algorithm-II,” *International Journal of Electrical Power & Energy Systems*, pp. 53:54-63, Dec 1, 2013.
25. ML Kothari, J. Nanda “Application of optimal control strategy to automatic generation control of a hydrothermal system,” In *IEEE Proceedings D (Control Theory and Applications)* ,Vol. 135, no. 4, pp. 268-274. IET Digital Library, 1988 Jul 1.
 26. GG. Bhise, ML. Kothari, J. Nanda “Optimum selection of hydro governor parameters for automatic generation control of a hydrothermal system,” In 1993 2nd International Conference on Advances in Power System Control, Operation and Management, APSCOM-93. pp. 910-915. IET, 1993 Dec 7.
 27. Y. Pal Verma, A. Kumar, “Participation of doubly fed induction generator-based wind turbine in frequency regulation with frequency-linked pricing,” *Electric Power Components and Systems*, vol. 40, no. 14, pp. 1586-1604, 2012.
 28. Ayodele, T. R., et al., “Challenges of grid integration of wind power on power system grid integrity: A review,” *world 3*, 2020.
 29. Wang, Siqi, and Kevin Tomsovic, “Fast frequency support from wind turbine generators with auxiliary dynamic demand control,” *IEEE Transactions on Power Systems*, vol.34, no.5, pp.3340-3348, 2019.
 30. Xu, Chen, Xiaodong Chu, and Haoyi Huang. "Wide-area synthetic inertia control of multiple resources incorporating primary frequency control of wind turbines." *Journal of Physics: Conference Series*. Vol. 1176, no. 6, IOP Publishing, 2019.
 31. A. H. A. Elkasem, S. Kamel, A. Rashad, and F. Jurado, “Optimal Performance of DFIG Integrated with Different Power System Areas Using Multi-Objective Genetic Algorithm,” 2018 20th Int. Middle East Power Syst. Conf. MEPCON 2018 - Proc., pp. 672–678, 2019, doi: 10.1109/MEPCON.2018.8635243.
 32. A. Annamraju and S. Nandiraju, “Load Frequency Control of an Autonomous Microgrid Using Robust Fuzzy PI Controller,” *2019 8th Int. Conf. Power Syst. Transit. Towar. Sustain. Smart Flex. Grids, ICPS 2019*, 2019, doi: 10.1109/ICPS48983.2019.9067613.
 33. A. Bouaddi, R. Rabeh, and M. Ferfra, “Load Frequency Control of Autonomous Microgrid System Using Hybrid Fuzzy logic GWO-CS PI Controller,” 2021 9th Int. Conf. Syst. Control. ICSC 2021, pp. 554–559, 2021, doi: 10.1109/ICSC50472.2021.9666683.
 34. C.C. Wu, W.J. Lee, C.L. Cheng and H.W. Lan, “Role and value of pumped storage units in an ancillary services market for isolated power system-simulation in the Taiwan

- power system,” IEEE Transaction Ind. Appl., vol. 44, no. 6, pp. 1924–1929, Nov./Dec. 2008
35. M. H. Albadi, E. F. El-Saadany, “A summary of demand response in electricity markets,” *Electric power systems research*, vol.78, no.11, pp. 1989-1996, 2008.
 36. S. Braithwait, K. Eakin “The role of demand response in electric power market design,” Edison Electric Institute, pp.1-57, 2002.
 37. E. Nekouei, T. Alpcan and D. Chattopadhyay, "Game-Theoretic Frameworks for Demand Response in Electricity Markets," in *IEEE Transactions on Smart Grid*, vol. 6, no. 2, pp. 748-758, March 2015, doi: 10.1109/TSG.2014.2367494.
 38. C. B. Field, V. R. Barros, K. Mach, and M. Mastrandrea, “Climate Change 2014: Impacts, Adaptation, and Vulnerability,” New York, USA: Cambridge University Press, 2014.
 39. F. C Schweppe, R. D. Tabors, J. Kirtley, H. Outhred, F. Pickel, & A. Cox, “Homeostatic utility control,” *IEEE Transactions on Power Apparatus and Systems*, PAS-vol. 99, no. 3, pp. 1151–1163, 1980, May, <https://doi.org/10.1109/TPAS.1980.319745>.
 40. T. K. Chau, et al., “Demand-side regulation provision from industrial loads integrated with solar PV panels and energy storage system for ancillary services,” *IEEE Transactions on Industrial Informatics* vol. 14, no. 11, pp. 5038-5049, 2017.
 41. D. J. Shiltz, et al., “Integration of automatic generation control and demand response via a dynamic regulation market mechanism,” *IEEE Transactions on Control Systems Technology*, Vol. 27, no.2, pp. 631-646, 2017.
 42. D. Jay & K. S. Swarup, “Frequency restoration using dynamic demand control under smart grid environment,” In *Proc. IEEE PES Innovative Smart Grid Technologies—India (ISGT India)*, Kerala, pp. 311–315, IEEE, 2011.
 43. K. Samarakoon, J. Ekanayake, & N. Jenkins, “Investigation of domestic load control to provide primary frequency response using smart meters,” *IEEE Transactions on Smart Grid*, vol. 3, no. 1, pp. 282–292, 2012, <https://doi.org/10.1109/TSG.2011.2173219>.
 44. R. Raman, S. K. Dutta, P. Sarmah, M. Das, A. Saikia & P.K. Sadhu, “Feasible evaluation of shunt active filter for harmonics mitigation in induction heating system,” *HighTech and Innovation Journal*, vol. 2, no. 3, pp. 235–245, (2021, September). <https://doi.org/10.28991/HIJ-2021-02-03-08>.
 45. M. Beiraghi & A.M. Ranjbar, “Adaptive delay compensator for the robust wide-area damping controller design,” *IEEE Transactions on Power Systems*, vol. 3, no. 6, pp. 4966–4976, 2016. <https://doi.org/10.1109/TPWRS.2016.2520397>.

46. I. Abdulrahman, R. Ismael & G. Belkacemi, "Power oscillations damping using wide-area-based solar plant considering adaptive time- delay compensation". *Energy Syst*, vol. **12**, pp.459–489,2021, <https://doi.org/10.1007/s12667-019-00350-2> Springer.
47. J. Ma et al., "Application of dual youla parameterization based adaptive wide-area damping control for power system oscillations," *IEEE Trans. Power Syst.*, vol. 29, no. 4, pp. 1602–1610, 2014, doi: 10.1109/TPWRS.2013.2296940.
48. P. Zhang, et al, "Adaptive wide area damping control scheme with stochastic subspace identification and signal time delay compensation," *IET Generation, Transmission & Distribution*, vol. 6, no. 9, pp. 844–852. <https://doi.org/10.1049/iet-gtd.2011.0680>.
49. M. Mokhtari & F. Aminifar, "Toward wide-area oscillation control through doubly-fed induction generator wind farms," *IEEE Transactions on Power Systems*, vol. 29, no. 6, pp. 2985–2992, 2014, November. <https://doi.org/10.1109/TPWRS.2014.2309012>.
50. P. Babahajiani, Q. Shafiee & H. Bevrani, "Intelligent demand response contribution in frequency control of multi-area power systems," *IEEE Trans on Smart Grid*, vol. 9, no. 2, pp. 1282–1291, 2018, June. <https://doi.org/10.1109/TSG.2016.2582804>.
51. S. A. Hosseini, M. Toulabi, A. S. Dobakhshari, A. M. Ranjbar & A. M. Ranjbar, "Delay compensation of demand response and adaptive disturbance rejection applied to power system frequency control," *IEEE Transactions on Power Systems*, vol. 35, no. 3, pp. 2037–2046, 2019, November. <https://doi.org/10.1109/TPWRS.2019.2957125>.
52. T.S. Mahmoud, B.S. Ahmed, M.Y. Hassan, "The role of intelligent generation control algorithms in optimizing battery energy storage systems size in microgrids: A case study from Western Australia" *Energy Conversion and Management*. 2019 Sep 15; 196:1335-52.
53. Z. Tan, X. Li , L. He , Y. Li, J. Huang, "Primary frequency control with BESS considering adaptive SoC recovery," *International Journal of Electrical Power & Energy Systems*, 2020 May;117:105588.
54. X. Li , Y. Huang, J. Huang, S. Tan, M. Wang, T. Xu, X. Cheng, "Modelling and control strategy of battery energy storage system for primary frequency regulation," In2014 International Conference on Power System Technology 2014 Oct 20 (pp. 543-549). IEEE.
55. X. Li , S. Wang, "Energy management and operational control methods for grid battery energy storage systems," *CSEE Journal of Power and Energy Systems*. vol. 7, no. 5, pp. 1026-40, 2019 Jun 13.
56. P. Mercier, R. Cherkaoui, A. Oudalov, "Optimizing a battery energy storage system for

- frequency control application in an isolated power system,” *IEEE transactions on Power Systems*, vol. 24, no. 3, pp. 1469-77, 2009 Jun 23.
57. M. Torkashvand, A. Khodadadi, M. B. Sanjareh, and M. H. Nazary, “A Life Cycle-Cost Analysis of Li-ion and Lead-Acid BESSs and Their Actively Hybridized ESSs with Supercapacitors for Islanded Microgrid Applications,” *IEEE Access*, vol. 8, pp. 153215–153225, 2020, doi: 10.1109/ACCESS.2020.3017458.
 58. S. Sitompul, Y. Hanawa, V. Bupphaves, and G. Fujita, “State of charge control integrated with load frequency control for BESS in islanded microgrid,” *Energies*, vol. 13, no. 18, 2020, doi: 10.3390/en13184657.
 59. S. Som, S. De, S. Chakrabarti, S. R. Sahoo, and A. Ghosh, “A robust controller for battery energy storage system of an islanded ac microgrid,” *IEEE Trans. Ind. Informatics*, vol. 18, no. 1, pp. 207–218, 2022, doi: 10.1109/TII.2021.3057516.
 60. J. Tan and Y. Zhang, “Coordinated Control Strategy of a Battery Energy Storage System to Support a Wind Power Plant Providing Multi-Timescale Frequency Ancillary Services,” *IEEE Trans. Sustain. Energy*, vol. 8, no. 3, pp. 1140–1153, 2017, doi: 10.1109/TSTE.2017.2663334.
 61. S.K. Aditya, D. Das, “Battery energy storage for load frequency control of an interconnected power system,” *Electric power systems research*, vol. 58, no. 3, pp. 179-85, 2001 Jul 20.
 62. L. Wang, *Model predictive control system design and implementation using MATLAB®*. Springer Science & Business Media; 2009 Feb 14.
 63. Z. Chen, Z. Liu, and L. Wang, “A modified model predictive control method for frequency regulation of microgrids under status feedback attacks and time-delay attacks,” *Int. J. Electr. Power Energy Syst.*, vol. 137, no. May 2021, p. 107713, 2022, doi: 10.1016/j.ijepes.2021.107713.
 64. A. Oshnoei, M. Kheradmandi, R. Khezri, and A. Mahmoudi, “Robust Model Predictive Control of Gate-Controlled Series Capacitor for LFC of Power Systems,” *IEEE Trans. on Ind. Informatics*, vol. 17, no. 7, pp. 4766–4776, 2021, doi: 10.1109/TII.2020.3016992.
 65. B. Khokhar and K. P. S. Parmar, “A novel adaptive intelligent MPC scheme for frequency stabilization of a microgrid considering SoC control of EVs,” *Appl. Energy*, vol. 309, no. August 2021, p. 118423, 2022, doi: 10.1016/j.apenergy.2021.118423.
 66. A. Mohammadi, H. Asadi, S. Mohamed, K. Nelson, and S. Nahavandi, “Multiobjective and Interactive Genetic Algorithms for Weight Tuning of a Model Predictive Control-

- Based Motion Cueing Algorithm,” *IEEE Trans. Cybern.*, vol. 49, no. 9, pp. 3471–3481, 2019, doi: 10.1109/TCYB.2018.2845661.
67. H. Mahmoudi, M. Aleenejad, and R. Ahmadi, “A New Multiobjective Modulated Model Predictive Control Method with Adaptive Objective Prioritization,” *IEEE Trans. Ind. Appl.*, vol. 53, no. 2, pp. 1188–1199, 2017, doi: 10.1109/TIA.2016.2624738.
 68. S. Kayalvizhi and D. M. Vinod Kumar, “Load frequency control of an isolated micro grid using fuzzy adaptive model predictive control,” *IEEE Access*, vol. 5, pp. 16241–16251, 2017, doi: 10.1109/ACCESS.2017.2735545.
 69. M. Elsis, M. Soliman, M. A. S. Aboelela, and W. Mansour, “Optimal design of model predictive control with superconducting magnetic energy storage for load frequency control of nonlinear hydrothermal power system using bat inspired algorithm,” *J. Energy Storage*, vol. 12, pp. 311–318, 2017, doi: 10.1016/j.est.2017.05.009.
 70. M. Dashtdar et al., “Frequency control of the islanded microgrid based on optimised model predictive control by PSO,” *IET Renew. Power Gener.*, vol. 16, no. 10, pp. 2088–2100, 2022, doi: 10.1049/rpg2.12492.
 71. S. Zhang, Y. Mishra and M. Shahidehpour, "Fuzzy-Logic Based Frequency Controller for Wind Farms Augmented with Energy Storage Systems," in *IEEE Transactions on Power Systems*, vol. 31, no. 2, pp. 1595-1603, March 2016, doi: 10.1109/TPWRS.2015.2432113.
 72. Y. Han, P. M. Young, A. Jain and D. Zimmerle, "Robust Control for Microgrid Frequency Deviation Reduction With Attached Storage System," in *IEEE Transactions on Smart Grid*, vol. 6, no. 2, pp. 557-565, March 2015, doi: 10.1109/TSG.2014.2320984.
 73. H. Bevrani, M. R. Feizi and S. Ataei, "Robust Frequency Control in an Islanded Microgrid: H_∞ and μ -Synthesis Approaches," in *IEEE Transactions on Smart Grid*, vol. 7, no. 2, pp. 706-717, March 2016, doi: 10.1109/TSG.2015. 2446984..
 74. I. Pan, S. Das, “Fractional order fuzzy control of hybrid power system with renewable generation using chaotic PSO,” *ISA Trans.* 2016, vol. 62, pp.19–29.
 75. Y. Mi, D. Li, C. Wang, P. Loh, “The sliding mode load frequency control for hybrid power system based on disturbance observer,” *Int. J. Electr. Power Energy Syst.* vol. 74, pp. 446–452, 2016.
 76. L. B. Armenio, E. Terzi, M. Farina and R. Scattolini, "Model Predictive Control Design for Dynamical Systems Learned by Echo State Networks," in *IEEE Control Systems Letters*, vol. 3, no. 4, pp. 1044-1049, Oct. 2019, doi: 10.1109/LCSYS.2019.2920720.

77. T.H. Mohamed, et al. "Model predictive based load frequency control design concerning wind turbines." *International Journal of Electrical Power & Energy Systems* vol. 43, no. 1, pp. 859-867, 2012.
78. A. M. Ersdal, L. Imsland and K. Uhlen, "Model Predictive Load-Frequency Control," in *IEEE Transactions on Power Systems*, vol. 31, no. 1, pp. 777-785, Jan. 2016, doi: 10.1109/TPWRS.2015.2412614.
79. Y. Zheng, J. Zhou, Y. Xu, Y. Zhang, Z. Qian, "A distributed model predictive control based load frequency control scheme for multi-area interconnected power system using discrete-time Laguerre functions," *ISA Transactions*, vol. 68, pp.127140,2017,<https://doi.org/10.1016/j.isatra.2017.03.009>.
80. M. Khan and H. Sun, "Complete Provision of MPC-Based LFC By Electric Vehicles with inertial and droop support from DFIG-Based Wind Farm," in *IEEE Transactions on Power Delivery*, vol. 37, no. 2, pp. 716-726, April 2022, doi: 10.1109/TPWRD.2021.3069740.
81. M. Dashtdar, et al. "Frequency control of the islanded microgrid based on optimised model predictive control by PSO." *IET Renewable Power Generation*, vol. 16, no. 10, pp. 2088-2100, 2022.
82. Z. Chen, Z. Liu, and L. Wang. "A modified model predictive control method for frequency regulation of micro grids under status feedback attacks and time-delay attacks." *International Journal of Electrical Power & Energy Systems*, vol. 137 (2022): 107713, <https://doi.org/10.1016/j.ijepes.2021.107713>.
83. Y. Cao, et al. "Multiscale model predictive control of battery systems for frequency regulation markets using physics-based models." *Journal of Process Control*, vol. 90, pp. 46-55, 2020.
84. A. Oshnoei, M. Kheradmandi and S. M. Muyeen, "Robust Control Scheme for Distributed Battery Energy Storage Systems in Load Frequency Control," in *IEEE Transactions on Power Systems*, vol. 35, no. 6, pp. 4781-4791, Nov. 2020, doi: 10.1109/TPWRS.2020.2997950.
85. B. Khokhar, and K.P. Singh Parmar. "A novel adaptive intelligent MPC scheme for frequency stabilization of a microgrid considering SOC control of EVs." *Applied Energy*, vol. 309, 2022: 118423, <https://doi.org/10.1016/j.apenergy.2021.118423>.
86. N. S. G. E., C. A. Cañizares, K. Bhattacharya and D. Sohm, "Frequency Regulation Model of Bulk Power Systems with Energy Storage," in *IEEE Transactions on Power Systems*, vol. 37, no. 2, pp. 913-926, March 2022, doi: 10.1109/TPWRS.2021.3108728.

87. A.Al-Hinai, H.Alyammahi, H.H. Alhelou, “coordinated intelligent frequency control incorporating battery energy storage system, minimum variable contribution of demand response, and variable load damping coefficient in isolated power systems,” *Energy Reports*. Vol. 7: 2021 Nov 1, pp. 8030-41.
88. SA.Hosseini, M. Toulabi, A. Ashouri-Zadeh , AM. Ranjbar, “Battery energy storage systems and demand response applied to power system frequency control,” *International Journal of Electrical Power & Energy Systems*, vol. 136:107680, 2022 Mar 1.
89. M. O. Qays, Y. Buswig, M. L. Hossain and A. Abu-Siada, "Recent progress and future trends on the state of charge estimation methods to improve battery-storage efficiency: A review," in *CSEE Journal of Power and Energy Systems*, vol. 8, no. 1, pp. 105-114, Jan. 2022, doi: 10.17775/CSEEJPES.2019.03060.
90. S., Braithwait, and Kelly Eakin, “The role of demand response in electric power market design,” Edison Electric Institute, 2002.
91. Y. Chai, Y. Xiang, J. Liu, C. Gu, W. Zhang and W. Xu, "Incentive-based demand response model for maximizing benefits of electricity retailers," in *Journal of Modern Power Systems and Clean Energy*, vol. 7, no. 6, pp. 1644-1650, November 2019, doi: 10.1007/s40565-019-0504-y.
92. J. Kennedy and R. Eberhart, “Particle swarm optimization,” in *Proc. IEEE Int. Conf. Neural Networks*, Piscataway, NJ, vol. 4, pp. 1942–1948, 1995.
93. Riccardo Poli, James Kennedy, Tim Blackwell, “Particle swarm optimization: An overview,” *Swarm Intelligence*, vol.1, pp. 33-57, 2007.
94. J. Vuelvas, F. Ruiz, “A novel incentive-based demand response model for Cournot competition in electricity markets,” *EnergySystems*, vol.10, no.1, pp. 95-112, 2019.
95. R. Shankar, K. Chatterjee & R. Bhushan, “Impact of energy storage system on load frequency control for diverse sources of interconnected power system in deregulated power environment,” *International Journal of Electrical Power & Energy Systems*, vol. 79, pp. 11–26, 2016, <https://doi.org/10.1016/j.ijepes.2015.12.029>.
96. S. Rajasomashekar, P. Aravindhababu, “Biogeography based optimization technique for best compromise solution of economic emission dispatch. *Swarm and Evolutionary Computation*,” vol. 71, pp. 47–57,2012. <https://doi.org/10.1016/j.swevo.2012.06.001>.
97. R. Walawalkar, S. Blumsack, J. Apt and S. Fernands, "Analyzing PJM’s economic demand response program," 2008 IEEE Power and Energy Society General Meeting - Conversion and Delivery of Electrical Energy in the 21st Century, Pittsburgh, PA, USA, 2008, pp. 1-9, doi: 10.1109/PES.2008.4596905.

98. D.Stroe, F. Yongcun, C.Wen, Z. Chen, C. Fernandez, S. Wang, Y. Chunmei, Battery System Modeling. Netherlands: Elsevier Science, 2021.
99. A. Oudalov, D. Chartouni and C. Ohler, "Optimizing a Battery Energy Storage System for Primary Frequency Control," in IEEE Transactions on Power Systems, vol. 22, no. 3, pp. 1259-1266, Aug. 2007, doi: 10.1109/TPWRS.2007.901459.
100. Knap V, Sinha R, Swierczynski M, Stroe DI, Chaudhary S. Grid inertial response with Lithium-ion battery energy storage systems. In: 2014 IEEE 23rd international symposium on industrial electronics (ISIE), Istanbul; 2014. p. 1817–22.
101. M. Schwenzer, et al. "Review on model predictive control: An engineering perspective." The International Journal of Advanced Manufacturing Technology, vol. 117, pp. 1327–1349 ,2021. <https://doi.org/10.1007/s00170-021-07682-3>.
102. K. Charles, N. Urasaki, T. Senjyu, LM. Elsayed, L. Liu, “Robust load frequency control schemes in power system using optimized PID and model predictive controllers,”Energies. 2018 Nov vol. 7:11:3070.
103. Z. Chen, Z. Liu, and L. Wang, “A modified model predictive control method for frequency regulation of microgrids under status feedback attacks and time-delay attacks,” Int. J. Electr. Power Energy Syst., vol. 137, no. May 2021, 2022, doi: 10.1016/j.ijepes.2021.107713.
104. N. Mukherjee and D. De, "A New State-of-Charge Control Derivation Method for Hybrid Battery Type Integration," in IEEE Transactions on Energy Conversion, vol. 32, no. 3, pp. 866-875, Sept. 2017, doi: 10.1109/TEC.2017.2695242.

APPENDIX A

Details of Components of Power System under Investigation:

A.1. Nominal parameters for DFIG The parameters used in DFIG based WECS are T_A =time constant of non-conventional generator, T_R = transducer time constant, T_w = washout time constant, H_e = inertia constant of WECS, P_{out}^{max} is maximum output of non-conventional generator, P_{out}^{min} is minimum output of non-conventional generator, K_{wp} , K_{wi} are proportional and integral constant of speed regulator respectively. These variables are presented in Table A-1

Table A-1. Nominal Parameters of DFIG based WECS

T_A (sec)	T_R (sec)	T_w (sec)	H_e	K_{wp}	K_{wi}	P_{out}^{max} (p.u)	P_{out}^{min} (p.u)
0.2	0.1	6	3.5	1.5	0.15	1.2	0

Table A-2.

BESS Parameters											
<i>Battery voltages = 1755 – 2925V DC</i>			$C_{bp} = 52597F$				$K_{BESS} = 100KV/pu. MW$				
$R_{bs} = 0.013\Omega$			$X_{CO} = 0.0274\Omega$				$\alpha^\circ = 15^\circ$				
$R_{bt} = 0.0167\Omega$			$I_{BESS}^0 = 0.02213 p.u.$				Base voltage = 10KV, Base current = 200KA				
$R_b = 0.001\Omega$			$R_{bp} = 10k\Omega$				$C = 40MWh$				
$C_b = 1F$			$T_{BESS} = 0.026sec$				$SOC_{ref} = 0.5$				
Nominal value of parameters for wind two area power system (<i>Base power = 2000MW</i>)											
Area no.	K_P (Hz/pu.MW)	K_r	T_r (sec)	T_p (sec.)	f (Hz)	T_g (sec)	T_i (sec)	R (Hz/pu.MW)	H	D (pu.MW/Hz)	B (pu.MW/Hz)
1	120	0.5	10	20	60	0.08	0.3	3	4.7104	8.33×10^{-3}	0.3417
2	120	0.5	10	20	60	0.08	0.3	3	4.7104	8.33×10^{-3}	0.3417

A-2. MPC Parameters:

prediction horizon = 10,

control horizon = 2,

weights on manipulated variables = 0.8,

weights on manipulated variable rates = 0.10, weight on output signals = 0.10

A-3. PSO Parameter:

Number of particles = 20,

maximum inertia weight = 0.9,

minimum inertia weight = 0.4,

acceleration factor (c1 & c2 are): $c1 = 2$; $c2 = 2$,

Maximum number of steps = 20,

Dimension of the problem = 3

Swetalina Bhuyan

A-4. Answer to the queries raised by the examiners of the thesis:

Q-1. Number of Objectives are more and that needs to be presented in a concise manner, if possible.

Ans: The new concise form of objectives are formed as follows:

- I. To introduce DR in ALFC of both hydrothermal system and wind integrated two-area thermal power system for checking the role of DSM in ALFC.
- II. To design the DR control loop to compensate for the delay issues in DR for smooth frequency control in an interconnected power system.
- III. To implement a new SOC-based strategy for the incremental BESS model in coordination with DR in ALFC of each area of a wind-integrated two-area thermal power system for smooth frequency regulation.
- IV. To propose a new state space based MPC concerning all the variables in the incremental BESS model.
- V. To analyse specially the proposed MPC-based ALFC including inertia issues arising from WECS.
- VI. To examine the saving of battery life when DR is present in the proposed MPC based ALFC.
- VII. To compare the MPC based ALFC with a robust PSO-optimized integral controller based ALFC in co-ordination with PD controller from wind used for inertia issues to confirm the effectiveness of the proposed MPC controller for the studied power system.
- VIII. To implement the delay compensator in DR loop in coordination with formulation and tuning of MPC for ALFC study in an isolated MG.
- IX. To verify the frequency control scheme having simple BESS with a strategy-based SOC controller in BESS in MG.
- X. To validate the proposed PSO tuned MPC in collaboration with lead compensator-based DR and BESS for frequency control in the studied isolated MG through OPAL-RT OP5600 with RT lab version of 19.3.0.228.

Q-2. In Fig. 3.4 to Fig. 3.6, using (a), (b) and (c) for three figures enhance clarity. Why utilizing DR, the deviation curves are smoother?

Ans: The three sub-figures of each of the figures from Fig.3 4 to 3.6 are marked as (a), (b) and (c) to enhance their clarity with the related discussion in the thesis.

DR is an effective method to provide grid frequency support since it can reduce peak load in advance or shed load immediately when a contingency occurs. Hence, the frequency deviation curves become smoother when DR is utilized.

Q-3. How the deviation of frequency affected by integration of wind?

Ans: The randomness and fluctuation nature of the wind energy conversion system affects the security concern of grid frequency deviation. This intermittent nature of wind power can significantly influence grid stability causing frequency deviations. Thus, a better control methodology needs to be developed to smooth the frequency fluctuation without excessive spillage.

Q-4. How and where a delay compensator is used in a practical power system?

Ans: Generally, the delay compensator is used before the controller like the automatic voltage controller (AVR) or automatic load frequency control (ALFC) of the power system. The scheme for a delay compensator in a practical power system is shown in Fig.A.1. In the figure, the delay compensator is used for a wide-area power system. In the wide-area systems, the remote signals are equipped with a stamp demonstrating the precise time of measurement. The measurement sites render an opportunity for exact computation of time delays with the help of dedicated global positioning system (GPS) devices that are used in the control locations, and the time stamp data in the controller. To do so, the phasor measurement unit (PMU) measurements at a time are collected and resynchronized in a data centre referred to as the phasor data concentrator (PDC). When, one or multiple transmission channels experience congestion, the PDC waits until it acquires data from all the measurements. Next, it starts sending data to the central wide-area damping controller (WADC) that is installed nearby. Afterward, the measurements are processed by the central WADC to obtain the control signal with the time stamp. When the adaptive delay compensator (ADC) receives the control signal, the time delay of the control loop is calculated, which denotes a new time stamp freshly acquired from the GPS. Through real-time measurement of time delay, the ADC is adapted to

reimburse the latency of the remote signal. Next, the delay-compensated signal is fed to the AVR/ ALFC input of the excitation system to meet the required dynamic performance [45].

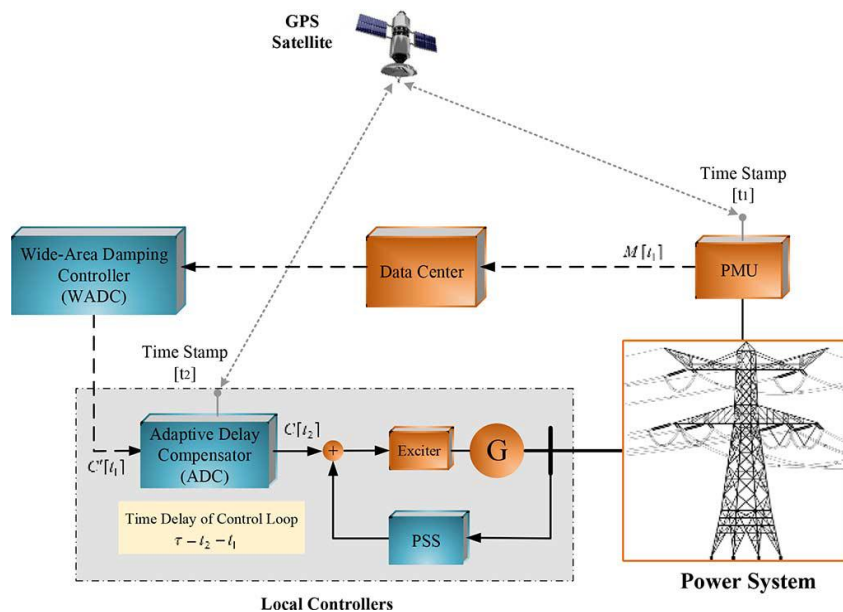


Fig.A.1. Control Structure of power system with delay compensator [45].

Q-5. Why upper bound (maximum value) of SOC is kept at 0.7 (refer 5.4.1)?

Ans: The value of the SOC varies between 0% and 100%. If the SOC is 100%, then the cell is said to be fully charged, whereas a SOC of 0% indicates that the cell is completely discharged. In practical applications, the SOC is not allowed to go below 50% and therefore the cell is recharged when the SOC reaches 50%. The wide variations of charge affect the battery life. So, the deviation in SOC is kept narrow. In the present study, SOC_{ref} is assumed as 0.5. Moreover, plus minus 20% variation is assumed to be allowed for dynamic load change and hence SOC_{max} and SOC_{min} are set at 0.7 and 0.3 respectively for the present analysis.

Q-6. Last para of section 5.5.2: “while analyzing system performance with proposed SOCsmooth frequency regulation.” what is “inertia controller” and how is it practically used?

Ans: The inertia controller is the controller, practically used by wind generators to avoid inertial issues arising from wind due to its randomness and fluctuation. In the case of variable-speed wind turbines driving the double-fed induction generator (DFIG), the rotational kinetic energy will not naturally contribute to the inertia of the grid as the rotational speed is decoupled from the grid frequency by the grid side converter. Therefore, to emulate the inertia and to

facilitate the excess active power injection from the wind turbine for frequency support, an additional auxiliary signal is augmented. The inertia controller used in wind generator improves the inertia issues by imposing an increased power step beyond the steady state power setting. The corrected power setting can be fed to the controller of the grid side converter of DFIG to extract more rotational energy from the rotor blades [22].

In this thesis, an inertia controller is used in the DFIG-based wind energy conversion system which is presented in Fig-2.2 of chapter-2. It can be seen from the figure that, the inertia controller of DFIG is meant for providing an additional signal as ΔP^* defined in equation (2.2). That additional power signal is added to the power reference output that is being tracked by the equivalent controller of the nonconventional machine. In equation (2.2), the values of the control parameters affect the inertia of the system. As the grid frequency exceeds certain limits, this additional PD controller became active and adds the signal to the torque control to set the torque demand. As load increases, the system frequency drops, the set point torque is increased and the rotor slows down and kinetic energy is released.

Swetalina Bhuyan